(2)

Research and Development Technical Report

SLCET-TR-88-0845-F

IMPROVEMENT IN THE CAPACITY AND SAFETY OF LITHIUM/ INORGANIC ELECTROLYTE SULFUR DIOXIDE RECHARGEABLE CELLS, PHASE 2

Carl R. Schlaikjer
Medlinda D. Jones
Arden P. Johnson
James E. Torkelson
Walter VanSchalkwijk
Ljiljana Marincic

Battery Engineering Inc.
1636 Hyde Park Ave.
Hyde Park, MA 01636

November 1990

Final Report for Period September 1988 - November 1990

DISTRIBUTION STATEMENT

Approved for public release;
distribution is unlimited.

Prepared for
Electronics Technology and Devices Laboratory

US ARMY LABORATORY COMMAND

FORT MONMOUTH, NEW JERSEY 07703-5000

91 4 26 023

NOTICES

Disclaimers

The findings in this report are not to be construed as an official Department of the Army position, unless so designated by other authorized documents.

The citation of trade names and names of manufacturers in this report is not to be construed as official Government indorsement or approval of commercial products or services referenced herein.

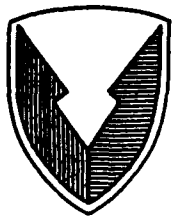

Research and Development Technical Report

SLCET-TR-88-0845-F

IMPROVEMENT IN THE CAPACITY AND SAFETY OF LITHIUM/ INORGANIC ELECTROLYTE SULFUR DIOXIDE RECHARGEABLE CELLS, PHASE 2

Carl R. Schlaikjer
Medlinda D. Jones
Arden P. Johnson
James E. Torkelson
Walter VanSchalkwijk
Ljiljana Marincic

Battery Engineering Inc.
1636 Hyde Park Ave.
Hyde Park, MA 01636

November 1990

Final Report for Period September 1988 - November 1990

DISTRIBUTION STATEMENT

Approved for public release;
distribution is unlimited.

Prepared for
Electronics Technology and Devices Laboratory

US ARMY
LABORATORY COMMAND
FORT MONMOUTH, NEW JERSEY 07703-5000

NOTICES

Disclaimers

The findings in this report are not to be construed as an official Department of the Army position, unless so designated by other authorized documents.

The citation of trade names and names of manufacturers in this report is not to be construed as official Government indorsement or approval of commercial products or services referenced herein.

REPORT DOCUMENTATION PAGE

Form Approved
OMB No. 0704-0188

1a. REPORT SECURITY CLASSIFICATION Unclassified	1b. RESTRICTIVE MARKINGS
2a. SECURITY CLASSIFICATION AUTHORITY	3. DISTRIBUTION/AVAILABILITY OF REPORT Approved for public release; distribution is unlimited.
2b. DECLASSIFICATION/DOWNGRADING SCHEDULE	
4. PERFORMING ORGANIZATION REPORT NUMBER(S)	5. MONITORING ORGANIZATION REPORT NUMBER(S) SLCET-TR-88-0845-F
6a. NAME OF PERFORMING ORGANIZATION Battery Engineering Inc. 6b. OFFICE SYMBOL (If applicable)	7a. NAME OF MONITORING ORGANIZATION U.S. Army Laboratory Command (LABCOM) Electronics Technology and Devices Lab (ETDL)
6c. ADDRESS (City, State, and ZIP Code) 1636 Hyde Park Avenue HYde Park MA 02136	7b. ADDRESS (City, State, and ZIP Code) ATTN: SLCET-PR Fort Monmouth NJ 07703-5000
8a. NAME OF FUNDING/SPONSORING ORGANIZATION 8b. OFFICE SYMBOL (If applicable)	9. PROCUREMENT INSTRUMENT IDENTIFICATION NUMBER DAAL01-88-C-0845
8c. ADDRESS (City, State, and ZIP Code)	10. SOURCE OF FUNDING NUMBERS PROGRAM ELEMENT NO. ?.1 / PROJECT NO. 62705 / TASK NO. AH94 / WORK UNIT ACCESSION NO. DA317720

11. TITLE (Include Security Classification)
IMPROVEMENT IN THE CAPACITY AND SAFETY OF LITHIUM/INORGANIC ELECTROLYTE SULFUR DIOXIDE RECHARGEABLE CELLS, PHASE 2

12. PERSONAL AUTHOR(S) Carl R. Schlaikjer, Melinda D. Jones, Arden P. Johnson, James E. Torkelson, Walter vanSchalkwijk, Ljiljana Marincic

13a. TYPE OF REPORT	13b. TIME COVERED	14. DATE OF REPORT (Year, Month, Day)	15. PAGE COUNT
Final Report	FROM Sep 88 TO Nov 90	1990 November	216

16. SUPPLEMENTARY NOTATION

17. COSATI CODES			18. SUBJECT TERMS (Continue on reverse if necessary and identify by block number)
FIELD	GROUP	SUB-GROUP	Lithium; Sulfur Dioxide; Rechargeable Batteries; Lithium Batteries
10	02		
07	04		

19. ABSTRACT (Continue on reverse if necessary and identify by block number)

Our objective during this Phase II SBIR program was to develop a prototype rechargeable lithium/ sulfur dioxide/ carbon cell, using practical AA size hardware, in which the electrolyte was to be a sulfur dioxide solution of lithium bromide or thiocyanate, together with a highly soluble "cosolute", a second non-lithium salt of the same anion. The cosolute was intended to replace the organic "cosolvents" familiar from the primary cells, and hopefully, to improve lithium plating efficiency and electrolyte stability during cycling.

The primary discharge capacities for AA size cells containing 1.25M CsBr/ 0.12M LiBr/ SO_2 were only about 400 mAh, while secondary and subsequent capacities were less than 200 mAh. The rates of solvolysis of bromide and of thiocyanate were exacerbated apparently both by the high anion concentrations and by increased lithium ion concentration.

We then studied lithium/ sulfur dioxide/ carbon rechargeable cells in which the (contd)

20. DISTRIBUTION/AVAILABILITY OF ABSTRACT ☐ UNCLASSIFIED/UNLIMITED ☒ SAME AS RPT. ☐ DTIC USERS	21. ABSTRACT SECURITY CLASSIFICATION Unclassified
22a. NAME OF RESPONSIBLE INDIVIDUAL Dr. Michael Binder	22b. TELEPHONE (Include Area Code) (908) 544-4795 / 22c. OFFICE SYMBOL SLCET-PR

19. Abstract (contd)

electrolytes were mixtures of tetrachloroaluminate salts in sulfur dioxide, to take advantage of the better performance, but to face the problem of limited capacity. By better design of the positive electrode, we built AA size cells (6.0ml; 15g) delivering 500 to 600 mAh at 3.1 volts, 50 mA, representing 260-310 wH/l; 100-125 wH/kg; 26 W/l; and 10 W/kg.

Potentiostatic and galvanostatic measurements using AA cells with positive electrode screens but no carbon implied that explosions occasionally observed during charge cycles were not likely initiated by "hard" short circuits, but by chemical reactions between lithium dendrites and possibly hydrolysis products. We determined how to measure and to remove moisture from carbon positive electrodes.

We determined that the capacity of lithium/ bromine soluble positive cells was being limited by the loss of electrical contact between the carbon and the positive electrode current collector. Also, lithium plating efficiency was poor.

SUMMARY

Our overall objective during this Phase II SBIR program was to develop a rechargeable lithium/ sulfur dioxide cell, using practical AA size hardware, in which the electrolyte was to be a lithium salt together with a "cosolute", a second non-lithium salt of the same anion dissolved in liquid sulfur dioxide. The cosolute was chosen such that it was by itself highly soluble, and was added specifically to increase the dielectric constant of the solution and therefore increase the solubility of the lithium salt. The anions chosen were thiocyanate and bromide, both of which are capable of providing overcharge protection through reversible electrochemical reactions.

We found several examples of non-lithium thiocyanates and bromides which did substantially increase the solubility of lithium thiocyanate or lithium bromide. Salts with organic cations were incompatible with lithium, but potassium, cesium, and guanidinium compounds were compatible and produced solutions with useful concentrations of lithium ion.

We compared the capacities of identically constructed wound electrode AA size cells containing cosolute electrolytes with cells containing a conventional primary cell electrolyte including acetonitrile, propylene carbonate, and lithium bromide. Cells with the primary cell electrolyte all gave in excess of one amp hour at 50 mA, ambient temperature. The primary discharge capacities for AA size cells containing 1.25M CsBr/ 0.12M LiBr/ SO_2 were only about 400 mAh, while secondary and subsequent capacities were less than 200 mAh, and lower than capacities delivered to the cells during time limited charge cycles. We were able to increase the lithium concentration by using 1M guanidinium bromide/ 1M cesium bromide/ 0.7M LiBr. However, the rate of solvolysis of bromide to bromine and sulfur monobromide, and of thiocyanate to parathiocyanogen was apparently exacerbated by the high anion concentrations, and by increased lithium ion concentration.

We turned to the study of lithium/ sulfur dioxide/ carbon rechargeable cells in which the electrolytes were mixtures of tetrachloroaluminate salts in sulfur dioxide, to take advantage of the better chemical stability, cycling efficiency, and cycle life, but to face the problem of limited capacity, which had become apparent during earlier studies. We have shown in principle that the capacity can be improved by better design of the positive electrode. AA size cells (6.0ml; 15g) delivering 500 to 600 mAh at 3.1 volts, 50 mA, represent 260-310 wH/l; 100-125 wH/kg; 26 W/l; and 10 W/kg. With glass fiber separators, cells ran a maximum 50-60 cycles before short-circuiting.

We have used glass fiber separators purposely to explore the relationships between safety during short-circuiting and the presence of extensive concentrations of hydrolysis products known to be present in sulfur dioxide solutions containing mixed tetrachloroaluminates. Coordinating our efforts with related work, we discovered how to remove hydrolysis products quantitatively from

electrolytes such as $2LiCl \cdot CaCl_2 \cdot 4AlCl_3 \cdot 12SO_2$, how to determine low levels of water present in carbon positive electrodes, and we have discovered a method of removing moisture from the electrodes without damaging their structure.

Potentiostatic and galvanostatic measurements using AA cells with positive electrode screens but no carbon showed that, in $2LiCl \cdot CaCl_2 \cdot 4AlCl_3 \cdot 12SO_2$, the overpotential for oxidation of the electrolyte on a carbon surface was lower than that for the oxidation of the electrolyte, or of nickel, on a metal surface. The implication was that "hard" short circuits through lithium dendrites to positive electrode hardware during charging are unlikely. The further implication was that rapid reactions in these cells are also not caused by "hard" short circuits, but are more likely initiated by other reactions, such as those involving lithium dendrites in the presence of hydrolysis products.

We also studied lithium/ bromine soluble positive cells, attempting to redesign the positive electrode to increase the capacity. The capacity of carbon electrodes was being limited by the loss of electrical contact between the carbon and the positive electrode current collector. While lithium and all hardware appeared to be stable in electrolytes containing purified $CH_2ClCClO$/ $LiAlCl_4$/ and up to 30 volume percent of bromine, lithium plating efficiency was poor.

FOREWORD

Battery Engineering Inc, is pleased to acknowledge financial support from the ETD Laboratory for this contract as part of the Small Business Innovative Research Program. This document, the eighth quarterly and final report of our current two-year Phase II program, represents the continuation of DAAL01-87-C-0751, the Phase I contract which ran from July 1 through December 31, 1987.

This current effort, under Contract DAAL01-88-C-0845 between Battery Engineering, Inc. and Fort Monmouth, originally studied lithium/ sulfur dioxide/ carbon rechargeable cells in which the electrolyte is liquid sulfur dioxide containing one or more non-lithium "cosolute" salts, the purpose of which has been to make a lithium salt more soluble. During cell discharge, lithium dithionite is produced in the carbon electrode. The anticipated advantage was that cells with the high capacities characteristic of lithium/ sulfur dioxide organic electrolyte primary cells could be produced, but without the need for organic cosolvents to increase the solubility of the lithium salt. There would then be no organic solvents to degrade during charge cycles.

Battery Engineering Inc., has also undertaken other Contracts to study lithium/ sulfur dioxide rechargeable cells. Contract F33615-87-C-2798 to Battery Engineering from Wright-Patterson Air Force Base, Ohio, was an SBIR Phase I effort which ran from 15 June through 15 December 1987. Negotiations to obtain Phase II funding were not successful. Contract N60921-89-C-0148 to Battery Engineering from the Naval Surface Warfare Center, Silver Spring, Maryland, was an SBIR Phase I effort which ran from 20 June through 20 December, 1989. The important distinctions between the Ft. Monmouth Contracts (DAAL01-87-C-0751 and DAAL01-88-C-0845) and the Air Force and Navy contracts are as follows.

Contracts F33615-87-C-2798 and N60921-89-C-0148 studied cells containing mixed tetrachloroaluminate electrolyte salts. During discharge, the sulfur dioxide was reduced not to lithium dithionite but to a complex including the aluminum. The discharge/charge reaction was more reversible, but the capacity was considerably lower than in cells without tetrachloroaluminate, in which the sulfur dioxide/ lithium dithionite reaction was allowed to occur. The objective of the Navy and Air Force projects was therefore in part to determine whether the positive electrode could be designed to increase the capacity, relative to state-of-the-art cells containing tetrachloroaluminate based electrolytes. The Army contracts considered only cells without tetrachloroaluminate salts in which the discharge product was lithium dithionite, in order hopefully to take advantage of the higher capacity.

While we developed electrolytes with which viable cells could be prepared, their capacities were not greater than what we were able to obtain using tetrachloroaluminate salts. Further, evidence indicated that the shelf life of "cosolute" cells would be inferior to cells containing tetrachloroaluminate salts. We therefore decided to include cells with tetrachloroaluminate salts as part of our studies under this current Contract DAAL01-88-C-0845, in order to take advantage of the greater charging efficiency and longer cycle life which this chemistry offers when compared with the existing data for our "cosolute" cells, and continue the work suggested by the results obtained during Contracts F33615-87-C-2798, N60921-89-C-0148, and F33615-87-C-2785.

TABLE OF CONTENTS

TABLE OF CONTENTS
(Continued).

TABLE OF CONTENTS
(Continued).

ILLUSTRATIONS

ILLUSTRATIONS (Continued).

ILLUSTRATIONS (Continued).

ILLUSTRATIONS (Continued).

ILLUSTRATIONS (Continued).

ILLUSTRATIONS (Continued).

LIST OF TABLES

CHAPTER 1.

INTRODUCTION

Our overall objective during this Phase II SBIR program has been to develop a rechargeable lithium/ sulfur dioxide cell, using practical AA size hardware, in which the capacity at the C/20 rate is at least 1 amp hour and the running potential is at least 2.85 volts. The study of the lithium/ sulfur dioxide cell as a soluble positive secondary system is a departure from most of the currently studied solid positive cells with liquid or polymeric organic electrolyte. The advantages of a liquid inorganic electrolyte lithium/ sulfur dioxide/ carbon cell include a simply constructed positive electrode, a highly conductive electrolyte with no organic solvents to degrade during cycling, and an electrolyte which does not depend on lithium hexafluoroarsenate. Carbon positive electrodes require no elaborate synthetic techniques and use less expensive materials than do electrodes based on insoluble positives. During cycling in lithium cells with cyclic ethers, hexafluoroarsenate is known to decompose to oxides of arsenic and to be reduced to elemental arsenic.

The study of the rechargeable lithium/ sulfur dioxide cell began at the same time as the discovery of the primary cell in 1969 by Maricle and Mohns at American Cyanamid [1]. It was the first substantial advancement in the study of primary lithium power sources. Unlike the lithium/ solid cathode primaries studied up to that time, the new cells were relatively stable during storage and ran at a steady potential throughout their useful life. They could be operated efficiently at rates comparable with aqueous zinc/ alkaline manganese cells, but with far superior volumetric and gravimetric energy density. The chemistry showed promise as a basis for a secondary cell in that the product of the electrochemical reduction, lithium dithionite, could be readily oxidized back to sulfur dioxide. Lithium/ sulfur dioxide primary cells have since found wide use in military communications in substantially the same chemical formulation as that first developed at American Cyanamid. However, this chemistry was not successful as a secondary cell.

The major difficulty appeared to be that the cosolvents acetonitrile and propylene carbonate were interfering with charging. Without the organic cosolvents, the lithium bromide electrolyte salt was essentially insoluble in sulfur dioxide. Kuo and others at Duracell studied rechargeable lithium/ sulfur dioxide cells using lithium salts which were soluble in liquid sulfur dioxide without organic cosolvents [2]. Those found to be substantially soluble in pure sulfur dioxide included the closoborate salts $Li_2B_{10}Cl_{10}$ and $Li_2B_{12}Cl_{12}$; $LiGaCl_4$, and $LiAlCl_4$. Cells containing the closoborates or $LiGaCl_4$ all gave large primary capacities, but despite attempts to realize improvements, showed dramatic capacity fading after just a few cycles. In addition, the closoborate salts as reducing agents reacted violently with sulfur dioxide if accidentally heated. Lithium tetrachlorogallate, even

at concentrations as low as 1 molar, tended to aggravate lithium corrosion.

Lithium tetrachloroaluminate, potentially the most valuable salt because of its low cost and low reactivity, severely limited even the primary discharge capacities. It was later discovered that the aluminum was involved in the discharge reaction [3, 4], and that the positive electrode material needed to be a high surface area carbon such as Ketjenblack. After a two year program to develop a C size cell using Ketjenblack and $LiAlCl_4 \cdot 6SO_2$, Kuo et al. were only able to realize about half the capacity which should have been available, based on the amount of sulfur dioxide present [5]. Somewhat higher capacity and better resistance to capacity fading was realized by increasing the concentration of tetrachloroaluminate, but capacities were lower than could be obtained with sulfur dioxide/ dithionite positives [6].

We wished to build a lithium/ sulfur dioxide rechargeable cell in which the discharge product was lithium dithionite, in order to take advantage of the higher capacity, but which contained no organic solvents to interfere with charging. The choice of lithium salts soluble in sulfur dioxide alone had been exhausted. However, we knew that Ballard had tried to prepare SO_2/ dithionite positive cells using lithium negative electrodes of the "second kind", that is, electrodes on which the lithium was supposed to cycle between the metal and a slightly soluble salt on the surface of the metal [7]. They had chosen supporting electrolytes from among several non-lithium salts soluble in sulfur dioxide alone. They discovered that as soon as they tried to increase the conductivity of the supporting electrolyte by increasing its concentration, the solubility of the corresponding lithium salt would also increase, therefore interfering with the operation of the lithium electrode as one of the second kind. Rather than limiting the solubility of the lithium salt by the "common ion effect", a concept familiar from aqueous solution chemistry, the supporting electrolyte salts were apparently increasing the solubility of lithium salts by increasing the dielectric constant of the solution.

Believing a lithium electrode of the second kind to be unnecessary, we wished to take advantage of this unexpected property to increase the solubility of lithium salts as much as possible. The approach was essentially equivalent to trading in organic cosolvents for a non-lithium "cosolute". We knew, for example, that ammonium thiocyanate was soluble in sulfur dioxide to at least 5 molar, and might increase the solubility of lithium thiocyanate. Many quarternary ammonium bromides were also substantially soluble, and might increase the solubility of lithium bromide. Since thiocyanate could be reversibly oxidized to thiocyanogen and bromide to bromine, both at potentials versus lithium greater than the lithium/ sulfur dioxide (dithionite) potential, either could serve as an electrochemical mechanism for preventing damage during overcharge.

During our Phase I work, we established that soluble non-lithium

salts did in fact increase the solubility of corresponding lithium salts, and that lithium/ carbon cells could be cycled without short circuiting, venting, or exploding. Our test vehicles were hermetic wound electrode AA size cells with a common electrode area of about 50 cm^2, which we cycled at 1 mA/cm^2 at ambient temperature. The electrolyte consisted of sulfur dioxide and ammonium thiocyanate with lithium thiocyanate prepared by metathesis from lithium chloride, in which the concentration of ammonium thiocyanate was 3 molar and the lithium thiocyanate was 1 molar, assuming that the metathesis had gone to completion. Alternatively, we used 4 molar N-methylpyridinium bromide with 1 molar lithium bromide. The highest capacity obtained was only 360 mAh, although the amount of sulfur dioxide present was nearly 1.5 amp hours. We showed that the choice of material for the positive electrode screens affected the electrical capacities, indicating that hardware corrosion was likely occurring.

During Phase II, we planned to continue our efforts to build lithium/ sulfur dioxide (dithionite) cells which would perform as well as the currently used primaries, but which would be efficient secondaries cells as well, based on the principle of a "cosolute" to increase the solubility of a lithium salt. The causes for the observed low cell capacities had to be identified. We planned to begin by determining the best hardware, electrolyte salt, and the best way to prepare the electrolyte salt to limit or prevent corrosion of the positive contact hardware. Instead of preparing lithium thiocyanate by metathesis in sulfur dioxide, we would prepare it from LiOH and NH_4SCN in water, followed by drying, to exclude chloride from the electrolyte. We planned to increase the rate at which we were able to screen potential hardware material by carrying out separate corrosion studies, and to determine whether an improved method for filling and sealing cells would improve performance.

We have also continued our studies of lithium/ sulfur dioxide/ carbon rechargeable cells in which the electrolytes are mixtures of tetrachloroaluminate salts in sulfur dioxide, to take advantage of the better chemical stability, cycling efficiency, and cycle life, but to face the problem of limited capacity which had become apparent during earlier studies [3-5]. Some improvements in the capacity, resistance to capacity fading, morphology of lithium plating, and rate capability were realized by increasing the aluminum concentration [6]. To prevent freezing, the aluminum was added as calcium tetrachloroaluminate instead of lithium tetrachloroaluminate. The calcium did not interfere with the lithium electrode, but instead improved the morphology of the lithium plate and the efficiency of the positive electrode, when compared with control cells or alternative additives such as sodium tetrachloroaluminate.

The approach used to increase the capacity still further was to examine positive electrode form, composition and method of manufacture [8]. Hydrolysis products, believed to be capable of initiating rapid chemical reactions during charge cycles, were removed quantitatively from the electrolyte using a newly

discovered process [8]. We set out to develop means to measure and remove adsorbed water from carbon positive electrodes as well, and determine how the complete removal of moisture from this system would affect capacity and safety.

Lithium/ bromine soluble positive cells containing chloro- or dichloroacetyl chloride, $LiAlCl_4$ or $LiBr \cdot AlCl_3$, and up to 40 volume percent bromine had been previously shown both to discharge and to charge at 1 mA/ cm^2 with only 3 to 4 millivolts of polarization. Hermetically sealed AA size wound electrode cells could accept extended overcharge without increasing in impedance, bulging, shorting, or exploding [9, 10]. We had resolved to reexamine this system, using $LiAlCl_4$ and chloroacetyl chloride dried according to the newly discovered techniques [8].

CHAPTER 2.

EXPERIMENTAL

REAGENTS

The chemicals used were of the highest purity commercially available. Their sources are listed below:

Salts and metals

aluminum, 99.999%	Alfa/ Ventron
aluminum chloride (anhydrous)	Fluka
ammonium thiocyanate	Baker
calcium	Pfizer
calcium chloride dihydrate, reag.	Baker
cesium bromide	Aldrich
cesium carbonate	Johnson Matthey
cesium thiocyanate	(synthesized as described below)
ferrous sulfate	Fisher
guanidine carbonate	Kodak
guanidine hydrochloride	Fisher
lithium	Foote Mineral
lithium bromide	Aldrich
lithium carbonate	Fisher
lithium chloride	Foote Mineral
lithium tetrafluoroborate	Johnson Matthey
lithium thiocyanate	(synthesized as described below)
lithium trifluoromethanesulfonate ("triflate")	3M Company
potassium bromide	Aldrich
potassium thiocyanate	Baker
potassium trifluoromethanesulfonate ("triflate")	Johnson Matthey
sodium chloride	Aldrich
tetrabutylammonium thiocyanate	Aldrich
tetramethylammonium thiocyanate	(synthesized as described below)

Solvents

acetone	Fisher
acetonitrile	Eastman
anisole	Aldrich
benzene	Aldrich
bromine	Fisher

1,2- dimethoxyethane	Baker
chloroacetyl chloride	Aldrich
ethyl acetate	Fisher
ethyl bromide	Fisher
ethyl iodide	Fisher
methyl bromide	Matheson
methyl chloride	Matheson
methyl iodide	Fisher
methyl sulfide	Aldrich
methylene chloride	Baker
propylene carbonate	Eastman
pyridine (reagent)	Fisher
sulfur dioxide (40 ppm H_2O)	Matheson
sulfuryl chloride	Eastman
tetrahydrofuran	EM Science
tetramethylguanidine	Aldrich
thioanisole	Aldrich

Acids and bases

cesium hydroxide	Aesar
hydrobromic acid (reagent)	Fisher
lithium hydroxide monohydrate	Lithcoa
tetramethylammonium hydroxide (in methanol)	Aldrich
p-toluenesulfonic acid	Fluka
trifluoromethane-sulfonic acid	Aldrich

N-methylpyridinium bromide was prepared at room temperature from a stoichiometric mixture of pyridine and methyl bromide in benzene. The ammonium, substituted ammonium, and pyridinium salts were dried *in vacuo* at 100°C. for about 16 hours.

After titration of the lithium hydroxide monohydrate and the ammonium thiocyanate to confirm their equivalent weights, one mole batches of lithium thiocyanate were prepared by mixing a 2 mole percent excess of ammonium thiocyanate with lithium hydroxide in a 250 ml roundbottom flask with enough water to bring the level about two thirds of the way to the top. The dissolution and reaction cooled the mixture substantially. The flask was connected to an empty fractionation column, transfer tube, cold water condenser, and receiving flask, which contained enough 1M sulfuric acid to absorb the ammonia released, and the system was evacuated through an adapter tube and then closed off. The roundbottom flask was heated in a water bath and stirred with a magnetic stirrer, while the solution in the receiving flask was stirred. When the mixture in the roundbottom became a pasty solid, it was removed to a beaker, placed in a vacuum oven, heated to about 100°C, ground to a fine powder, and heated in the vacuum oven again to 200°C. for 16 hours. It did not discolor. Lithium and calcium halides were also dried *in vacuo* at 200°C.

for 16 hours.

Ammonium, tetrabutylammonium, and potassium thiocyanates were dried *in vacuo* at 100°C. for about 16 hours. Titration potentiometrically with silver nitrate confirmed their equivalent weights. Titration of the methanolic solution of the tetramethylammonium hydroxide with standardized acid established its equivalent volume. Titration of the partially hydrated cesium hydroxide established its equivalent weight.

About 0.5 mole of tetramethylammonium thiocyanate was prepared by mixing a 1.5 mole percent excess of methanolic tetramethylammonium hydroxide with ammonium thiocyanate in a 250 ml roundbottom flask. The flask was connected to an empty fractionation column, transfer tube, cold water condenser, and receiving flask, which contained enough 1M sulfuric acid to absorb the ammonia released, and the system was evacuated through an adapter tube and then closed off. The roundbottom flask was heated in a water bath and stirred with a magnetic stirrer, while the solution in the receiving flask was stirred. When the mixture in the roundbottom became a pasty solid, it was removed to a beaker, placed in a vacuum oven, heated to about 100°C, ground to a fine powder, and heated in the vacuum oven to 155°C. for three days before potentiometric titration showed that the water had finally been removed. The salt showed a minor amount of discoloration.

In a similar fashion, about 0.56 mole of cesium thiocyanate was prepared in aqueous solution from cesium hydroxide (solid, with about 20 weight percent water) with a 2 mole percent excess of ammonium thiocyanate. The cesium hydroxide was added to the 250 ml roundbottom flask with about 150 ml. of water and allowed to dissolve and cool in an ice bath. The ammonium thiocyanate was then added to this cooled solution to avoid rapid reaction and boiling. The solid recovered from the flask after evaporation was ground to a fine powder and dried overnight in the vacuum oven at 120°C. Heating at a higher temperature was found to be unnecessary and even caused some melting and decomposition.

Cesium triflate was prepared by the dropwise titration of 0.16 M triflic acid into a 1.6 M solution of cesium carbonate. The end point of the reaction was detected by removing a drop of liquid from the solution and testing it on a spot plate versus bromocresol green. The product was recovered and dried under vacuum for 24 h at 125°C.

The aluminum chloride was distilled in the dryroom at an average relative humidity of 2% at 70°F., at 120 to 150°C. and at atmospheric pressure in a Pyrex sublimator from molten lithium tetrachloroaluminate over calcium turnings. The vapor crystallized as pure white flakes and plates on the outside surface of the sublimator condenser while the condenser was being cooled with dry ice. Transfer of the crystallized product to sealed containers was carried out in the dryroom.

Lithium tosylate was prepared by addition of p-toluene sulfonic

acid to suspension of Li_2CO_3 in water. When the pH was neutral, the solution was boiled to reduce the volume; the solid which precipitated was recrystallized from water and then dried under vacuum.

Trimethylsulfonium triflate and dimethylphenylsulfonium triflate were prepared by the method of Badet and Julia [11]. In the case of trimethylsulfonium triflate, 10 ml methyl sulfide, 15 ml anisole and 12 ml trifluoromethane sulfonic acid were added to 25 ml methylene chloride in a 250 ml roundbottom flask. The mixture was allowed to stand at room temperature for 5 days. The product was precipitated by gradual addition of toluene accompanied by vigorous shaking. The liquid was decanted off from the resulting solid. The solid was first air-dried, then dried under vacuum at room temperature. Dimethylphenylsulfonium triflate was prepared analogously, with thioanisole used in place of methyl sulfide. Trimethylsulfonium bromide was prepared by addition of a solution of trimethylsulfonium triflate in acetone to a solution of LiBr in acetone; the sulfonium bromide salt precipitated immediately. It was filtered and dried under vacuum.

Tetramethyl- and tetraethylammonium sulfite were prepared by dissolving sodium sulfite and the tetraalkylammonium bromide together in water. The solution was boiled to reduce the volume. The solid which formed on cooling was recrystallized from water and dried overnight under vacuum at 50°C.

Guanidine hydrobromide, $H_2N^+=C(NH_2)_2 \cdot Br^-$ or $H_6(N_3C)^+Br^-$, was prepared by neutralization of a suspension of guanidine carbonate in water with the appropriate amount of concentrated HBr. The resulting solution was boiled to reduce the volume. The solid which precipitated was recrystallized from dilute aqueous HBr or methanol/ methylene chloride and dried under vacuum at 50°C overnight.

Pentasubstituted guanidine derivatives were prepared starting with tetramethyl guanidine (Aldrich) by reaction with alkyl bromides and iodides in benzene (slowly dropping the tetramethylguanidine into the hot benzene/ excess alkyl halide mixture), followed by crystallization from methylene chloride, acetone, ethyl acetate, or mixtures of these solvents. Hexasubstituted derivatives were prepared by reacting pentasubstituted halide salts in methanol with a 95% stoichiometric amount of lithium methoxide, followed by fractionation with benzene to remove methanol, filtration of the pot residue to remove all but the guanidine/ benzene solution, and reaction with a 15% excess of alkyl chloride or bromide in benzene at room temperature, which produced pure white crystals.

N-methylpyridinium chloride and hexamethylenetetramine·CH_3Cl were likewise prepared by the equilibration of methyl chloride with pyridine or hexamethylenetetramine in benzene solution at room temperature over a period of several weeks. The halide equivalent weights of the products were checked by argentimetric titration.

Tetrahydrofuran (THF) was first shaken together with an aqueous solution of ferrous sulfate to destroy peroxides. The ether was predried with calcium chloride, and was then fractionally distilled over phosphorus pentoxide using a Berl porcelain saddle column. The THF was stored in a sealed flask in the dry room and was used within a few days after distillation.

The acetonitrile was fractionated on a two foot Berl saddle column until infrared spectra showed that the solvent could not be further dried. The propylene carbonate was fractionated on a similar column during vacuum distillation, using the same criterion. The 1,2- dimethoxyethane (analyzed reagent) was used as received.

The chloroacetyl chloride and sulfuryl chloride were purified by fractionation from a solution of lithium tetrachloroaluminate, using a Berl saddle column. The bromine was used as received.

SOLUBILITY TESTS

The solubility test solutions were prepared by grinding dried salts in a glass mortar and pestle and by weighing into the bottom of a 7 ml Savillex (Teflon) vessel. The vessel was then charged with liquid sulfur dioxide from a pressurized 100 ml Savillex vessel to a final volume of 5 ml. In cases where the reactivity of lithium was tested, a clean piece of Li was added carefully to the vial after the SO_2 had been added, and the mixture was checked for dangerous reactivity before the vial was sealed. The threads of the 7 ml vessel were wrapped with Teflon tape and the vessel was sealed shut. The solution was then agitated in order to dissolve as much of the salt mixture as possible. The agitation time was always at least 20 minutes beyond the time taken for the solution to reach room temperature. The vials were allowed to stand overnight or for several days.

ELECTROLYTES

Electrolyte solutions were prepared in the dryroom hood at a relative humidity of 2% or less at 70°F. by weighing dried salts, transferring to 100 ml Savillex Teflon pressure vessels containing magnetic stir bars, and then by directly adding liquid sulfur dioxide slowly. The sulfur dioxide was condensed in a 100 ml volumetric flask by leading SO_2 vapor into it through a 10 ml pipette. The volumetric was cooled in a small Dewar flask containing dry ice/ isopropyl alcohol. The liquid sulfur dioxide was allowed to cool practically to the temperature of the dry ice mixture before it was added to the Savillex vessels. Even so, by boiling, the SO_2 displaced the air from the vessel during the addition of the solvent. Once filled to the mark with the sulfur dioxide, the vessels were capped and tightened. Each top had a Teflon valve with a fitting through which the vessel could be connected to the cell filler.

Tetrachloroaluminate/ sulfur dioxide solvates were also prepared

in the dryroom hood. First, enough dried LiCl/ $CaCl_2$/ NaCl and distilled $AlCl_3$ were weighed, sufficient to prepare 120 ml of the desired sulfur dioxide solvate. The salts were transferred to a 250 ml roundbottom flask, and dried according to a previously described procedure [8]. Sulfur dioxide gas was then led into the roundbottom using a hose to 24/40 adapter and vacuum distillation adapter, which led to an oil filled bubbler to allow the regulation of the gas so that it was not added faster than it was being absorbed. The salt mixture quickly absorbed the gas, even at room temperature, forming a warm, light tan solution. The stirrer kept the solution agitated until the requisite weight of sulfur dioxide had been added, or until the solution no longer accepted sulfur dioxide vapor at room temperature. Liquid sulfur dioxide was <u>not</u> added to the glass roundbottom, to avoid having the pressure increase beyond one atmosphere. Solids suspended in the solution, present apparently as the result of the drying procedure, were then allowed to settle. The solution was decanted at ambient temperature and pressure into a 100 ml Teflon Savillex pressure vessel, and capped.

One molar $LiAlCl_4$/ two molar acetyl chloride in sulfur dioxide was prepared in the dryroom hood by adding lithium chloride and aluminum chloride into a glass roundbottom and drying them [8]. The salt mixture was dissolved by first adding sulfur dioxide gas, then the requisite amount of purified chloroacetyl chloride. The solution was transferred to a 100 ml Savillex Teflon pressure vessel containing a magnetic stir bar, and then liquid sulfur dioxide was directly added, as described above.

The electrolytes containing bromine, chloroacetyl chloride, and lithium tetrahaloaluminate were prepared several different ways. If the salt was $LiAlCl_4$, lithium chloride and distilled aluminum chloride were dried [8]. The salt mixture was dissolved in the requisite amount of distilled chloroacetyl chloride in order to make 50-100 ml of solution in a 100 ml Savillex vessel. Portions of this "stock" solution were then used with bromine to make 4-10 ml electrolyte batches. No attempt was made to remove hydrolysis products from solutions of $LiBr \cdot AlCl_3$, beyond using the dried lithium bromide and the distilled aluminum chloride. Solutions of $LiAlBr_4$ were made by adding 99.999% aluminum as 330 mg nuggets to distilled acetyl chloride containing a slight excess of lithium bromide and enough bromine to supply both the soluble cathode and the required bromide for the aluminum. The aluminum was attacked and dissolved during a steady if somewhat vigorous reaction.

The infrared spectra were run on a Perkin Elmer model 137 spectrophotometer. A type I 10 mm pathlength quartz cell containing the sample, transferred to the cell in the dryroom, was placed in the sample port and run versus an identical empty cell. Because of the limited transmittance of the quartz, the machine did not respond at wavelengths longer than 4.5 microns. Solution spectra were also run in demountable cells with sodium chloride windows, using 0.1mm spacers, between 4,000 and 660 cm^{-1}.

AA SIZE CELLS

All of the AA size screened electrode cells, with the exception of those with reference electrodes, shared the following characteristics:

Cases:

Hermetic, size AA, 304 stainless steel, with 52 alloy feedthrough/ filler tubes, annealed soft; capable of being cold welded.

Dimensions, 0.5" O.D. x 1.875" long; 6.03 cm^2.

Polarity: case negative

Negatives:

3.5" x 1.5" x 0.015"; solid Li; 2.66 Ah.

Positives ("standard" form):

3.00" x 1.5" x 0.023"

25 weight % Ketjenblack; 75% Chevron acetylene black; Teflon binder 5 or 10% by weight of carbon present; average weight of positive material, 0.4 to 0.56g.

Common electrode area ("standard" form):

58.1 cm^2

Cell void volume, all components present except electrolyte: about 4.0 ml, measured as the maximum amount which cells would accept from the graduated syringe. "Calculated" values appearing in the tables were found from the weight of the electrolyte added, assuming that the electrolyte density was 1.4 g/cm^3. Electrolytes containing cesium bromide in particular may have been significantly denser.

Variations between cells were as follows.

Negatives:

1. Electrical contact was a single strand of nickel ribbon pressed diagonally across the lithium.
2. Electrical contact was a nickel tab, to which was welded nickel expanded foil screen, only as wide as the 3/32" tab. The end of the lithium foil was wrapped once around the tab and rolled down to cover completely the nickel contact.
3. The length was varied from 1.88 to 3.75 inches (1.70 to 2.65 Ah), depending upon the thickness of the positive electrode.

Separators: one layer each of either

1. Craneglass 0.007" nonwoven Pyrex fabric, 5% polyvinyl alcohol binder
2. Scimet type 200/60, 60% microporous Tefzel; 0.002"
3. "Hovosorb" #B605298 (Hollingsworth and Vose), binderless Pyrex fabric, 0.005" to 0.008"
4. "Fluortex", either 9-PFK-590 (coarser) or 9-210/46, type 906 (finer) Tefzel screening (Tetko, Inc.) placed next to negative; Rayperm type 200/60, 60% microporous Tefzel, 0.002", placed next to positive.
5. Gelman Sciences microporous PVC film, 0.008" thick; "Lot 303"

Positive electrodes:

Dimensions: In "regular" length positives, the carbon was scraped away from 0.375" of the length to provide a

purchase for the mandrel to roll the electrodes together. Net common electrode area, 50.8 cm^2. In "increased surface area" positives, the total length was 3.5", for a net common electrode area of 60.5 cm^2. Positives varied in length from 1.88 to 3.75 inches (36.4 to 72.6 cm^2), depending upon the thickness. Individual thicknesses, loadings, and weights are shown in the tables.

"Wet rolled" process: The carbon mix was blended with a 50/50 mixture of isopropyl alcohol and water. While stirring, DuPont Teflon suspension was added. The carbon mix was then rolled on to expanded foil screens, allowed to air dry, and cured at 280°C. for 15 minutes

"Dry pressed" process: Carbon/ Teflon/ 50:50 water: isopropanol mixture from the above process was extruded through a multifaceted die to increase the surface area and allow rapid air-drying. The mixture was then cured at 280°C. for 15 minutes, cooled, and chopped to a fine powder in a blender. A steel die 14" x 1.75" was used to prepare a sheet from which several positives could be cut. Equal amounts of cured carbon mixture were weighed for each side of the positive electrode screen. The carbon was distributed as evenly as possible. The die was placed in a hydraulic press between 800 and 4,000 lbs/ in^2.

"Flooded" electrode AA size cells had each a single flat piece of positive electrode, 1.5 x 3/8 x 0.023", which fit inside cylindrical anodes cold welded to the inside of the stainless steel cases and covered by one layer of the "Hovosorb" separator. The positives were suspended only by aluminum tabs welded to the feedthrough/ fillports.

Wound electrode AA cells used with electrolytes containing bromine were similar, except the positive electrode substrates were nickel or graphite fiber as well as nickel screen.

Positive electrode composition: Varied considerably, according to the information included with the tables.

Positive electrode support screens (expanded metal foil):

1. 5 Al 10-125
2. 5 Al 10-125 anodized in 50/ 50 isopropyl alcohol, 0.2M NH_4HCO_3, to 160 mV positive of a Ag/AgCl/0.1M KCl/ salt bridge/ indicating electrode
3. Same as 2., anodized to +200 mV
4. 5 Ni 10-125
5. 5 Ti 10-125
6. 4 (Inconel 600) 7-077. Inconel = 76% Ni, 15.5% Cr, 8% Fe, 0.5% Mn
7. 4 Zr 10-12

Positive electrode support tabs:
(occasionally varied from support screen material)

Electrical feedthroughs:

1. 52 alloy hollow tube was used both as the fillport and the positive electrode contact.

2. Solid tantalum wire feedthrough in glass-to-metal seal; glass-to-metal seal at the other end of the cell case contained 52 alloy fillport cathodically protected against the cell case.

Electrolytes:

1. 0.85M LiBr; 21.5 v/o CH_3CN; 6.5 v/o $C_3H_6CO_3$; 13.8 M SO_2 ("control" electrolyte)
2. 4M NH_4SCN; 1M LiSCN; 16.25 M SO_2 (clear light yellow solution; all salts dissolved)
3. 3M NH_4SCN; 1M LiSCN; 17.55 M SO_2 (clear light yellow solution; all salts dissolved)
4. 2M NH_4SCN; 0.5M LiSCN (two liquid phases, the lighter about one third the total volume)
5. 2M NH_4SCN; 0.75M LiSCN (two liquid phases, the lighter one about 40% of the total volume, with a greater difference in density than in 4.)
6. 1M NH_4SCN; 0.1M LiSCN (clear light yellow solution)
7. 3M $N(CH_3)_4Br$; 1M LiBr (clear red solution, nearly completely dissolved)
8. 2M $N\text{-}CH_3(C_5H_5)Br$; 0.75M LiBr (clear red solution, nearly completely dissolved)
9. 2M NH_4SCN; 0.4M LiSCN; 17.7 M SO_2 (clear light yellow solution; all salts dissolved)
10. 2M NH_4SCN; 0.25M LiSCN; 17.9 M SO_2 (clear light yellow solution; all salts dissolved)
11. 2M NMe_4SCN; 0.5M LiSCN; ($\approx$ 18M SO_2); all salts dissolved, forming orange-red solution
12. 2M $N(nBu)_4SCN$; 0.5M LiSCN (viscous red solution; all salts dissolved)
13. 1M KSCN; 0.5M LiSCN; 19M SO_2 (clear light yellow solution; nearly all salts dissolved)
14. 2M CsSCN; 1M LiSCN; 15.8M SO_2 (clear yellow solution; all salts dissolved)
15. 0.85M LiBr; 21.5 vol. % 1,2- dimethoxyethane; 6.5 vol. % propylene carbonate; 14.2M SO_2
16. 0.85M LiBr; 28 vol. % 1,2- dimethoxyethane; 14.2M SO_2
17. 0.85M LiBr; 28 vol. % propylene carbonate; 14.2M SO_2
18. 0.85M LiBr; 21.5 vol. % acetonitrile; 6.5 vol. % propylene carbonate; 14.2M SO_2
19. 1M CsBr; 0.5M LiBr; (not all salts dissolved, composition of solid salt phase not determined)
20. 2M CsBr; 0.5M LiBr; 18M; 0.48 Ah/ml (slightly cloudy light yellow solution; nearly all salts dissolved)
21. 0.85M LiBr; 14 vol. % 1,2- dimethoxyethane; 14 vol. % propylene carbonate; 14.2M SO_2; 0.381 Ah/ml.
22. 1.0M LiBr; 34 vol. % 1,2- dimethoxyethane; 11 vol. % propylene carbonate; 10.7M SO_2; 0.285 Ah/ml.
23. Salts weighed to provide the following concentrations; not necessarily all soluble; SO2 was the only solvent:
    - 1.25M CsBr; 0.12M LiBr
    - 1.5M CsBr; 0.12M LiBr
    - 1.0M CsBr; 0.12M LiBr
    - 1.25M $Cs(CF_3SO_3)$; 0.12M LiBr
    - 0.75M $Cs(CF_3SO_3)$; 0.15M LiBr

24. 5M $H_2N^+=C(NH_2)_2$ Br^-/ 0.7M LiBr; all salts dissolved in a clear red solution
25. $2LiCl \cdot CaCl_2 \cdot 4AlCl_3 \cdot 12SO_2$
26. $3LiCl \cdot CaCl_2 \cdot NaCl \cdot 6AlCl_3 \cdot 18SO_2$
27. $4LiCl \cdot CaCl2 \cdot 6AlCl_3 \cdot 18SO_2$
28. $LiCl \cdot CaCl_2 \cdot 4AlCl_3 \cdot 12SO_2$ (acid electrolyte, with excess $AlCl_3$)
29. SO_2/ 1M $LiAlCl_4$/ 2M $CH_2ClCClO$
30. $CH_2ClCClO$/ $LiAlCl_4$ or $LiAlBr_4$ or $LiBr \cdot AlCl_3$/ Br_2:
    $LiAlCl_4$ = 1M
    $LiAlBr_4$ = 1M
    $LiBr \cdot AlCl_3$ = 2M
    Br_2 = 15, 20, 30, or 40 vol %

The least expensive, lightest, and most conductive positive grid material would be aluminum, and during the tests carried out in Phase I, aluminum appeared to be superior to nickel in resisting corrosion. We had planned to investigate whether anodization of the aluminum grids (numbers 2 and 3 under "positive electrode support screens") would increase their stability, similar to what had been observed by the senior author at Mallory in 1972 during work on lithium/ sulfur dioxide primary cells, as we now explain.

The cathodes for lithium/ sulfur dioxide primary cells were prepared by mixing Shawinigan acetylene black with 50/50 isopropanol/ water and adding a small portion of Teflon suspension in water. The mixture was then rolled onto the aluminum screens, blotted, and allowed to dry. When no alcohol was included, the water in the presence of the carbon and the atmosphere completely corroded the aluminum screens by the time the water had evaporated. If only isopropanol was used with the mix during the rolling operation, the screens in the finished cathodes appeared perfectly sound, but then corroded quickly in the cells as soon as the electrolyte (SO2/ LiBr/ acetonitrile/ propylene carbonate) was added. During the rolling operation, the carbon, air, solvent mixture, and the emulsifying agents, which are electrolytes, were acting together to anodize the aluminum. If only water was present, the anodization continued until the aluminum was completely oxidized. If only alcohol was present, no anodization occurred at all. If the 50/50 solvent mixture was present and the aluminum contained about 1% iron, an electronically conductive oxide coating formed which allowed the cathodes in the finished cells to function without corroding.

If the screens were preanodized to the correct potential versus a silver/ silver chloride/ 0.1 molar potassium chloride reference electrode, using 50/50 isopropanol/ water containing a volatile neutral electrolyte salt such as ammonium carbonate, the carbon could be applied to the treated screens using only isopropanol. The cells not only functioned well, but their capacity and impedance were much more consistent.

In our present situation, the carbon/ binder mixture was pressed dry, rather than rolled wet, onto the positive electrode screens to maintain a consistent loading and thickness. The aluminum

screens therefore would not have had the benefit of a chemically produced conductive oxide layer. We therefore felt that preanodization of the aluminum screens might prove beneficial.

Cells containing "painted" positives used anodized aluminum foil, on which was applied one layer of aqueous carbon emulsion (Acheson Colloids) mixed with 10% DuPont Teflon aqueous suspension, followed by a 50/ 50 mixture of emulsion with Ketjenblack, followed by another layer of emulsion. The foil was treated briefly at 280°C. after each application of emulsion. The positives were 7" long and 8 to 12 mils thick. The common electrode area, based on the 6", 10 mil thick anode, was 116 cm^2, and the total amount of carbon per cell, about 350 mg.

AA SIZE REFERENCE ELECTRODE CELLS

The reference electrode cells were similar to the other AA size cells except the can bottoms had been machined off. In their place were glass/ metal feedthrough seals, each with circular nickel screens welded to nickel tabs, the tabs then welded to the feedthroughs. Circular pieces of lithium foil were pressed to the circular screens, and the resulting electrode placed concentrically inside the can bottom. The reference electrode was isolated from the can and from the electrode spiral, which was to be inserted into the can from the opposite end, by "Hovosorb" separator material. The feedthroughs were then TIG welded to the bottoms of the cans. In each cell, the positive and negative electrodes were each cut one eighth of an inch narrower, for a total width of 1.375", in order to leave room for the reference electrode. The positive electrode screens and tabs were 5 Ti 10-125. In each cell, the plane of the reference electrode disk was perpendicular to the axis of the electrode spiral, and spread out over nearly the entire area at the end of the spiral.

Electrolytes for AA cells with reference electrodes:

1. 1M KSCN; 0.5M LiSCN; 19M SO_2; 0.51 Ah/ml (clear light yellow solution; nearly all salts dissolved)
2. 1M CsBr; 0.5M LiBr; (not all salts dissolved, composition of solid salt phase not determined)
3. 0.5M KBr; 0.5M LiBr; (Not all salts dissolved, composition of solid phase not determined. Reported solubility of KBr alone, about 0.11M [12]).
4. 1.25M CsBr; 0.12M LiBr (complete solution).

AA CELL FILLING AND CLOSING; ELECTRICAL CONNECTIONS

An aluminum frame situated in the dryroom hood held the essential parts of the filling apparatus. The boiling points of some of the electrolytes tested were lower than ambient temperature, and so were under pressure in the storage vessels. All electrolytes were handled using the same apparatus. A thin Teflon line led from the valve at the bottom of a 100 ml Savillex vessel containing one of the electrolytes to a four-way Teflon lined Hamilton valve. The

valve was first set to allow electrolyte into a 10 ml air tight glass syringe, at the same time connecting a cell to be filled to a mechanical vacuum pump, suitably protected from the corrosive sulfur dioxide. When the syringe contained 4 ml of electrolyte, the valve below the electrolyte reservoir was closed and the four way valve turned to admit electrolyte into the cell. After the cell was filled, the fill tube was crimped just below the Teflon tube leading from the four-way valve. The cell was removed from the Teflon tube and crimped twice more to ensure that the tube had been cold welded shut. Nickel tabs were then resistance welded on to the cans, and lead wires soldered to the tabs and to the crimped tubes. The lead wires were soldered to banana plug connectors, which fit the computer terminals.

TUBE CELLS

Experimental tube cells were prepared in the dryroom from test tubes and glass disposable pipettes. Their purpose was to test positive electrodes in a flooded condition, with noble metal contacts not likely to take part in any electrochemical reactions. The boiling point of the electrolyte was higher than room temperature. Test tubes 16 mm in diameter were cut to 48 mm long, and the glass pipettes with thinned tips were 6.5 mm at the base, cut to 146 mm long. Pieces of expanded metal screen about 12 mm wide were bent into cylinders that just fit around the bases of the pipettes, and welded to metal tabs which extended past the tips of the pipettes. The assemblies were secured into the tubes with Teflon stoppers drilled with appropriate holes.

Lithium squares 8 x 8 mm x 0.120" were cut from foil 20 to 50 mils thick. The lithium disks were placed on a clean surface in the dryroom and the pipette bases were pressed into them such that the lithium was concentric with the pipette bases and sealed against the glass. 20 mil straight nickel wires were passed through the tip ends of the pipettes and imbedded in the lithium at their bases. In this way, the pipettes could be placed upside down into electrolyte inside the test tubes, the lithium and cathode both being immersed without the electrolyte touching the nickel wire anode contacts. The volume of electrolyte per cell was about 10 ml. The net area of lithium facing the cathode assembly was about 0.94 cm^2. Pressing the pipettes into the lithium expanded the surface area facing the cathode to about 1 cm^2.

Positive electrodes were constructed using metal screens fabricated from 0.020" tantalum wire, 0.003" tantalum foil, or perforated molybdenum foil (Figure 1). It was difficult to prepare cathodes with reproducible weight and consistent contact with the metal screen. To circumvent this problem, a piece of metal foil was cut to four inches long times 1/10" wide with a 8 x 12 mm area at one end. Small pieces of metal foil, 1 mm in width were spot welded to the face of the square area with the foil twisted between the welds so that they could act as a screen to hold a pressed carbon cathode. The carbon was pressed into the square

area of the metal foil. The carbon was then trimmed to fit the square area. A cathode prepared in this way was about 1 mm thick and presented an area to the electrolyte, including the edges of the pressed electrode, of about 0.96 cm2. The weight of active material was 20- 22 milligrams.

Painted positive electrodes on metal foil were prepared on a square area of 10 x 10 mm. The weight of cathode material was 2 to 3 milligrams. The painted cathodes were approximately 0.004" thick (0.007" including the substrate). The discharge load of 501 ohms provided a current density of 5 to 6 mA/cm^2. In both cases the stem of the positive substrate foil was secured to the glass pipette with Teflon tape. In order to facilitate the discharge of a tube cell the lithium electrode was increased in thickness to 0.120". A lithium reference electrode identical in design to the anode was constructed and placed adjacent to the cathode with the two glass pipettes secured to each other with Teflon tape.

Electrolyte for tube cells with and without reference electrodes:

1.7M LiBr; 43 vol. % 1,2- dimethoxyethane; 13 vol. % propylene carbonate; 8.1M SO_2; 0.22 Ah/ml.

The tube cells were cycled using the computer or discharged through a constant load and monitored with a strip chart recorder.

BUTTON CELLS

The button cells were 13/16" in diameter times 1/16" thick, the cans and covers made from 304 stainless steel. Calculations showed that the entire volume of the can was 0.531 cm^3. The cans were lined with tantalum to prevent participation of the stainless steel in electrochemical reactions. Disks were cut from 3 mil tantalum foil, using the lathe to prevent the formation of creases or burrs in the foil, so that the disks just fit inside the cans. Tantalum screens prepared by welding twisted narrow strips of tantalum foil to the disks held the pressed carbon material in the cans.

The positive electrode material for the pressed electrodes was the same 25%/ 75% carbon mixture used for the AA cells. One hundred milligram portions of the carbon/ Teflon mixture were compacted with a die into the cell cans, using a hand press. The die had a collar which prevented the carbon from extending to the edges of the cans and interfering with the gaskets, which were press fitted to the cell covers and sealed with a halocarbon grease. The gaskets were Tefzel (ethylene tetrafluoroethylene copolymer), machined from a rod to fit the covers.

The button cell cans containing the painted cathodes were prepared with a mixture of isopropyl alcohol, 25/ 75 carbon mix, and Hostaflon (Höchst), a suspension of ethylene/ tetrafluoroethylene

copolymer in water. The carbon/ Hostaflon/ isopropanol mixture was applied to the Tantalum inserts using a small paintbrush. The mixture was allowed to air dry followed by curing at 250°C for 15 minutes. This procedure was repeated five more times until the substrate was occluded from view by the carbon. Electrodes prepared by painting were not more than 0.010" thick.

Lithium disks just wide enough to fit into the base of the covers were cut from 0.020" foil (14.5 mils needed for the required volume) and pressed into the covers with a polypropylene die using a hydraulic press in the dryroom. The volume of the lithium, 0.103 cm^3, represented 254 mAh. It was intended that the lithium would be cold welded to the stainless covers and be extruded far enough towards the edges to seal against the gaskets, which were pressed on to the covers after the lithium was in place. Later, it was found to be more convenient to place lithium over the stainless steel cover, then put the gasket in place before pressing the lithium to the cover to create the cold weld. This provided an improved occlusion of the stainless steel cover from the electrolyte.

The cans, with the carbon mixture pressed or painted on, and Craneglass Pyrex nonwoven fabric disks cut from 0.007" sheet to the same diameter as the cathodes, were dried at 150°C. for two hours in an oven inside the dryroom. The cans were transferred to the dryroom hood and placed on the base of the hand press. The separators were positioned and the cells filled with electrolyte, using a dried glass disposable pipette. The boiling point of the electrolyte used for the button cells was above room temperature. The covers were positioned and the cells crimped shut. The crimping tool touched only the can, to avoid short-circuiting the cell.

Electrolyte for button cells:
1.7M $N(C_2H_5)_4Br$; 43 vol. % 1,2- dimethoxyethane; 13 vol. % propylene carbonate; 8.1M SO_2; 0.22 Ah/ml.

THIN WALLED D WIDTH WOUND CELLS

Cylindrical cells measuring 1.25" O.D. x 0.625" tall contained wound electrodes about 12" long, the surface area in common being about 115 cm^2. The reason for constructing these cells was because D size tops with tantalum electrical feedthroughs and 52 alloy fillports were immediately available. Using tantalum feedthroughs in place of the 52 alloy tubes for the positive electrode contacts would prevent iron and nickel from entering the electrolyte by corrosion of the tubes. The positive electrode collectors were 5 Al 10-125 screens, anodized in 50/ 50 isopropyl alcohol, 0.2M NH_4HCO_3, to 160 mV positive of a Ag/AgCl/ 0.1M KCl/ salt bridge/ reference electrode.

AA CELL CYCLING TESTS

All AA size cells except those with reference electrodes were tested using the computer controlled cycler, with the following parameters:

Discharge/ charge constant currents: variable, not greater than 1 $mA \cdot cm^{-2}$/ 1 $mA \cdot cm^{-2}$ of common electrode area (36 to 73 mA)
Discharge/ charge time limits: variable; not longer than 20 h/ 20 h
Discharge/ charge potential limits: 2.0 V/ 4.0 V
Rest after discharge/ rest after charge:
10 minutes/ 10 minutes
Temperature range: 19 to 25°C.

The tests were conducted within the building, but in a brick-walled safe room with one outside wall. A ventilator was capable of removing gases from the room within a few minutes. The power supplies had separate current leads and potential sensing leads to correct for IR drop within the 100 foot shielded cable between the computer and the test area. The cells were started on "rest after charge" to establish a record of the initial open circuit potentials.

The potentiostatic and galvanostatic measurements were performed with AA size cells located in the same safe room, and with similar cables allowing two sets of leads for each cell. The cells were the same as the AA size cells described above, except that no carbon was present on the nickel positive electrode screens. Figure 2 shows the schematic for the polarization measurements. The first channel of the Yokogawa model 3021 dual channel recorder measured the current by keeping track of the potential across a standardized carbon resistor of about ten ohms. The Electrosynthesis model 410 potentiostat, which included its own reference input circuit, was set at incremental values either anodic or cathodic to the rest potential of the screen with respect to the lithium electrode, and the current read on the first recorder channel. The potential between the reference and the working electrode at the potentiostat was unavoidably affected by the current, but the second recorder channel measured the potential across the cell without interference from current through the leads. The input impedance for each recorder channel was one megohm, and the input differential amplifiers allowed the measurement of potential difference without interference from current leakage to ground.

Figure 3 shows the similar circuit used to measure lithium plate/ strip efficiencies. The circuit now includes a Harrison Laboratories model 855B constant current power supply. The same AA cells with positive electrode screens without carbon were used, so that lithium was being transferred from the solid metal negative electrodes to nickel screens, not to foil electrodes or to electrodes with thin layers of lithium on metal substrates as in previous studies involving sulfur dioxide solutions of tetra-

chloroaluminate salts [2]. Lithium was transferred to the nickel screen for various amounts of time at a current density of about 1 mA/ cm^2 of solid lithium surface, then stripped immediately at the same current. The potentiostat was appropriately set to divert only anodic current from the constant current power supply, and then only when the potential of the nickel screen reached 0.5 volts anodic to the lithium foil. The efficiency was calculated by dividing the time required for stripping the electroactive deposited lithium by the time required for plating.

AA REFERENCE ELECTRODE CELL TESTS

The first AA reference electrode cells were discharged using a constant load of 100 ohms and a two channel strip chart recorder to monitor both the cathode versus the reference electrode and the cathode versus the anode, as shown in Figure 4. The cathode was connected to the negative input of each channel, and via the 100 Ω resistor to the anode, which was connected to the cell can. The cell can was connected to the positive input of the first channel, and the lithium reference electrode disk was connected to the positive input of the second channel.

Figure 5 is a schematic diagram of the electrical connections used for the second series of reference electrode cell tests. Three cycler power supplies were connected as shown, in order to monitor all three possible potential differences: the cell potential (lithium versus carbon), the reference versus the carbon, and the reference versus the lithium. This time, cells were cycled at constant current, just as were the other AA cells. The first power supply carried the discharge and charge currents, while the other two were used only as recording voltmeters. These two supplies were set on "rest after charge" for a period of time exceeding the length of the test. To prevent short circuits between the power supplies, the negative power carrying leads in the second and third supplies were disconnected. As shown in Figure 5, the reference electrode was connected to the negative inputs of the second and third power supplies. Because the power supplies were capable of reading only positive potentials, the readings for the reference versus the anode were taken only during the discharge half cycles.

CORROSION STUDIES

Both lithium/ negative hardware and carbon/ positive hardware were tested by immersing samples in each of the electrolytes, using 4 ml Savillex Teflon vials with gas tight tops. Pieces of lithium were pressed on to nickel screens, which had been welded to nickel tabs, in turn welded to samples cut from AA cell cases. 20-50 milligram samples of the carbon mixture were pressed to samples of the positive screen material to be tested, to which had been welded samples cut from the feedthrough tube stock. These assemblies were kept in an oven in the dryroom at 150°C. for 2 hours, then transferred to the 4 ml Savillex vials. The 100

ml vessels containing the electrolyte samples were inverted over the 4 ml vials, and about 2 to 3 ml of electrolyte allowed to enter the smaller vials through the valves. The caps were secured to the 4 ml vials before very much of the sulfur dioxide had boiled away.

The vials, although not transparent, were clear enough to observe changes in the color and clarity of the electrolyte, and any drastic changes in the appearance of the solid samples. At the conclusion of the tests, the vials were opened in the laboratory hood, the solid samples washed with water and blown dry, and the metal surfaces examined at once under the optical microscope. The electrolyte samples were hydrolyzed as a quick test to determine whether any obvious reactions had occurred during the storage period (all substances should have been soluble, although aqueous solutions of thiocyanate and sulfur dioxide are yellow).

CYCLIC VOLTAMMETRIC ANALYSIS

Corrosion studies were also carried out on a more quantitative scale using cyclic voltammetry. The absolute corrosion rates were measured by the technique of Polarization Resistance (or "Linear Polarization") and from Tafel slopes, which provide a direct measurement of corrosion currents (i_{corr}). The corrosion current, in turn, can easily be correlated to corrosion rate, expressed in milli-inches per year (mpy). Cyclic voltammetry studies and corrosion rate measurements were carried out using a PAR Model 273 potentiostat/ galvanostat in conjunction with a Hewlett-Packard/ Moseley Model 7001A X-Y recorder. The applied waveforms (the potential-time relationships) were varied in order to cover the potential range of interest (between the OCP and Li redox potential) and to record the currents approaching the steady tate conditions. Unless otherwise stated, delay 1 (D_1) was 120 sec., cathodic sweep rate (S_1) was 5mV/sec., delay 2 (D_2) 10 sec. and anodic sweep rate (S_2) 5 mV/sec.

The Savillex Teflon pressure vessel assembly served as a three-electrode electrochemical cell. The working electrodes consisted of 0.25 inch rods of the metal or alloy to be tested, each inserted into the 0.25 inch side port of a 100 ml Savillex vessel. A typical exposed geometrical surface area was 2 cm^2. Reference and counter electrodes were lithium foil cold welded to Kovar wires sealed into 0.25 inch hollow glass rods, inserted through fittings located in the middle of threaded caps at either end of the 40 mm I.D. barrel of the 100 ml Savillex Teflon vessels. The vessels were supported in a vertical position so that the side port holding the metal sample was at the lower end of the barrel and the glass rods holding the reference and counter electrodes were vertical. The required electrolyte salt and liquid SO_2 were admitted to the vessel with the upper cap removed, and the cap then replaced and tightened.

The electrolyte used in the voltammetric corrosion analyses was a mixture of CsBr (0.25M - 1.677M) and LiBr (0.09M - 0.58M) in SO_2.

As a result of the solubility studies, the electrolyte used contained LiBr concentrations between 0.09M and 0.134M. In an evaluation of the experimental set-up, 1.0M $LiAlCl_4$ in 60 parts of SO_2Cl_2 and 40 parts of $SOCl_2$ were used because of the simplicity in handling (boiling point above ambient temperature).

CHAPTER 3.

RESULTS AND DISCUSSION

"CONTROL" CELLS: ACETONITRILE/ PROPYLENE CARBONATE/ LITHIUM BROMIDE

Table 1 summarizes the cell data and primary discharge capacity for cells which contained the organic electrolyte, 0.85M LiBr with 21.5 volume percent CH_3CN and 6.5 volume percent $C_3H_6CO_3$, the balance being sulfur dioxide, about 13.8 molar. This formulation is similar to the electrolyte used in lithium/ sulfur dioxide primary cells. The purpose of the test was to determine whether carbon cathodes, prepared as we did them from dried pressed powder, would function effectively in a lithium/ sulfur dioxide cell.

TABLE 1. Capacity of AA cells containing 21.5 v/o CH_3CN/ 6.5 v/o $C_3H_6CO_3$/ 0.85 M LiBr/ 13.8 M SO_2

Cell #	Separator	Positive contact scrn.	tab	Electrolyte Salt	Conc.	Approx. vol(ml)	Other	Dischg. Capac., mAh	Fig. #'s
37-54-2	Tefzel	adz.16V Al	Ni	LiBr	0.85 M	3.4	PC/AN= 3/10	159	6
37-54-6	Pyrex	adz.16V Al	Ni	LiBr	0.85 M	3.87	PC/AN= 3/10	450	
37-62-1	Pyrex	adz .2V Al	aAl	LiBr	0.85 M	3.91	PC/AN= 3/10	1,250	
39-39-2	Tefzel	adz .2V Al	aAl	LiBr	0.85 M	3.74	PC/AN= 3/10	1,267	7
39-39-4	Pyrex	adz .2V Al	aAl	LiBr	0.85 M	3.6	PC/AN= 3/10	1,093	

Cells with aluminum screens anodized to +160 mV versus the Ag/ AgCl reference electrode ran flat at about 2.75 volts, while those with screens anodized to +200 mV dipped below 2.6 volts during the first three hours, then ran at about 2.8 volts. Those with nickel tabs between the cathodes and the feedthrough tubes showed low capacity and their discharge ended abruptly, while those whose aluminum cathode tabs were connected directly to the feedthrough tubes gave more than one amp hour. By way of example, Figure 6 shows the discharge/ charge profile for cell 37-54-2, and Figure 7 for cell 39-39-2.

When cells 37-54-2 and 37-54-6 were opened, the nickel connecting tabs were found to have been completely corroded away. The remaining cells, in which the aluminum tabs were successfully welded directly to the feedthrough tubes, showed that the nickel connectors were unnecessary. When cell 37-62-1 was opened, no

internal pressure was encountered. The aluminum screen and tab were not visibly affected, but the feedthrough tube was tarnished with an easily removed black deposit. This amount of corrosion evidently did not affect the operation of the cell over the 25 hours or so that it was being tested.

The data demonstrated that carbon electrodes made by pressing dried powdered cathode mixture on screens make effective dithionite cathodes. We had therefore established that if we were to encounter poor performance in lithium salt/ cosolute electrolyte cells, the poor performance would not have resulted from badly designed positive electrodes.

THIOCYANATE ELECTROLYTES

Corrosion tests. The results of the corrosion tests involving thiocyanate electrolytes in the 4 ml Savillex sample vials are summarized in Table 2. The notation "uaAl" refers to unanodized aluminum, "aAl$^{\text{superscript}}$" to anodized aluminum and the potential to which it was anodized in 50/50 isopropanol/ water, "Inc" to Inconel 600, and "AA" to a section cut from a 304 stainless steel AA size cell can. The "/" marks indicate that the components in the sample tested were electrically connected.

TABLE 2. Corrosion Tests in Thiocyanate Electrolytes. Samples Biased with Lithium or Carbon at Ambient Temperature in 4 ml Savillex Gas Tight Teflon Vials.

	Electrolyte			Storage	
Sample	LiSCN	(R)SCN	R=	time	Result
Li	1 M	3 M	NH_4^+	10 days	No tarnish or corrosion, some elect.-insol. solid
Li	1 M	4 M	NH_4^+	9 days	No tarnish or corrosion, some elect.-insol. solid
Li	0.5 M	2 M	NH_4^+	6 days	No changes
Li/Ni/AA	0.5 M	2 M	NH_4^+	10 days	Electrolyte a deeper color, minor amount of H_2O-insol. solid after hydrolysis
uaAl/C	1 M	4 M	NH_4^+	1 day	No tarnish, some pitting
Ni/C	1 M	4 M	NH_4^+	1 day	Obvious tarnish, minor corrosion
Ti/C	0.5 M	2 M	NH_4^+	4 days	No changes
Inc/C	1 M	3 M	NH_4^+	3 days	No tarnish or corrosion; minor cloudiness
Inc/C	1 M	4 M	NH_4^+	3 days	No tarnish or corrosion; minor cloudiness
Inc/C	0.2 M	2 M	NH_4^+	2 days	No changes
Ti/C	0.2 M	2 M	NH_4^+	2 days	No changes
Ti/C	0.5 M	1 M	K^+	38 days	No changes
Li/Ni/AA	0.5 M	2 M	NMe_4^+	--	Immediate rapid reaction; red color in solution
Li/Ni/AA	0.5 M	2 M	$N(nBu)_4^+$	--	Slow reaction evident

The corrosion tests indicated that lithium in contact with cell hardware and LiSCN/ NH_4SCN/ SO_2 at the same time should be stable at least for short cell discharge tests. The corrosion tests also suggested that the cathode contact support hardware could be chosen from either aluminum, titanium, or Inconel 600. However, lithium and anode contacted hardware were found to be incompatible with electrolyte containing substituted ammonium ions. We suspected at that time that ammonium cations may also have been interacting with lithium and anode contacted hardware in unfavorable ways which were not evident from the limited corrosion information we had obtained.

We then considered widening the study to include alkali thiocyanates to accompany LiSCN, to provide salts where the cation could not be reduced by lithium. Table 3, containing information first compiled by Jander [12], compares the approximate molar solubilities of various salts in liquid sulfur dioxide. The available information was very limited. Initially, we had not considered using potassium thiocyanate because the reported solubility in sulfur dioxide was only about 0.63 molar. Since potassium thiocyanate was more soluble than sodium thiocyanate, the possibility existed that cesium thiocyanate would have a solubility high enough to act as a reasonable cosolute for lithium thiocyanate. Because we felt that the expense of the cesium salt would preclude its use in a practical rechargeable lithium cell, potassium thiocyanate was also considered as an alternative, less expensive cosolute. Its solubility was higher than 1M at ambient temperature.

TABLE 3. Approximate Molar Solubilities of Various Inorganic Salts in Liquid Sulfur Dioxide (after [12]). 100g SO_2 ≈ 76.9 ml. at 0°C.

	f.wt.	Solubility, g/100g liq.SO_2	salt density (g/ml)	vol. of salt in 100g liq.SO_2	Approx. solubility, M/l. 0°C.
NH_4SCN	76.12	46.89	1.305	35.93	5.46
KSCN	97.18	4.879	1.886	2.587	0.631
NaSCN	81.08	0.653	(≈1.5)	0.43	0.104
KBr	119.01	0.976	2.75	0.355	0.106
NaBr	102.91	0.014	3.2	0.004	0.00177
LiBr	86.84	0.052	3.464	0.015	0.00778

AA size cell tests. Table 4 summarizes the results of cycling tests for cells containing thiocyanate. Shown are the separator material, the metals used for the cathode screens and tabs, the composition of each electrolyte and the approximate volume of electrolyte present in each cell, and the capacity in milliamp hours for up to the first three cycles. The term "uaAl" refers to aluminum positive electrode support screen which had not been anodized, and "aAl" to support screen which had been anodized in isopropanol/ water/ 0.2M ammonium carbonate to +.160 millivolts

TABLE 4. Capacity of AA cells containing lithium thiocyanate with cosolute thiocyanates in liquid sulfur dioxide

Cell #	Separator	Positive contact scrn.	tab	Electrolyte: Li^+ conc (moles/l)	$(R)^+$ conc.	Approx. volume (ml)	(R)=	Discharge capacity, mAh pri.	sec.	3rd	Figure numbers
37-48-2	Pyrex	aAl-2V	Ni	1	3	3.89	NH_4^+	67.5	33.3	25	8
(Cell was aspirated to remove air. All subsequent cells were vacuum pumped)											
37-53-2	Pyrex	Al	Ni	1	4	3.71	NH_4^+	104.2	33	12	
37-53-5	Tefzel	Al	Ni	1	4	3.67	NH_4^+	127.5	would not charge		
37-54-1	Tefzel	aAl-16	Ni	1	4	3.35	NH_4^+	98.3	would not charge		
37-54-5	Pyrex	aAl-16	Ni	1	4	3.80	NH_4^+	192.5	35.8; maintained open circuit potential		13
37-57-1	Tefzel	Inc	Ni	1	3	2.69	NH_4^+	112.5	45	25.8; exploded during charge	
37-57-2	Tefzel	Inc	Ni	0.5	2	4.12	NH_4^+	163.3	29.2; would not maintain o.c.p.		
37-57-3	Pyrex	Inc	Ni	1	3	3.97	NH_4^+	206.7	58.3		9
37-57-4	Pyrex	Inc	Ni	0.5	2	3.97	NH_4^+	277.5	38.3; maintained open circuit potential		10
37-62-2	Pyrex	aAl-2V	aAl	0.5	2	> 3	NH_4^+	232	81.7		
37-66-1	Tefzel	Inc	Inc	0.1	1	4.0	NH_4^+	167.5	59.2	25	
37-66-3	Pyrex	Inc	Inc	0.1	1	4.0	NH_4^+	149.2	30	15	
37-69-1	Pyrex	Ti	Ti	0.75	2	3.66	NH_4^+	193.3	71.7		11
37-69-3	Tefzel	Ti	Ti	0.75	2	3.95	NH_4^+	145.8	30	20.8	
37-66-2	Tefzel	Inc	Inc	0.1	1	1.53	NH_4^+	refused to run; ocp=2.95V			
37-66-4	Pyrex	Inc	Inc	0.1	1	4.0	NH_4^+	78.3	28.3	5.8	12
37-54-3	Tefzel	aAl	Ni	0.5	2	--	$N(nBu)_4^+$	35	refused to cycle		
37-54-8	Tefzel	aAl	Ni	0.5	2	--	$N(nBu)_4^+$	23.3	refused to discharge		
37-53-3	Crane	naAl	Ni	0.25	2	4.13	NH_4^+	240	refused to discharge		14
37-53-6	Tefzel	naAl	Ni	0.25	2	3.21	NH_4^+	41.7	refused to cycle		15
37-75-3	Tefzel	aAl	aAl	0.25	2	--	NH_4^+	158	27.5 refused to cycle		
37-75-5	Crane	aAl	aAl	0.25	2	--	NH_4^+	151	33.3	17.5 refused to dischg.	
37-81-2	Novosorb	Ti	Ti	0.4	2	4.30	NH_4^+	124	57.5	29.2	16
37-81-6	Tefzel	Ti	Ti	0.4	2	4.12	NH_4^+	104	30.3	14.2	17
37-54-4	Tefzel	aAl	Ni	0.5	1	4.32	K^+	285	127	exploded.	18
37-54-7	Crane	aAl	Ni	0.5	1	4.10	K^+	289	63.3		19
37-81-3	Novosorb	Ti*	Ti	0.4	2	4.31	NH_4^+	34.2	0.83 refused to discharge		
37-81-5	Tefzel	Ti*	Ti	0.4	2	4.05	NH_4^+	29.2	13.3 refused to discharge		
37-88-3	Novosorb	Ti**	Ti	0.4	2	4.10	NH_4^+	127	20.8	13.3	
37-88-4	Novosorb	Ti**	Ti	0.4	2	3.94	NH_4^+	105	33.3	17.5	
37-88-1	Novosorb	Ti**	Ti	0.4	2	4.46	NH_4^+	226	130	100	20
37-88-2	Novosorb	Ti**	Ti	0.4	2	4.16	NH_4^+	230	116	81.7	21
37-90-2	Novosorb	aAl**	Ni	1	2	4.29	Cs^+	291	118	60.3	27,28,29
37-90-3	Novosorb	aAl**	Ni	1	2	4.93	Cs^+	62.5	400	113	30
37-90-4	Novosorb	aAl**	Ni	0.5	1	4.33	K^+	322	101	72.5	22
37-90-5	Novosorb	aAl**	Ni	0.5	1	4.29	K^+	307	121	80.8	23
37-90-6	Novosorb	aAl**	Ni	0.5	1	3.74	K^+	230	64.2	145	24,25,26
37-87-4	Novosorb	Zr**	Zr	0.5	1	4.64	K^+	223	76.7	44.2	

TABLE 4 (Continued).

Cell #	Separator	Positive contact scrn. tab	Electrolyte: Li⁺ conc (moles/l)	(R)⁺ conc.	Approx. volume (ml)	(R)=	Discharge capacity, mAh pri.	sec.	3rd	Figure numbers
37-87-5	Novosorb	Zr**	Zr	0.5	1	4.67	K⁺	244	107	exploded.

* Discharged one week after filling
** Negative electrode contact was buried in the lithium.

versus the silver chloride reference electrode described in Chapter 2. For each cell in which an asterisk appears after the composition of the positive screen material, the cell was stored on open circuit for one week at ambient temperature before being cycled. For each cell in which a double asterisk appears after the composition of the positive screen material, the negative electrode contact was buried in the lithium so that it did not directly face cathode material. For all other cells, the negative electrode contact was nickel ribbon pressed diagonally into the lithium electrode.

Most of the cells accepted charge at 3.25 volts, 50 mA, and were able to maintain an open circuit potential. However, the primary capacities were low, and secondary and higher capacities were lower. Figure 8 shows the discharge/ charge profile for cell 37-48-2, which was filled after being pumped down on the pneumatic aspirator only to about 22" of mercury. Although the electrolyte volume was adequate, the capacity and running potential were particularly low, compared with cells thoroughly pumped down on the vacuum pump before filling. In addition, cell 37-48-2 failed to accept any substantial charge. For comparison, Figure 9 shows the discharge/ charge profile for cell 37-57-3, filled with about the same amount of the same electrolyte. Cell 37-48-2 ran between 2.4 and 1.5 volts at a lower and lower potential as the discharge proceeded, for a total of 248 mAh during four attempts, while cell 37-57-3 ran nearly flat at an average potential of 2.8 volts, giving 207 mAh on the first cycle. The thorough pumping may be required to ensure complete displacement of air and wetting of the cathode material.

Cells containing electrolyte originally intended to be 2M ammonium thiocyanate were filled with solution from the heavier of the two phases formed. The compositions of these phases were not determined, but the highest primary capacities recorded were obtained from these cells, the better when the lithium thiocyanate originally added was equivalent to 0.5M rather than 0.75M. Figure 10 shows the cycling profile for cell 37-57-4, while Figure 11 shows cell 37-69-1. We may find more satisfactory capacities from cells with still lower concentrations of lithium thiocyanate, starting with 2M ammonium ion. Lowering the ammonium thiocyanate to 1M and the lithium thiocyanate to 0.1M, as shown

in Figure 12 for cell 37-66-4, gave poor results. Raising the concentration of ammonium ion to 4 M produced cells which did not charge well, as shown in Figure 13 for cell 37-54-5.

The only cell to have exploded during this work or Phase I was cell 37-57-1, which was underfilled because of difficulty in adequately crimping the fill tube. We therefore did not test more cells which had not been completely filled.

Cells 37-54-3 and 37-54-8 each contained 2M tetrabutylammonium thiocyanate/ 0.5M lithium thiocyanate. The primary capacities were low. While 37-54-8 stayed at about 2.7 volts during charging, 37-54-3 refused to accept charge below 4 volts. As explained above under the corrosion tests, the anode/ negative contact hardware was likely reducing the cation, causing lithium passivation. A noticeably higher viscosity may also have contributed to early passivation.

It was discovered that two liquid phases would form if the concentration of ammonium thiocyanate was higher than two molar. The concentration of ammonium thiocyanate was therefore held at 2M, and the lithium thiocyanate concentration varied in order to obtain the maximum primary capacity. Cells 37-53-3 (Figure 14) and 37-53-6 (Figure 15) each contained 2M ammonium thiocyanate/ 0.25 molar lithium thiocyanate. 37-53-3, with the Craneglass separator, gave a primary capacity of 240 mAh and sustained a charging current, but refused to deliver any more capacity. 37-53-6, with the Tefzel separator, gave only 41.7 mAh and refused either to charge or discharge further. Replicate cells 37-75-3 and 37-75-5 behaved in similar fashions. In cells 37-81-2 (Figure 16) and 37-81-6 (Figure 17), the concentration of LiSCN was raised from 0.25 to 0.4M. The capacity did not improve. On cycling past six complete cycles, the cells refused either to discharge or charge. The capacity and running potential this time were not affected by whether the separator was binderless glass or Tefzel. Cells 37-81-3 and 37-81-5 were replicates of 37-81-2 and 37-81-6, except they were allowed to stand one week at room temperature before they were cycled. The primary capacities were disastrously low.

At this point, we began tests with electrolyte in which the salt mixture weighed into the 100 ml Savillex vessel was equivalent to 1M KSCN/ 0.5M LiSCN. To our surprise, nearly all of the salts present dissolved at room temperature, forming a light yellow solution. Cells 37-54-4 (Figure 18) and 37-54-7 (Figure 19) behaved similarly, although the separators differed. The primary capacities were respectively 286 and 289 mAh, which was higher than they had been for cells containing ammonium thiocyanate, but still unacceptably low. The capacities dropped sharply during the second cycle. Cell 37-54-4 exploded during the second charge cycle, disconnecting cell 37- 54-7 in the process. The cells were both adequately filled, so that low electrolyte volume could not have been the cause of the explosion.

In order to prevent undercutting between the nickel tab contact and the lithium electrode, we changed the design of the negative

electrode such that the nickel was buried in the lithium at one end, instead of being exposed to one surface of the positive electrode along its diagonal. Cells 37-88-3 and 37-88-4 each contained 2M NH_4SCN/ 0.4M LiSCN, but did not fare any better than the earlier cells with diagonally tabbed anodes. Likewise, cells 37-88-1 (Figure 20) and 37-88-2 (Figure 21), each with 1M KSCN/ 0.5M LiSCN, gave primary capacities which were even about 9% lower than their diagonally tabbed predecessors.

When anodized aluminum screen and tabs were used as the positive electrode substrates in place of titanium, also using the potassium electrolyte with the separator "Hovosorb", the primary capacity increased to more than 300 mAh (cell 37-90-4 and Figure 22; cell 37-90-5 and Figure 23). Cell 37-90-6, a third replicate but containing less electrolyte, gave some 30% less capacity during the first discharge cycle. The continuation of discharge cycle 1 and discharge cycle 2 are shown in Figure 24, and cycles 3 to 6 in Figures 25 and 26. The terminal potential during charge became more and more unsteady as the testing proceeded. During the sixth charge cycle, the cell was set on open circuit to check for "soft" short circuits between the carbon and lithium dendrites from the anode. The potential remained steady during open circuit stand, indicating that short circuits had not formed during the charge cycles, and were not responsible either for the reduced capacity or the unsteady terminal potential during charging. Extended cycling showed that the cells could take repeated overcharge without shorting or passivating, but the capacity still fell off sharply with continued cycling.

Cells 37-87-4 and 37-87-5 were similar to cells 37-90-4 and 37-90-5, except 37-87-4 and -5 had zirconium positive substrate hardware. The capacity/ cycling behavior were not significantly different. However, 37- 87-4 exploded during its 9^{th} charge cycle, and -5 during its 3^{rd}.

The solubility of cesium thiocyanate in liquid sulfur dioxide at room temperature was beyond 2 molar, as we suspected, and salts weighed out to the equivalent of 2M CsSCN/ 1M LiSCN dissolved completely. While the solubility of CsSCN in liquid sulfur dioxide was considerably higher than that of KSCN, no dramatic improvement in the capacity resulted when the cesium salt was used in place of the potassium salt. Cell 37-90-2 (Figures 27, 28, and 29) gave a primary capacity of 291 mAh, using Hovosorb with an anodized aluminum positive electrode support screen. While the discharge cycles lasted about 2 hours before the two volt cutoff, the charge cycles lasted the full ten hours for which the cycler was set without reaching the high potential cutoff. The terminal potential during charge became more and more unsteady as the testing proceeded, as it had before for cell 37-90-6. During the sixth charge cycle (Figure 29), the cell was put on open circuit. The steady decay in the potential with time suggested this time that a "soft" short circuit had developed.

Cell 37-90-3 (Figure 30) was the other which was successfully filled and sealed and which contained cesium. During the first

discharge cycle, an intermittent connection prevented complete discharge to two volts. The cell then charged for ten hours, equivalent to an overcharge of about 440 mAh, or seven times the charge which had been withdrawn during the first discharge cycle. During the second discharge cycle, the cell delivered over 400 mAh, but with an initial plateau, apparently corresponding to the discharge of some of the thiocyanogen produced by the oxidation of the thiocyanate during the first charge cycle. However, the capacity also decreased substantially during the first few cycles.

Corrosion of components during cycling in cells containing thiocyanate. Table 5 summarizes the observations made of components taken from cells containing thiocyanate after they had been cycled and disassembled in the dryroom. Unlike the samples examined after the tests in the gas tight vials, these represented cell parts subjected to cycling. The observations were made to determine whether there had been corrosion particularly of the positive electrode screen and tab during charging. Both aluminum anodized to + 200mV and Inconel were unaffected by the cycling.

TABLE 5. Observations of the corrosion of hardware in cells containing thiocyanate, opened after cycling.

Cell #	Separator	Positive contact scrn.	tab	Electrolyte: Li^+ conc (moles/l)	NH_4^+ conc.	Approx. volume (ml)	Observations
37-53-5	Tefzel	uaAl	Ni	1	4	3.67	Cycling had pitted screen. Ni tab and feedthrough were slightly corroded.
37-54-1	Tefzel	aAl-16	Ni	1	4	3.35	Al screen was clearly pitted.
37-57-1	Tefzel	Inc	Ni	1	3	2.69	Cell had exploded. Inconel screen was untouched.
37-57-3	Pyrex	Inc	Ni	1	3	3.97	Inconel screen was untouched.
37-54-5	Pyrex	aAl-16	Ni	1	4	3.80	Al screen was slightly pitted.
37-62-2	Pyrex	aAl-2V	aAl	0.5	2	> 3	All solids were water soluble; all cell parts were intact
37-84-2		Ti	Ti	0.4	2	--	Ti screen unaffected after cycling
37-84-3		Ti	Ti	0.5	1M K^+	--	Ti screen unaffected after cycling

Stability of SO_2 electrolytes containing thiocyanates. During the first two quarters of this contract, we observed that sulfur dioxide solutions of substituted ammonium thiocyanates were not sufficiently stable in the presence of lithium to serve as cosolutes for lithium thiocyanate. We suspected the same was true for ammonium thiocyanate as well. When we substituted potassium or

cesium thiocyanate for ammonium or organic cations, the lithium was more stable and cells delivered more capacity. During these studies, we had the opportunity to observe the stability of solutions of potassium and cesium thiocyanates in liquid sulfur dioxide for some months at room temperature. Over this time, the internal parts of the Savillex vessels below the electrolyte level have become coated with an intractable yellow solid, insoluble in water or organic solvents. The solid may be a mixture of sulfur and parathiocyanogen, or polymerized thiocyanogen. The thiocyanogen would be formed from the solvolysis of thiocyanate according to reactions similar to those discussed by Jander [12]:

$$2SO_2 + 2K^+ + 2SCN^- \text{---> } SO(SCN)_2 + K_2SO_3 \quad (1)$$

$$4SO(SCN)_2 \text{---> } 4(SCN)_2 + 2S + 2SO_2 \quad (2)$$

$$n(SCN)_2 \text{---> } 2(SCN)_n \quad (3)$$

Since these reactions are expected to be irreversible, deterioration of the electrolyte and reduced shelf life would be predicted for cells containing thiocyanate. At this point, we therefore abandoned our study of electrolytes containing thiocyanate.

AA SIZE REFERENCE ELECTRODE CELLS

The reference electrode cell studies were undertaken in order to determine whether the lithium electrodes or the carbon electrodes were limiting the cell capacities. As described in Chapter 2, the first tests were carried out using a constant load with a two channel strip chart recorder to monitor the potentials between the cathode and the anode, and between the cathode and the reference electrode. The tests were carried out using cells containing either 2M NH_4SCN/ 0.4M LiSCN, 1M KSCN/ 0.5M LiSCN, or the organic electrolyte used in primary cells, 21% acetonitrile/ 6.5% propylene carbonate/ 0.85M LiBr. In each case, the anode appeared to be the electrode which passivated first.

We doubted that the anodes could be passivating first, particularly in the cell containing the primary electrolyte. We then tried using cycler power supplies, each with an input impedance exceeding 10 megohms, to monitor all three possible potentials: the carbon versus the negative electrode, the carbon versus the reference, and the lithium negative versus the reference electrode. With these data, we would be able to determine whether the total cell resistance was changing with discharge depth.

During the revised tests with the cycler power supplies, we repeated the thiocyanate cosolute mixture, using 1M KSCN/ 0.5M LiSCN. We also attempted two inorganic cosolute bromides, 0.5M KBr/ 0.5M LiBr and 1.0M CsBr/ 0.5M LiBr, although undissolved salts remained in both of the bromide mixtures.

Table 6 summarizes the construction materials, the electrolyte compositions, and the discharge capacities versus cycle number

for each of the reference electrode AA cells. Cell 43-2-2 contained sulfur dioxide saturated with lithium bromide/ potassium bromide, cell 43-2-3 1M KSCN/ 0.5M LiSCN, and cell 43-2-4, what was originally weighed out to be 1.0M cesium bromide/ 0.5M lithium bromide.

TABLE 6. Capacities of Reference Electrode AA Cells

Cell No.	Separator	Positive contact scrn.	Positive contact tab	Electrolyte Salt	Conc.	Approx. volume	Discharge capacity, mAh ori.	sec.	3rd	4th	5th	Figures
43-2-2	Hovosorb	Ti	Ti	LiBr	0.5M*	4.13ml	30.8	9.17	8.33			37-39
				KBr	0.5M							
43-2-3	Hovosorb	Ti	Ti	LiSCN	0.5M	4.86ml	77.5	77.5	68.3	63.3		31-36
				KSCN	1.0M							
43-2-4	Hovosorb	Ti	Ti	LiBr	0.5M*	5.77ml	188	152	214	145	60.0	40-42
				CsBr	1.0M							

* Not all of salt mixture dissolved.

Figure 31 shows the first two discharge profiles, the first and part of the second charge profiles for cell 43-2-3. Shown is the potential of the lithium versus the carbon as a function of time. Figure 32 shows the reference electrode versus the carbon, and Figure 33 shows the reference electrode versus the lithium over the same time period. The computer was not capable of recording potentials less than zero volts, so that during charge, the reference versus the lithium electrode remained at zero. We had intended that the discharge time be ten hours, but a malfunction terminated the primary discharge at 1.5 hours. A slight potential delay apparent in Figure 31 at the onset of the first discharge cycle was not caused by the carbon electrode (Figure 32), but by partial passivation of the lithium (Figure 33). During the second discharge cycle, the cell polarization noted in Figure 31 was caused both by the carbon electrode (Figure 32) and by the lithium (Figure 33), which by the end of the half cycle had polarized about 376 millivolts. Figures 34, 35, and 36 show the second discharge half cycle for cell 43-2-3 in greater detail. By the end of the half cycle, the carbon electrode had polarized about 500 mV. The profiles start with a period of open circuit, then discharge, then rest after discharge, then part of the following charge cycle.

If there were no IR loss, that is, no potential drop across the electrolyte and separator during the entire discharge half cycle, then the cell potential (C-Li) should equal the potential of the carbon with respect to the reference (C-Ref) minus the potential of the lithium with respect to the reference (Li-Ref). If there were any potential drop across the electrolyte, then the potential across the cell should be reduced by the extent of the drop, and

$$(C\text{-}Li) + (IR\ loss) = (C\text{-}Ref) - (Li\text{-}Ref) \quad (4)$$

or

$$IR\ loss = (C\text{-}Ref) - (C\text{-}Li) - (Li\text{-}Ref) \quad (5)$$

Table 7 shows the data collected by the computer and calculations of IR induced potential drop for each three point set of data. During the entire discharge half cycle, the IR loss did not exceed 10 millivolts, even at the very end of the discharge half cycle. During the third and fourth discharge half cycles, the carbon electrode contributed less and less to the total cell polarization, while the lithium electrode contributed more, reaching 586 millivolts by the end of the fourth cycle. The IR induced potential drop also did not exceed 10 millivolts throughout the test.

Figures 37 through 39 show each of the three profiles for cell 43-2-2, in which the electrolyte was sulfur dioxide saturated with a mixture of potassium and lithium bromide. As we explained on page 25, Jander reported that the solubility of potassium bromide by itself in liquid sulfur dioxide was only about 0.11 molar. A KBr/ LiBr salt mixture was attempted in spite of the limited solubility of potassium bromide, to determine whether a cell would function at all. At 1 mA/cm², the capacities were very low, as shown in Table 6. At the end of the discharge cycles, both the lithium and the carbon electrodes polarized about 500 millivolts. The cell refused to accept any substantial charge, the carbon electrode polarizing about 200 mV and the lithium electrode, we assume about 800 mV from the difference between the potential of the carbon electrode and the charge cutoff potential, which was set at 4 volts.

Figures 40 through 42 show each of the three profiles for cell 43-2-4, including the second, third, and fourth discharge half cycles. The first discharge cycle was stopped at 188 mAh while the cell was running at about 2.87 volts. The charge half cycles were ten hours. The electrolyte consisted of 1 molar cesium bromide saturated with lithium bromide, which we estimate was at no greater than 0.1 molar. The cell started each discharge half cycle without potential delay, but the anode polarized up to about 100 mV at the very end of the first four discharge half cycles. At the end of the fifth discharge half cycle, the lithium polarized about 370 mV, while the carbon polarized 450 mV (not shown). Plateaus appeared during the charge half cycles, the first roughly equivalent to the discharge capacities, but the second of indefinite length.

The plateaus were clearly related to the positive electrode (Figure 41), and very little of the polarization was caused by the anode (Figures 40 and 41). We would expect the first plateau to represent the oxidation of the dithionite back to sulfur dioxide, but the average of the discharge potential and the first charge plateau was about 3.05 volts, some 100 millivolts above the open

TABLE 7. Cell 43-2-3. Cell and reference potentials for discharge cycle 2. Calculated IR drop across separator/ electrolyte.

MINUTES	Li vs C	Ref vs C	Ref vs Li	HOURS	IR DROP
721	2.957	2.964	0.002	0.0167	0.005
722	2.949	2.957	0.002	0.0333	0.006
723	2.947	2.952	0.002	0.0500	0.003
724	2.944	2.952	0.002	0.0667	0.006
725	2.878	2.925	0.032	0.0833	0.015
726	2.864	2.913	0.042	0.1000	0.007
727	2.854	2.908	0.042	0.1167	0.012
728	2.849	2.905	0.051	0.1333	0.005
729	2.844	2.903	0.054	0.1500	0.005
730	2.839	2.905	0.059	0.1667	0.007
731	2.837	2.903	0.059	0.1833	0.007
732	2.837	2.903	0.063	0.2000	0.003
733	2.832	2.903	0.066	0.2167	0.005
734	2.832	2.9	0.061	0.2333	0.007
5	2.832	2.903	0.063	0.2500	0.008
736	2.834	2.905	0.061	0.2667	0.010
737	2.832	2.888	0.061	0.2833	-0.005
738	2.834	2.903	0.063	0.3000	0.006
739	2.834	2.905	0.061	0.3167	0.010
740	2.834	2.905	0.066	0.3333	0.005
741	2.834	2.903	0.066	0.3500	0.003
742	2.832	2.903	0.061	0.3667	0.010
743	2.832	2.903	0.066	0.3833	0.005
744	2.832	2.903	0.066	0.4000	0.005
745	2.83	2.903	0.061	0.4167	0.012
746	2.832	2.903	0.066	0.4333	0.005
747	2.83	2.903	0.066	0.4500	0.007
748	2.83	2.903	0.068	0.4667	0.005
749	2.827	2.903	0.068	0.4833	0.008
750	2.832	2.903	0.073	0.5000	-0.002
751	2.825	2.903	0.068	0.5167	0.010
752	2.82	2.898	0.071	0.5333	0.007
753	2.82	2.9	0.076	0.5500	0.004
754	2.817	2.898	0.073	0.5667	0.008
755	2.813	2.896	0.081	0.5833	0.002
756	2.81	2.898	0.083	0.6000	0.005
757	2.805	2.898	0.088	0.6167	0.005
758	2.8	2.896	0.09	0.6333	0.006
759	2.793	2.896	0.095	0.6500	0.008
760	2.788	2.891	0.098	0.6667	0.005
761	2.781	2.893	0.107	0.6833	0.005
762	2.771	2.888	0.11	0.7000	0.007
763	2.769	2.888	0.117	0.7167	0.002
764	2.756	2.888	0.12	0.7333	0.012
765	2.749	2.883	0.132	0.7500	0.002
766	2.742	2.883	0.142	0.7667	-0.001
767	2.732	2.886	0.144	0.7833	0.010
768	2.722	2.881	0.154	0.8000	0.005
769	2.712	2.878	0.156	0.8167	0.010

TABLE 7 (Continued).

MINUTES	Li vs C	Ref vs C	Ref vs Li	HOURS	IR DROP
770	2.703	2.876	0.168	0.8333	0.005
771	2.693	2.874	0.176	0.8500	0.005
772	2.683	2.874	0.176	0.8667	0.015
773	2.676	2.871	0.188	0.8833	0.007
774	2.668	2.869	0.195	0.9000	0.006
775	2.659	2.866	0.2	0.9167	0.007
776	2.651	2.864	0.208	0.9333	0.005
777	2.644	2.861	0.212	0.9500	0.005
778	2.639	2.859	0.215	0.9667	0.005
779	2.632	2.856	0.217	0.9833	0.007
780	2.625	2.854	0.225	1.0000	0.004
781	2.62	2.854	0.225	1.0167	0.009
782	2.612	2.849	0.227	1.0333	0.010
783	2.605	2.844	0.237	1.0500	0.002
784	2.6	2.844	0.237	1.0667	0.007
785	2.593	2.839	0.244	1.0833	0.002
786	2.585	2.839	0.249	1.1000	0.005
787	2.576	2.834	0.254	1.1167	0.004
788	2.566	2.83	0.256	1.1333	0.008
789	2.556	2.825	0.261	1.1500	0.008
790	2.549	2.825	0.264	1.1667	0.012
791	2.539	2.82	0.271	1.1833	0.010
792	2.532	2.815	0.281	1.2000	0.002
793	2.52	2.81	0.283	1.2167	0.007
794	2.505	2.808	0.291	1.2333	0.012
795	2.498	2.8	0.298	1.2500	0.004
796	2.488	2.798	0.303	1.2667	0.007
797	2.476	2.791	0.31	1.2833	0.005
798	2.463	2.793	0.317	1.3000	0.013
799	2.449	2.77?	0.322	1.3167	0.007
800	2.437	2.771	0.33	1.3333	0.004
801	2.419	2.761	0.337	1.3500	0.005
802	2.407	2.754	0.342	1.3667	0.005
803	2.39	2.742	0.344	1.3833	0.008
804	2.371	2.732	0.354	1.4000	0.007
805	2.356	2.715	0.352	1.4167	0.007
806	2.334	2.695	0.354	1.4333	0.007
807	2.312	2.673	0.356	1.4500	0.005
808	2.292	2.656	0.356	1.4667	0.008
809	2.271	2.637	0.361	1.4833	0.005
810	2.249	2.615	0.364	1.5000	0.002
811	2.224	2.595	0.361	1.5167	0.010
812	2.202	2.573	0.364	1.5333	0.007
813	2.175	2.549	0.369	1.5500	0.005
814	2.151	2.524	0.371	1.5667	0.002
815	2.122	2.505	0.376	1.5833	0.007
816	2.092	2.473	0.376	1.6000	0.005
817	2.063	2.449	0.376	1.6167	0.010
818	2.031	2.419	0.381	1.6333	0.007
819	2	2.434	0.256	1.6500	0.178
820	2.639	2.803	0.164	1.6667	0.000
821	2.651	2.813	0.159	1.6833	0.003
822	2.659	2.815	0.161	1.7000	-0.005
823	2.661	2.813	0.156	1.7167	-0.004
824	2.664	2.817	0.149	1.7333	0.004

TABLE 7 (Continued).

MINUTES	Li vs C	Ref vs C	Ref vs Li	HOURS	IR DROP
825	2.668	2.82	0.151	1.7500	0.001
826	2.673	2.815	0.146	1.7667	-0.004
827	2.676	2.82	0.146	1.7833	-0.002
828	2.678	2.82	0.144	1.8000	-0.002
829	3.079	3.093	0.02	1.8167	-0.006
830	3.105	3.132	0.034	1.8333	-0.007
831	3.123	3.147	0.034	1.8500	-0.010
832	3.132	3.159	0.032	1.8667	-0.005
833	3.132	3.159	0.037	1.8833	-0.010
834	3.12	3.152	0.039	1.9000	-0.007
835	3.11	3.147	0.039	1.9167	-0.002
836	3.103	3.142	0.044	1.9333	-0.005
837	3.101	3.137	0.046	1.9500	-0.010
838	3.105	3.137	0.039	1.9667	-0.007
839	3.103	3.145	0.042	1.9833	0.000
840	3.115	3.147	0.039	2.0000	-0.007
841	3.123	3.152	0.037	2.0167	-0.008
842	3.132	3.159	0.032	2.0333	-0.005

circuit of the sulfur dioxide/ dithionite potential with respect to lithium. Yet the second charge plateau was about 200 millivolts below the value expected for the lithium/ bromine potential (3.65 volts). We currently have no satisfactory explanation for the plateaus.

Cells 41-53-1 and 41-53-2 were identical to cells 41-50-1, 41-50-2, 41-51-1, and 41-51-2 except that the 52 alloy fillport tubes were connected to lithium reference electrodes. The tests differ from earlier ones in that the cells were placed on constant load using the computer controlled power supplies to monitor the potentials. Earlier tests used constant loads and a two channel recorder with a relatively low input impedance, or the computer in conjunction with discharge at constant current. The voltmeters in the computer controlled power supplies have much higher input impedances. Running cells at constant load helps prevent local polarization of the stronger electrode by the weaker electrode. Both cells were connected to 100 ohm loads about ten minutes after the computer began reading potentials.

Figures 43, 44, and 45 show respectively the carbon electrode versus the lithium, the carbon versus the reference, and the lithium versus the reference for cell 41-53-1. Figures 46, 47, and 48 show the same for cell 41-53-2. A power failure about 15 hours into the test prevented our collecting complete discharge data. However, for each cell, by far the greater polarization occurred in the positive electrode, the negative electrodes polarizing no more than 40 millivolts. The plateau in the discharge profile of cell 41-53-1 is actually not as pronounced as it appears. Cell 41-53-1 ran between 2.84 and 2.56 volts, while data collected for cell 41-53-2 ran between a much wider range, 2.85 and 1.46 volts. The capacity represented by a discharge at 2.85 volts through a resistance of 100 ohms for 12 hours (Figure 46) is 342 mAh.

BROMIDE ELECTROLYTES

Corrosion tests. The results of the corrosion tests involving bromide electrolytes in the 4 ml Savillex sample vials are summarized in Table 8. The cations (R) of the cosolute are described in the body of the table, as are their concentrations. Some of the electrolytes contained only lithium bromide with organic cosolvents. The notation "aAl" refers to anodized aluminum (the superscript refers either to +160 mV or +200 mV, the potential to which the aluminum was anodized), "Inc" to Inconel 600, "52" to 52 iron/nickel alloy feedthrough tubes, and "AA" to a section cut from a 304 stainless steel AA size cell can. The "/" marks indicate that the components in the sample tested were electrically connected.

The organic cation bromide cosolute electrolytes appeared to be at least superficially stable by themselves, but were reduced by lithium, particularly when in contact with other hardware such as nickel or stainless steel. While there were differences in the

TABLE 8. Corrosion Tests in Bromide Electrolytes. Samples Biased with Lithium or Carbon at Ambient Temperature in 4 ml Savillex Gas Tight Teflon Vials.

Sample	Electrolyte LiBr	(R)Br	Storage time	Result
Li	1M	3M NMe_4	3 days	Tarnish around cut edges.
Li/Ni/AA	1M	3M NMe_4	3 hours	Lithium tarnish and corrosion. Electrolyte darkened.
Li/Ni/AA	0.75M	2M N-MePy	6 days	No pitting on hardware, but Li tarnish; solids formed, insol. in H_2O; water solution was orange-yellow.
(none)	0.75M	2M N-MePy	13 days	On hydrolysis: clear, colorless solution; minor amt. of precipitate.
Li	1M	3M NMe_4	1 day	Some lithium tarnish. On hydrolysis: solid insol. in H_2O was not sulfur
uaAl/C	1M	3M NMe_4	1 day	No effect
aAl/52/C	0.75M	2M N-MePy	16 h	Al O.K.; 52 alloy corroded
aAl/52/C	0.75	2M NEt_4	4 days	Al O.K.; 52 alloy corroded
Ti/C	1M	3M NMe_4	4 days	slight tarnish
Ti/52/C	0.75M	2M NEt_4	6 days	Ti O.K., 52 alloy corroded
Ti/52/C	0.75M	2M N-MePy	3 days	Severe corrosion
Ni/52/C	1M	3M NMe_4	3 hrs	Electrolyte darkened
Inc/52/C	0.75M	2M N-MePy	6 days	Screen destroyed, 52 alloy corroded
Inc/C	1M	3M NMe_4	1 day	Screen destroyed
Inc/C	0.85M LiBr 21.5 % DME 6.5 % PC		2 d	No obvious changes in metal; electrolyte: yellow changed to orange
Ti/C	0.85M LiBr 21.5 % DME 6.5 % PC		2 d	No changes
Zr/C	0.85M LiBr 21.5 % DME 6.5 % PC		38 d	No changes

rate of decomposition, the situation did not seem to improve sufficiently when the cosolute cation was changed between NMe_4^+, NEt_4^+, and $N\text{-}MePy^+$. Electrolyte samples, when hydrolyzed following storage with lithium or lithium pressed to cell hardware, were orange-yellow in color and contained yellow solids which were insoluble in the aqueous solution. The solids apparently represented products from the reduction of the cations by lithium, since the products did not appear to contain elemental sulfur.

The qualitative test for sulfur was as follows. The solid was filtered and washed with water, and transferred to a test tube with 40% KOH. The mixture was boiled until the solid dissolved. It was then cooled, diluted 4:1 with cold water, and added to

aqueous cupric sulfate/ ammonium hydroxide complex. The deep blue solution produced a blue-white precipitate. The same test repeated with an authentic sample of sulfur produced a brown precipitate.

The electrolytes were also superficially stable in the presence of either aluminum or titanium electrochemically biased with pressed carbon samples, but rapidly oxidized Inconel and 52 nickel/iron alloy.

The first bromide cells contained 0.75 molar lithium bromide and 2M N-methylpyridinium bromide in sulfur dioxide only. The cells refused to run, and their open circuit potentials were about 1 volt. The corrosion tests suggested that the negative electrodes were to blame for the failure of these cells, although there were no reference electrodes to confirm that the negative electrodes had failed. During Phase I, bromide cells with aluminum-gridded positives and saturated with N-methylpyridinium bromide and lithium bromide did discharge, but only briefly.

The lithium dithionite which formed on the surface of the lithium and negative electrode contact hardware in these cells was evidently not sufficient to prevent reduction of the cosolute cation. It is possible that while in a conventional Li/SO_2 primary cell the acetonitrile increases the solubility of lithium bromide without increasing the solubility of lithium dithionite, in a solution containing a quarternary ammonium cation the solubility of lithium dithionite is increased as well. One approach to limiting the solubility of lithium dithionite, if this is the problem, might be to saturate the solution with lithium bromide and use as little as possible of the cosolute salt. A second approach would be to broaden the tests to include electrolytes with lithium bromide and organic cosolvents such as propylene carbonate and 1,2- dimethoxyethane, which are more likely to resist oxidation or reduction in this particular chemical environment than is acetonitrile.

A third approach was to use a cosolute bromide in which the cation was thermodynamically stable 'n the presence of metallic lithium. We prepared one molar ces m bromide/ saturated lithium bromide (about 0.1 molar)/ SO_2. Three samples were stored for 24 days at ambient temperature in 4 ml gas tight Savillex containers. The first contained a piece of lithium pressed to a nickel screen welded to a nickel tab, in turn welded to a piece of stainless steel cut from an AA can. The second contained a piece of titanium screen to which positive electrode carbon mixture had been pressed. The third was the same as the second, except that a sample of 52 nickel/ iron alloy used for the glass/ metal feedthroughs was welded to the titanium screen, in order to bias both the titanium and the 52 alloy at the potential of the carbon electrode while the assembly was immersed in the electrolyte.

After 24 days at ambient temperature, the colors of the solutions were compared. The first was still yellow. The second was reddish brown, and the third a deep reddish brown. All three mixtures had

developed a fine white precipitate. The metal samples were removed from the first container and washed with liquid sulfur dioxide in the dryroom hood. The sample was then hydrolyzed, acidified with hydrochloric acid, and treated with aqueous barium chloride solution. A white precipitate indicated the presence of sulfite or sulfate adhering to the original metal samples. Hydrolysis of the contents of the other two containers showed that the titanium remained unaffected, but that the 52 alloy had been deeply corroded. The hydrolyzed mixtures were not completely soluble in water and gave a foul odor.

In addition to the corrosion of the 52 alloy by the electrolyte, the electrolyte was likely undergoing solvolysis [12]:

$$2SO_2 + 2Li^+ + 2Br^- \longrightarrow SOBr_2 + Li_2SO_3 \qquad (6)$$

$$4SOBr_2 \longrightarrow 3Br_2 + S_2Br_2 + 2SO_2 \qquad (7)$$

Sulfur dioxide solutions of cesium bromide as high as three molar, but without lithium present, have remained stable over the same length of time. Lithium ion therefore likely was participating in or catalyzing the solvolysis reaction.

AA size cell tests. Table 9 summarizes the construction materials, the electrolyte compositions, and the discharge capacities versus cycle number for each of the AA cells containing bromide mixtures, either sulfur dioxide with organic solvents and lithium bromide, or sulfur dioxide with mixtures of inorganic bromides. The term "aAl" refers to aluminum positive electrode support screen which had been anodized in isopropanol/ water/ 0.2M ammonium carbonate to +.160 millivolts versus the silver chloride reference electrode described in Chapter 2. For each cell in which an asterisk appears after the composition of the positive screen material, the negative electrode contact was nickel ribbon pressed diagonally into the lithium electrode. For all other cells, the negative electrode contact was buried in the lithium so that it did not directly face cathode material.

TABLE 9. Capacity of AA Cells Containing Lithium Bromide Electrolytes with Organic Cosolvents or with Cesium Bromide

Cell	Separator	Positive contact		Electrolyte				Discharge capacity, mAh					
number		scrn.	tab	Salt	Conc.	Approx. volume	Other	pri.	sec.	3rd	4th	5th	Figure
37-69-4	Tefzel	Ti[1]	Ti	LiBr	0.85M	3.73ml	DME, 21% PC, 6.5%	799	700	525	expld.	. . . . .	49,50
37-75-2	Tefzel	aAl[1]	aAl	LiBr	0.85M	4.07ml	DME, 21% PC, 6.5%	772	525	106.7			
37-75-4	Crane	aAl[1]	aAl	LiBr	0.85M	3.86ml	DME, 21% PC, 6.5%	694	213	became disconnected			
37-81-1	Novosorb	Ti[1]	Ti	LiBr	0.85M	3.86ml	DME, 20%	278	66.7	100.3	expld.	. . . . .	51
37-81-4	Tefzel	Ti[1]	Ti	LiBr	0.85M	4.20ml	DME, 20%	406	83.0	5.0.	. . . . .		52
37-88-5	Novosorb	Ti	Ti	LiBr	0.85M	3.30ml	DME, 20%	169	stopped; low elect. wt.				

TABLE 9 (Continued).

Cell number	Separator	Positive contact scrn.	Positive contact tab	Electrolyte Salt	Conc.	Approx. volume	Other	Discharge capacity, mAh pri.	sec.	3rd	4th	5th	Figure
37-87-1	Novosorb	Zr[1]	Zr	LiBr	0.85M	4.19ml	PC, 28%	500	500	500	533	160 . . .	53-55
37-87-2	Novosorb	Zr[1]	Zr	LiBr	0.85M	4.18ml	PC, 28%	500	632	268	12.5		
37-87-3	Novosorb	Zr[1]	Zr	LiBr	0.85M	4.36ml	PC, 28%	500	500	443	101	expld.	
32-77-3	Novosorb	aAl[2]	aAl	LiBr	0.50M	6.66ml							
				CsBr	1.00M			297	214	208	134	158 . . .	61,62
32-77-4	Novosorb	aAl	aAl	LiBr	0.85M	5.64ml	DME, 14%						
							PC, 14%	500	425	160	107	. . . . .	56,57
32-77-5	Novosorb	aAl	aAl	LiBr	0.85M	5.53ml	DME, 14%						
							PC, 14%	500	500	183	85.8	. . . . .	
32-77-6	Novosorb	aAl	aAl	LiBr	0.85M	5.43ml	DME, 14%						
							PC, 14%	500	500	159	110	. . . . .	
32-85-1	Novosorb	Ti	Ti	LiBr	1.00M	5.40ml	DME, 34%						
							PC, 11%	520	102	113	66.7	23.3. . .	60
32-85-2	Novosorb	Ti	Ti	LiBr	1.00M	5.38ml	DME, 34%						
							PC, 11%	568	163	108	75.8	56.7. . .	
32-85-3	Novosorb	Ti	Ti	LiBr	1.00M	5.36ml	DME, 34%						
							PC, 11%	83.3[2]	488	64.2	28.3	27.5. . .	
32-85-4	Novosorb	Ti	Ti	LiBr	1.00M	5.51ml	DME, 34%						
							PC, 11%	157[2]	206	162	53.3	67.5. . .	
32-85-5	Novosorb	Ti	Ti	LiBr	0.5M	5.51ml							
				CsBr	2.0M			397	297	271	181	163 . . .	65
32-85-6	Novosorb	Ti	Ti	LiBr	0.5M	5.51ml							
				CsBr	2.0M			250	250	250	250	250 . . .	66
37-95-1	Tefzel[4]	Ti	Ti	LiBr	0.85M	5.79ml	DME, 14%						
							PC, 14%	500	refused to discharge			. . . . .	
37-95-2	Tefzel[4]	Ti	Ti	LiBr	0.85M	5.40ml	DME, 14%						
							PC, 14%	368	112	refused to discharge		. .	
37-95-3	Tefzel[4]	Ti	Ti	LiBr	0.50M	6.52ml							
				CsBr	1.00M			154	132	127	118	108 . . .	
37-95-4	Tefzel[4]	Ti	Ti	LiBr	0.50M	6.77ml							
				CsBr	1.00M			179	156	147	133	101 . . .	63
37-95-5	Tefzel[5]	Ti	Ti	LiBr	0.85M	5.01ml	DME, 14%						
							PC, 14%	500	500	500	143	. . . . .	58,59
37-95-6	Tefzel[5]	Ti	Ti	LiBr	0.85M	5.59ml	DME, 14%						
							PC, 14%	500	500	403	108	. . . . .	
37-95-7	Tefzel[5]	Ti	Ti	LiBr	0.50M	6.36ml							
				CsBr	1.00M			187	164	131	113	88.8 . .	64

[1] Negative electrode contact was a nickel strip running diagonally across the surface of the lithium.
[2] Aluminum, anodized in 50/ 50 isopropanol/ water/ 0.2M ammonium carbonate to +160 mV versus a silver/ silver chloride/ 0.1M potassium chloride electrode
[3] Cell did not complete cycle and was restarted
[4] Coarser Tefzel screen (Fluortex 9-PTK-590) plus one layer of Raypern next to carbon electrode.
[5] Finer Tefzel screen (Fluortex 9-210/46, type 906) plus one layer of Raypern next to carbon electrode.

AA cells with lithium bromide and organic cosolvents in sulfur dioxide. The discharge/ charge time limits for cell 37-69-4 were set to 17 hours/ 17 hours after the first discharge half cycle

reached two volts in about 16 hours (Figures 49 and 50). The electrolyte contained both 1,2- dimethoxyethane (DME) and propylene carbonate (PC). The positive electrode grid material was titanium. The primary capacity, about 800 mAh, was the highest of any cell except for the "control" cells containing 21.5 volume percent acetonitrile, 6.5 volume percent propylene carbonate, and 0.85M lithium bromide, which delivered in excess of one amp hour. The capacity decreased to 700 mAh on the second discharge half cycle, and to 525 on the third. 37-69-4 exploded during the third charge cycle (Figure 50).

Cells 37-75-2 and 37-75-4 were replicates also containing DME and PC, but with anodized aluminum positive electrode screens. Their behavior was similar, each giving closer to 700 mAh on the primary discharge cycle than the 800 delivered by 37-69-4. The second and third discharge capacities were also lower than those of 37-69-4.

The electrolyte for cells 37-81-1 and 37-81-4 also contained about 28 volume percent organic solvents, but this time, only DME. 37-81-1 contained a "Hovosorb" binderless Pyrex separator, and 37-81-4, a Tefzel separator. 37-81-1 (Figure 51), while its primary capacity was low, accepted a six hour charge cycle. It exploded during the third charge cycle. 37-81-4 gave slightly over 400 mAh on the primary discharge cycle, but then refused to accept either charge or discharge (Figure 52). 37-81-4 contained a Tefzel separator. The pair 37-81-1/ 37-81-4 then behaved similarly to the pair 37-53-3 and 37-53-6 (Figures 14 and 15) in that the Tefzel separator prevented charging. Our conclusion was that a pure DME cosolvent was inferior to the 21.5% DME/ 6.5% PC mixture, since 37-69-4, also with a Tefzel separator, did accept charge.

The electrolyte in cells 37-87-1, 37-87-2, and 37-87-3 also contained 28 volume percent organic solvent, but this time, only propylene carbonate. The three were replicates of one another. We limited the discharge/ charge times to just ten hours (500 mAh at 50 mA).

Cell 37-87-1 discharged the entire ten hour period for each of the first three cycles (Figures 53 and 54). The fourth cycle was interrupted when 37-87-5 exploded, but 37-87-1 was connected again and the fourth discharge cycle continued (Figure 55). The discharge timer had been reset, so that 37-87-1 discharged beyond ten hours to the set potential limit, 2.00 volts, for a total of 533 mAh. Then, during the fifth discharge cycle, the capacity was substantially less, only 167.5 mAh. After about five hours into the fifth charge cycle, the cell was left on open circuit. Over a 14 hour period, the potential remained steady, indicating that there were no internal shorts (Figure 55). The primary discharge of cell 37-87-2 likewise lasted the entire ten hour period. During the second discharge cycle, 37-87-2 became disconnected. It too was later reconnected, and its second discharge cycle continued, but to the two volt cutoff at 632 mAh. The capacity during the third discharge cycle was 268 mAh, and during the

fourth, only 12.5 mAh, each to a two volt cutoff. Cell 37-87-3 delivered 500 mAh during its first two discharge cycles, but then on the third cycle reached two volts at 443 mAh. During the fourth cycle, 37-87-3 delivered only 101 mAh. During the fourth charge cycle, 37-87-3 exploded.

We concluded that the cathode capacities of 37-87-1, -2, and -3 had been limited by discharging the cells to two volts, which amounted to discharging the cathodes to passivation. We resolved to try preparing flooded electrode cells, using a double separator with Tefzel screen next to the lithium and a less porous separator against the carbon electrode. We hoped that the greater electrolyte convection might postpone positive electrode passivation.

The highest capacities were obtained from cells 37-69-4, 37-75-2, and 37-75-4, each with the 21.5%/ 6.5% = DME/ PC mixed electrolyte. Higher capacities might be available by using an electrolyte mixture which is closer to 14%/ 14% = DME/ PC. Higher cycle lives might also be available by limiting the charge withdrawn to just 500 mAh and by using Tefzel separators to help prevent explosions through dendrite short circuits.

Cell 32-77-4 contained the same approximate volume of organic solvents (28%) and the same concentration of lithium bromide (0.85M) as that commonly used in the lithium/ sulfur dioxide primary cells, except that the solvent was an equal volume mixture of propylene carbonate and 1,2- dimethoxyethane. The objective of the test was to determine whether the organic cosolvent mixture could produce a higher primary capacity, and whether this could be maintained if the discharge depth were kept below 100%. Figure 56 shows most of the first two cycles, and Figure 57, the third and fourth cycles. The charge half cycles all lasted for the preset ten hour period, but the discharge capacities faded quickly from the preset ten hours (500 mAh). Cells 32-77-5 and 32-77-6 were replicate tests and behaved similarly.

The electrolyte of cell 37-95-1 was identical to that of cells 32-77-4, -5, and -6, but the separator consisted of a layer of Fluortex 9-PFK-590 (Tetko) Tefzel screen next to the anode and a layer of Rayperm microporous Tefzel next to the carbon electrode. The object was to provide a spiralled electrode configuration but with flooded electrodes to determine if greater convection in the electrolyte would provide improved mass transport and higher capacity. The common electrode area and the carbon content of the cell were lower than for AA cells with 5 to 8 mil separators. Cell 37-95-1 refused to deliver any substantial secondary capacity. Its replicate, cell 37-95-2, gave only two discharge half cycles.

Cells 37-95-5 and 37-95-6 were similar to 37-95-1 and 37-95-2 except that the Tefzel screen was a finer mesh, Fluortex 9-210/ 46, type 906. The potential during cycling was much steadier for both cells, as shown in Figure 58 for cell 37-95-5. However, the

capacity quickly faded (Figure 59), even though the first few discharge cycles were time limited at ten hours rather than potential limited at two volts. The behavior was similar to that of cells containing only the Hovosorb binderless Pyrex separators.

The solvent ratio was changed from 14%/ 14% dimethoxyethane/ propylene carbonate to 34% DME/ 11% PC for cells 32-85-1, 32-85-2, 32-85-3, and 32-85-4. The total percent by volume of organic cosolvent had been raised from 28% to 45%, and the boiling point of the electrolyte raised nearly to ambient temperature. The mixture represented the largest amount of organic solvent mixture which could be present and still contain enough sulfur dioxide to represent slightly more than one amp hour in an AA cell. As shown in Figure 60 and in Table 9, the capacity fading was severe for all of these cells in spite of the increased concentration of organic solvents.

Solubility of lithium bromide in CsBr/ SO_2. We had discovered that cesium bromide by itself was soluble to at least three molar in sulfur dioxide. We suspected that the solubility of lithium bromide, while it was being favorably affected by the increase in dielectric constant provided by the cesium bromide, was also being adversely affected by the common (bromide) ion effect. One of our goals was to determine what concentration of cesium bromide was required to maximize the solubility of lithium bromide.

The concentration of cesium bromide was varied in steps of 0.10M between 0.1 and 0.5M, then in steps of 0.25M between 0.5 and 2.0M, using the 4 ml Savillex sample vials. Then for each case (11 concentrations of CsBr), the amount of LiBr added to a 4 ml vial was varied, starting from an amount equivalent to 0.5M back down to 0.1M. The solutions were observed to determine whether all of the lithium bromide present had dissolved. The maximum concentration of LiBr was 0.12 molar, when the concentration of CsBr was 1.25 molar. While the maximum solubility of lithium bromide was disappointingly low, solvolysis was slowest when there was no solid LiBr present in the 4 ml vials. 1.25M CsBr/ 0.12M LiBr was used to fill cells either with 52 alloy fillports/ electrical feedthroughs or with negative electrode biased 52 alloy fillport/ tantalum wire glass-to-metal electrical feedthroughs.

AA size cells with alkali bromide electrolytes. Before we had determined how the concentration of cesium bromide affected the solubility of lithium bromide, we worked only with saturated lithium bromide, probably less than 0.2 molar, and either one or two molar cesium bromide. We used either anodized aluminum or titanium as the positive current collector, and Hovosorb or Tefzel screen in conjunction with Rayperm microporous Tefzel as the separator.

Figures 61 and 62 show the first five cycles for cell 32-77-3. The double plateaus during the charge half cycles appeared again, as they had in cell 43-2-4, but were less pronounced during the fourth and fifth cycles. Cell 37-95-4 (Figure 63), with the

titanium as opposed to the anodized aluminum screen, also showed the double plateaus. The capacities were lower than for cell 32-77-3, which had an anodized aluminum screen, but were similar to the reference electrode AA cell, which also had a titanium screen. Replacing the Hovosorb separator either with the coarse or the finer Tefzel screen plus the Rayperm membrane made little difference in the capacity or the appearance of the discharge/ charge profiles (cells 37-95-3; 37-95-4, Figure 63; and 37-95-7, Figure 64).

Cells 32-85-5 and 32-85-6 both contained two molar as opposed to one molar cesium bromide. Cell 32-85-5 (Figure 65) was set at ten hour discharge and charge limits, while cell 32-85-6 (Figure 66) was set at five hour limits, in order to compare potential limited with time limited cycles and their effect on the cycle life. The capacity of cell 32-85-5 faded quickly, while cell 32-85-6 maintained 250 mAh during the five cycle test. Table 10 compares the discharge capacities of cells 32-85-5 with 32-85-6 as a function of cycle number until the capacity of each cell was about 100 mAh.

The total accumulated capacity for cell 32-85-5 was 1.58 Ah, while that for cell 32-85-6 was 2.09 Ah. By the fifth cycle, the discharge profile of cell 32-85-6 showed that its capacity was also fading, but the total capacity delivered was higher.

TABLE 10. Discharge Capacities, in milliamp hours, of AA cells with 2M CsBr/ 0.5M LiBr

Cycle #	Cell #32-85-5	Cell #32-85-6
1	396.7	250.0
2	296.7	250.0
3	271.7	250.0
4	180.8	250.0
5	163.3	250.0
6	169.2	231.7
7	100.8	197.5
8		164.2
9		139.2
10		102.5
Totals	1,579.2	2,085.1

Table 13 includes some cells which contained mixtures of cesium and lithium bromide. The amount of LiBr weighed into the Savillex electrolyte vessels remained equivalent to 0.12 molar, while the cesium bromide concentration was either 1, 1.25, or 1.5 molar. Figure 67 shows the beginning cycle profile for cell 41-26-1. Figure 68 shows both the discharge and the charge capacities as a function of cycle number. The discharge half cycles were allowed to run for as long as the cell could remain above 2 volts. The charge cycles were limited to five hours or 4 volts, whichever came first. The primary capacity was 388 mAh at 38.1 mA, and the primary charge capacity was 5 hours times 38.1 mA, or 190.5 mAh.

All of the subsequent charge capacities were time limited at 190.5 mAh. While the cell did continue to cycle without shorting, none of the succeeding discharge cycles gave capacities equivalent to the charge capacity. The test was terminated after 16 cycles. Cells 41-26-2 (Figure 69), 41-26-4 (Figure 70), 41-26-5 (Figure 71), 41-27-1 (Figure 72), and 41-27-2 (Figure 73) all behaved in a manner similar to cell 41-26-1.

We had available D size covers with both tantalum wire glass-to-metal electrical feedthroughs and 52 alloy fillports welded to the rims. We cut D size cans to a height of 5/8 inch and used wound electrodes to prepare case negative cells. Of the two such cells tested, 41-31-3 exploded during its primary discharge cycle (Figure 74) after delivering a capacity of 462 mAh at 1 mA/ cm^2, or about 4 mAh/ cm^2. The second, cell 41-31-4, gave a primary capacity of 466 mAh, a secondary capacity of 28.7 mAh, and a tertiary capacity of only 7.7 mAh (Figure 75). All of the charge cycles were time limited, although a plateau at about 3.5 volts appeared during the first charge cycle, perhaps as the result of the formation of bromine.

Test tube cells. The purpose of the test tube cells was to determine whether the capacity of carbon electrodes in the AA cells was being limited by the geometry or by the chemistry. In the test tube cells, the carbon electrode was completely flooded by a large excess of electrolyte. In addition, the carbon substrate could be made entirely from an inert metal such as tantalum. Imbedding the glass pipettes into the lithium reference and working electrodes provided a seal which prevented electrolyte from reaching the electrode contact hardware and causing local discharge reactions. The disadvantage was that the boiling point of the electrolyte had to be above ambient temperature, which meant using 56 volume percent cosolvent mixture with the sulfur dioxide and the electrolyte salt. Cosolute electrolytes could not be used.

Table 11 summarizes the results of tests where the carbon electrodes were either pressed or painted onto tantalum or molybdenum substrates. The electrolyte salt was tetraethylammonium bromide. The carbon electrode would not be expected to passivate during discharge, since the anticipated product, tetraethylammonium dithionite, would be soluble in the sulfur dioxide/ organic solvent mixture. A resistive load of 1 KΩ corresponds to a current density of about 5 mA/cm^2, and 500 ohms, 10 mA/cm^2, both considerably greater than the current density used in the AA cells. The discharge profiles for cells 39-91-1, 41-1-1, 41-4-1, and 41-5-1 are shown Figures 76 and 77. The running potentials were lower than they had been for the AA cells, but the primary specific capacities were roughly 4.6 times higher, even at the higher current densities. A capacity of 500 mAh in an AA cell corresponds to only 8.6 mAh/ cm^2.

While the specific capacities of the cells in Table 11 were expected to be high because of the electrolyte salt used, test tube cells 41-13-1 and 41-14-1 contained 1.7 molar lithium

TABLE 11. Capacities of Test Tube Cells Containing Quarternary Ammonium Bromide Electrolytes

(Cathode area = 0.42 cm²)

Cell No.	Separator	Positive contact scrn. cath.	Electrolyte Salt	Conc.	Approx. volume	Other	Load (KΩ)	Average Potential (V)	Specific Capacity (mAh/cm²)	Figure
39-91-1	(none)	Ta painted	NBt_4^+	1.70M	4ml	DME, 43% PC, 13%	1.02	2.2	45.7	76
41-1-1	(none)	Ta painted	NBt_4^+	1.70M	4ml	DME, 43% PC, 13%	1.02	2.1	36.7	77
41-4-1	Crane-glass	Ta pressed	NBt_4^+	1.70M	4ml	DME, 43% PC, 13%	0.50	2.12	37.5	77
41-5-1	Crane-glass	Mo pressed	NBt_4^+	1.70M	4ml	DME, 43% PC, 13%	0.50	2.2	39.9	77

bromide. The anticipated product was lithium dithionite, which was expected to accumulate in the carbon electrode. These cells contained reference electrodes (Figure 1) and were cycled on the computer at 1 mA/ cm², using two extra power supplies to monitor each of the electrodes versus the lithium reference electrode (Figure 5). A summary of the results is given in Table 12 and in Figures 78-83.

TABLE 12. Capacities of Test Tube Reference Electrode Cells Containing LiBr/ Organic Solvents

Cell No.	Separator	Positive contact scrn. cath.	Electrolyte Salt	Conc.	Approx. volume	Other	Discharge capacity, mAh, to 2V or to preset cutoff time (Positive electrode area, 1cm²) pri.	sec.	3rd	4th	5th	Figure
41-13-1	Crane-glass	Mo pressed	LiBr	1.7M	10 ml	DME, 43% PC, 13%	15.0*	32.5	9.33	8.79	7.04. . .	78-83
41-14-1	Crane-glass	Mo pressed	LiBr	1.7M	10 ml	DME, 43% PC, 13%	44.5	47.2	8.83	12.8	14.3. . .	

* Cell did not complete cycle and was restarted.

Perhaps the most important result was that the polarization at the end of the discharge half cycles was due exclusively to passivation of the carbon electrode. The lithium electrode showed its greatest polarization during the onset of the discharge half cycles (Figure 83). In the wound electrode AA cells with limited electrolyte (for example cell 43-2-3), the greatest lithium polarization had occurred near the end of the discharge half cycle. Since the carbon electrode area for cells 41-13-1 and 41-14-1 was about 1 cm², the capacities noted in Table 12 are also specific capacities. A specific capacity of 20 mAh/ cm² corresponds to about 1.2 Ah from an AA cell. The specific capacity of the carbon electrodes in flooded electrode test tube cells with electrolyte containing lithium ranged widely, but

reached a value about 5.5 times higher than was obtained in the AA cells.

Button cells. The purpose of the button cell tests was to determine whether the chemistry available from test tube cells, numbers 39-91-1, 41-1-1, 41-4-1, and 41-5-1, could be packaged into a practical configuration with starved electrodes. With an area of roughly 3.3 cm^2, a flooded carbon electrode in a test tube cell would be expected to deliver about 132 mAh. Button cells 41-2-2, 41-3-1, 41-3-2, and 41-3-3 were all discharged and charged at 10 mA constant current, or 3 mA/ cm^2. The carbon electrode in the first of these was painted; in the others the carbon electrodes were pressed. The highest capacity obtained from any discharge cycle was only 3.3% of the expected value (results not shown).

TRIFLUOROMETHANESULFONATE (TRIFLATE) ELECTROLYTES

Solubility of LiBr in $CsCF_3SO_3$/ SO_2. Cesium triflate was investigated as a possible cosolute to increase the solubility of lithium triflate or bromide. We believed that some bromide was necessary to provide overcharge protection, but a lower concentration of bromide in the presence of another anion might mean that there would be less of a tendency for the bromide tc undergo solvolysis to sulfur monobromide.

Cesium triflate by itself was soluble to at least 0.75 molar in liquid sulfur dioxide. The solubility of potassium triflate was between 0.35 and 0.5 molar. Lithium triflate and lithium tetrafluoroborate were essentially insoluble in sulfur dioxide. All solutions containing only triflate salts were water white. Solutions in which bromides had been included with the salt mixture were various shades of yellow, indicating at least that bromide was present in solution.

Cells with trifluoromethanesulfonates. Table 13 is a summary of the cell constructions, electrolyte compositions, and Figure references for cells containing lithium bromide with cesium triflate or cesium bromide. Included are AA size cells, AA cells with reference electrodes, and thin walled D width cells.

Cells 41-36-1 and 41-36-2 were similar to the previous AA cells in that the positive electrode contacts were also 52 alloy tubes. However, the weight of the salts in the electrolyte reservoir corresponded to 0.75 molar cesium triflate/ 0.15 molar lithium bromide. Both cells failed to discharge even on light loads. As shown in Figures 84 and 85, the open circuit potentials were not steady as a function of time.

When AA size tantalum feedthrough tops were available, cells were prepared with the tantalum feedthroughs at one end and 52 alloy tube fillports at the other. As explained above, the tubes were connected to the cases of case negative cells to provide cathodic protection against corrosion. Cells 41-50-1, 41-50-2, 41-51-1,

TABLE 13. Summary of Cell Construction and Electrolyte Composition: Cells Containing Lithium Bromide with Cesium Bromide or Triflate

CELL #	POSITIVE ELECTRODE[2]							ELECTROLYTE		FIGURE #s
	Const. Type[2]	Carbon/ Teflon[3]	Thickness (mils)	Loading mg/cm²	Carbon Wt./mg	Method[4]	Common Area/cm²	Composition	Weight (g)	
41-26-1	A	75/25/10	23	28.3	753	P&R	53.2	1.25 M CsBr 0.12 M LiBr	5.68. . .	67,68
41-26-2	A	75/25/10	23	24.2	643	P&R	53.2	1.5 M CsBr 0.12 M LiBr	5.66. . .	69
41-26-4	A	75/25/10	26	35	842	P&R	48.0	1.0 M CsBr 0.12 M LiBr	5.50. . .	70
41-26-5	A	75/25/10	21	20.7	620	P&R	60.0	1.0 M CsBr 0.12 M LiBr	5.83. . .	71
41-27-1	A	75/25/10	30	21.9	481	PO	44.0	1.25 M CsBr 0.12 M LiBr	5.81. . .	72
41-27-2	A	75/25/10	31	26	494	PO	38.0	1.5 M CsBr 0.12 M LiBr	5.21. . .	73
41-31-3	D	75/25/5	23	22.1	2,540	P&R	115	1.5 M CsBr 0.12 M LiBr	32.1. . .	74
41-31-4	D	75/25/5	23	22.2	2,551	P&R	115	1.5 M CsBr 0.12 M LiBr	30.2. . .	75
41-36-1	A	75/25/5	23	21.7	471	P&R	43.3	0.75 M CsTr 0.15 M LiBr	5.23. . .	84
41-36-2	A	75/25/5	23	20.5	468	P&R	45.6	0.75 M CsTr 0.15 M LiBr	5.25. . .	85
41-50-1	T	75/25/5	23	22.8	418	P&R	36.3	0.75 M CsTr 0.15 M LiBr	5.23. . .	
41-50-2	T	75/25/5	23	22.5	426	P&R	36.3	0.75 M CsTr 0.15 M LiBr	4.43. . .	
41-51-1	T	75/25/5	23	25.4	461	PT	36.3	0.75 M CsTr 0.15 M LiBr	4.35. . .	
41-51-2	T	75/25/5	23	25.8	468	PT	36.3	0.75 M CsTr 0.15 M LiBr	4.05. . .	
41-53-1	R	75/25/5	23	22.5	433	P&R	38.4	1.25 M CsBr 0.12 M LiBr	5.60. . .	43-45
41-53-2	R	75/25/5	23	22.5	433	P&R	38.4	1.25 M CsBr 0.12 M LiBr	5.74. . .	46-48

[1] Screen & Tab for Positive Electrode:
Collector screen: Aluminum anodized in 50/50 isopropanol/ water/ 0.2M NH_4HCO_3 at 160 mV vs Ag/ AgCl/ 0.1M KCl. The tabs were non-anodized aluminum.

[2] Construction type:
A: AA size cell; 52-Alloy feedthrough/fillport, case negative
D: D width cell; 52-Alloy Fillport cathodically protected, Tantalum feedthrough to positive, case negative
T: AA size cell; 52-Alloy Fillport cathodically protected, Tantalum feedthrough to positive, case negative
R: AA size cell; 52-Alloy Fillport with reference electrode, Tantalum feedthrough to positive, case negative. Discharge at 100Ω constant load

[3] Carbon:
75/25/10: Carbon ratio, 75 weight percent Chevron acetylene black, 25 weight percent Ketjenblack. The Teflon binder content was 10 percent of the weight of the carbon mixture.
75/25/5: Carbon ratio, 75 weight percent Chevron acetylene black, 25 weight percent Ketjenblack.

TABLE 13 (Continued).

The Teflon binder content was 5 percent of the weight of the carbon mixture.
[4])Positive Electrode Construction:
P&R = Pressed and Rolled; PO = Pressed Once; PT = Pressed Twice
Separators: "Novosorb" #8605298, 0.010"

and 41-51-2, even though they had tantalum positive feedthroughs, also showed unsteady open circuit potentials over a sixteen hour period.

When we began the study of the solubility of lithium bromide in solutions of cesium triflate/ SO_2, we believed at first that we could alleviate bromide common ion effect, bromide solvolysis, and increase the concentration of lithium, simply by lowering the overall concentration of bromide. In fact, common ion effects with lithium will exist for any combination of salts, since for example the introduction of cesium triflate into CsBr/ LiBr/ SO_2 or into LiBr/ SO_2 is equivalent to introducing both cesium triflate and lithium triflate. Although the yellow color of solutions prepared with lithium bromide indicated the presence of bromide, the solutions may have been devoid of lithium because of metathesis:

$$Cs^+ + Tr^- + \underline{LiBr} \longrightarrow Cs^+ + Br^- + \underline{LiTr} \qquad (8)$$

If lithium triflate were completely insoluble in sulfur dioxide solutions of cesium triflate, then lithium ions attempting to pass from a discharging lithium anode through a salt film (solid electrolyte interphase) would be precipitated by the triflate present in the solution. It would therefore have been impossible to discharge cells because the lithium anodes would become passivated with insoluble lithium triflate.

During the corrosion studies, described in the next section, various metal samples were used as working electrodes in cyclic voltammetric measurements. Cathodic currents in the vicinity of the lithium potential were found in CsBr/ SO_2 only when lithium bromide was also present in solution. CsTr/ SO_2 in which we had made an effort to dissolve LiBr also showed no cathodic current in the vicinity of the lithium potential.

The reduction of the cation of an active metal such as lithium or cesium from electrolytes based on sulfur dioxide is made possible by the ability of the cation to be transported through the solid electrolyte interphase. The mobility of lithium in the salt films is adequate, but the mobility of the large cesium cation is low. The failure of the corrosion samples to show cathodic currents near the lithium potential from SO_2 solutions of CsTr/ LiBr was accepted as confirmation that lithium ions were essentially absent from the triflate solution, and that the AA size cells had failed to function because lithium triflate was insoluble.

CYCLIC VOLTAMMETRIC CORROSION MEASUREMENTS

The original purpose of these measurements was to identify quantitatively the corrosion rates, in milli-inches per year, of various metals of potential use as positive electrode supports and contact hardware for lithium/ sulfur dioxide cells containing alkali bromides. Table 14 is a summary of the results taken from the corrosion current measurements.

TABLE 14. Quantitative Estimation of Corrosion Rates of Various Metals in Sulfur Dioxide Solutions of Cesium and Lithium Bromide, using Cyclic Voltammetric Analysis

Working electrode	Electrolyte CsBr	LiBr	Result
SS 303	(1M $LiAlCl_4$/ $SOCl_2$/ SO_2Cl_2)		System test: geometric configuration
Pt	0.98M	0.10	Severe corrosion: used as reference and counter electrode contacts.
Kovar	0.98M	0.10	Qualitative: stable as reference and counter electrode contacts.
Mo	0.98M	0.10	Corrosion of surface was evident.
Ti	1.5M	0.12	Current oscillations: poor Li^+ diffusion in high Cs^+ concentration. Corrosion rate at ambient temperature, 0.90; 0.84 mils per year.
Ta	0.25M	0.10M	Excessive IR drop
	1.5M	0.12M	Corrosion rate at ambient temperature: 0.55 mils per year.
	0.5M	none	High cathodic currents at dithionite potential; no cathodic current at lithium potential
Nb	1.5M	0.12	Corrosion rate at ambient temperature: 0.14 mils per year (from linear polarization); 0.59 mils per year (from Tafel slope)

Using the tantalum working electrode, the behavior of a 0.75 molar solution of cesium triflate "saturated" with lithium bromide was similar to 0.5M cesium bromide without lithium bromide, in that there was no cathodic current when the potential of the working electrode was reduced to the lithium potential. We concluded that lithium ion was absent from the triflate solution, and therefore that lithium triflate was insoluble. Cesium was not reduced, apparently because the large cations were unable to migrate through the solid electrolyte interphase which had formed on the working electrode. Corrosion currents were higher if electrolyte solutions were allowed to stand, evidently because solvolysis allowed the formation of bromine.

DERIVATIVES OF LITHIUM TETRACHLOROALUMINATE

Attempts to Prepare bridged oxidoaluminate. By preparing an alu-

minate of much larger size than $AlCl_4^-$, we hoped to produce a sulfur dioxide solution containing aluminum where the anion could not participate in the reduction of sulfur dioxide during cell discharge. Bailey and Blomgren have reported that when water is slowly added to a refluxing solution of $AlCl_3$ in thionyl chloride, a species is formed which gives rise to infrared absorbances at 795 and 670 cm^{-1}. They identify the species as the bridged oxido- aluminate $[Cl_3Al\text{-}O\text{-}AlCl_3]^{2-}$ [13]. The same species was also said to form by the reaction of $AlCl_3$ with Li_2O in thionyl chloride.

We attempted to prepare this oxidoaluminate by heating distilled anhydrous aluminum chloride with lithium oxide, lithium carbonate, and by reacting water with solutions or mixtures of $AlCl_3$ in sulfuryl chloride, tetrahydrofuran, and methylene chloride. We avoided thionyl chloride to prevent side reactions. None of the resulting solids would dissolve in sulfur dioxide. We then attempted to repeat the results reported by Bailey and Blomgren, by refluxing 1M $LiAlCl_4$/ $SOCl_2$ with water equivalent to 0.5, 1.0, and 1.5 times the number of moles of aluminum present. In each case, the solution apparently reverted to $LiAlCl_4$/ $SOCl_2$.

Attempts to prepare mixed aluminate species. As an alternative approach to finding lithium salts of large aluminate anions which would be soluble in sulfur dioxide, much work was directed toward preparing mixed aluminate ions of the type $(AlCl_3X)^-$:

$$AlCl_3 + LiX \text{ ---> } Li^+AlCl_3X^- \qquad (9)$$
$$X = \text{triflate, tosylate, bromide, etc.}$$

The following salts were either heated with aluminum chloride or equilibrated in sulfuryl chloride or sulfur dioxide at a molar ratio of 1 to 1: lithium triflate, lithium tosylate, and lithium chloroacetate. None of the resulting mixtures were substantially soluble in sulfur dioxide.

Similar reactions were carried out in attempts to prepare mixed chloro- and bromoaluminates such as $AlCl_3Br^-$ or $AlCl_2Br_2^-$ which would be soluble in sulfur dioxide. Enough $AlCl_3$ and LiBr were added to a 4 ml Savillex vial to prepare a 1 M solution of each. Liquid SO_2 was added and the vial sealed. Even after the mixture had stood over the weekend, most of the LiBr had not dissolved. If the salt mixture were first melted in the absence of air and allowed to solidify, the resulting $LiBr \cdot AlCl_3$ also did not dissolve. Disproportionation to insoluble $AlBr_3$ or $LiAlBr_4$ may have been occurring.

Sequestered lithium tetrachloroaluminate. When the electrolyte of a lithium/ sulfur dioxide cell contains a mixture of alkali and alkaline earth tetrachloroaluminates, the sulfur dioxide is reduced not to lithium dithionite, but to a complex salt involving the aluminum Report 6, [2-6, 8-9]. The aluminum interferes with the formation of dithionite, so that the primary capacity of lithium cells with identically designed carbon-based cathodes is lower if the electrolyte salt is $LiAlCl_4$ than if it is, for

example, $LiGaCl_4$ or LiBr with acetonitrile.

We wished to determine whether lithium tetrachloroaluminate at 1 molar could be sequestered to prevent it from participating in the reduction of sulfur dioxide. Since $LiAlCl_4$ is so extremely soluble in oxyhalides, we chose two molar chloroacetyl chloride, $CH_2ClCClO$, as most nearly resembling an oxyhalide, with a reduction potential sufficiently lower than the sulfur dioxide/ lithium dithionite potential to prevent its being reduced on the carbon along with or instead of the sulfur dioxide.

Among five AA cells, the capacities were all less that 300 mAh at 50 mA. All discharged above three volts, indicating that the chloroacetyl chloride did not succeed in preventing the aluminum from participating in the discharge reaction. All of the cells except one exploded. One cell initiated the explosion, while nearby cells were apparently shock sensitive and exploded as the result of the initiating cell.

Sulfito-aluminates. Reaction between aluminum chloride and a soluble sulfite in SO_2 leads to precipitation of aluminum sulfite. In the presence of an excess of the sulfite, however, the precipitate is reported to redissolve to form a soluble sulfito-aluminate [14]. Neither the tetramethyl- nor the tetraethylammonium sulfite proved to be sufficiently soluble in SO_2, in each case being well below 1 molar. Addition of aluminum chloride in amounts such that the sulfite ion would always be present in at least a 3:1 excess did not appear to change the amount of undissolved solid present.

SULFUR AND NITROGEN BASED COSOLUTE CATIONS

Sulfonium salts. Tetraalkylammonium and tetraalkylphosphonium salts are highly soluble in SO_2, and have been used to "modify" or increase the solubility of lithium salts in that solvent [7b]. Trialkylsulfonium ions are similarly ions of low charge containing large organic groups, and might also be soluble. Three sulfonium compounds were prepared and their solubility and behavior in sulfur dioxide were tested.

The bromide and triflate salts of trimethylsulfonium and the triflate salt of dimethylphenylsulfonium were found to be very soluble in sulfur dioxide, and increased the solubility of lithium salts. In a 1 M solution of $S(CH_3)_3Br$, lithium bromide was soluble to at least 0.2 molar.

When SO_2 solutions of the sulfonium salts were tested for reactivity with lithium metal, the lithium reacted in each case over the course of a few minutes to a few hours. Reddish-brown to black solids formed, and eventually the chunks of lithium completely disintegrated.

Nitrogen bases: N-methylpyridinium, hexamethylenetetramine and guanidine derivatives. Alkyl-substituted ammonium bromides and

N-methylpyridinium bromide had shown good solubility in sulfur dioxide, but were reactive towards lithium. We had never investigated how lithium would behave in the presence of salts other than bromides or thiocyanates. A series of compounds was therefore investigated as possible agents for increasing the solubility of other lithium salts in SO_2, as well as lithium bromide.

N-methylpyridinium chloride proved to be soluble in SO_2, to greater than 5 molar. A series of solutions was prepared containing 5 molar N-methylpyridinium chloride and enough of various lithium salts to make a concentration of 0.5 molar. Lithium tosylate, triflate, trifluoroacetate, tetrafluoroborate, and chloride were tested. In each case there was little or no corrosion of the lithium metal by the solution. However, very little if any of the lithium salts dissolved. Sulfur dioxide solutions which were 2, 3, 5, and 7 molar in N-methylpyridinium chloride failed to make LiCl substantially soluble. The stability of lithium metal in high concentrations of N-methylpyridinium chloride was not expected, in light of the observation that lithium was not stable in SO_2 solutions of N-methylpyridinium bromide/ lithium bromide.

N-methylhexamethylenetetramine chloride was also very soluble in sulfur dioxide, up to at least 4 molar. No reaction with lithium metal was observed in these solutions. However, neither lithium bromide nor lithium chloride was soluble at 0.5 molar even in concentrated solutions of the amine salt.

A series of guanidine derivatives were tested for solubility and reactivity with lithium. We believed that the hexa-substituted derivatives would react less with lithium, since they did not contain any labile nitrogen-hydrogen bonds. Lithium showed no reaction with ethylpentamethylguanidinium chloride, but lithium did decompose slowly in solutions of tetramethylguanidinium bromide and diethyltetramethylguanidinium bromide. Lithium bromide did not appear to be significantly soluble in any of these solutions.

Solutions of unsubstituted guanidine hydrobromide in sulfur dioxide surprisingly did not react significantly with lithium metal at ambient temperature on exposure for one week. Both guanidine hydrochloride and guanidine hydrobromide were soluble to over 5 molar. In solutions of the hydrobromide at intermediate concentrations, two phases were present. At 2 molar, the upper phase was about three times the volume of the lower, or denser layer. As the concentration increased, the volume of the upper layer decreased. At 4 molar, only a very small upper layer was present. A 5 molar solution was homogeneous. In mixtures with two layers, neither layer reacted with lithium.

Lithium bromide was found to be soluble in concentrated solutions of guanidine hydrobromide in liquid sulfur dioxide. At 5 molar guanidine hydrobromide, LiBr dissolved to at least 0.7 molar, though it did not reach 1 molar. A 52 alloy feedthrough tube was tested at the positive electrode against an aluminum screen with

pressed cathode material, and caused the 5M $H_6(N_2C)^+Br^-$/ 0.7M LiBr to become dark reddish brown. Electrolyte samples underwent noticeable solvolysis, apparently with the formation of minor amounts of sulfur monobromide, within a few weeks.

AA cells with guanidinium bromide/ lithium bromide. Cells 45-88-2, -3, and -4 all contained screened positive electrodes and 5M $H_6(N_2C)^+Br^-$/ 0.7M LiBr. All showed low primary capacity, and during the charge cycles, each ran 10 hours without exceeding 4 volts. All failed to deliver substantial capacities during subsequent discharge cycles. Cell 45-88-2 had the highest primary capacity, but only 155.8 mAh (Figure 86).

Cells 46-88-1 and -2 contained the same electrolyte, but painted positive electrodes on aluminum foil. The behavior of each of these cells was similar to the other. The discharge/ charge profiles for cell 46-88-1 are shown in Figure 87 as an example. The positive electrodes could not maintain a current density of 1 mA/ cm^2, and so the cells were restarted at 50 mA, or about 0.43 mA/ cm^2. The discharge capacities were low, and again the charge cycles lasted the allowed ten hour limit without exceeding four volts.

The same electrolyte was used in similar cells with positives containing 25 weight percent Ketjenblack/ 75% acetylene black, and 10% instead of 5% Teflon binder. The result was even more disappointing. Cell 51-5-3 gave only 25.4 mAh during its first discharge cycle. It accepted charging current, but refused to deliver any substantial capacity during a second discharge half cycle. A replicate, cell 51-5-4, behaved similarly.

Electrolytes with guanidinium bromide/ cesium bromide/ lithium bromide. The high concentration of guanidinium ion may have been impeding the mobility of lithium ion, a phenomenon we noticed also when high concentrations of cesium were causing unstable currents during the reduction of lithium ion from SO_2/ CsBr/ LiBr. It was not possible to prepare solutions in which the concentration of $H_6(N_2C)^+Br^-$ was lower than 5 molar, since as we explained above, two liquid phases were formed if the average concentration of $H_6(N_2C)^+Br^-$ was lower than about 5 molar.

We then tried mixing all three of LiBr, CsBr, and $H_6(N_2C)^+Br^-$ in order to lower the total concentration of non-lithium cation without excessively lowering the concentration of lithium ion, and without encouraging the corrosion of lithium metal. We successfully prepared 1M $NH_2^+=C(NH_2)_2$ Br^-/ 1M CsBr/ 0.5M LiBr, as having a reasonably high concentration of lithium and a reduced concentration of non-lithium cation. However, these solutions soon developed a deep brown color at ambient temperature, and were likely undergoing solvolysis rapidly. Hydrolysis of samples of electrolyte solutions showed that water-insoluble substances with powerful and obnoxious aromas, perhaps including sulfur monobromide, had formed.

Lichtin believes that it is oxygen and traces of moisture, and

not sulfur dioxide, which are responsible for the oxidation of bromide in solutions of sulfur dioxide [15]. However, we had taken what we believed were adequate precautions to exclude air and moisture from sulfur dioxide solutions of bromide salts, and noted that the degree of decomposition seemed more extensive than what could be explained based on the likely concentration of oxygen in these solutions. In addition, Audrieth has discussed other reactions in sulfur dioxide involving solvolysis without redox, which apparently are similar in nature to the first step in the solvolysis of bromide in sulfur dioxide to thionyl bromide, and its subsequent disproportionation to bromine and sulfur monobromide [16]. It is possible that moisture or lithium ion exert a catalytic effect on the solvolysis of bromide in sulfur dioxide, since the solutions were stable in the absence of lithium bromide, and lithium bromide is nearly impossible to dry completely, simply by heating in vacuo.

Extreme measures, such as the use of vacuum line techniques to exclude oxygen and moisture, were thought impractical in a situation where the most important objective has been to prepare inexpensive, reliable rechargeable cells. We therefore decided at last to abandon the concept of the "cosolute" as a means to increase the solubility of a lithium salt in sulfur dioxide, in favor of lithium rechargeable cells containing sulfur dioxide solutions of tetrachloroaluminate salts.

MIXED TETRACHLOROALUMINATES

AA size cells. We then transferred our attentions to lithium/ sulfur dioxide AA size cells in which the electrolyte contained a high concentration of mixed tetrachloroaluminate salts. We resolved to take advantage of the known high degree of reversibility and the superior shelf life of this system. The major purposes of studying variations in the electrolyte, the composition of the positive electrodes, and the design of the electrodes were first to determine whether the capacity could be improved compared with previous cells, and second, to determine whether cells could maintain improved capacity as a function of cycle life. Our purpose in determining how to measure and remove moisture from the carbon electrodes, and in carrying out extensive cycle tests, was to establish whether we could eliminate explosions during charge cycles by removing moisture.

We tried four dried electrolytes, all with the molar ratio of aluminum to sulfur near 1:3. The first, designated "2/1", was $2LiCl \cdot CaCl_2 \cdot 4AlCl_3 \cdot 12SO_2$, the same composition, except for the drying process, which had been used during the previous contracts [6, 8]. Its main purpose was to compare different carbon types, carbon ratios, and carbon/ binder ratios with what we considered to be the "baseline" cells, which contained "2/1" with 25% Ketjenblack/ 75% acetylene black/ 10% Teflon binder [8]. We also prepared 2/1 with sulfur trioxide equivalent to half of the aluminum present.

The second electrolyte combined three basic salts, lithium, calcium, and sodium chlorides, with aluminum chloride, such that lithium constituted half of the cationic content of the mixture, as it had in "2/1": $3LiCl \cdot CaCl_2 \cdot NaCl \cdot 6AlCl_3 \cdot 18SO_2$. It was designated "3/1/1".

The third electrolyte was "4/1", or $4LiCl \cdot CaCl2 \cdot 6AlCl_3 \cdot 18SO_2$. We had already studied cells with a few different combinations of lithium and calcium chloride, including 4/1, and $LiCl \cdot NaCl \cdot 2AlCl_3 \cdot 6SO_2$ [8], and wished to determine what effect 4/1 would have on alternative positives.

The fourth was "1/1", or $LiCl \cdot CaCl_2 \cdot 4AlCl_3 \cdot 12SO_2$, an acid electrolyte, with excess $AlCl_3$ in an attempt to increase the capacity by dissolving the lithium chloride formed during primary discharge. The hope was that the carbon electrode would become "conditioned" to the higher capacity during subsequent discharges.

Most cell positives contained Chevron 50% compressed acetylene black, with various amounts of high surface area blacks such as Ketjenblack, but including also Darco S51 and KB-B, Norit SX-2 activated carbon, Ensari Super S, and polyparaphenylene [17]. The specific surface areas of Darco S-51, KB-B, and Norit SX-2 are respectively 650, 1,500, and 800 m^2/g.

Four types of positive electrodes were studied. The first consisted of expanded and anodized aluminum foil on which carbon/ binder mixtures which had been "cured" at 280°C. for 15 minutes, then chopped in a blender, were pressed. The second was anodized aluminum foil on which mixtures including "Aquadag" or "Electrodag" (Acheson Colloids) with DuPont Teflon suspension and various carbon samples were painted, then cured. The third type of positive electrode was carbon/ binder kneaded with 50/50 water/ isopropanol and spread wet onto an expanded foil screen, which avoided having the binder damaged during the dry blending operation, but which made it difficult to prepare positives with reproducible thickness and loading. The positives were air dried, then cured. The fourth was the annular bobbin case positive, in which a tight fitting cylindrical carbon ring was placed inside the cell case, held there through a cylinder of separator and two semi-cylindrical pieces of lithium by a central spring made of a coil of stainless steel ribbon. The two lithium pieces were electrically connected to each other and to the 52 alloy feedthrough tube.

Data for cells containing mixed tetrachloroaluminate salts are summarized in Table 15. Included are the cell number, the electrolyte composition, and a summary of each positive electrode composition, both of which are explained at the foot of Table 15. Next is the capacity of the first discharge half cycle followed by the capacity and the number of the last discharge half cycle. Tests were terminated either because the discharge capacity was below 400 mAh, or the cell shorted or exploded during the last charge cycle. The charging regime for most cells was 10 hours or 4.1 volts, whichever came first. Charging occurred between 3.75

and 3.85 volts, with overcharge plateaus near 4.05 volts. If discharge capacities exceeded 500 mAh, the charging time was increased to 15 hours.

TABLE 15. SUMMARY OF AA SIZE CELL DATA: CELLS CONTAINING MIXED TETRACHLOROALUMINATE SALTS IN SULFUR DIOXIDE

Cell #	Electrolyte[1]	Cathode composition[2]	Primary discharge capacity (mAh)	Discharge capacity, last cycle (mAh)	# of last cycle[3]	Figure numbers
45-79-3	3/1/1	25Kj/75ab/10T	419	352 (no chg.>cy.25)		91,92
45-79-4	3/1/1	25Kj/75ab/10T	325.1	282 (no chg.>cy.4)		
45-94-1	2/1	100Kj/5T	364.1	381 (no chg.>cy.2)		95
45-94-2	2/1	100Kj/5T	610	(would not accept charge)		
45-94-3	2/1	100Kj/5T	483	(would not accept charge)		
45-94-4	2/1	100Kj/5T	467.4	578 (no chg.>cy.2)		
45-94-5	2/1	100Kj/5T	466	(would not accept charge)		
46-81-1	2/1	100A/10T;75Kj/25A/	341	(shorted, 1st charge cycle)		
46-82-4	2/1	10T;2 more layers	283	(would not accept charge)		
46-82-5	2/1	on Al foil	278	(would not accept charge)		
46-87-1	2/1	A/T;50Kj/50A/T;41/f	244	(would not accept charge)		
46-87-6	2/1	A/T;50Kj/50A/T;41/f	241	(would not accept charge)		
46-95-1	2/1	25Kj/75ab/14T;2xC	436	284	52,exp!	
46-92-5	2/1	25Kj/75ab/14T;A/10T	298	(would not accept charge)		
50-15-1	3/1/1	25Kj/75ab/10T	378	(shorted, 1st charge cycle)		
50-15-2[5]	3/1/1	25Kj/75ab/10T	372	378 (short,cy21chg)		
50-15-3[5]	2/1	25Kj/75ab/10T	410	421 (short,cy19chg)		88-90
50-28-2	3/1/1	100Kj/10T	575	(would not accept charge)		
50-28-3	3/1/1	100E/10T;3x/f	102	(would not accept charge)		
50-29-4	3/1/1	87Pp/13ab/10T	82.5	(poor charging efficiency)		
50-29-5	3/1/1	87Pp/13ab/10T	79.4	(poor charging efficiency)		
50-34-3[5]	2/1	100N/10T	199	197	32	
50-34-4[5]	2/1	100N/10T	164	222	36	
50-36-1	2/1	100D_1/10T	302	276 (no chg.>cy.4)		
50-36-2	2/1	100D_1/10T	271	291 (no chg.>cy.3)		
51-1-1	3/1/1	100ab/3T	245	(would not accept charge)		
51-1-2	3/1/1	100ab/3T	309	248 (no chg.>cy.2)		
51-1-4	3/1/1	100ab/3T	224	(would not accept charge)		
51-3-1	3/1/1	100ab/3T	206	(would not accept charge)		
51-3-2	3/1/1	100ab/3T	212	(would not accept charge)		
51-6-1[4]	3/1/1	25Kj/75ab/10T	410	(would not accept charge)		
51-6-2[4]	3/1/1	25Kj/75ab/10T		(refused to function)		
51-6-6	3/1/1	100ab/3T	262	220 (no chg.>cy.2)		
51-13-1[5]	2/1	25Kj/75ab/20T(wr)	346	216	21,short.	
51-13-2[5]	2/1	25Kj/75ab/20T(wr)	356	300	12,short.	
51-13-4[5]	2/1	25Kj/75ab/5T(Ni,wr)	352	233	21,short.	
50-38-2[5]	4/1	25Kj/75ab/10T	309	289	5,short.	
50-38-3	4/1	25Kj/75ab/10T	194	(refused to function)		
50-45-3	4/1	E.Super S/10T	143	(refused to function)		
50-46-1	4/1	E.Super S/10T	143	(would not accept charge)		
51-17-1	2/1	25Kj/75ab/5T(Ni,wr)	191	(would not accept charge)		
51-18-1	2/1	25Kj/75ab/5T(Ni,wr)	452	(would not accept charge)		

TABLE 15 (Continued).

Cell #	Electrolyte[1]	Cathode composition[2]	Primary discharge capacity (mAh)	Discharge capacity, last cycle (mAh)	# of last cycle[3]	Figure numbers
50-46-2[5]	2/1	E.Super S/10T	179	(poor discharge capacity)		
52-65-3[6]	2/1	25Kj/75ab/10T(Ni,wr)	414	423	7,short	
50-61-1	2/1	D_2/10T	(refused to function)			
50-61-2	2/1	D_2/10T	(refused to function)			
50-41-3[5]	2/1	25Kj/75ab/10T(PF)	409	356	18,short.	
50-41-4[5]	2/1	25Kj/75ab/10T(PF)	434	356	17,exp!	107
51-15-2[5]	2/1(SO_3)	25Kj/75ab/20T(wr)	307	279	13,remv'd.	
51-15-3[5]	2/1(SO_3)	25Kj/75ab/20T(wr)	301	279	13,short.	
51-15-1[5]	2/1	25Kj/75ab/20T(wr)	382	330	19,remv'd.	
50-67-3[5]	2/1	25Kj/75ab/10T(Tfz/HV)	451	175	7,short.	
50-67-4[5]	2/1	25Kj/75ab/10T(Tfz/HV)	423	156	3,short.	
50-66-1[5]	2/1	25Kj/75ab/10T(Tfz/HV)	405	225	5,short.	
50-74-4[5]	2/1	25Kj/75ab/10T(+ s.a.)	531	567	11,short.	
50-73-2[5]	2/1	25Kj/75ab/10T(+ s.a.)	517	554	11,short.	
50-71-4[5]	2/1	25Kj/75ab/10T(PVC)	371	401	7,remv'd	
50-69-7	2/1	25Kj/75ab/10T(Tefzel)	575	(soft short)		
50-70-1	2/1	25Kj/75ab/10T(Tefzel)	588	(soft short)		
50-70-3	2/1	25Kj/75ab/10T(PVC)	373	390	13	96
50-73-1	2/1	25Kj/75ab/10T(+ s.a.)	62.7	428	20	
50-77-1	2/1	25D_1/75ab/10T(+ s.a.)	313	(remv'd, poor 1st cap.)		
50-77-2	2/1	25D_1/75ab/10T(+ s.a.)	319	(remv'd, poor 1st cap.)		
50-83-2	2/1	25D_1/25Kj/50ab/10T	473	--	1,short.	
50-83-3	2/1	25D_1/25Kj/50ab/10T	571	473	17,exp!	97
50-83-4	2/1	25D_2/25Kj/50ab/10T	554	497	9	
50-84-5	2/1	25D_2/25Kj/50ab/10T	569	538	11,short	
50-85-1	2/1	[25Kj/75ab/10T	372	--	1,short.	
50-85-2	2/1	(Tfz, + s.a.)]	397	185	2,short.	
50-89-1	2/1	25Kj/75ab/10T	469	437	14	
50-95-3	2/1	[25Kj/75ab/10T	318	(remv'd, poor 1st cap.)		
50-95-4	2/1	(Tfz,2 layers]	387	(remv'd, poor 1st cap.)		
56-2-1	2/1	25N/25Kj/50ab/10T	495	550	11,short.	98-100
56-2-2	2/1	25N/25Kj/50ab/10T	522	--	1,short.	
56-3-4	2/1	[25Kj/75ab/10T	452	237	5	
56-3-5	2/1	(anode,77cm²)]	456	200	5	
56-11-1	2/1	[25Kj/75ab/10T	472	461	7,short.	
56-11-3	2/1	(case pos.)]	473	173	8,short.	
56-20-1	2/1	25D_1/50Kj/25ab/10T	584	542	8,exp!	
56-20-2	2/1	25D_1/50Kj/25ab/10T	432	570	7,short.	
56-20-3	2/1	50Kj/50ab/10T	461	575	8,short.	
56-21-4	2/1	50Kj/50ab/10T	611	467	14,short.	
56-21-5	2/1	5Kr/25Kj/70ab/10T	275	389	9,short.	
56-21-6	2/1	5Kr/25Kj/70ab/10T	572	450	12,short.	
56-25-3	2/1	25D_2/50Kj/25ab/10T	546	55.9	3,short.	
56-26-5	2/1	25D_2/50Kj/25ab/10T	541	72.8	3,short.	
56-26-8	2/1	25D_1/25Kj/50ab/10T (acetone washed)	458	494	2,removed	
56-28-1	2/1	Al screen/no carbon	potentiostatic/ galvanostatic tests.			
56-28-2	2/1	Ni screen/no carbon				

TABLE 15 (Continued).

Cell #	Electrolyte[1]	Cathode composition[2]	Primary discharge capacity (mAh)	Discharge capacity, last cycle (mAh)	# of last cycle[3]	Figure numbers
56-25-2	2/1	25D_1/25Kj/50ab/10T (acid washed)	544	152	12,exp!	
56-26-7	2/1	50D_2/25Kj/25ab/10T	539	338	2,short.	
56-27-11	2/1	50D_1/25Kj/25ab/10T	485	292	20,removed.	101
56-47-1	2/1	25Kj/75ab/10T (dried 20hrs)	461	489	6,exp!	
56-47-2	2/1		449	--	1,short.	
56-56-1	2/1	5.7Kr/23.6D_1/23.6Kj 47.2ab/10T	519	85.5	4,short.	
56-56-2	2/1		519	105	3,short.	
56-56-3	2/1	10D_1/30Kj/60ab/10T	488	489	3,short.	
56-56-4	2/1	10D_1/30Kj/60ab/10T	496	74.5	4,short.	
51-26-1	2/1	25Kj/75ab/10T (wr)	359	342	16,short.	102
51-26-2	2/1	25Kj/75ab/10T (wr)	401	362	9,remv'd.	94
51-26-3	1/1	25Kj/75ab/10T (wr)	461	381	14,remv'd.	93
51-26-4	1/1	25Kj/75ab/10T (wr)	406	(remv'd, poor 1st cap.)		
51-26-5	1/1	25Kj/75ab/10T (wr)	403	285	10,remv'd.	
51-30-1	2/1	100ab/3T (ann. bob.)	230	168	21,remv'd.	103
51-30-2	2/1		252	181	19,remv'd.	104
51-33-1	2/1(SO_2)	25Kj/75ab/10T (wr)	346	disconnected after primary discharge		
51-33-2	2/1(SO_2)	25Kj/75ab/10T (wr)	397			
51-33-4	2/1	25Kj/75ab/10T (wr)	219			
51-33-5	2/1	25Kj/75ab/10T (wr)	236	228	10,remv'd.	
51-33-6	2/1	25D_2/25Kj/50ab/10T (+ s.a.)	512	377	20,exp!	
51-33-7	2/1		501	416	9,remv'd.	
51-37-1	2/1	25Kj/75ab/10T (wr) flooded cell, 7.26cm^2	49.1	7 mA/cm^2, 1st 2 cycles (unintentional)		
51-37-2	2/1		57.4	15.2	13,remv'd.	105
51-37-3	2/1		62.0	63.7	6,remv'd.	106
56-79-1	2/1	10D_2/30Kj/60ab/10T	513.9	61.8	3	
56-79-4	2/1	25D_1/25Kj/50ab/10T	515.6	482.6	3,short	
56-79-5	2/1	25D_1/25Kj/50ab/10T	468.2	(shorted,1st charge)		
56-79-2	2/1	10D_2/30Kj/60ab/10T	552.0	100.0	8,short	
56-80-6	2/1	25D_1/25Kj/50ab/10T	513.1	(remv'd,cap.fading)		
51-45-4[6]	2/1	25Kj/75ab/10T(Ni)	309.9	(remv'd,cap.fading)		
51-45-3[7]	2/1	25Kj/75ab/10T(Ni)	311.6	94.0	6,exp!	
56-79-3	2/1	10D_2/30Kj/60ab/10T	523.2	259.9	6,short	
51-45-5[6]	2/1	25Kj/75ab/10T(Ni)	259.1	3.4	9	
51-45-2[7]	2/1	25Kj/75ab/10T(Ni)	415.7	417.4	5,short	
51-45-1[7]	2/1	25Kj/75ab/10T(Ni)	382.7	200.7	8,short	
57-67-6	2/1	25Kj/75ab/10T htd. 2 days @ 180°C	557.1	(shorted,1st charge)		
57-67-1	2/1	25Kj/75ab/10T	583.4	78.7	8,short	
57-67-5	2/1	25Kj/75ab/10T	568.9	497.0	8,exp!	
61-20-1	2/1	25Kj/75ab/10T htd.5days @180°C	425.7	313.3	9,remv'd	
61-20-2	2/1	25Kj/75ab/10T	415.7	314.1	9,exp!	

TABLE 15 (Continued).

[1] All electrolytes were cleaned free of hydrolysis products.
1/1 = $LiCl \cdot CaCl_2 \cdot 4AlCl_3 \cdot 12SO_2$ (acid electrolyte, with excess $AlCl_3$)
2/1 = $2LiCl \cdot CaCl_2 \cdot 4AlCl_3 \cdot 12SO_2$
3/1/1 = $3LiCl \cdot CaCl_2 \cdot NaCl \cdot 6AlCl_3 \cdot 18SO_2$
4/1 = $4LiCl \cdot CaCl2 \cdot 6AlCl_3 \cdot 18SO_2$

[2] Cathode material was pressed dry to anodized aluminum screen except where indicated otherwise. Numbers indicate percent by weight. Percent carbon in mixtures totals 100%; percent Teflon binder is based on the total weight of carbon plus Teflon.

A = Aquadag
ab = Chevron 50% compressed acetylene black
ann.bob. = annular bobbin, case positive, with lithium at center
C = cured, 280°C., 15 min.
D_1= Darco S-51
D_2= Darco KB-B
case pos. = case positive
E = Electrodag 230
E. = Ensari Super S
f = anodized aluminum foil
Kj = Ketjenblack
l = number of painted layers
Ni = Nickel screen
N = Norit SX-2
PF = treated with pore former (ammonium bicarbonate)
Pp = polyparaphenylene
PVC = PVC separator (Gelman Sci.)
+ s.a. = increased surface area
T = Teflon binder, Dupont type 30 resin in aqueous dispersion
Tfz = Tefzel microporous separator (Scimet)
Tfz/HV = Both Tefzel and Hollingsworth/Vose separator
wr = wet-rolled
x = "times"

[3] exp! = exploded during last charge cycle.

[4] Positive electrode mix had been cured, finely ground in a blender, and pressed dry onto anodized aluminum screens.

[5] charge cutoff limit raised to 4.10 volts.

[6] Cells had lithium pressed on the can as opposed to being wound next to the cathode.

[7] Cells contained cathodes which had been dried for two days at 180°C and anodes composed of lithium pressed on the can as well as wound next to the cathode.

Effect of overcharge. The cell which most closely resembled those of previous efforts [6, 8] was 50-15-3. The electrolyte was "2/1" and the positive, 25/75/10. The profile of potential versus time at constant discharge and charge current for the first two cycles is shown in Figure 88. The capacity versus cycle number is shown in Figure 89. For the first 13 cycles, the charge cutoff potential was 4.0 volts, but subsequent to charge cycle 13 the charge cutoff potential was raised to 4.1 volts. Overcharge plateaus at about 4.08 volts then appeared during each subsequent charge cycle (Figure 90), and the charge cycles became time instead of potential limited. The cell short circuited without exploding

during charge cycle 19.

Variation of electrolyte formulation. Cells in which the electrolyte contained calcium tetrachloroaluminate have shown two discharge plateaus. When the current density was 1 mA/cm², the first plateau occurred at 3.3 volts and amounted to about 20 to 25% of the entire capacity, while the second was at about 3.1 volts (cell 50-[illegible]3, Figure 88, is an example). Since the first plateau occurred during the first as well as subsequent discharge half cycles, the cause could not have been dissolved chlorine present as the result of charging or overcharging. Since the first plateau persisted for most or all of the cycling, the calcium was not being permanently removed from the electrolyte, for example through reduction by the negative electrode. We currently believe that calcium is able partially to take the place of lithium in the discharge reaction and be absorbed by the carbon electrode [8].

Figure 91 shows the first three discharge half cycles and the first two charge half cycles for cell 45-79-3. Figure 92 shows the capacity as a function of cycle number for the same cell. Similar cells with 25/75/10 positives and 3/1/1 electrolytes were 45-79-4, 50-15-1, 50-15-2, 51-6-1, and 51-6-2. At cycle 15, the charge cutoff potential for cell 50-15-2 was raised to 4.1 volts. The discharge capacity had decreased to as low as 353 mAh, but regained its original capacity (378 mAh) when the charge cutoff potential was raised. Overcharge plateaus at 4.08 volts appeared just as they had for cell 50-15-3. The positive material for cells 51-6-1 and 51-6-2 had been reduced to a fine powder by prolonged chopping in the blender. The prolonged chopping increased the primary capacity, but damaged the integrity of the carbon. Changing the electrolyte from 2/1 to 3/1/1 does not seem significantly to have changed the capacity or cycle life.

Cells 50-38-2, 50-38-3, 50-45-3, and 50-46-1 all contained 4/1 electrolyte. Their capacity and cycle life were inferior to cells containing 2/1. The viscosity of 4/1 electrolyte was found to increase dramatically after it had been stored for several weeks at ambient temperature. The increase in viscosity may have been caused by a partial crystallization of $LiAlCl_4 \cdot 3SO_2$ from the mixture. We found no advantage in replacing $2LiCl \cdot CaCl_2 \cdot 4AlCl_3 \cdot 12SO_2$ with any other electrolyte.

Cells 51-26-3, -4, and -5 were filled with the acid electrolyte "1/1", or $LiCl \cdot CaCl_2 \cdot 4AlCl_3 \cdot 12SO_2$. The intent was to extend the capacity by postponing the accumulation of the discharge product lithium chloride in the positive electrode. With the primary capacity extended, the positive electrode might then become "conditioned" to the higher capacity. However, only the primary capacity was slightly improved. As an example, the subsequent discharge capacities of cell 51-26-3, which had the 1/1 electrolyte (Figure 93) were not higher than those for cell 51-26-2 (Figure 95), which had 2/1.

Cells containing calcium tetrachloroaluminate showed two plateaus

during primary as well as subsequent discharge half cycles. As we explained above, we concluded that the first plateau was caused by the participation of calcium ion in the discharge reaction in the positive electrode. The first plateaus might also have been caused by excess aluminum chloride if some had failed to react with the stoichiometric amount of calcium chloride present when the electrolyte was being prepared. The excess aluminum chloride might then have increased the initial discharge potential by allowing the formation of $LiAlCl_4$ during discharge instead of LiCl. The electrolyte in cells 51-26-3, -4, and -5 all contained both calcium and a clear excess of aluminum chloride. Their primary discharge profiles all showed three plateaus instead of two, for example, cell 51-26-3 shown in Figure 94. This additional initial higher plateau was evidently the one which was caused by the formation of $LiAlCl_4$ from the extra $AlCl_3$ present.

Variation of positive electrode composition. Cells containing 100% Ketjenblack/ 5% Teflon, at least when the positives were dry pressed, sometimes showed increased capacity (cell 45-94-2, 610 mAh; cell 50-28-2, with 3/1/1, 575 mAh), but were inconsistent, and did not charge well. A typical example is cell 45-94-1 (Figure 96). Cell 50-28-2, also with 100% Ketjenblack, did not fare better with 10% Teflon. We had found earlier that 100% Ketjenblack positives with 3% Teflon would cycle, if wet rolled rather than extruded, cured, chopped, and pressed dry [8]. As explained above, the chopping of dried, cured carbon mix may damage the Teflon binder.

Other cells contained dry pressed carbon positives which were 100% either of Chevron acetylene black, Norit SX-2, Darco S51, or Ensari Super S. Two cells contained positives with 87% polyparaphenylene (50-29-4 and 50-29-5). Of all of these, only the 100% Chevron acetylene black/ 5% Teflon gave significant capacity (cells 51-1-1, 51-1-2, 51-1-4, 51-3-1, 51-3-2, and 51-6-6).

Figure 97 shows the discharge and charge capacities as a function of cycle number for cell 50-70-3, which contained the previously studied 25% Ketjenblack/ 75% acetylene black mixture, and which gave capacities between 370 and 460 mAh for 13 cycles. The charge cycles were potential limited at 4.1 volts. Higher capacities were obtained when pressed positive electrodes contained 50% high surface area carbon, activated carbon, or a mixture of the two, with also 50% acetylene black and Teflon making up 10% by weight of the total carbon mixture. In one example, Figure 98 shows capacities versus cycle number for cell 50-83-3, whose discharge capacities averaged about 500 mAh over 17 cycles. The cells also showed less polarization during the charge cycles, and were time rather than potential limited. Other examples of such cells include 50-84-5, 56-2-1 (Figure 99, showing cycles 1 and 2; Figure 100, showing cycles 10 and 11, with overcharge; and Figure 101, showing capacities as a function of cycle number), 56-2-2, 56-20-1, 56-20-2, 56-20-3, 56-21-4, 56-26-8, and 56-25-2. Cell 56-27-11, which had more than 50% high surface area carbon, showed time limited charge cycles, but its capacity faded over just 20 cycles (Figure 102).

Variation of positive and negative electrode design. Cells with painted foil positives included the following:

46-81-1	46-87-1
46-82-4	46-87-6
46-82-5	50-28-3

The thinner carbon electrodes allowed their length to be increased to between 4.5 and 7.5 inches. The rationale was that if the capacity was being limited by the transport of aluminum into and out of the pores in the positive electrode, a thinner electrode should allow a larger capacity per unit weight of carbon. The cells were operated at 1 mA/ cm^2, similar to the cells with positives pressed on screens. All showed limited capacity and poor cycling efficiency.

Wet rolling of positive electrodes made it unnecessary to chop positive electrode material after curing, since the material was already attached to the current collecting screen. We therefore avoided disrupting the structure of the binder. Cells with wet rolled positives on screens included the following:

51-13-1	51-26-2
51-13-2	51-26-3
51-13-4	51-26-4
51-17-1	51-26-5
51-18-1	51-33-1
51-15-5	51-33-2
52-65-3	51-33-3
51-15-2	51-33-4
51-15-3	51-33-5
51-15-1	51-37-1
51-26-1	

The electrolyte for all cells was 2/1. Four contained 25/75/5 positives, five contained 25/75/20. Four had nickel-screened positives, which as far as we could determine were equivalent in performance to aluminum-screened positives [8]. The charge cutoff potential for all the cells which would cycle was 4.1 volts. The one with the highest capacity and the least fading was 52-65-3, also the one cell with 10% Teflon binder.

Cells containing positives prepared by the "wet rolled" process (51-26-1, -2, -3, -4, and -5; 51-33-1, -2, -3, -4, and -5; 51-37-1) were not as successful as those with dry pressed positives. The charge cycles were time limited, but the capacity faded markedly (Figure 103).

While more information is needed to draw any reasonable conclusions, there may be an optimum Teflon content for wet-rolled positives in cells with mixed tetrachloroaluminate salts. A high Teflon content will not prevent the capacity from fading, and a low Teflon content will not increase the capacity. A minimum amount is apparently needed to prevent disintegration during the primary discharge cycle, although earlier results indicate that

there are subjective factors as well [6]. For making large numbers of cells, a modified wet-rolled technique would be preferable to a dry pressed technique requiring the manufacture of individual electrodes.

Some of the most promising cells were those with "increased surface area". Electrode spools were wound with the positive electrodes on the outside, rather than the inside. The cells used 2/1 electrolyte and 25/75/10 dry pressed positives. Cell 50-74-4 started with a capacity of 531 mAh, increasing to 567 mAh on charge with the limit set at 4.1 volts, while cell 50-73-2 started at 517 mAh, increasing to 554 mAh, both shorting after 11 cycles. It was possible that the increased capacity resulted from the extra surface area of the cell case, which was electrically connected to the negative electrode. It could be argued that the cell case was acting as extra surface area for the anode even though the primary capacity was higher than expected, since the capacity increased for the first few cycles. Presumably, as more and more lithium became plated on the cell case, the capacity would rise still higher.

Cells 56-11-1 and -3 were case positive wound cells each with its positive electrode on the outside of the spool, to keep the physical configuration the same but to prevent the case from participating as part of the negative electrode. Both cells had capacities which resembled the earlier ones with outside negative electrodes. The observation reinforced the possibility that the cases were responsible for increasing the capacities of case negative cells with positives wound on the outside of the spools.

However, we could not obtain consistent results. Cells with "increased area" positive electrodes also included 50-73-1, 50-77-1, 50-77-2, 50-85-1, 50-85-2, 51-33-6, and 51-33-7. Their performance was not significantly improved when compared with cells containing the "regular" length positives. Cells with 77 cm^2 (4 inch long) anodes (56-3-4 and 56-3-5) could not sustain useful capacity.

Cells 51-30-1 and 51-30-2 contained annular bobbin positives with 97% acetylene black. They were cycled at the same current, 50.8 mA, as cells with wound electrodes, and therefore were operating at higher current density with thicker electrodes. The capacities were about half those of cells with wound electrodes. Since they showed little capacity fading (Figures 104 and 105), we also tried annular bobbin cells with Ketjenblack/ acetylene black = 25/ 75.

The area of the positives in cells with flooded electrodes (cells 51-37-2 and 51-37-3) was about 7.26 cm^2, although their thickness was the same as that in the wound electrode cells. Their capacities versus cycle number are shown in Figures 106 and 107, respectively. The total current was 7.26 mA, so that the current density was also 1 mA/ cm^2. Assuming the same capacity per unit surface area, 62 mAh from a flooded electrode cell is equivalent to about 434 mAh in a cell with "normal" length wound electrodes.

This capacity may seem low, but it should be compared with wound electrode cells containing positives prepared in the same way (cells 51-33-1, -2, -4, and -5). Positive electrodes operating in a flooded condition without mechanical pressure showed a moderate increase in capacity when compared with positive electrodes restricted in their access to electrolyte or mechanically confined by a wound electrode configuration. We could not conclude whether the capacity fading was caused by the lack of mechanical pressure or to inadvertently cycling cells 51-37-1 and -2 at 7 mA/ cm^2 for the first two cycles.

Explosions during charge cycles. Several cells containing dried mixed tetrachloroaluminate salts in sulfur dioxide exploded during charge cycles. In each case, the explosions occurred while each cell was in the normal part of its charge cycle, not during overcharge, and without any prior intermittent behavior. The following cells exploded during the charge cycles indicated:

cell #	cycle #
46-95-1	52
50-41-4	17
50-83-3	17
56-20-1	8
56-25-2	12
56-47-1	6
51-33-6	20
57-67-5	8
61-20-2	9

Figure 108 shows the 16^{th} and 17^{th} cycles for cell 50-41-4 as an example.

It has been our premise that hydrolysis products are contributing to the instability of cells during charge cycles. The possibility existed that moisture was being introduced by way of the positives or the separators during assembly of the cells, or during the filling operation. As we explain below, we found that significant quantities of moisture remained even in positives prepared from "cured" carbon mixture. Wnile acetylene black as received contained 0.2% by weight water and Ketjenblack contained 0.5%, the activated carbons initially contained 10% water. However, while four of the exploded cells contained activated carbon, cells 46-95-1, 50-41-4, and 56-47-1 did not. Cell 61-20-2 contained a wound positive which had been dried by equilibration twice with sulfur dioxide gas, as described below. While it was not completely dry, it did represent the driest cells we have been able to make.

The explosions could also have been initiated by lithium dendrites contacting Teflon binder within the positive electrode. Although Teflon reacts violently with lithium, ethylene tetrafluoroethylene copolymer (Tefzel) does not. While Tefzel emulsion is available commercially, we were not able to prepare wound positive electrodes using Tefzel as a binder.

RESIDUAL MOISTURE IN CARBON POSITIVE ELECTRODES

Determination of moisture in carbon electrodes. We established that equilibrating dry electrolyte with positive electrode samples could be used to determine the moisture left in the carbon after electrode preparation. Purified $2LiCl \cdot CaCl_2 \cdot 4AlCl_3 \cdot 12SO_2$, stored in 100 ml Savillex vessels, was transferred in the dryroom by pipette either to clean, empty 4 ml vials or to vials containing the samples to be tested. After equilibration, the electrolyte was pipetted into 10 mm pathlength quartz cuvettes and examined in the infrared between 4,000 and 2,000 cm^{-1}. Results indicated that if the positive electrode samples were equilibrated for 12-14 hours, the moisture present in the samples reacted quantitatively with the electrolyte, and the resulting $AlCl_3OH^-$ was distributed throughout the electrolyte in the vial. Reproducible values for the net absorption at 3,600 (OH stretch on $AlCl_3(OH)^-$) and 2,800 cm^{-1} (HCl) were reliably obtained.

Positive electrodes containing 50 weight percent Ketjenblack and measuring 1.5" x 3" could increase the concentration of hydrolysis products in cells with 4 ml of $2LiCl \cdot CaCl_2 \cdot 4AlCl_3 \cdot 12SO_2$ by as much as 2,500 ppm. The carbon material had been "cured" at 280°C in air to convert the Teflon binder to an elastomeric material. The positive electrodes were prepared from carbon mixture stored in air, then dried at 150°C for 1 hour, then at 150°C *in vacuo*, then cooled in the dryroom atmosphere. Positive electrodes were normally treated in this way before cells were wound.

Removal of moisture from carbon positive electrodes. We began simply by heating prepared positive electrodes *in vacuo* at various temperatures for various lengths of time. We discovered that prolonged heating did more to disrupt the structure of the positive electrodes than to dry them. The longer they were heated *in vacuo* (up to 8 hours), the more water was extracted when positive electrode samples were subsequently equilibrated with dried $2LiCl \cdot CaCl_2 \cdot 4AlCl_3 \cdot 12SO_2$. Heating for 16 hours again reduced the amount of water extracted by the electrolyte. Cells containing positives which had been dried by prolonged heating faded rapidly.

Evacuating carbon positive electrodes in a small vacuum desiccator, followed by equilibration with SO_2 gas at atmospheric pressure and ambient temperature for two to three hours, appeared to remove at least some of the moisture. We then tried using a second exposure to SO_2, evacuating the desiccator after the first treatment. Most of the moisture was removed from the carbon, apparently having been displaced by the sulfur dioxide. The amount remaining was equivalent to about 800 ppm in 4 ml of electrolyte, enough to fill an AA size cell.

We prepared wound electrode AA cells, but without welding the tops onto the cans. The purpose was to determine whether the SO_2 could displace the moisture from the carbon without tarnishing the lithium, keeping in mind a manufacturing situation where the

SO_2 treatment to remove moisture would be the last procedure before filling and sealing. After the double equilibration with SO_2 inside the desiccator, the electrode spirals were removed from the AA cans, the lithium examined, and the moisture in the carbon electrode determined. The procedure removed moisture, without having to heat the positives or the cells, and without corroding the lithium in the wound spirals.

LITHIUM/ BROMINE SOLUBLE POSITIVE CELLS

In the lithium/ bromine soluble positive cells, the electrolytes contained 15-40% bromine, with either chloroacetyl chloride/ $LiBr \cdot AlCl_3$ or dried $2LiCl \cdot CaCl_2 \cdot 4AlCl_3 \cdot 12SO_2$, with lithium and carbon as the negative and positive electrodes. The lithium was kinetically stable apparently because of an insoluble lithium bromide solid electrolyte interphase on the lithium surface.

The reasons for studying these cells further were clear [9,10]. Although we used only glass fiber separators, no cell ever shorted, exploded, bulged, or increased in impedance during charging. Samples taken from individual tests showed no tarnish or corrosion of any cells parts, including lithium, hardware attached to lithium, or nickel screens, 52 alloy feedthroughs, or stainless steel hardware attached to carbon. During discharge or charge, the overpotential and IR loss at 1 mA/ cm^2 was only 30 to 50 millivolts at ambient temperature. If an AA size cell contains 3.5 ml of electrolyte which is 30% bromine, the implications are as follows:

Total volume of bromine, 1 ml (about 1Ah)
Running potential, 3.49 to 3.45 V
Watt-hours available, 3.45
Cell volume, 6 ml
Energy density, 575 watt-hours per liter

The most important objective was to improve the adherence of carbon to the positive electrodes. Positive electrodes taken from cells during previous tests [9, 10] seemed to indicate that the observed low primary capacity and severe capacity fading were the result of the positive electrode material pulling away from the support screen. The particular Teflon polymer present in the DuPont suspension was tested by precipitating a sample with 50/50 water/ isopropanol, washing and drying it, and soaking it in electrolyte with 30% bromine. The material appeared to retain its original elastomeric properties. We had intended to use Ni feltmetal, sponge metal, or graphite felt to hold the carbon in place, or to mix carbon with graphite or glass fiber to increase binding.

AA size cells. The test results for cells containing bromine as a soluble positive are summarized in Table 16. The entries are explained at the bottom of the table.

TABLE 16. SUMMARY OF AA SIZE CELL DATA:
LITHIUM/ BROMINE CELLS[1]

Cell #	Electrolyte Composition[1]	Cathode Composition[2]	Primary discharge capacity (mAh)	Discharge capacity, last cycle (mAh)	# of last cycle	Figure numbers
52-63-2	40%/1A	25/75/10	341	(poor dischg. cap.)		
52-65-1	30%/1A	25/75/10	153	(poor dischg. cap.)		
52-65-2	30%/1A	25/75/10	153	(poor dischg. cap.)		
52-85-3	30%/1B_1	25/75/10	92.3	(poor dischg. cap.)		
52-85-4	30%/1B_1	25/75/10	69.4	(poor dischg. cap.)		
52-87-2	30%/1B_2	25/75/10	50.8	(refused to function)		
52-87-3	30%/1B_2	25/75/10	50.8	(refused to function)		
52-93-1	20%/2C	25/75/10	133	(refused to function)		
52-93-2	20%/2C	25/75/10	92.3	(poor dischg. cap.)		
52-93-3	15%/2C	25/75/10	92.3	(poor dischg. cap.)		
52-93-4	15%/2C	25/75/10	92.3	(poor dischg. cap.)		
52-87-5	30%/1B_2	25/75/10	70.0	(primary cap. only)		
55-3-1	15%/2C	25/75/10	(reference electrode cell)			109-111
55-5-2	20%/2C	25/75/10(wr)	(refused to function)			
51-26-6	20%/2C	25/75/10(wr)	203	(refused to function)		
55-15-1	20%/3C	25/75/10(etched)	145	≈50 mAh	2,removed.	
55-15-2	20%/3C	25/75/10(etched)	121	≈50 mAh	2,removed.	
55-15-3	20%/2C/2%I	25/75/10(etched)	119	≈50 mAh	2,removed.	
55-15-4	20%/2C/2%I	25/75/10(etched)	133	≈50 mAh	2,removed.	
55-15-5	20%/2C	Alupower	425	100	9,removed.	112,113
55-15-6	20%/2C	Alupower	390	113	9,removed.	
55-19-1	20%/2C	97ab/3T (ann.bob)	325	(refused to function)		
55-19-2	20%/2C	97ab/3T (ann.bob)	330	(refused to function)		
55-21-1	20%/2C	25/75/10 (Ni mat)	(refused to function)			
55-21-2	20%/2C	25/75/10 (Ni mat)	93.1	61	2,removed.	
55-21-3	20%/2C	97ab/3T(ann.bob.)	(refused to function)			
55-25-1	20%/2C	25/75/10(pocket)	(refused to function)			
55-33-1	20%/3C	97ab/3T(ann.bob.)	108	≈50 mAh	2,removed.	
52-93-6	40%/3C/2%I	25/75/10	121	≈50 mAh	2,removed.	
55-43-1	20%/2C	25/70/7.5/5Kr	148	14.4	6,removed.	
55-43-2	20%/2C	25/65/5/10Kr	104	68.6	8,removed.	
55-43-3	20%/2C	25/50/10/25Kr	156	62.7	6,removed.	
55-43-4	20%/2C	Panex(unT,no C)	(refused to function)			
55-55-1	20%/2C	25/75/10 (1P,unT,Ni mat)	288	104	6,removed.	
55-55-2	20%/2C	25/75/10 (1P,unT,Ni mat)	132	39.8	2,removed.	
55-55-3	20%/2C	(½)25/75/10 + (½)50/50/10[3]	(refused to function)			
55-55-4	20%/2/1	(½)25/75/10 + (½)50/50/10	314	(shorted, 1st charge cycle)		
55-63-1	20%/2C	25/75/10 (1P,T)	153	49.1	6,removed.	
55-63-2	20%/2C	25/75/10 (1P,T)	195	73.7	2,removed.	
55-63-3	20%/2C	50/50/10 (2P,T)	154	112	2,removed.	
55-63-4	20%/2C	25/75/10 (2P,T)	136	67.7	2,removed.	
55-63-5	20%/2C	25/75/10 (1P,T)	214	61.0	4,removed.	
55-63-6	20%/2C	25/75/10 (1P,T)	195	106	2,removed.	
55-63-7	20%/2C	48/48/10/4Kr (2P,T)	156	81.3	4,removed.	
55-63-8	20%/2C	25/65/5/10K (filt.)	295	76.2	3,removed.	
55-69-2	20%/2C	100Kj/10T (2P,T)	229	83.8	2,removed.	

TABLE 16 (Continued).

Cell #	Electrolyte Composition[1]	Cathode Composition[2]	Primary discharge capacity (mAh)	Discharge capacity, last cycle (mAh)	# of last cycle	Figure numbers
55-69-3	20%/2/1	100Kj/10T (2P,T)	559	(shorted, 1st charge cycle)		
55-69-4	20%/2/1	100Kj/10T (2P,T)	522	(shorted, 1st charge cycle)		114
55-73-1	20%/2/1	25/75/10	412	(shorted, 1st charge cycle)		
55-73-2	20%/2/1	25/75/10	278	51.7	4,short.	
55-81-4	20%/2/1	100Kj/10T (2P,T,alt.Kr)	470	(shorted, 1st charge cycle)		
57-11-1	20%/1A	23/67/10/10G	314.1	60.1	7	
57-11-2	20%/1A	20/60/10/20G	269.2	56.7	8	
57-11-5	20%/1A	Ni sint.	671.4	Refused to charge		
57-3-2	20%/1C	Ni sint.	583.4	Refused to charge		
57-67-3	20%/1C	Alupower	386.1	35.6	6	
57-67-4	20%/1C	Alupower	336.1	4.2	8	

[1] First entry = volume percent bromine
Second entry = salt concentration (moles per liter):
A = $LiAlCl_4$
B_1 = $LiAlBr_4$ (from melted salts)
B_2 = $LiAlBr_4$ (from Al plus bromine *in situ*)
C = $LiBr \cdot AlCl_3$
2/1 = $2LiCl \cdot CaCl_2 \cdot 4AlCl_3 \cdot 12SO_2$ (no cosolvent)
Solvent (for all other cells) = $CH_2ClCClO$
I = Iodine

[2] Positive electrode composition (nickel support):
First entry = w/o (weight percent) Ketjenblack
Second entry = w/o acetylene black
Third entry = w/o Teflon binder

ab = Chevron 50% compressed acetylene black
Alupower = carbon fiber composite; Alupower, Inc., Warren, NJ.
ann.bob. = annular bobbin
etched = screen soaked in aqua regia
filt. = carbon filtered as slurry over screen, dried, paper removed
G = nickel coated graphite: 75 w/o Ni; 25% graphite
I = iodine
Kj = Ketjenblack
Kr = Kreha F-205; (Japanese) carbon fiber cloth. Kreha Corp., New York
alt.Kr = Kr between layers
Ni mat = used in place of Ni screen
Ni sint. = sintered nickel plaque
no C = no carbon on screen
1P = carbon/Panex/screen/carbon
2P = carbon/Panex/screen/Panex/carbon. Stackpole, Inc., Lowell, MA
pocket = screen/carbon/screen
T = Teflon binder, Dupont type 30 resin in aqueous dispersion
Tfz = Tefzel separator
unT = no Teflon added
(wr) = wet rolled

[3] Signifies that the positive electrode mixture is half 25/75/10 and half 50/50/10 for both cells.

Cell 55-3-1 was a reference electrode cell, similar to others discussed above, in which both ends were fitted with feedthrough tops. One of the tops was attached to a nickel tab and screen, to which was pressed a concentrically placed lithium disc. Cell 55-3-1 was discharged through a 100 ohm resistor while the computer monitored the potentials between the positive and negative, the positive and reference, and the negative and reference electrodes (Figures 109-111). The polarization was caused essentially by the positive electrode, the lithium polarizing at most 350 millivolts at the point where the cathode had polarized about 50%.

Figure 112 shows the cycle profile, and Figure 113 the capacity versus cycle number for cell 55-15-5, a cell containing an Alupower positive bound with carbon fibers and Teflon. While the cell and its duplicate 55-15-6 at least maintained a capacity of 100 mAh or better, the capacity was still considerably less than that represented by the bromine present.

Several cells contained bromine with $2LiCl \cdot CaCl_2 \cdot 4AlCl_3 \cdot 12SO_2$ instead of bromine with chloroacetyl chloride/ $LiBr \cdot AlCl_3$. Figure 114 shows the discharge/ charge profile for cell 55-69-4, which contained 20% bromine with $2LiCl \cdot CaCl_2 \cdot 4AlCl_3 \cdot 12SO_2$. The primary discharge profile showed three plateaus at 3.65, 3.5, and 3 volts. Cell 55-69-4 and other cells containing this electrolyte short circuited easily, and delivered substantially less than the expected 800 mAh.

As explained below, we found that bromine could be reduced on a nickel screen from $CH_2ClCClO$/ 1M $LiBr \cdot AlCl_3$/ 20% Br_2. We attempted cells with no carbon, but instead positives made from sintered nickel powder similar to those used to prepare nickel/ cadmium cells. Cell 57-11-5 contained 1M $LiAlCl_4$/ 20% bromine/ $CH_2ClCClO$, and cell 57-3-2 contained the same but with 1M $LiBr \cdot AlCl_3$. The primary capacities were encouraging, but the cells polarized about 400 mV throughout discharge and refused to accept charge.

POTENTIOSTATIC/ GALVANOSTATIC STUDIES: AA SIZE CELLS

The objective in charging cells without carbon on their positive electrode contacts were to determine whether "hard" short circuits between lithium dendrites and positive electrode hardware could be produced, and if so, whether explosions could be made to take place in cells with completely "dry" electrolytes, but without carbon or Teflon binder. The other objectives were to establish the polarization behavior of a nickel surface under anodic conditions, and obtain a rough idea of the plating efficiency of lithium on nickel substrates from both high concentration tetrachloroaluminate/ sulfur dioxide and bromine based electrolytes.

The total surface area of the nickel in the 5 Ni 10-125 screen electrodes, geometric area about 50.8 cm^2, was estimated to be about 33.4 cm^2, including both the original surface area of the

metal foil and the area exposed by cutting the foil into expanded screen. The constant current used for the lithium plate/ strip measurements was about 43 mA, or a current density of about 1.3 mA cm^2.

AA cell containing $2LiCl \cdot CaCl_2 \cdot 4AlCl_3 \cdot 12SO_2$ (dried) with a nickel positive screen, but without carbon. The potentiostat was set at each potential for about 15 seconds. As the potential of the nickel screen was made progressively more anodic with respect to the lithium electrode, the measured currents were steady, as follows:

Potential, Ni vs. Li	Current, mA
3.20V	(open circuit)
4.3	0.1
4.4	0.3
4.5	0.8
4.6	1.6
4.7	2.5
4.8	5.6
4.9	9.1
5.0	13.

There was no measurable current before the nickel was 4.3 volts anodic to the lithium. Since all of the charging and overcharging of our AA test cells was done below 4.1 volts, all of the anodic current at the positive electrode must have been occurring on carbon surfaces, rather than on positive electrode contact support hardware. Any lithium dendrites from the negative electrode growing towards the positive would have to grow towards carbon, rather than towards the hardware. Any short circuits between the dendrites and the positive electrode would therefore have to be soft shorts to the carbon, rather than hard shorts to the more conductive metal surfaces.

Since at potentials higher than 4.3 volts anodic to lithium, the current may have represented the oxidation of the nickel rather than the electrolyte, we made no attempt to run the cell at constant current with the nickel as the anode. Rather, we plated and stripped lithium from the nickel screen, carrying the potential of the screen during each strip cycle no more anodic to the lithium electrode than 0.5 volts. The tests were carried out at ambient temperature, and the lithium was stripped immediately after plating. The result was as follows:

Li plated, Q/ cm^2	Plate/ strip efficiency, percent
0.05	92
0.058	73
0.062	84
0.124	58
0.184	75
2.9	94.7

Li plated, Q/ cm^2	Plate/ strip efficiency, percent
4.64	97.5
97.0	95.8

No short circuits were produced, although the separator was "Hovosorb" Pyrex fabric.

AA cell containing $CH_2ClCClO$/ 1M $LiBr \cdot AlCl_3$/ 20% Br_2 with a nickel positive screen, but without carbon. Polarization of the nickel screen anodic to the open circuit potential produced the following results:

Potential, Ni vs. Li	Anodic Current, mA
3.60V	(open circuit)
4.0	0.8
4.68	5.6
4.92	15.2

When the potential was set cathodic to the open circuit value, unexpected and persistent cathodic currents appeared:

Potential, Ni vs. Li	Cathodic Current, mA	Duration at steady value
3.2	4.2	2 min.
2.05	26.5	9 min.

The nickel appeared eventually to become passivated. At that point, the cathodic current was set at 40 mA, and the nickel stayed within 0.5 volt of the lithium potential. However, on attempting anodically to strip the lithium presumed plated by the cathodic current, we found no lithium. We repeated the experiment using dried $LiAlCl_4$, along with the distilled chloroacetyl chloride and 20% bromine, but the result was the same. After passing a cathodic current of 43 milliamps for about 3 hours, lithium appeared, but the time required for stripping was only 5 minutes (3%).

CHAPTER 4.

CONCLUSIONS

The following statements summarize the findings and conclusions described in Chapter 3.

Li/ "cosolute"; lithium salt; SO_2/ carbon cells:

1. Thiocyanate and bromide cosolute salts with organic cations were found to be unstable in the presence of lithium. A lithium dithionite film, if it does form on the surface of the metal, does not adequately protect the lithium.

2. Thiocyanate electrolytes such as LiSCN/ KSCN or CsSCN/ SO_2 could be prepared which were stable in the presence of lithium and had an adequate lithium ion concentration. However, significant solvolysis of thiocyanate salts to parathiocyanogen occurred during several months stand at ambient temperature, which effectively prevented their use for this application. AA size cells had low capacity and faded rapidly.

3. Cesium bromide increased the solubility of lithium bromide in sulfur dioxide, and solutions were stable in the presence of lithium. The maximum lithium ion concentration, 0.12 molar, occurred when the cesium concentration was 1.25 molar. AA size cells had low capacity, either because the concentration of lithium ion was too low, or because cesium ion interfered with lithium ion transport. Reference electrode cells showed that most of the polarization was occurring at the carbon positive electrode.

4. The best cosolute electrolyte which we were able to devise, which included a low reactivity with lithium and the highest concentration of lithium ion in combination with the lowest concentration of non-lithium cations, was liquid sulfur dioxide with 1M $NH_2^+=C(NH_2)_2$ Br^-/ 1M CsBr/ 0.5M LiBr. This electrolyte underwent significant solvolysis after a short time at room temperature, apparently producing bromine and sulfur monobromide. The solvolysis may have been exacerbated by the higher concentration of lithium ion in conjunction with the high bromide concentration.

5. When we tried to lower the concentration of bromide by using cosolute salts with other anions, such as cesium trifluoromethanesulfonate, these failed to produce adequate concentrations of lithium ion.

6. We concluded that a lithium/ sulfur dioxide (dithionite) cell based on the cosolute principal was not practical.

7. We tried cells containing lithium bromide in sulfur dioxide with organic solvents alternative to acetonitrile, such as 1,2- dimethoxyethane. Primary capacities were high, but cells faded rapidly with cycle number.

8. We tried to seguester $LiAlCl_4$ in solutions of sulfur dioxide with chloroacetyl chloride, to prevent the aluminum from participating in the discharge reaction. The solvewnt did not prevent the participation of aluminum, and the cells were shock sensitive.

9. Attempts to prepare derivatives of $AlCl_4^-$ by replacing one or more chlorides with larger groups did not result in salts with significant solubility in sulfur dioxide.

Li/ $2LiCl \cdot CaCl_2 \cdot 4AlCl_3 \cdot 12SO_2$/ carbon cells:

1. We established a reliable means of measuring the moisture content of positive electrodes for tetracloroaluminate/ sulfur dioxide cells. Samples are equilibrated overnight with dried electrolyte in gas tight Teflon containers, then the electrolyte is examined by infrared spectroscopy. Carbon electrodes may be dried by equilibration with sulfur dioxide gas.

2. Improvement in the capacity of Li/ SO_2 cells resulted when the high surface area carbon content of the positive electrodes was increased from 25 to 50%. The high surface area carbon could be Ketjenblack or activated carbon, along with acetylene black/ 10% Teflon. Higher levels of high surface blacks increased fading.

3. Cells with "increased surface area" electrodes are more difficult to prepare without shorting, and did not show improved performance when compared with cells containing three inch long electrodes.

4. Cells with 100% acetylene black/ 3% Teflon binder annular bobbin positives showed low capacity (100 mAh), but no capacity fading for about 20 cycles at 50 mA.

5. The capacity was higher for thin (0.023") positives when flooded, although the configuration is impractical.

6. In case negative cells, the stainless steel surface participates when the positive electrode faces the outside of the electrode spool.

7. Electrolyte containing excess aluminum chloride to delay the accumulation of lithium chloride in the positive electrode during discharge was not successful in increasing the capacity of the positive electrode. No advantage was found in replacing $2LiCl \cdot CaCl_2 \cdot 4AlCl_3 \cdot 12SO_2$ with any other combination.

8. Overcharging lithium cells containing dried sulfur dioxide solutions of mixed tetrachloroaluminate salts at 1mA/ cm^2 produced a plateau at about 4.05 volts, and charge cycles became time rather than potential limited. Cells with initial capacities from 400-500 mAh regained their original capacities if overcharged, even if discharged to passivation.

9. During charging, the formation of "hard" short circuits between growing lithium dendrites and positive electrode hardware is unlikely. Cells overcharging at 1 mA/ cm^2 ran below 4.1 volts, while reactions did not begin on bare nickel until it was more than 4.3 volts anodic to lithium. Dendrites would be more likely to grow towards carbon, producing only "soft" shorts. Explosions of some cells were observed during charge cycles, but cells were not known to be free of hydrolysis products. Lithium plated satisfactorily from $2LiCl \cdot CaCl_2 \cdot 4AlCl_3 \cdot 12SO_2$ on nickel.

Lithium/ bromine soluble positive cells:

1. An AA size cell with a reference electrode discharged at 100Ω constant load showed that the positive electrode was responsible for the premature polarization. Various cathode formulations, including nickel or graphite fiber, were not successful in increasing the capacity. Using bromine with $2LiCl \cdot CaCl_2 \cdot 4AlCl_3 \cdot 12SO_2$ in place of $LiBr \cdot AlCl_3$/ $CH_2ClCClO$ also did not improve the capacity or cycle life.

2. Metallic lithium had been found to be stable in 1M $LiBr \cdot AlCl_3$/ CH_2CClO/ 20% Br_2. However, galvanostatic plating/ stripping measurements showed that the plating efficiency of lithium from this same electrolyte was very poor. The bromine was reduced on the nickel surface, which did not passivate as quickly as expected.

3. A primary cell based on a more conductive sintered nickel cathode may operate at a considerably higher rate than would a carbon cathode, but some activation polarization would result.

CHAPTER 5

RECOMMENDATIONS

Based on the work for this entire contract, we feel that cells with mixed tetrachloroaluminate salts in sulfur dioxide hold the most promise for the successful development of a lithium/ inorganic electrolyte soluble positive rechargeable system. As currently designed, AA cells deliver about 269 Wh/ 1 and 100 Wh/ kg at 26 W/1 (10 W/ kg). We have now established how to dry both carbon electrodes and electrolyte mixtures, and the positive electrode composition most likely to take maximum advantage of the available capacity.

Although only one cell which we dried as extensively as possible did explode during a charge cycle, the system will require further development before any scaling up in size could be accomplished safely. We have shown that the rapid reactions leading to explosions during charge cycles are not likely caused by "hard" short circuits to positive electrode contact hardware, but are more likely caused by chemical reactions. The problem remains to establish what chemical reactions lead to the explosions. If they involve hydrolysis products or the Teflon binder, then the possibility exists that the problem can be successfully addressed.

We recommend that the work be continued in the following two general areas, using AA and C size wound and annular bobbin cells:

1. Determine to what extent carbon electrodes with 25-50 weight percent of Ketjenblack or other high surface area carbon can be dried by using sulfur dioxide. Cycle cells in a manner which allows them to short during charge cycles, for example by using macroporous glass fiber separators, in order to establish whether rapid reactions will still occur.

2. Since thin, flexible positive electrodes with Tefzel binder cannot be made, prepare case positive annular bobbin cells with Tefzel binder, and test as in (1). C and D size cells could presumably be prepared with several thin annular bobbin carbon electrodes positioned concentrically with cylindrical lithium electrodes.

REFERENCES

1. D.L. Maricle and J.P. Mohns, U.S. Patent 3,567,515 (1971).

2. H.C. Kuo, A.N. Dey, C.R. Schlaikjer, D.L. Foster, and M. Kallianidis, Contract DOE-DE-AC01-80ER10191, Subcontract LBL #4507410 (Lawrence Berkeley Laboratory), Final Report, November 1980 to June 30, 1985.

3. A.N. Dey, H.C. Kuo, D.L. Foster, C.R. Schlaikjer, and M. Kallianidis, presented at the Power Sources Symposium, Cherry Hill, New Jersey, May 1986.

4. C.R. Schlaikjer, D.L. Foster, H.C. Kuo, L. Chow, and A.N. Dey, "Proceedings of the Symposium on Lithium Batteries," A.N. Dey, ed., Electrochemical Society Proceedings Volume 87-1 (1987), page 437. The Electrochemical Society, Pennington NJ.

5. H.C. Kuo, C.R. Schlaikjer, M. Kallianidis, P. Keister, and A.N. Dey, Final Report for the period March, 1984 to February, 1986, Contract SLCET-TR-84-0379-F, Fort Monmouth, New Jersey.

6. C. Schlaikjer, Final Report for SBIR Phase I Contract #F33615-87-C-2798, December 15, 1987 (Wright-Patterson Air Force Base).

7a. Prater et al, European Patent #118,292, Sept. 12, 1984;
7b. J.F. Connolly, R.J. Thrash U.S. Patent #4,482,616, November 13, 1984;
7c. J.F. Connolly, R.J. Thrash, and R.A. Kretchmer, U.S. Patent 4,612,265, September 16, 1986.

8. C. R. Schlaikjer, M. D. Jones, and J. E. Torkelson, Final Report for SBIR Phase I Contract N60921-89-C-0148, December 14, 1989 (Naval Surface Warfare Center).

9. C. R. Schlaikjer, Final Report fo SBIR Phase I Contract # F33615-87-C-2785, January 14, 1988 (Wright-Patterson Air Force Base).

10. Carl R. Schlaikjer, U.S. Patent 4,849,310 (July 18, 1989).

11. B. Badet and M. Julia, Tetrahedron Lett. 1979, 1101.

12. G. Jander, "Die Chemie in Wasser-ähnlichen Lösungsmitteln," Springer Verlag, Berlin, 1949, pp. 209-307.

13. J. C. Bailey and G. E. Blomgren, Proc. Electrochem. Soc. Symposium on Primary and Secondary Ambient Temperature Lithium Batteries, Oct. 1987, Vol. 88-6, J. P. Gabano, Z. Takehara and P. Bro, eds., p. 301.

14. L. F. Audrieth, "Liquid Sulfur Dioxide: A Novel Reaction Medium," Stauffer Chemical Co., NY, 1969, p. 18.

15. N.N. Lichtin, Prog. Phys. Org. Chem. 1, 75, (1963).

16. L.F. Audrieth, "Liquid Sulfur Dioxide ...a Novel Reaction Medium," Stauffer Chemical Company, New York (1969), pages 15-17.

17. P. Kovacic and J. Oziomek, J. Org. Chem. 29, 100 (1964).

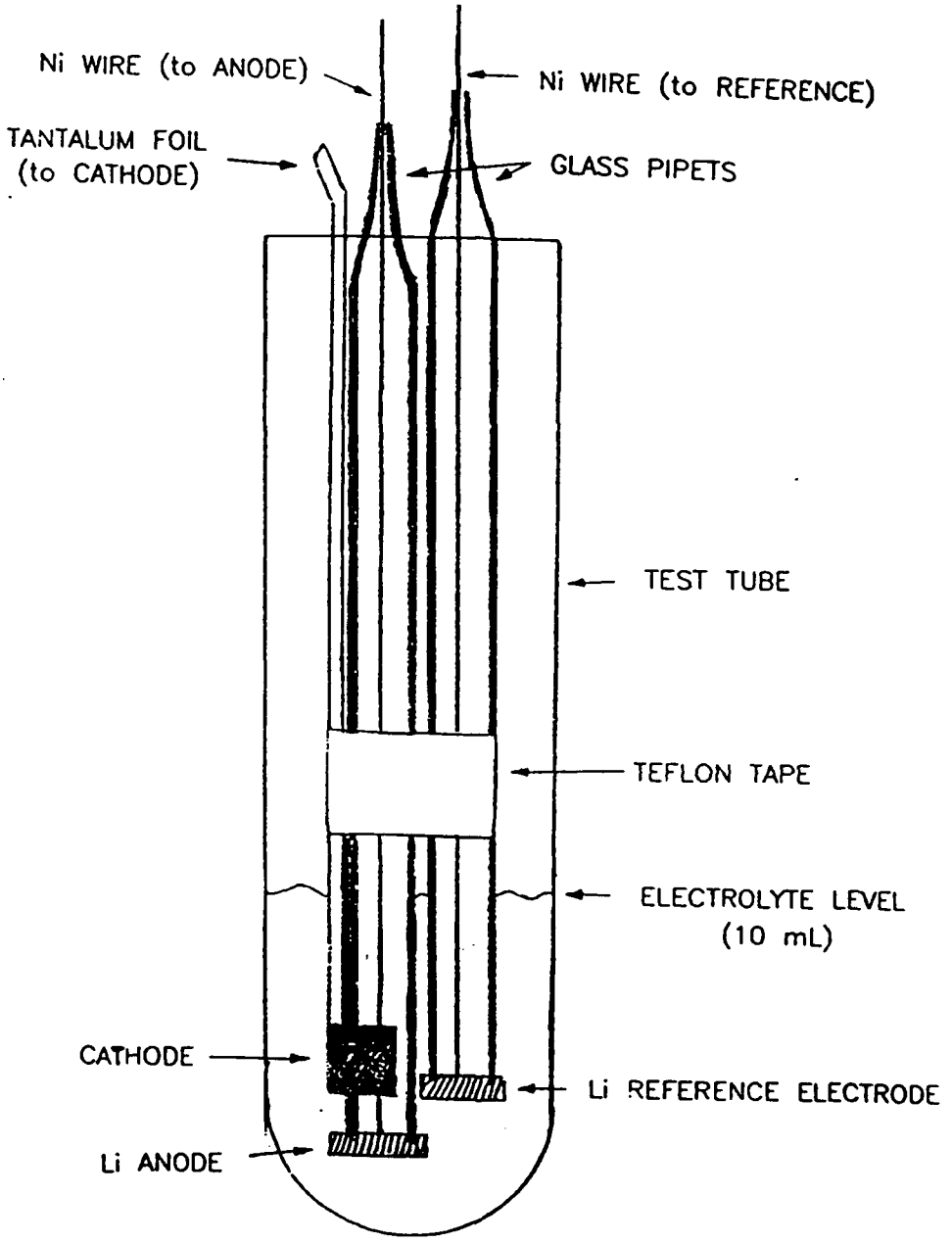

FIGURE 1. Three electrode test tube cell for use with noble metal positive electrode contacts and with electrolytes having boiling points above ambient temperature.

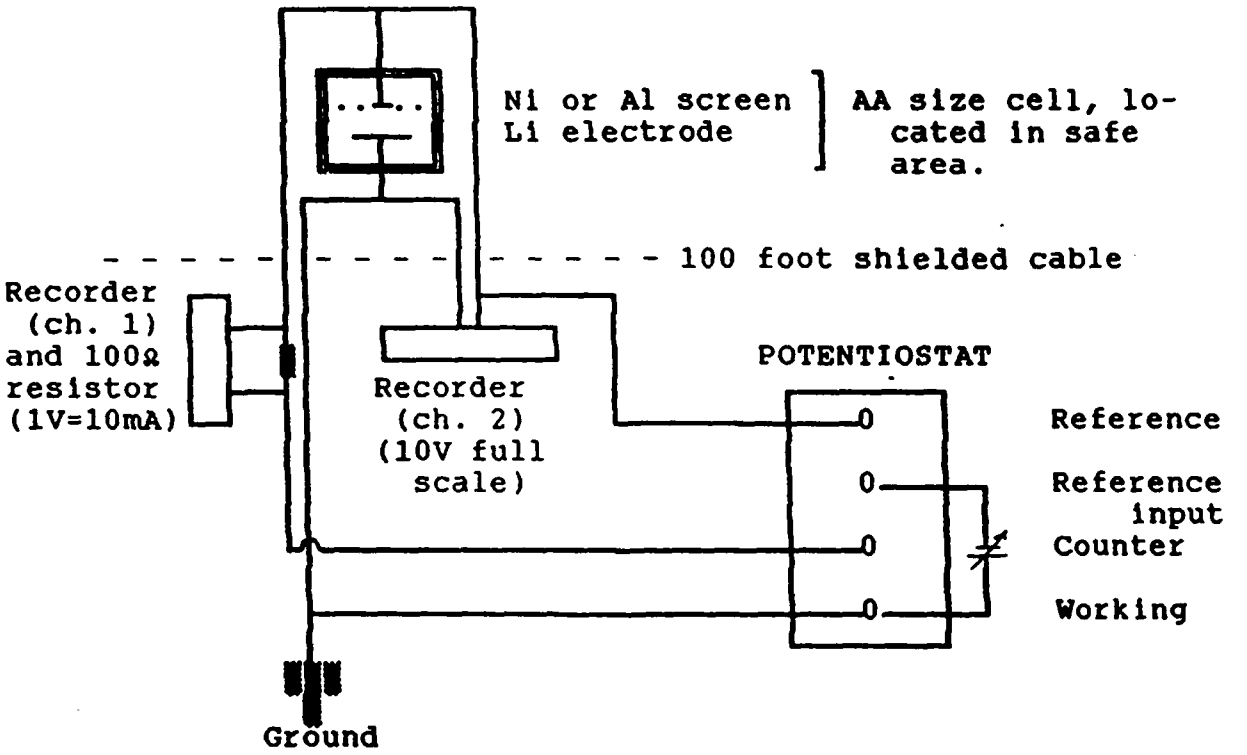

FIGURE 2. Schematic diagram of connections between AA cells without carbon and the potentiostat and recorder for measurements of anodic and cathodic currents at various potentials.

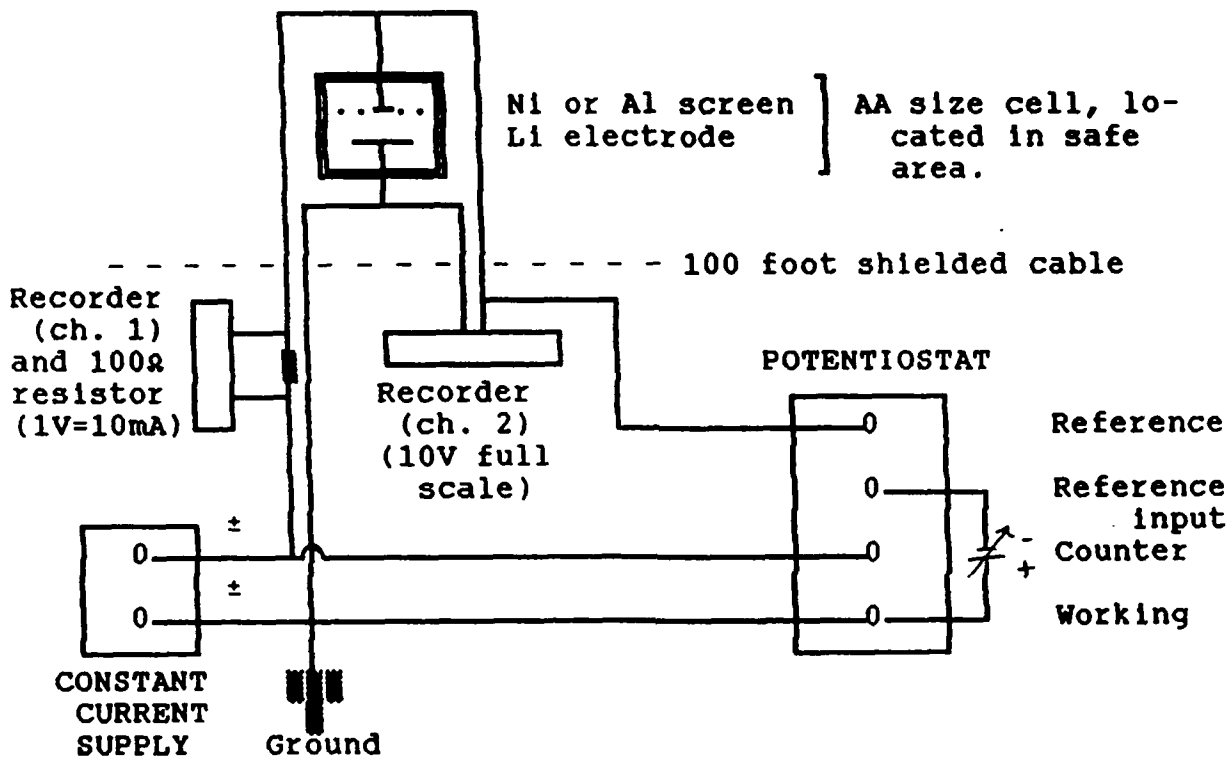

FIGURE 3. Schematic diagram of connections between AA cells without carbon and the potentiostat, the recorder and the galvanostat for measurements of lithium plate/ strip efficiencies.

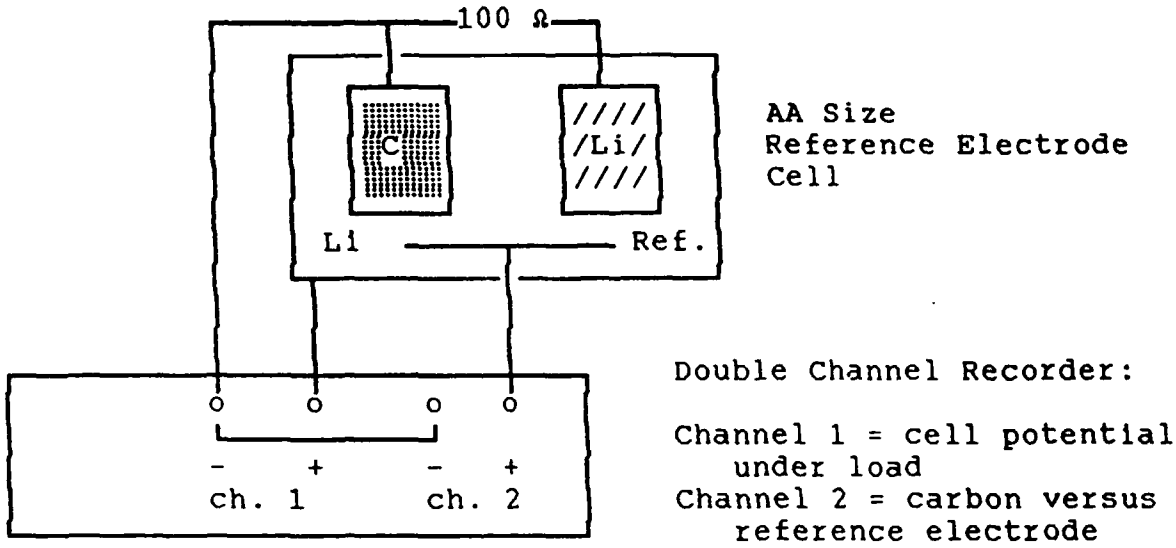

FIGURE 4. Schematic of connections for reference electrode cell tests, using strip chart recorder.

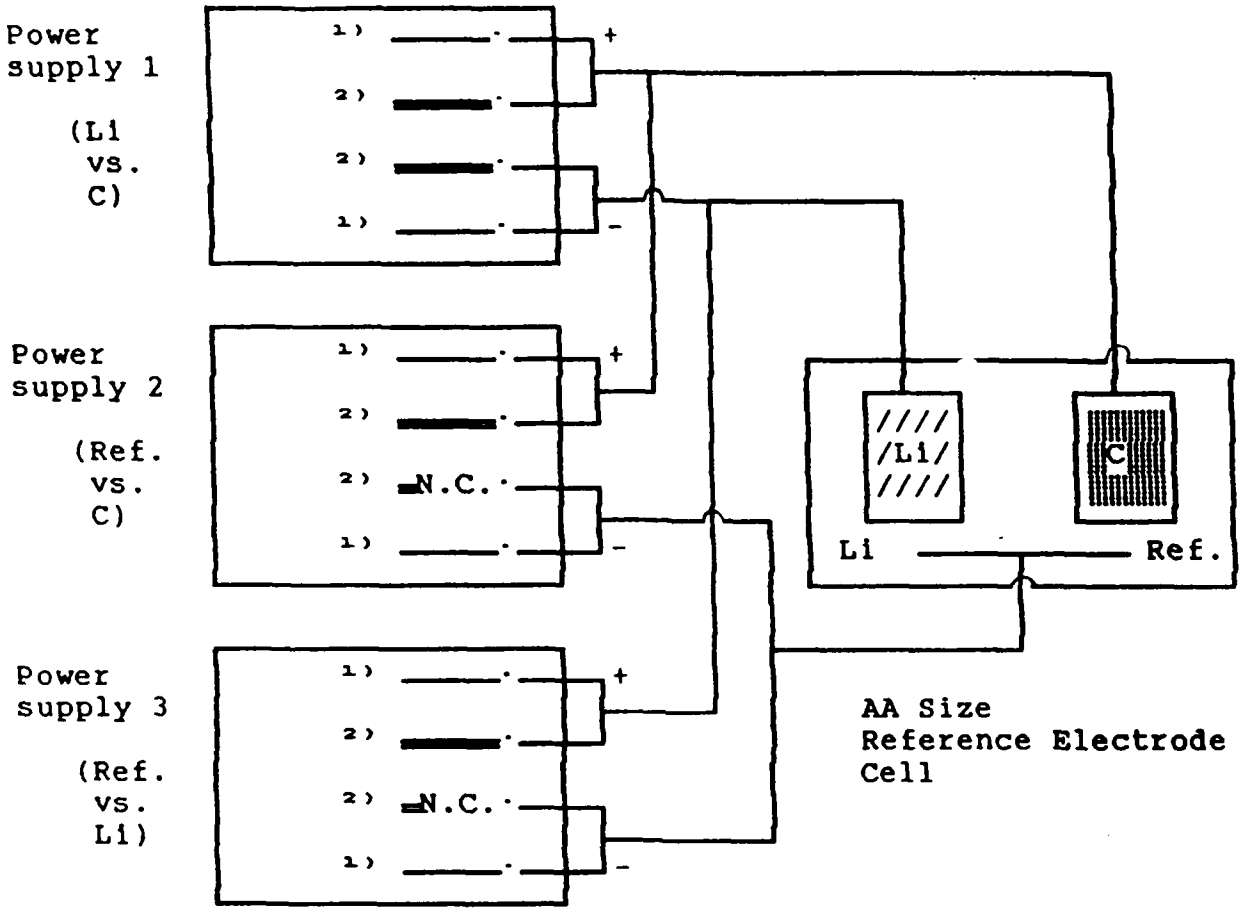

1) Potential sensing leads within computer regulated power supply
2) Current carrying leads within power supply

FIGURE 5. Schematic of connections for reference electrode cell tests, using high impedance cycler power supplies as voltmeters.

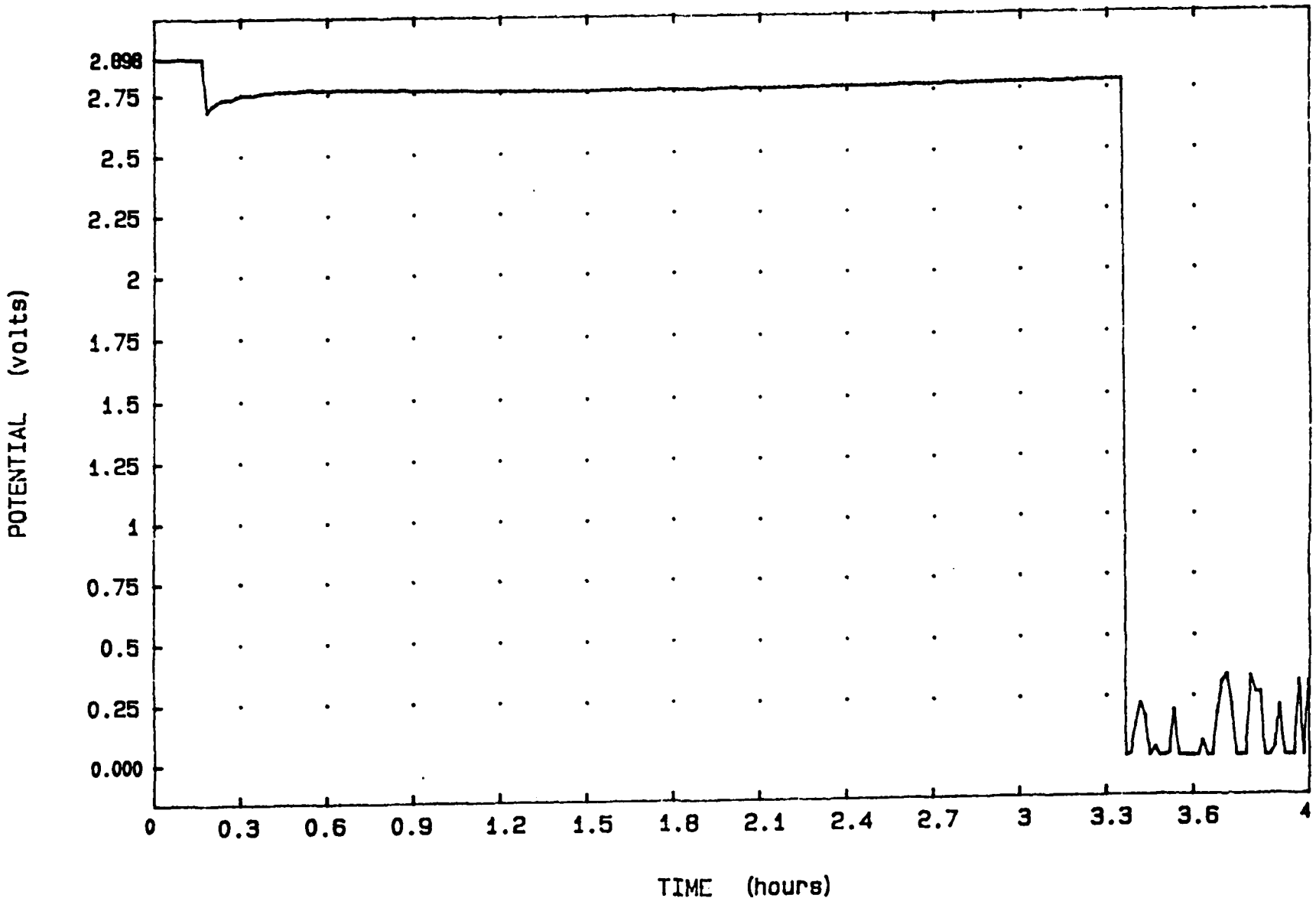

FIGURE 6. Cycle profile for cell #37-54-2.
Electrolyte: 0.85 M LiBr, 21.5 v/o acetonitrile, 6.5 v/o propylene carbonate, 13.8 M SO_2
Cathode screen: Al anodized to +160 mV versus Ag/ AgCl
Cathode tab: Ni
Separator: Tefzel

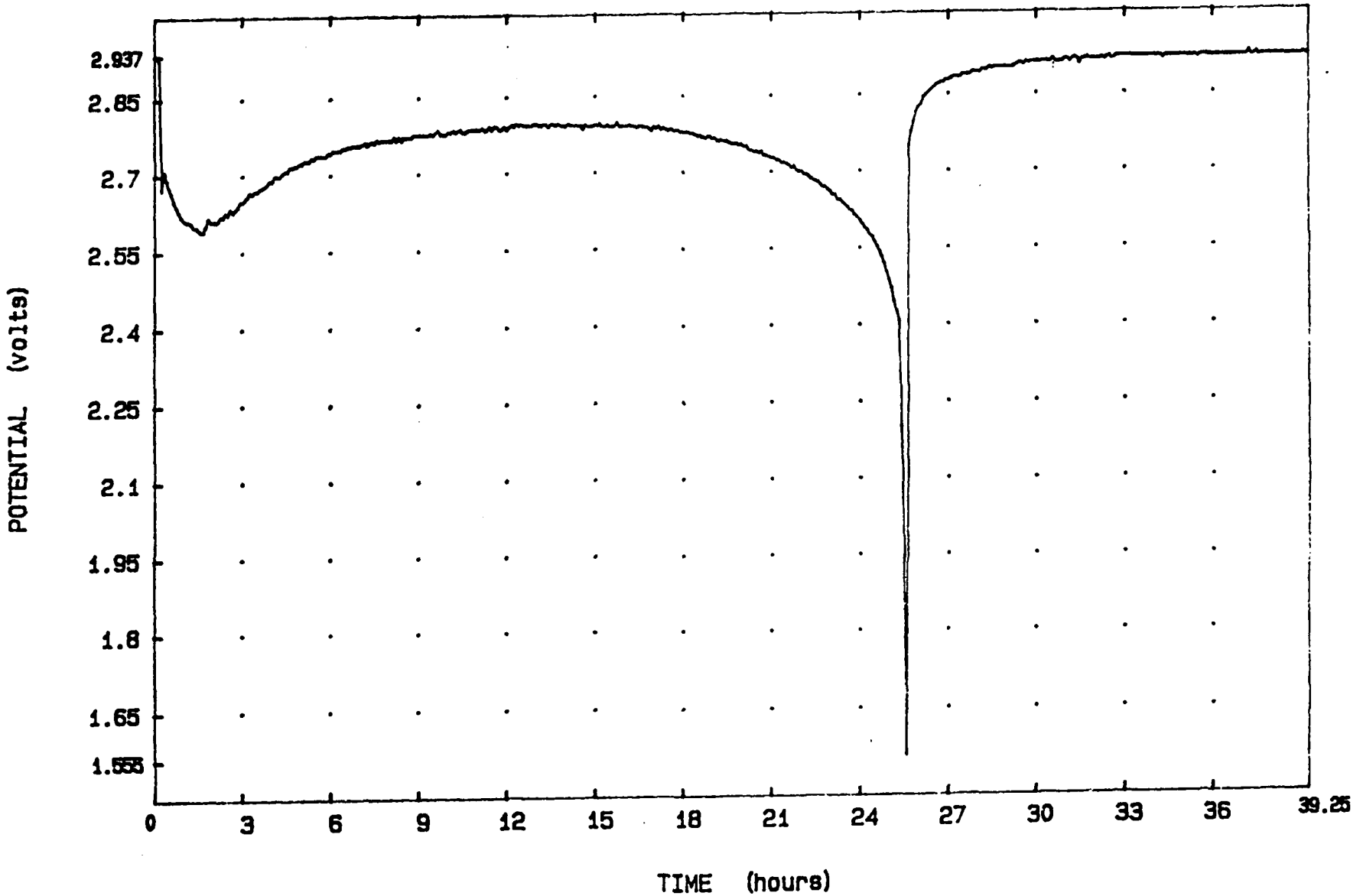

FIGURE 7. Cycle profile for cell #39-39-2.
Electrolyte: 0.85 M LiBr, 21.5 v/o acetonitrile, 6.5 v/o propylene carbonate, 13.8 M SO_2;
Cathode screen: Al anodized to +200 mV versus Ag/ AgCl; cathode tab, Al
Separator: Tefzel

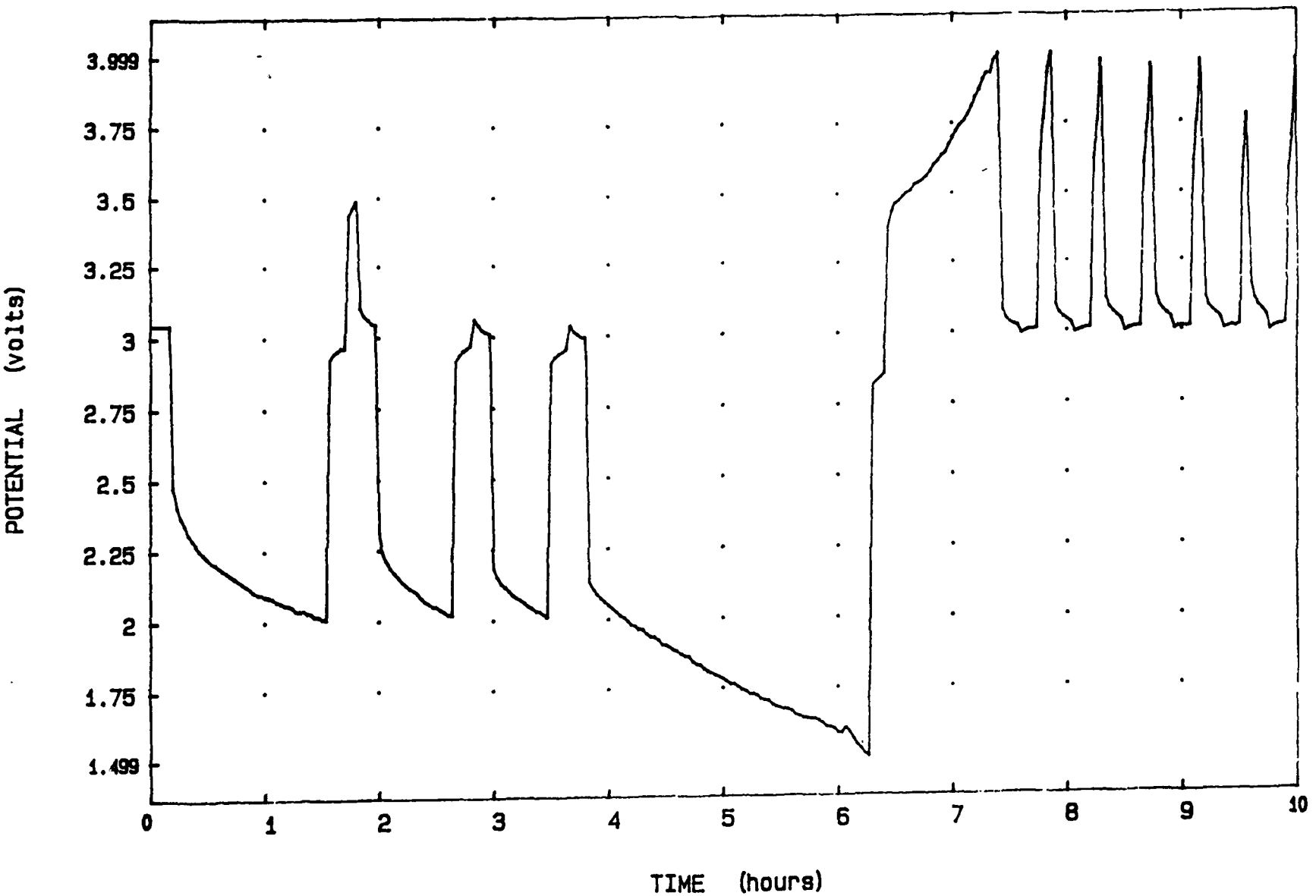

FIGURE 8. Cycle profile for cell #37-48-2.
Electrolyte: 3.89ml of 1M LiSCN/ 3M NH_4SCN, 17.55 M SO_2
Cathode screen: Al anodized to +200 mV versus Ag/ AgCl
Cathode tab: Ni
Separator: Pyrex

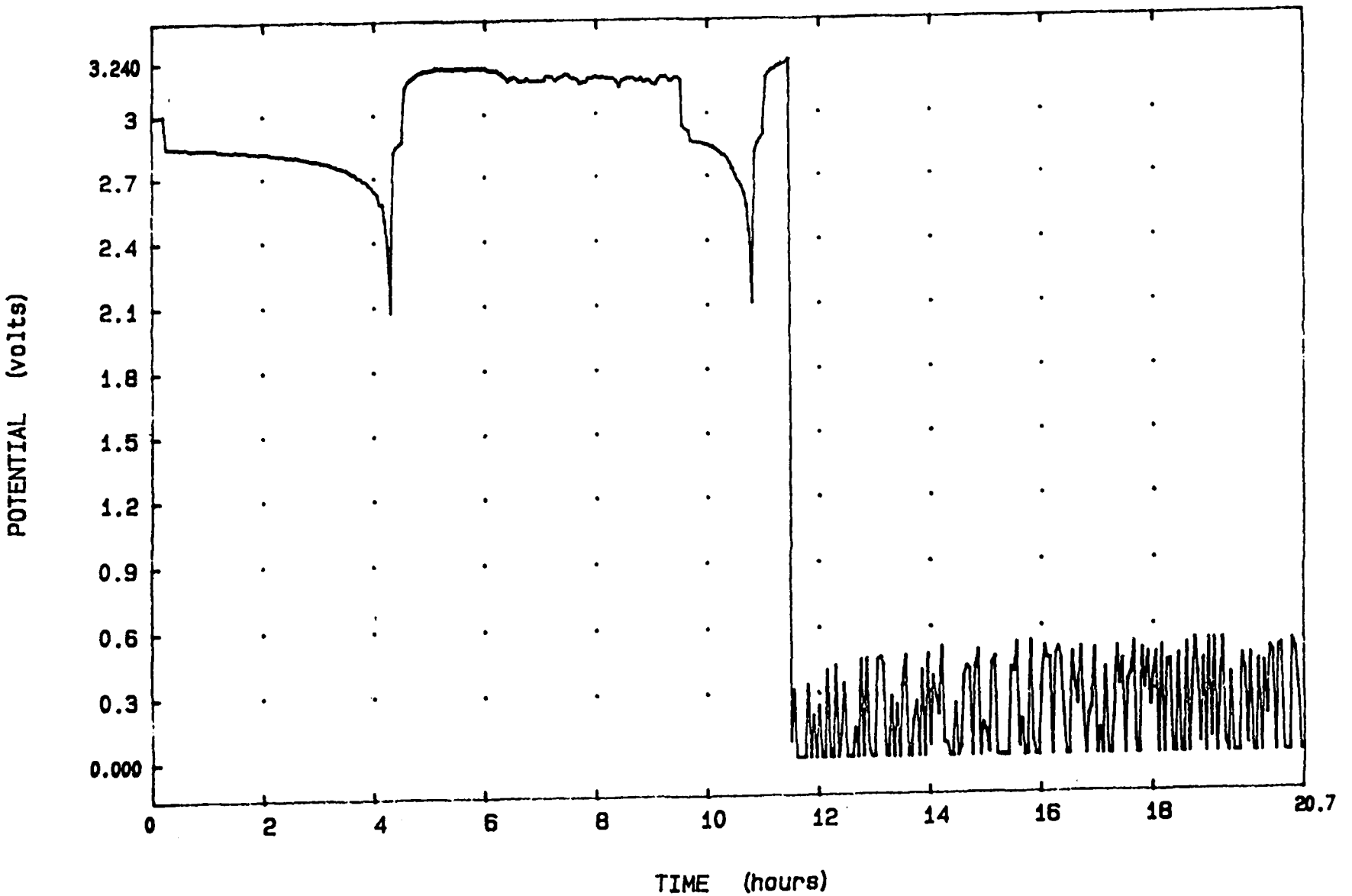

FIGURE 9. Cycle profile for cell #37-57-3.
Electrolyte: 3.97ml of 1M LiSCN/ 3M NH_4SCN, 17.55 M SO_2
Cathode screen, Inconel 600
Cathode tab, Ni
Separator, Pyrex

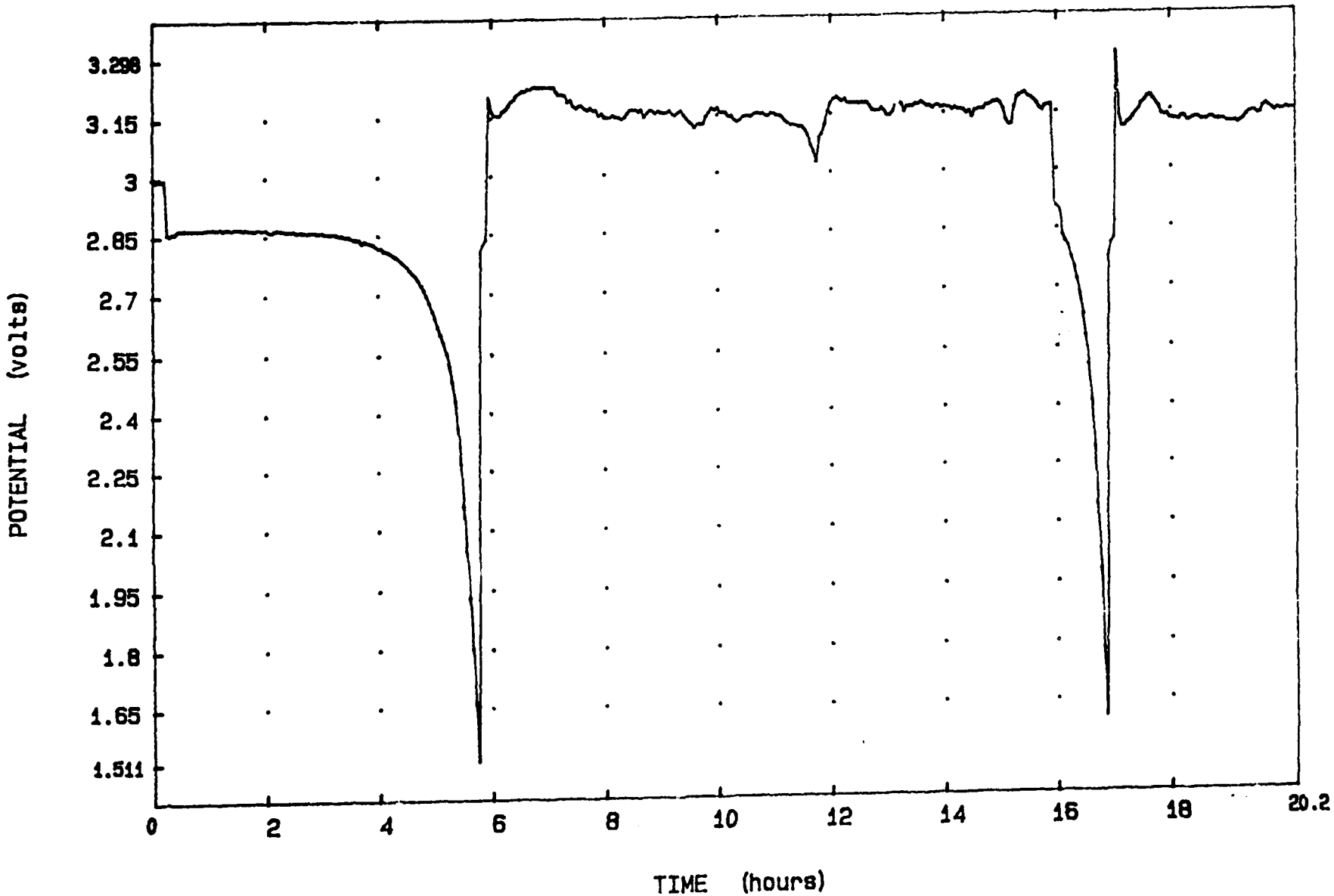

FIGURE 10. Cycle profile for cell #37-57-4.
Electrolyte: 3.97ml of 0.5M LiSCN/ 2M NH_4SCN (heavier phase)
Cathode screen: Inconel 600
Cathode tab: Ni
Separator: Pyrex

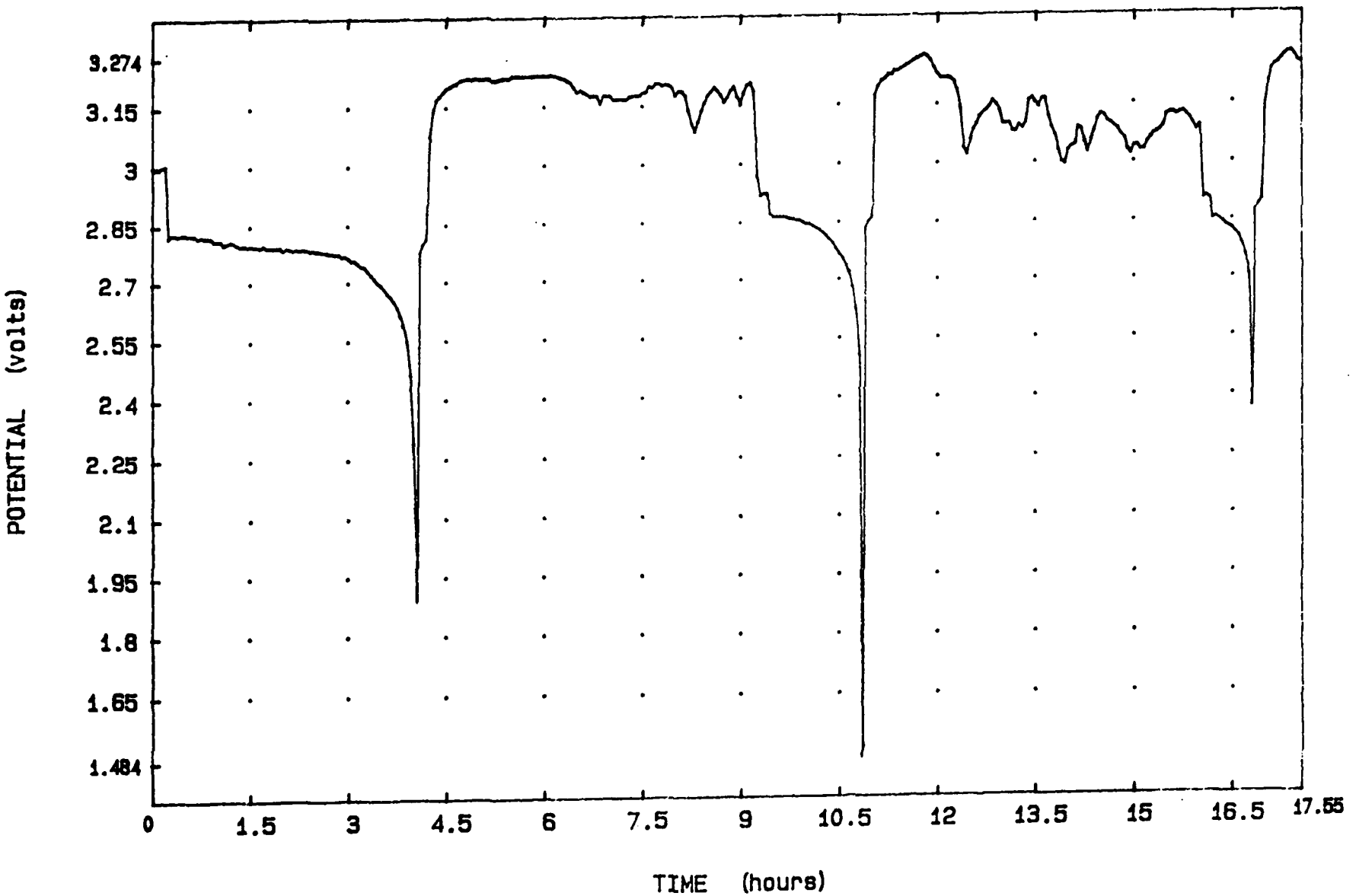

FIGURE 11. Cycle profile for cell #37-69-1.
Electrolyte: 3.66ml of 0.75M LiSCN/ 2M NH_4SCN, (heavier phase)
Cathode screen: titanium
Cathode tab: Ti
Separator: Pyrex

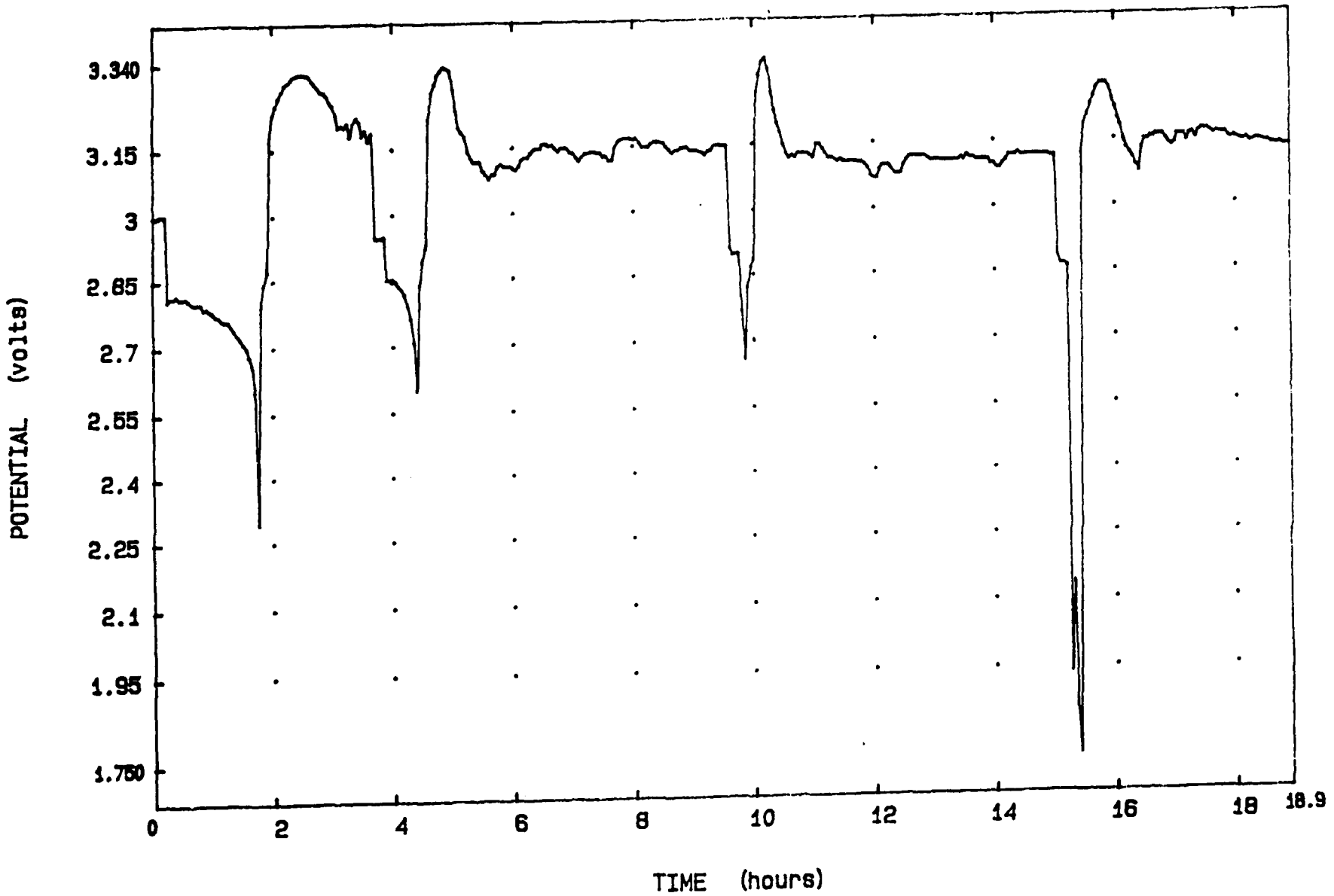

FIGURE 12. Cycle profile for cell #37-66-4.
Electrolyte: 4.0ml of 0.1M LiSCN/ 1M NH_4SCN
Cathode screen: Inconel 600
Cathode tab: Inconel
Separator: Pyrex

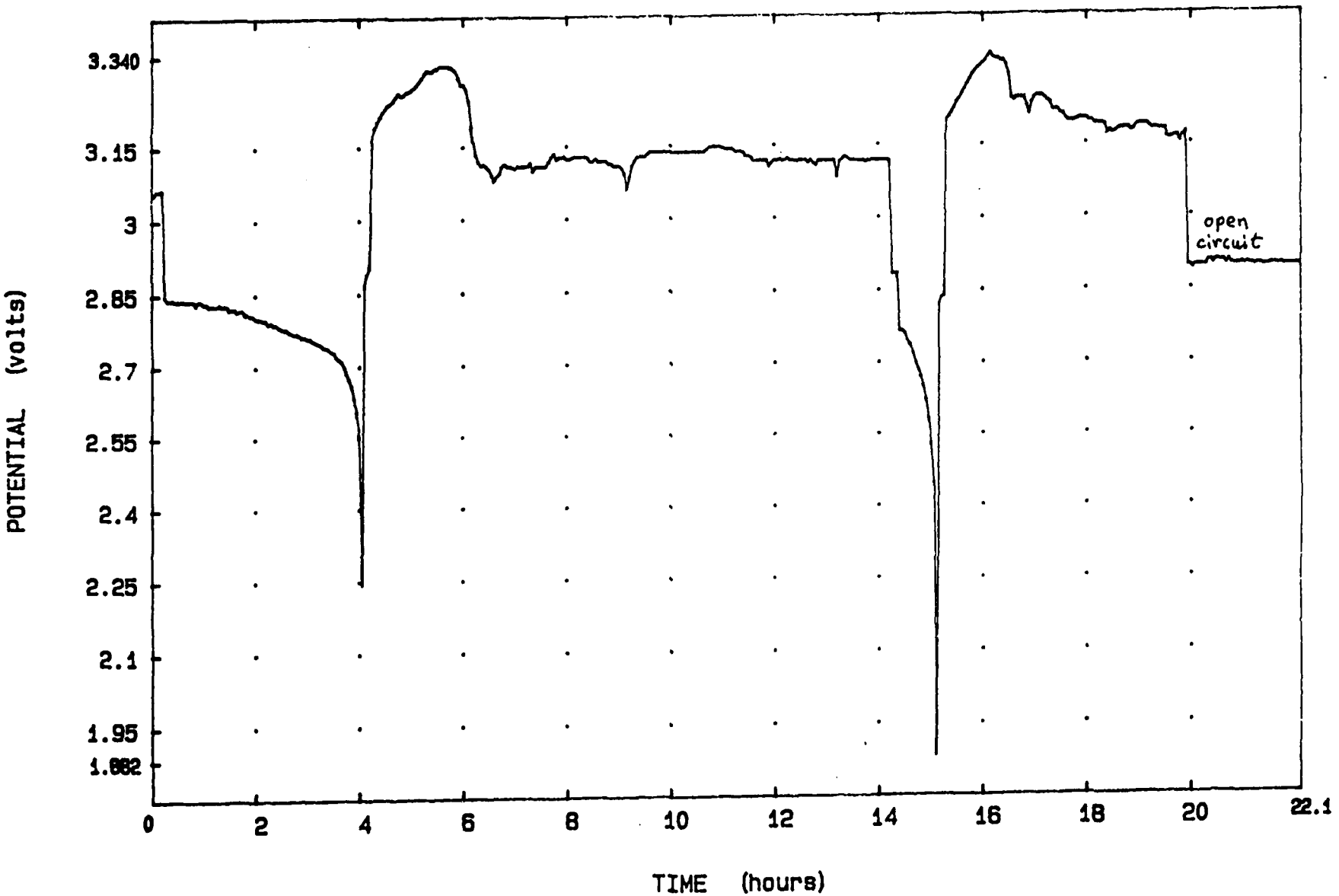

FIGURE 13. Cycle profile for cell #37-54-5.
Electrolyte: 3.80ml of 1M LiSCN/ 4M NH_4SCN, 17.55 M SO_2
Cathode screen: Al anodized to +160 mV versus Ag/ AgCl
Cathode tab: Ni
Separator: Pyrex

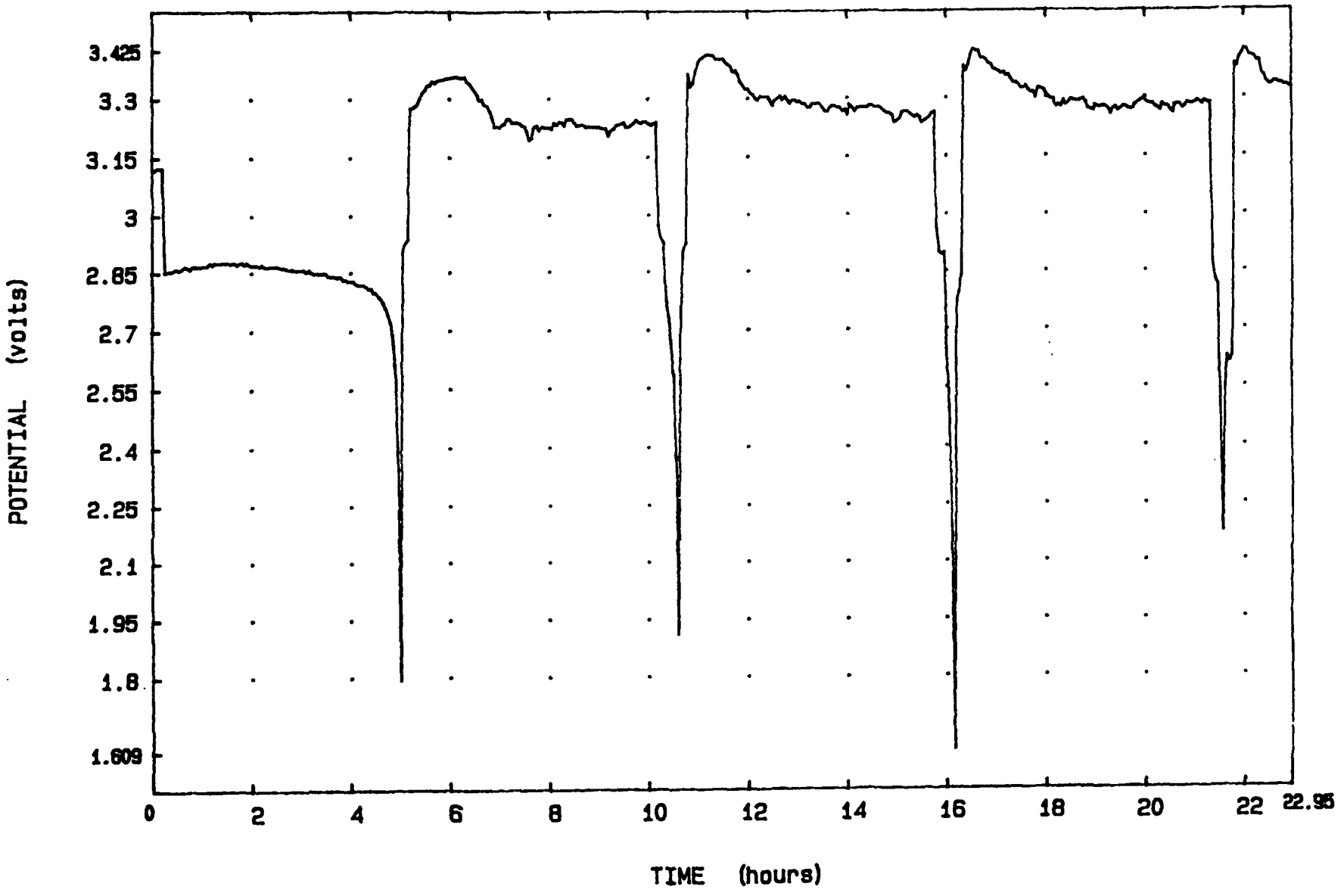

FIGURE 14. Cycle profile, cell #37-53-3, first four cycles
Separator: Craneglass
Pos. screen/contact: Al/Ni
Electrolyte: 2M NH_4SCN / 0.25M LiSCN

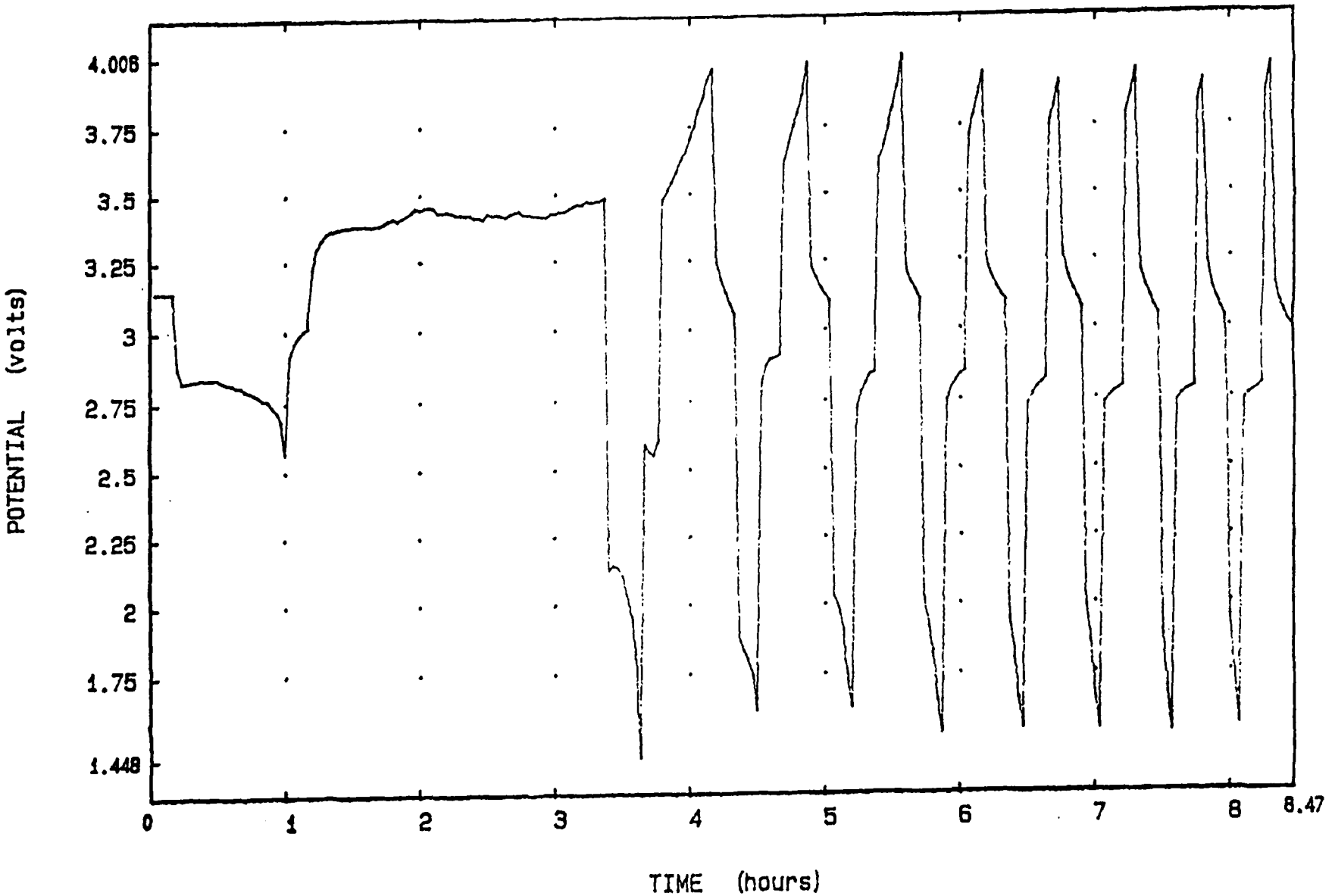

FIGURE 15. Cycle profile, cell #37-53-6, first nine cycles
Separator: Tefzel
Pos. screen/contact: Al/Ni
Electrolyte: 2M NH_4SCN / 0.25M LiSCN

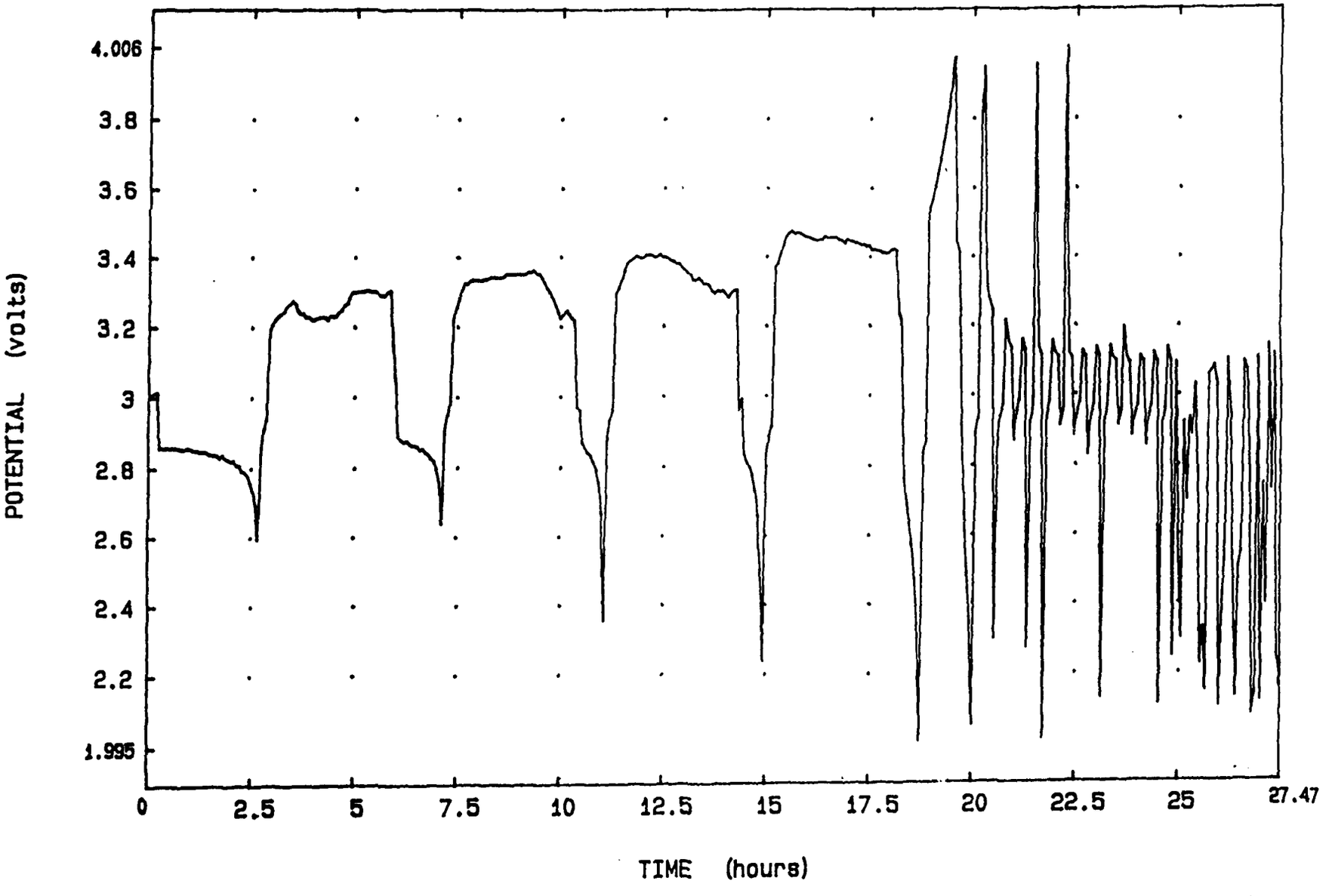

FIGURE 16. Cycle profile, cell #37-81-2,
Separator: Hovosorb
Pos. screen/contact: Ti/Ti
Electrolyte: 2M NH_4SCN / 0.4M LiSCN

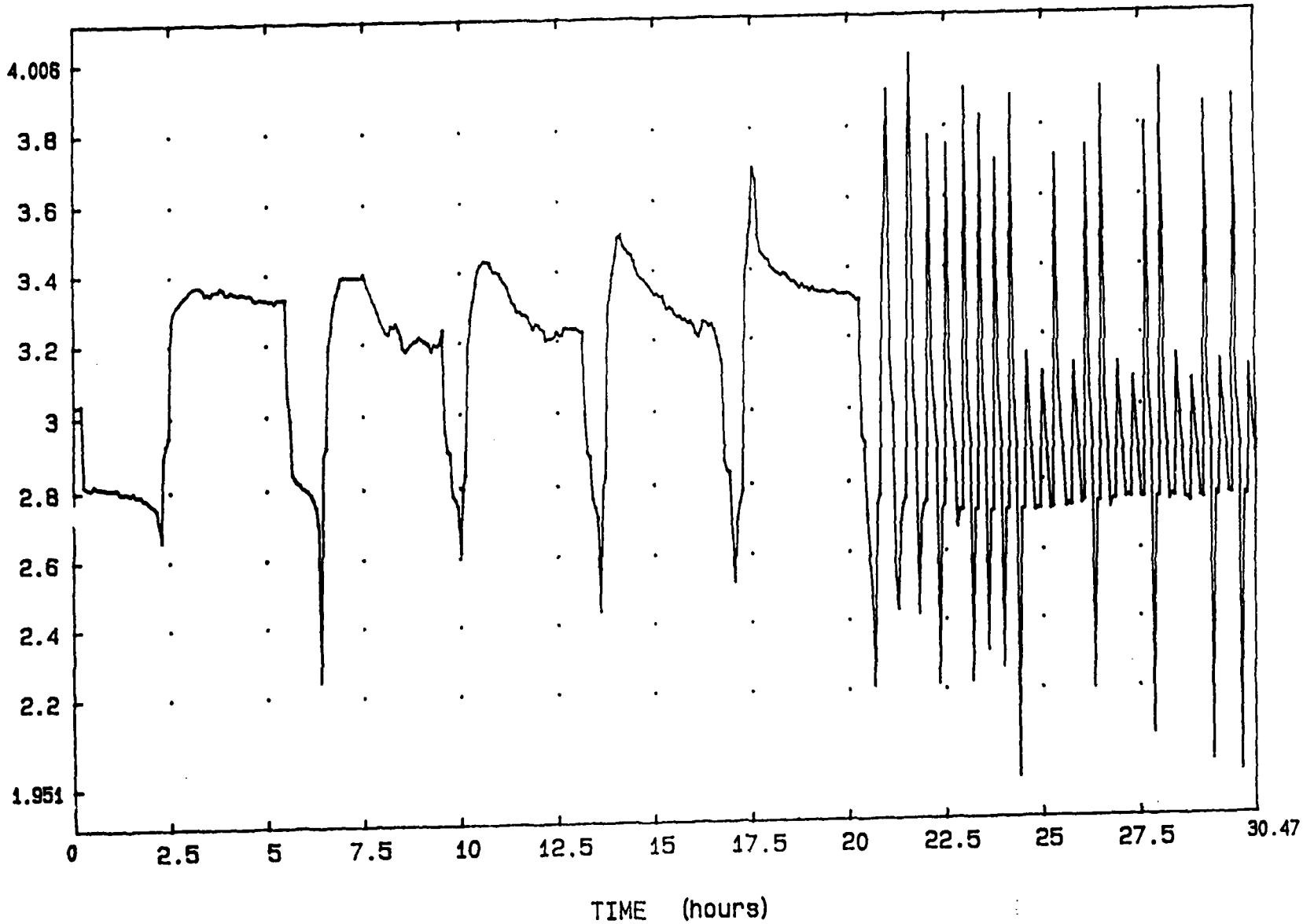

FIGURE 17. Cycle profile, cell #37-81-6
Separator: Tefzel
Pos. screen/contact: Ti/Ti
Electrolyte: 2M NH4SCN / 0.4M LiSCN

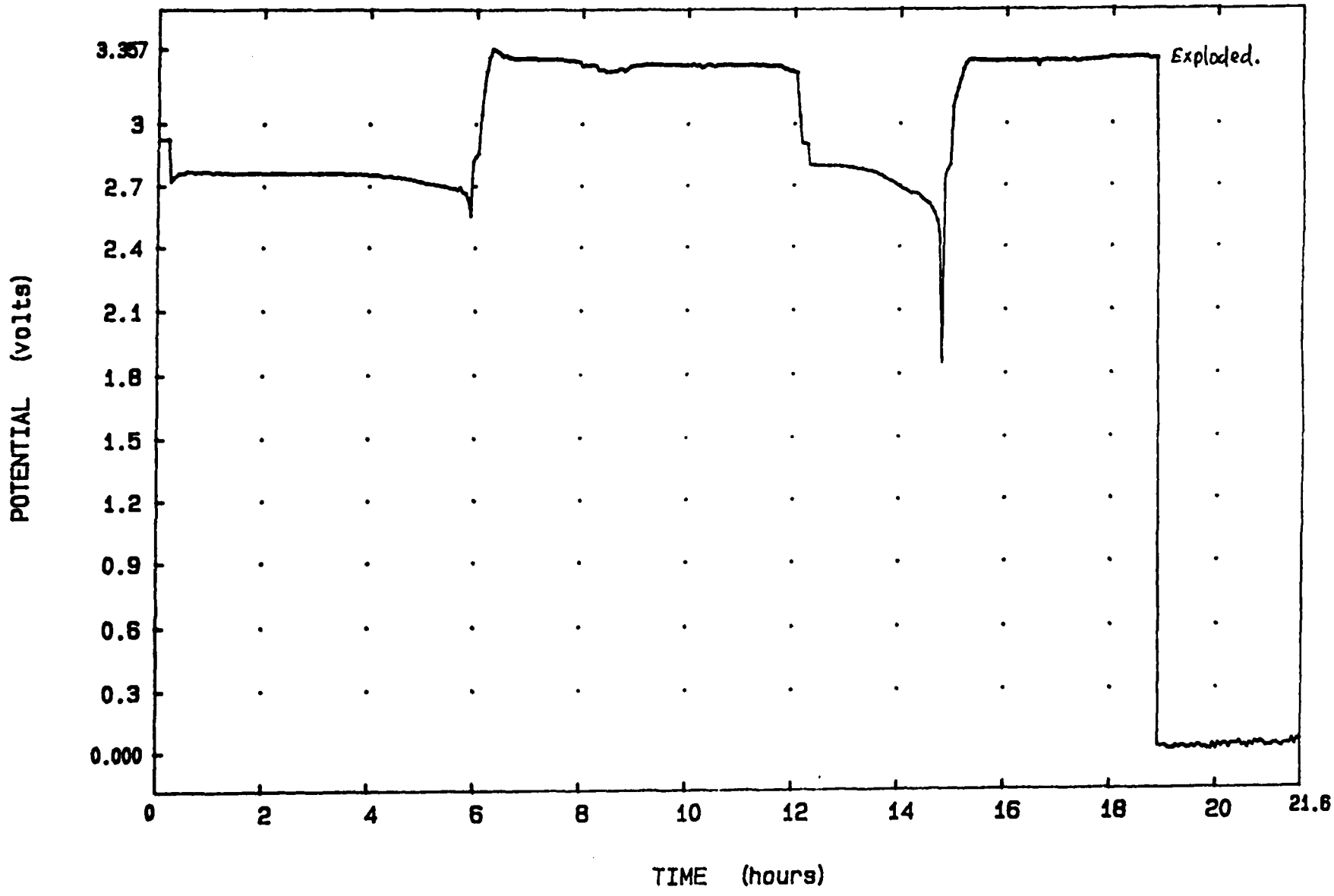

FIGURE 18. Cycle profile, cell #37-54-4, two cycles
Separator: Tefzel
Pos. screen/contact: anodized Al/ anodized Al
Electrolyte: 1M KSCN / 0.5M LiSCN

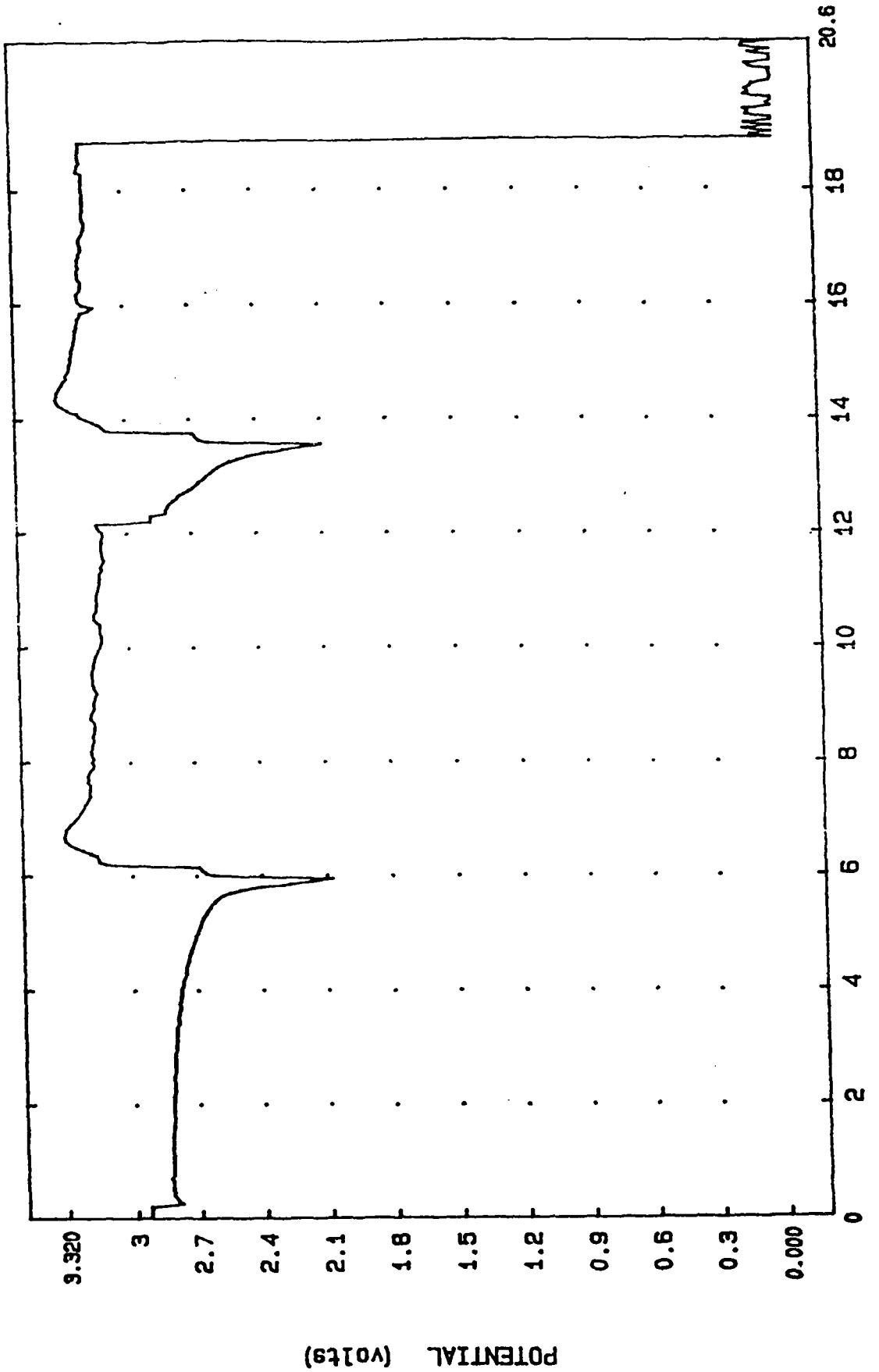

FIGURE 19. Cycle profile, cell #37-54-7, first two cycles
Separator: Craneglass
Pos. screen/contact: anodized Al/ Ni
Electrolyte: 1M KSCN / 0.5M LiSCN

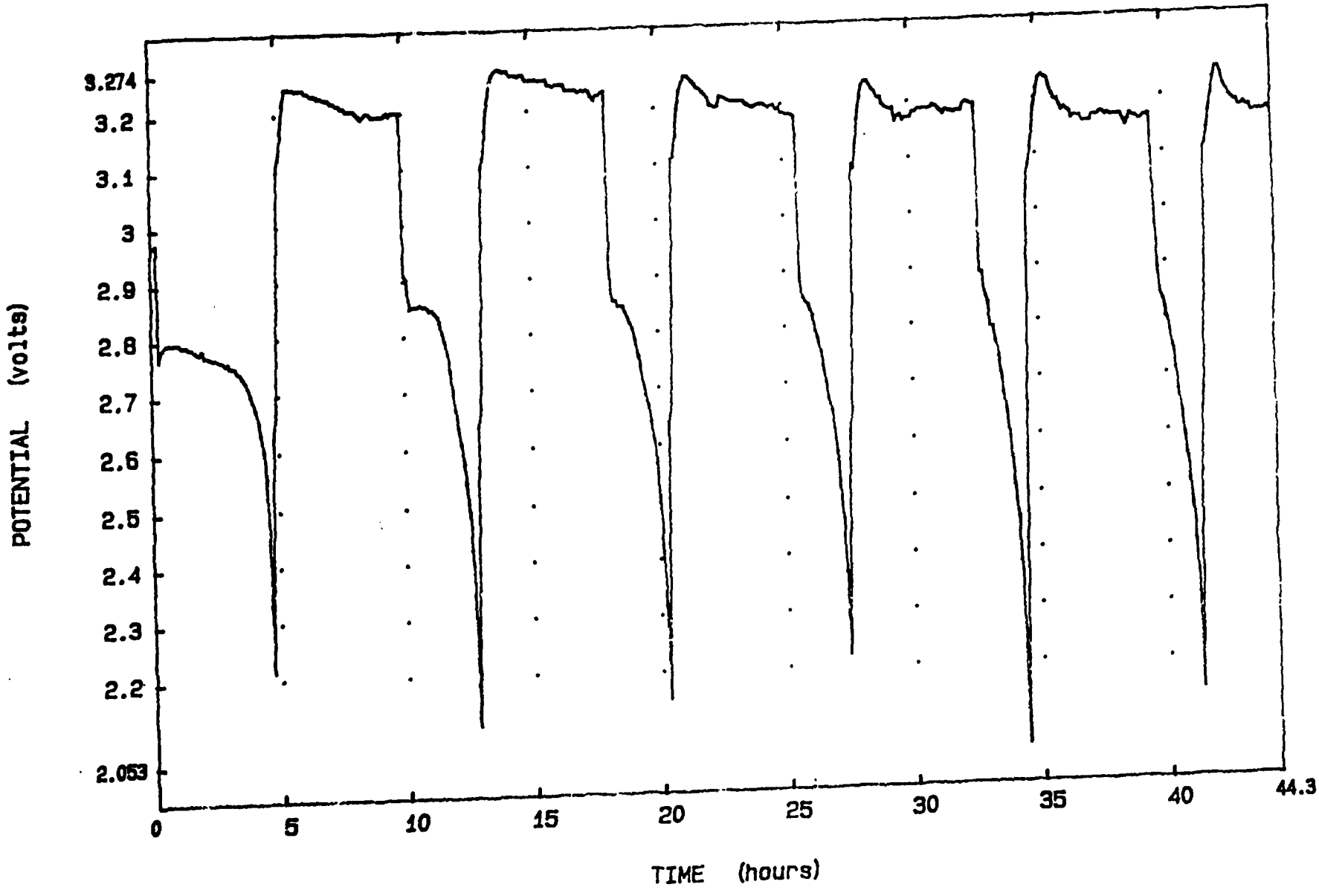

FIGURE 20. Cycle profile, cell #37-88-1, first six cycles.
Separator: Craneglass
Pos. screen/contact: Ti/ Ti
Electrolyte: 1M KSCN / 0.5M LiSCN

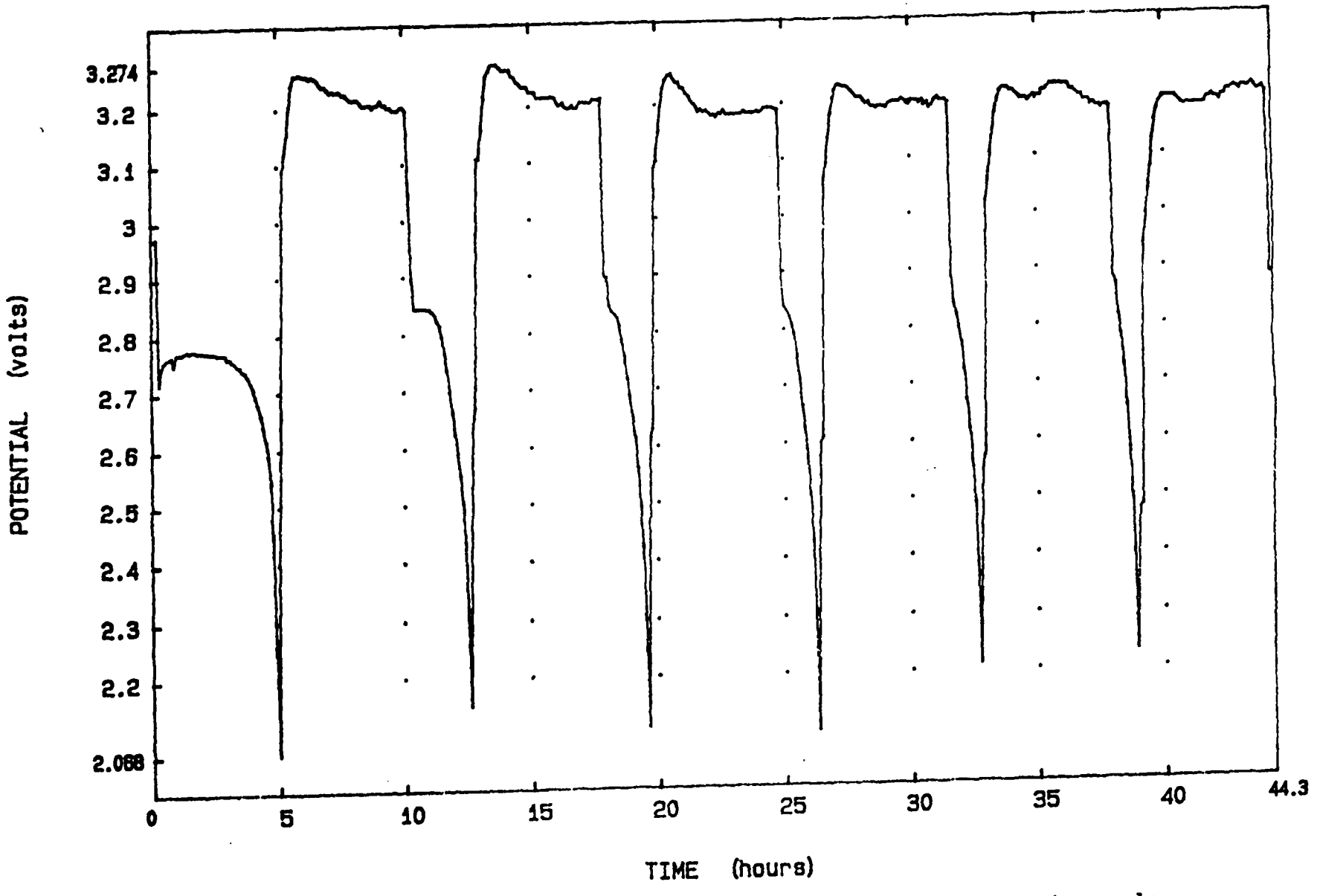

FIGURE 21. Cycle profile, cell #37-88-2, first six cycles.
Separator: Hovosorb
Pos. screen/contact: Ti/ Ti
Electrolyte: 1M KSCN / 0.5M LiSCN

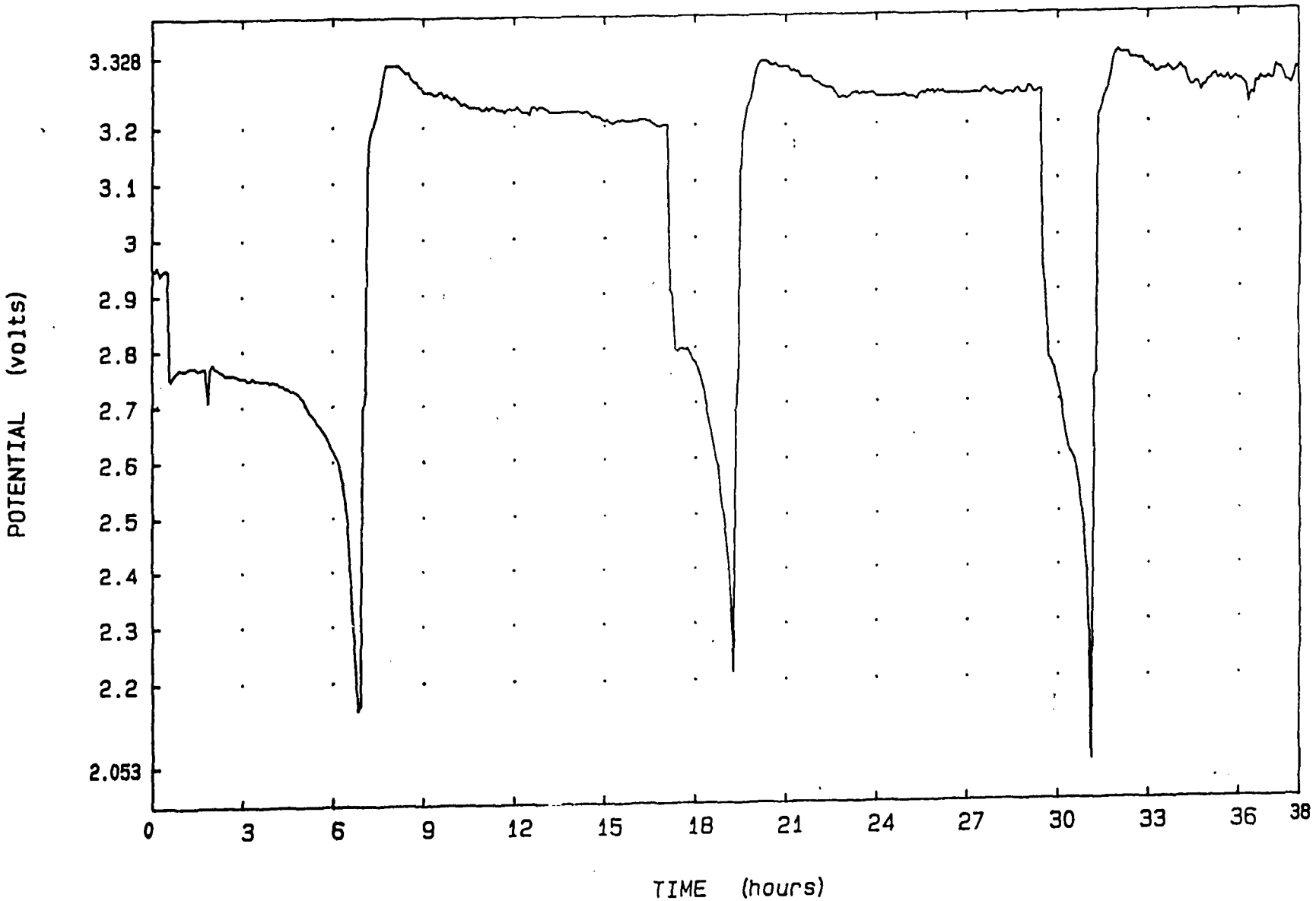

FIGURE 22. Cycle profile, cell #37-90-4, first three cycles.
Separator: Hovosorb
Pos. screen/contact: anodized Al/ anodized Al
Electrolyte: 1M KSCN/ 0.5M LiSCN

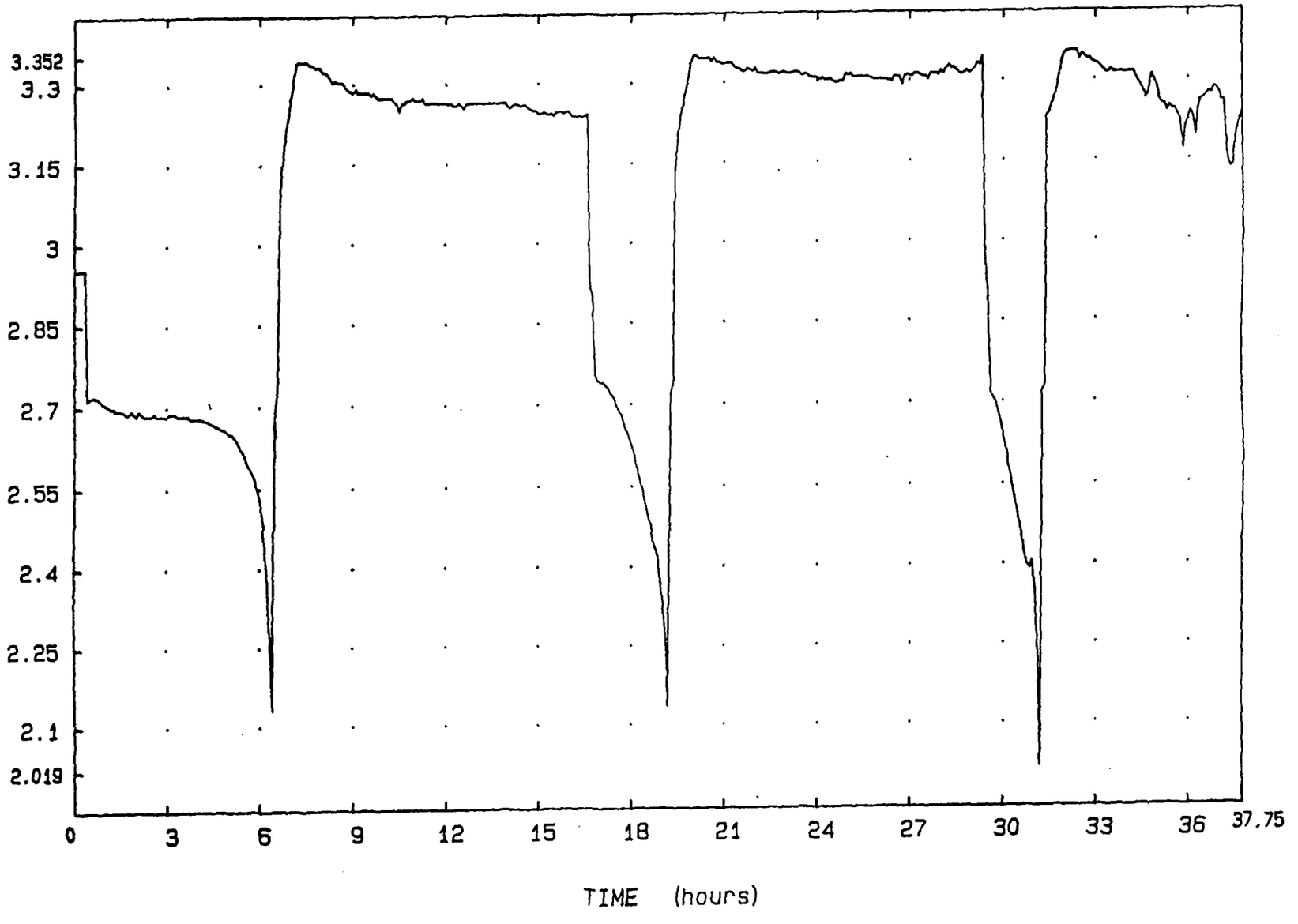

FIGURE 23. Cycle profile, cell #37-90-5, first three cycles
Separator: *Hovosorb*
Pos. screen/contact: anodized Al/ anodized Al
Electrolyte: 1M KSCN/ 0.5M LiSCN

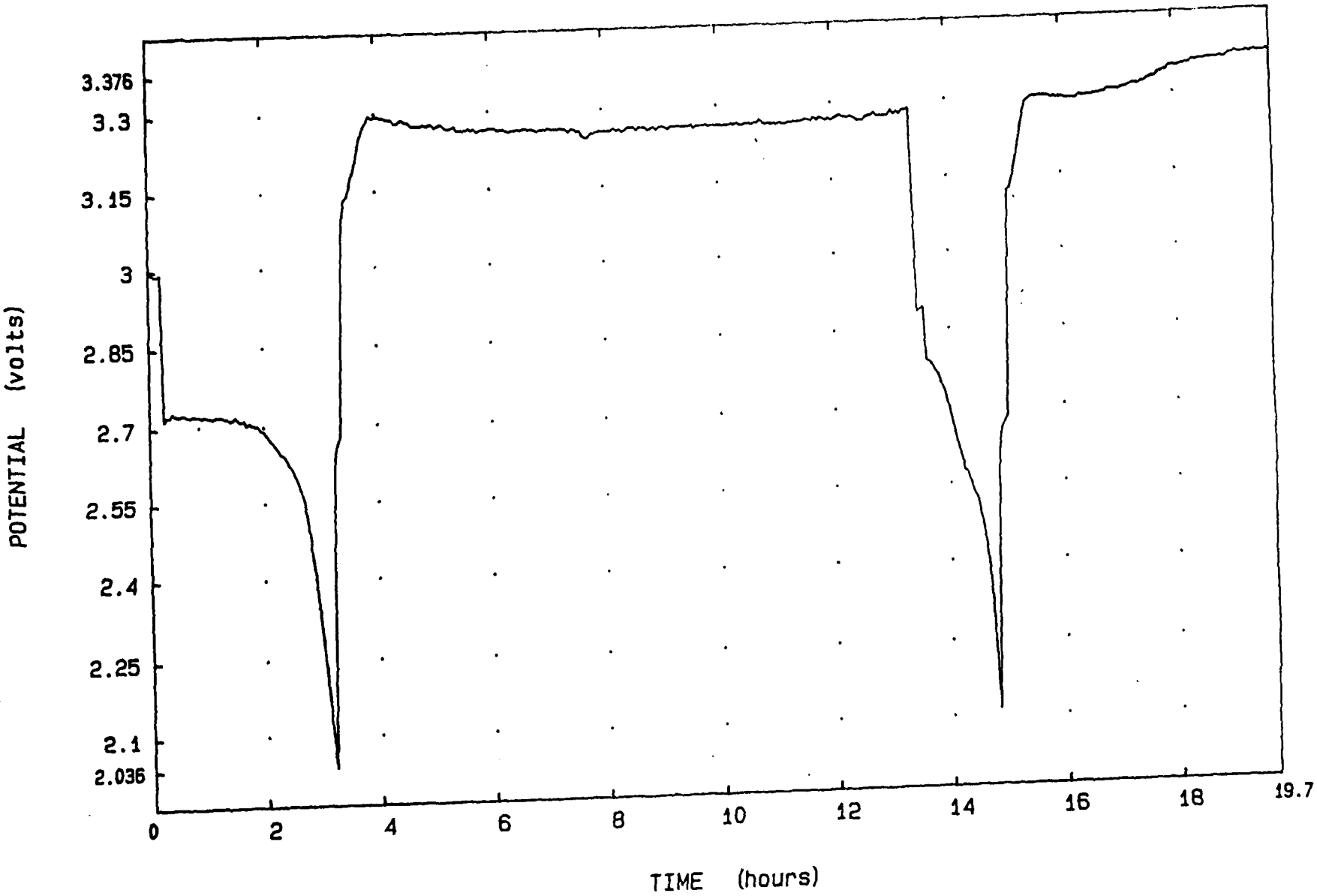

FIGURE 24. Cycle profile, cell #37-90-6, cycle 1, cont.; cycle 2.
Separator: Hovosorb
Pos. screen/contact: anodized Al/ anodized Al
Electrolyte: 1M KSCN/ 0.5M LiSCN

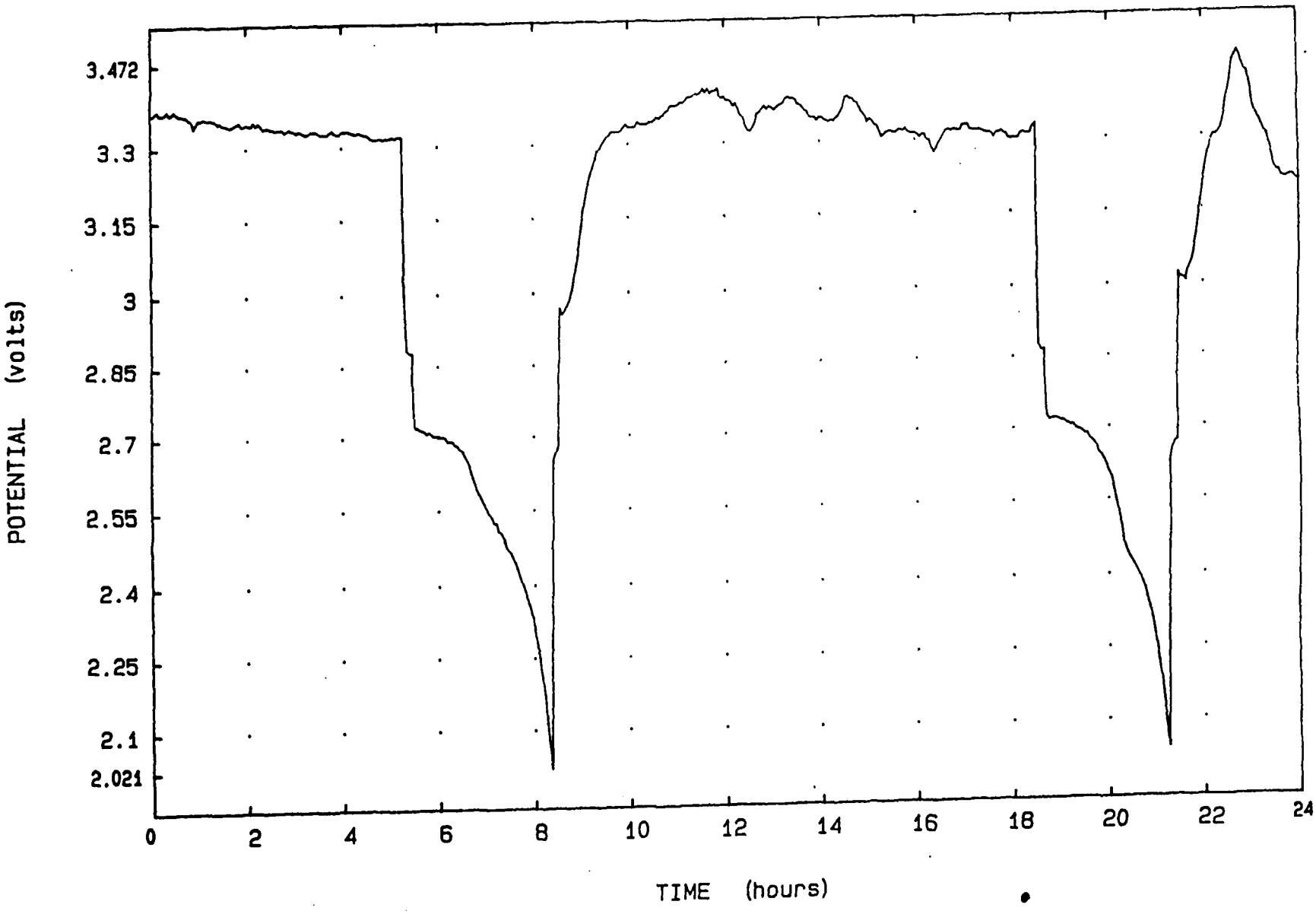

FIGURE 25. Cycle profile, cell #37-90-6, cycles 3,4
Separator: Hovosorb
Pos. screen/contact: anodized Al/ anodized Al
Electrolyte: 1M KSCN/ 0.5M LiSCN

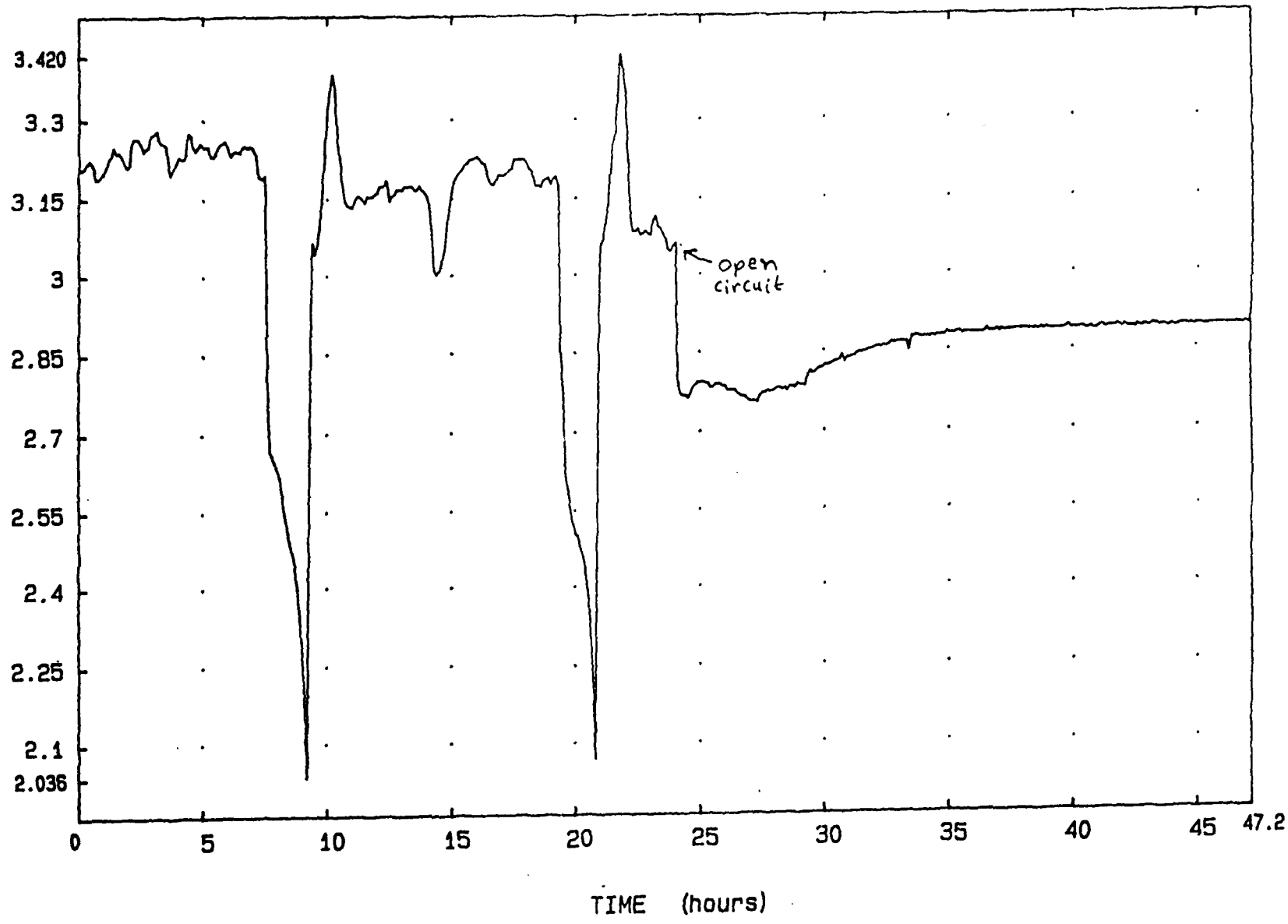

FIGURE 26. Cycle profile, cell #37-90-6, cycles 5,6;
open circuit
Separator: Hovosorb
Pos. screen/contact: anodized Al/ anodized Al
Electrolyte: 1M KSCN/ 0.5M LiSCN

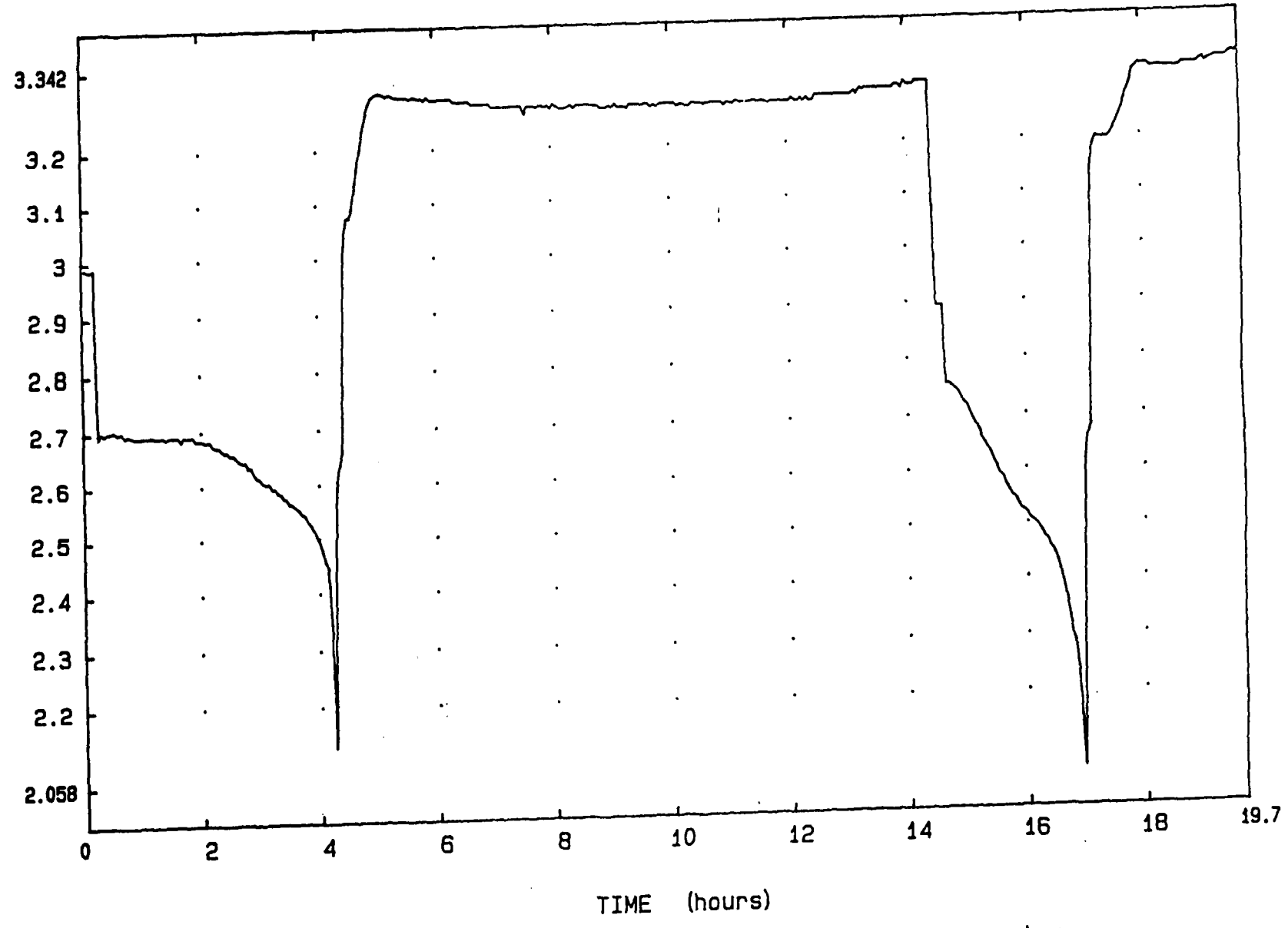

FIGURE 27. Cycle profile, cell #37-90-2, cycle 1, cont.; cycle 2
Separator: Hovosorb
Pos. screen/contact: anodized Al/ anodized Al
Electrolyte: 2M CsSCN/ 1M LiSCN

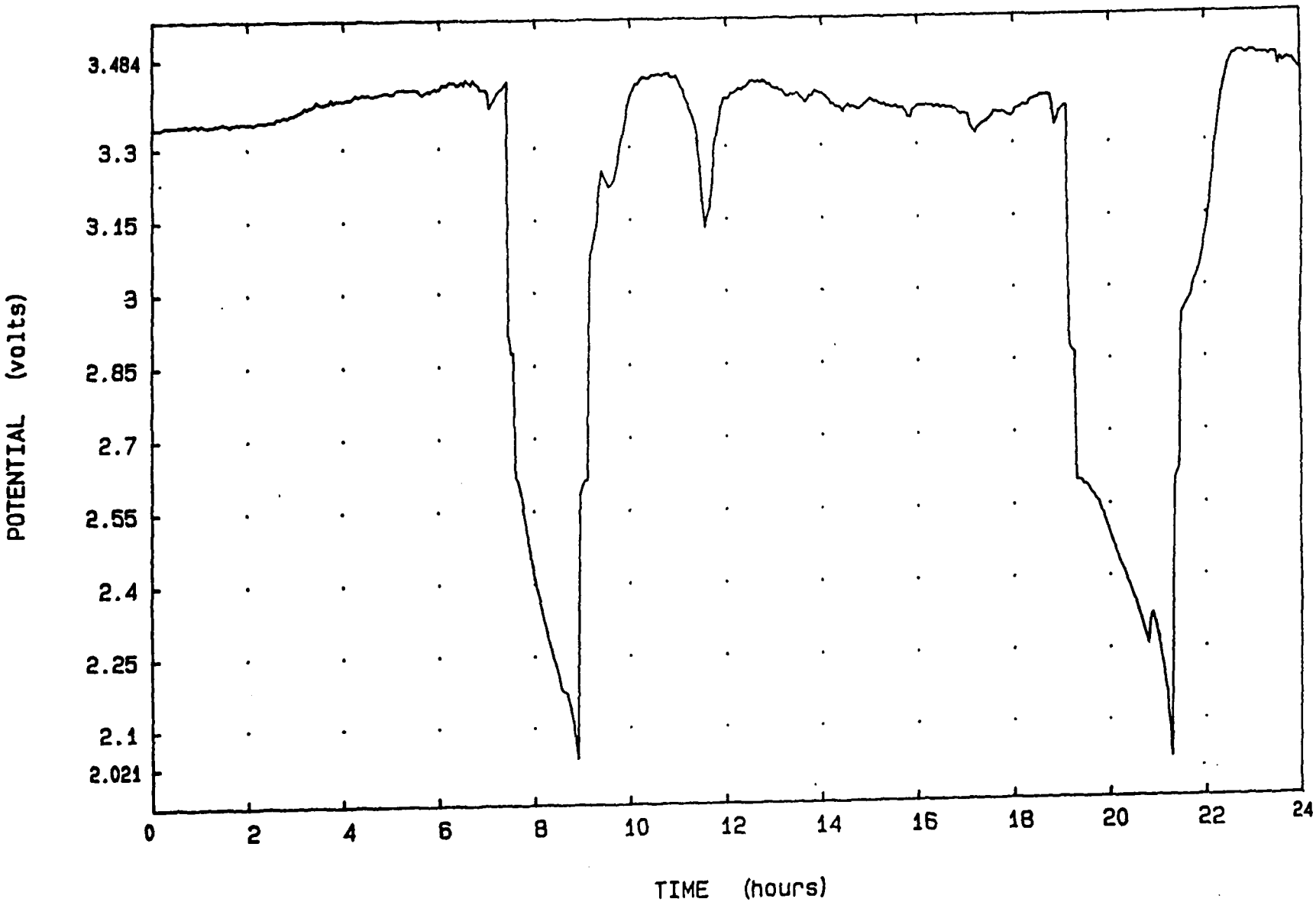

FIGURE 28. Cycle profile, cell #37-90-2, cycles 3,4
Separator: Hovosorb
Pos. screen/contact: anodized Al/ anodized Al
Electrolyte: 2M CsSCN/ 1M LiSCN

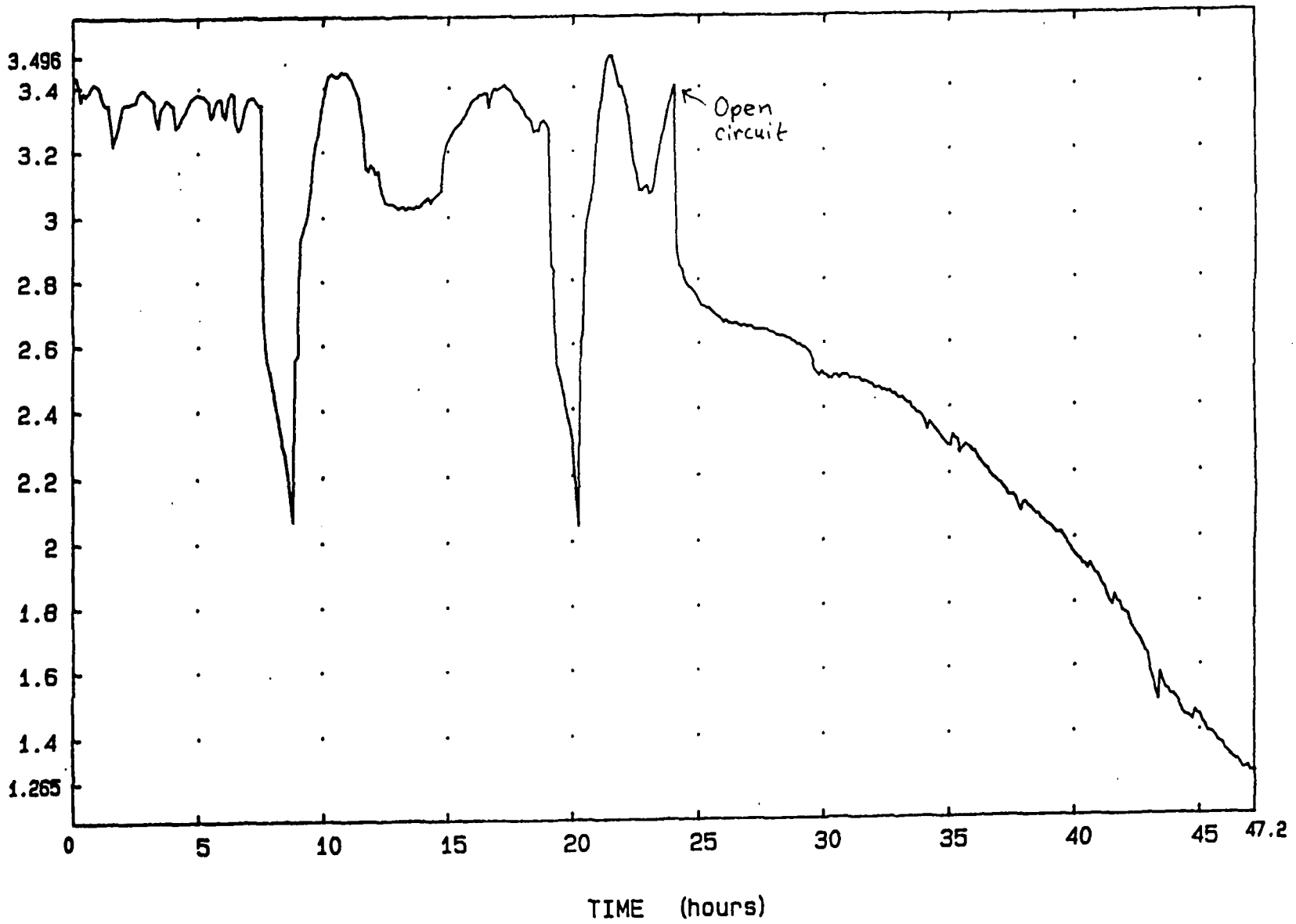

FIGURE 29. Cycle profile, cell #37-90-2, cycles 5,6;
open circuit
Separator: Hovosorb
Pos. screen/contact: anodized Al/ anodized Al
Electrolyte: 2M CsSCN/ 1M LiSCN

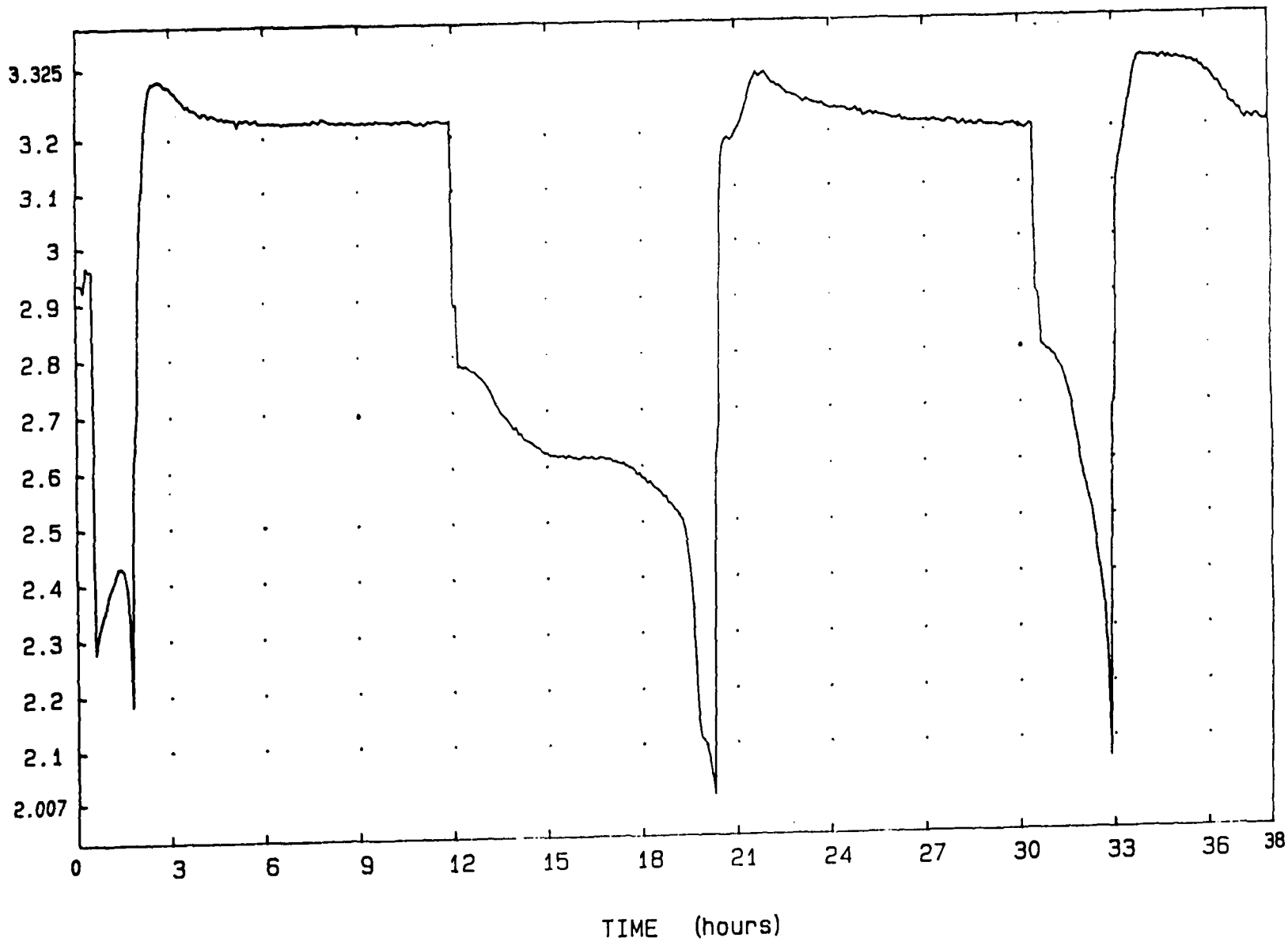

FIGURE 30. Cycle profile, cell #37-90-3, cycle 1 (intermittent connection); cycles 2,3
Separator: Hovosorb
Pos. screen/contact: anodized Al/ anodized Al
Electrolyte: 2M CsSCN/ 1M LiSCN

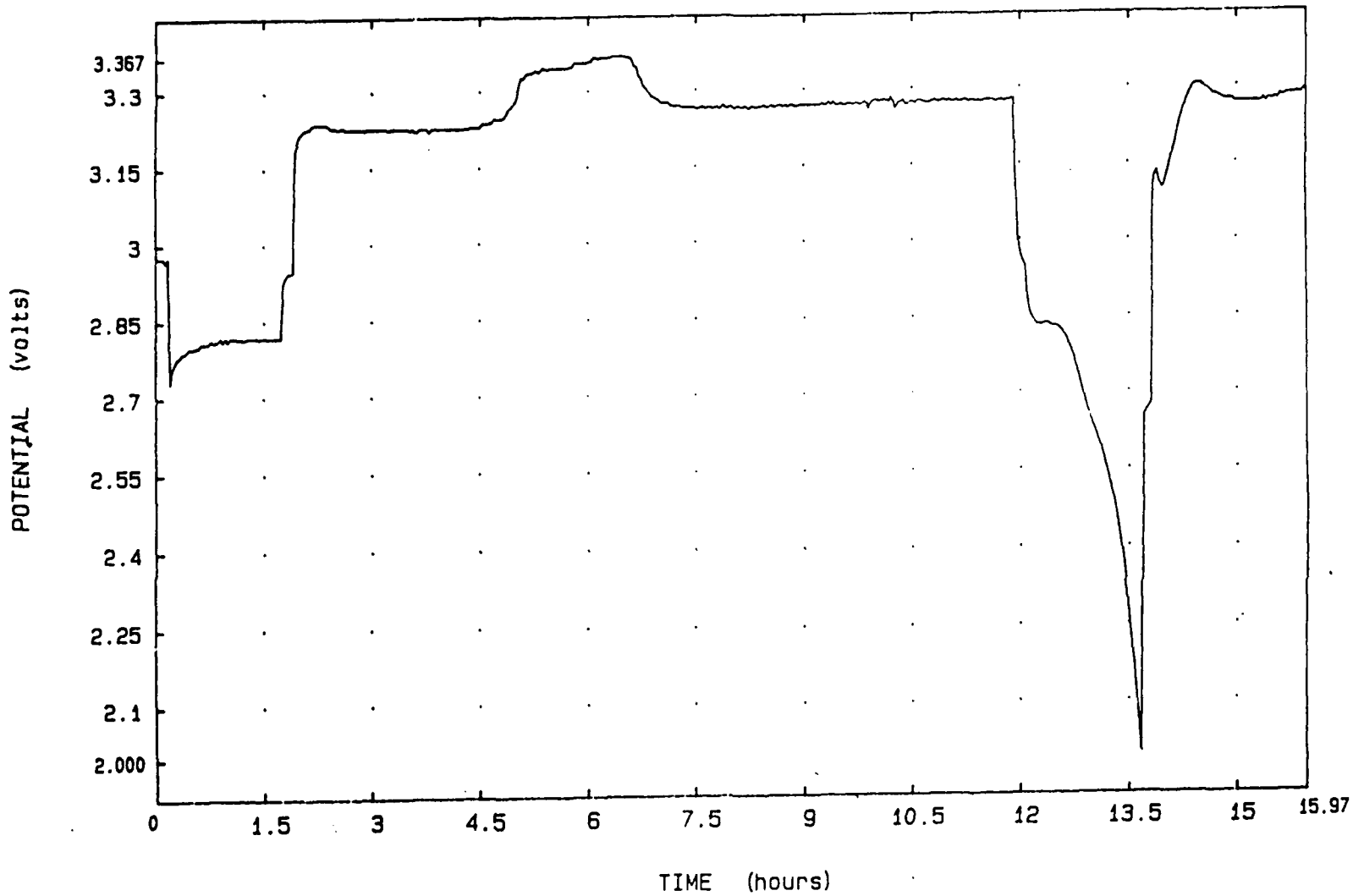

FIGURE 31. Cycle profile, cell #43-2-3: Li vs. C
Separator: Hovosorb
Pos. screen/contact: Titanium
Electrolyte: 1M KSCN; 0.5M LiSCN

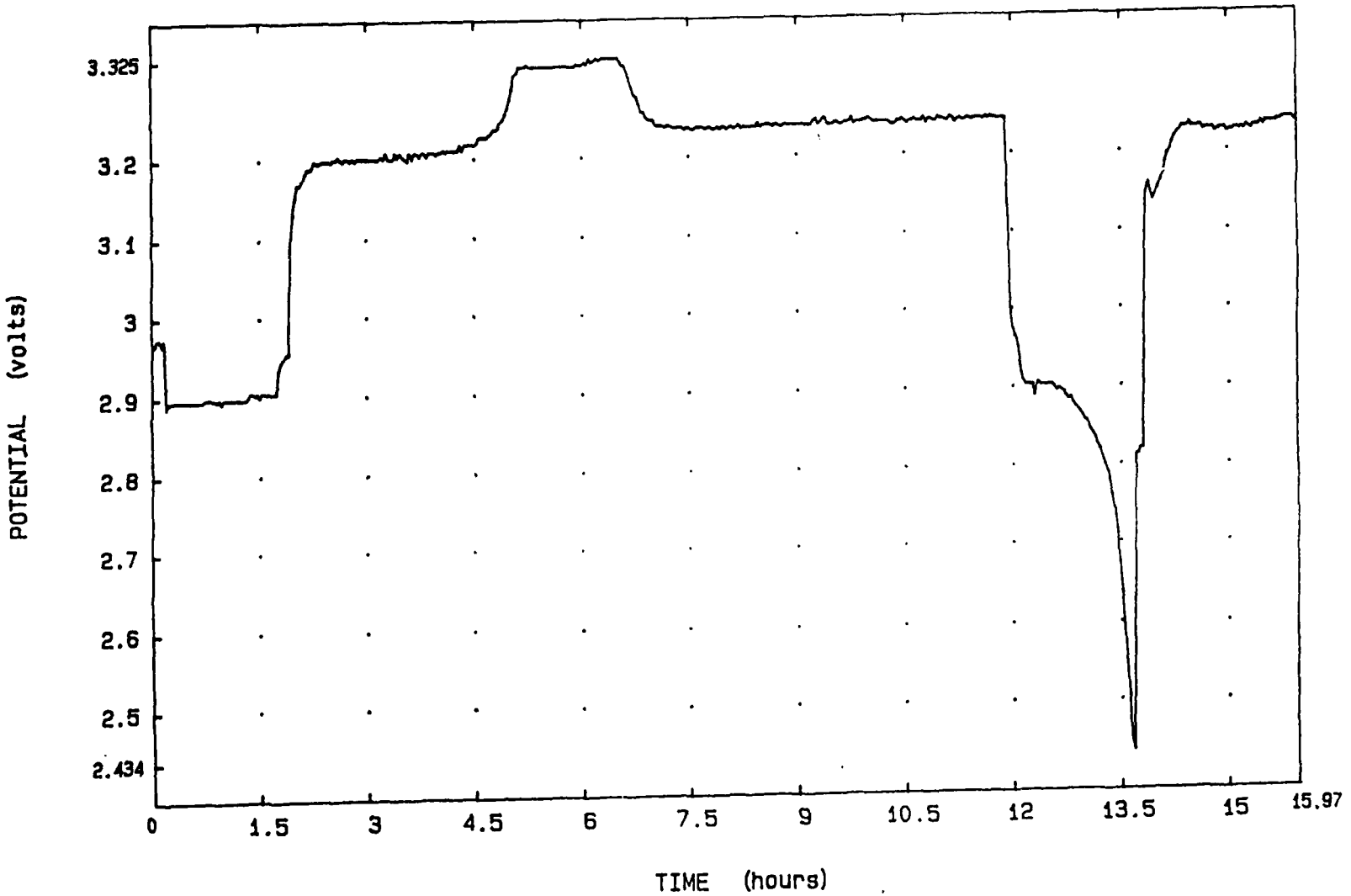

FIGURE 32. Cycle profile, cell #43-2-3: Ref. vs. C
Separator: Hovosorb
Pos. screen/contact: Titanium
Electrolyte: 1M KSCN; 0.5M LiSCN

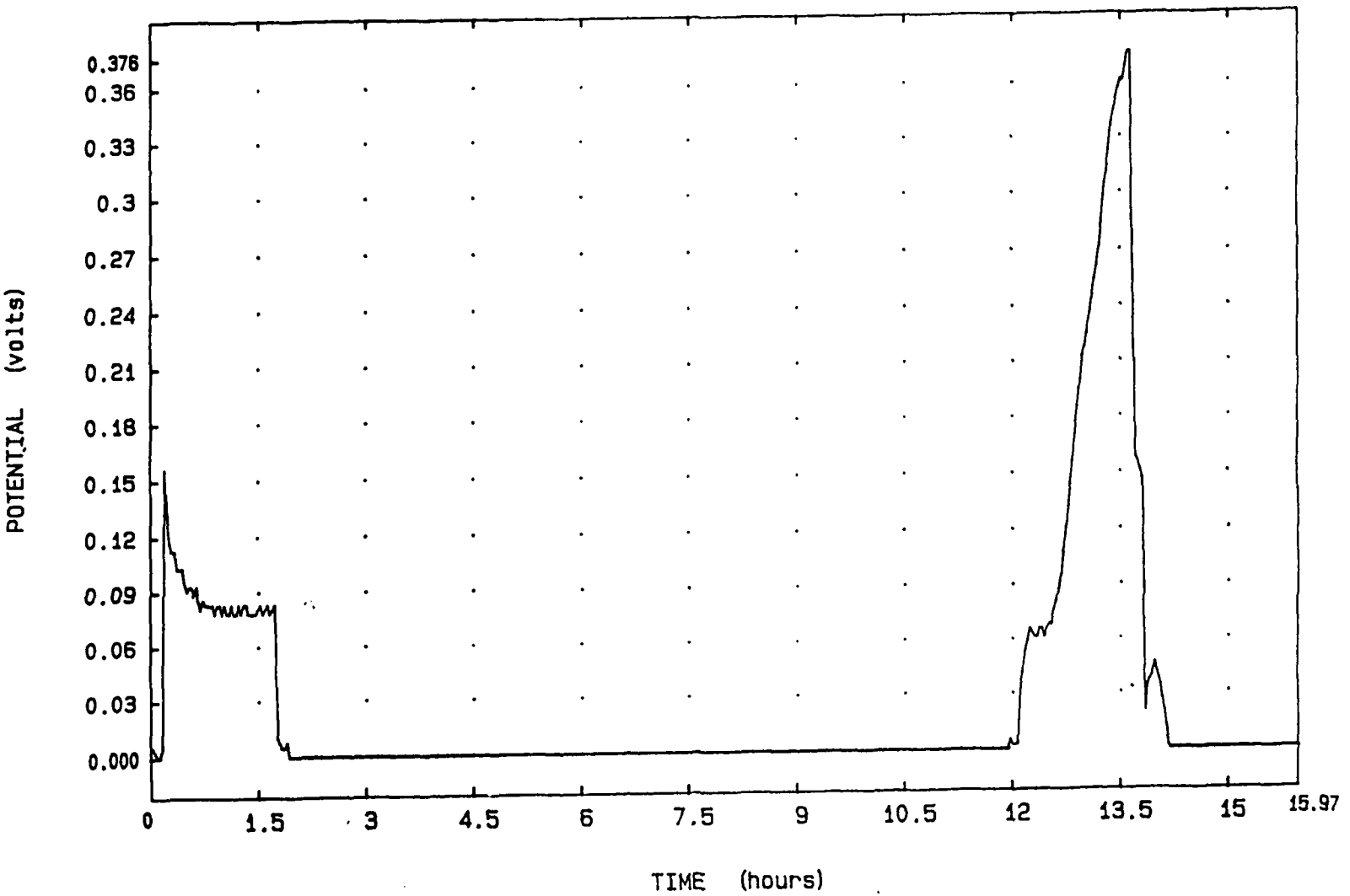

FIGURE 33. Cycle profile, cell #43-2-3: Ref. vs. Li
Separator: Hovosorb
Pos. screen/contact: Titanium
Electrolyte: 1M KSCN; 0.5M LiSCN

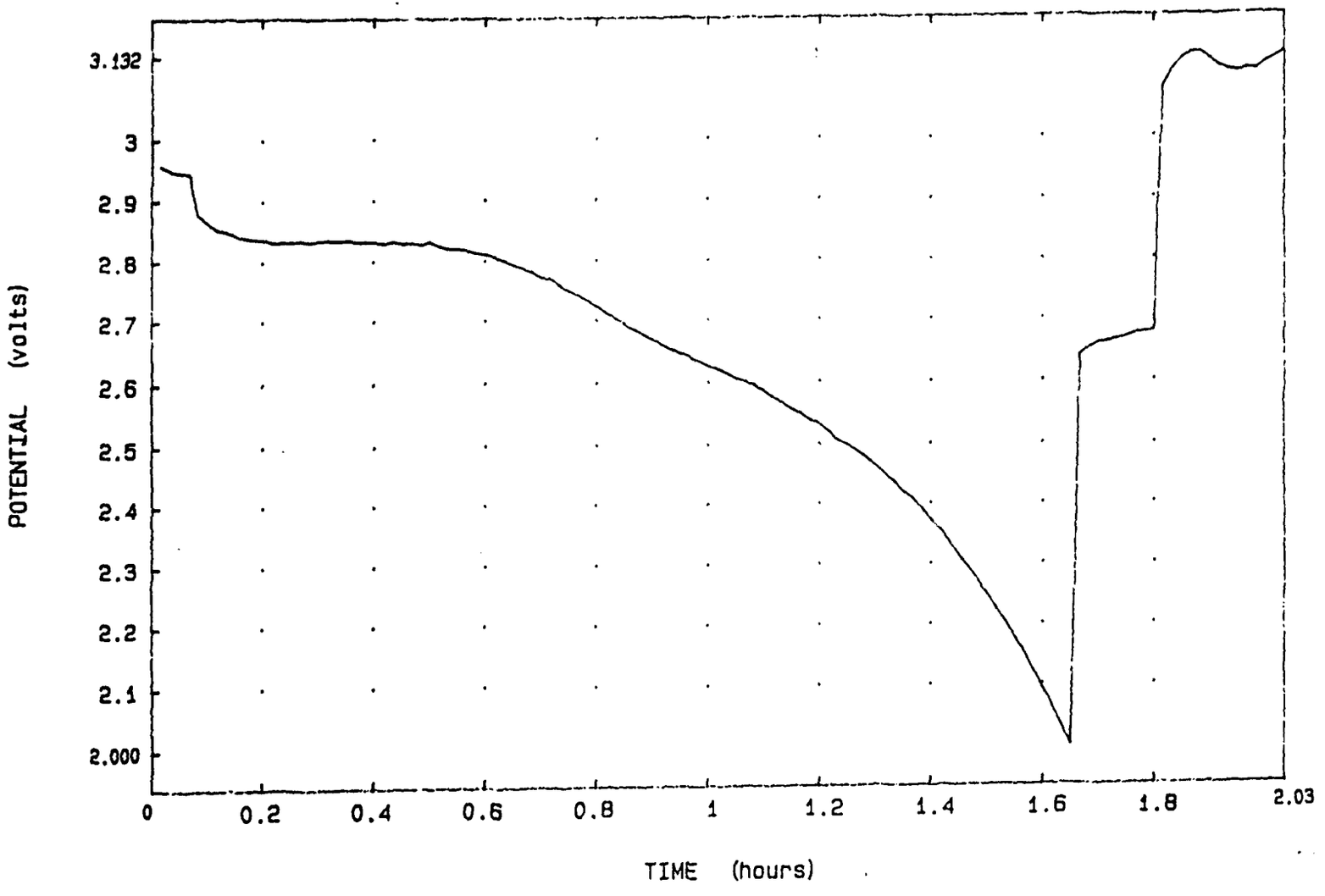

FIGURE 34. Cycle profile, cell #43-2-3: Li vs. C; cycle #2.
Separator: Hovosorb
Pos. screen/contact: Titanium
Electrolyte: 1M KSCN; 0.5M LiSCN

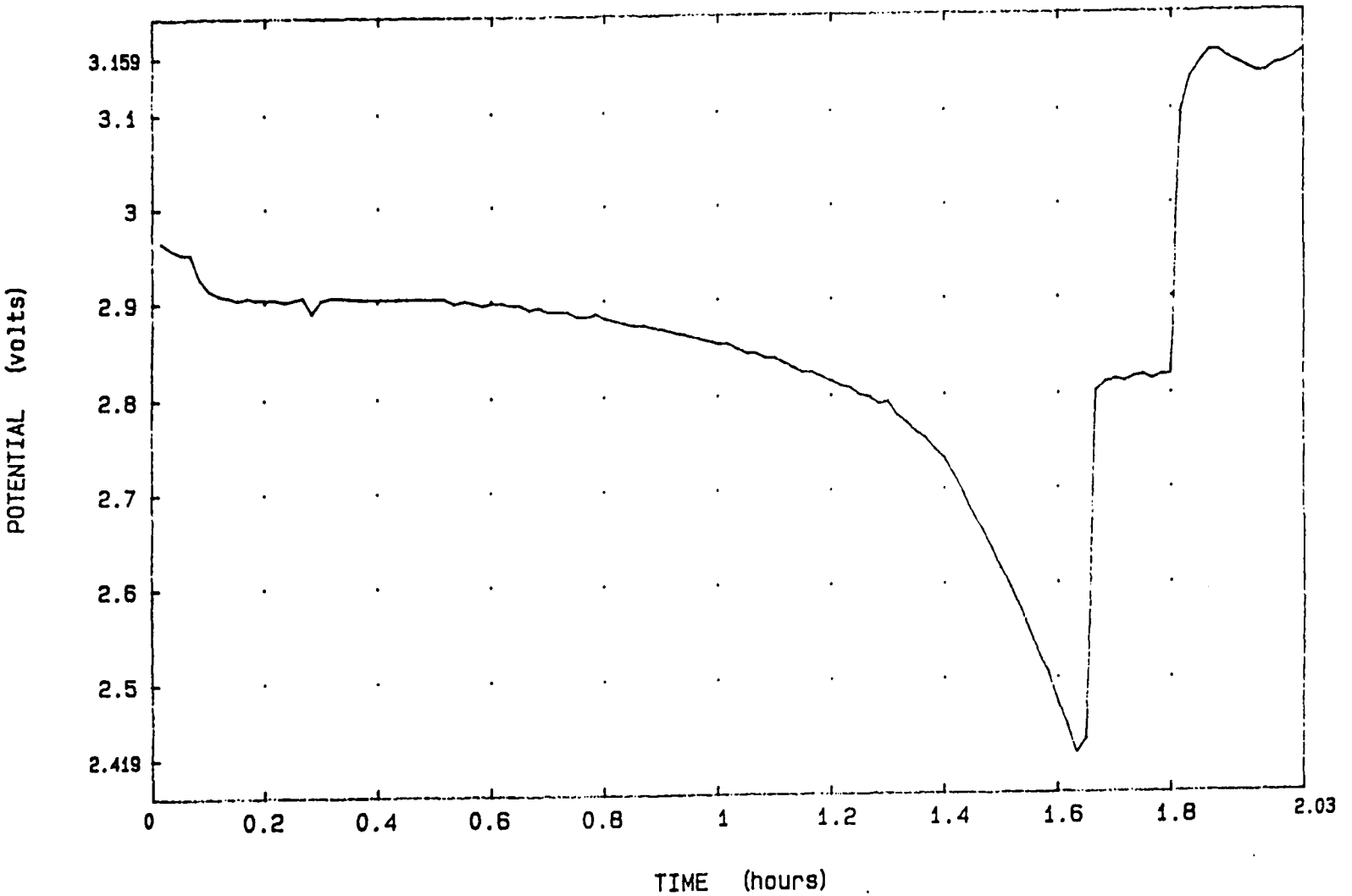

FIGURE 35. Cycle profile, cell #43-2-3: Ref. vs. C; cycle #2.
Separator: Hovosorb
Pos. screen/contact: Titanium
Electrolyte: 1M KSCN; 0.5M LiSCN

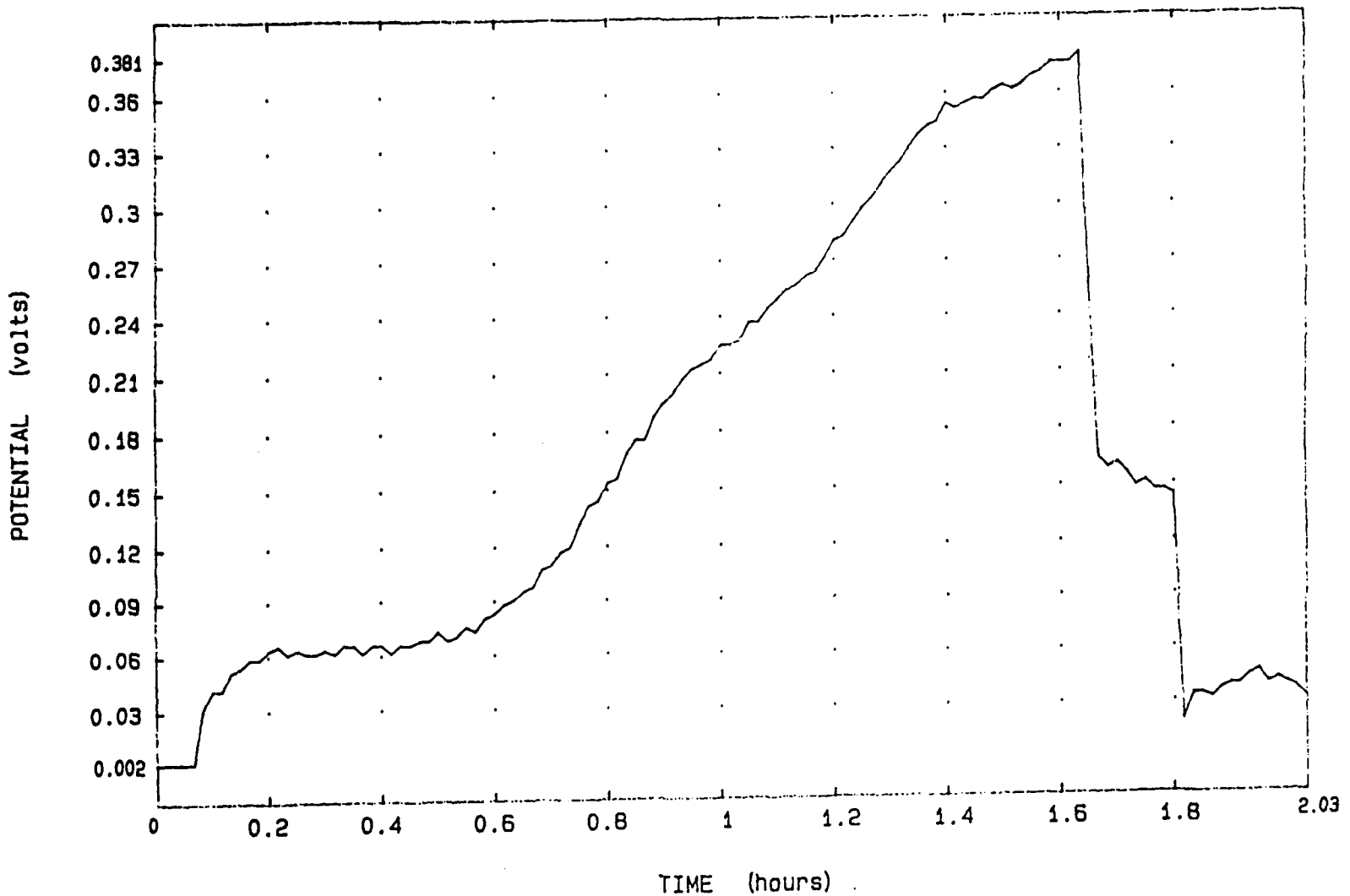

FIGURE 36. Cycle profile, cell #43-2-3: Ref. vs. Li; cycle #2.
Separator: Hovosorb
Pos. screen/contact: Titanium
Electrolyte: 1M KSCN; 0.5M LiSCN

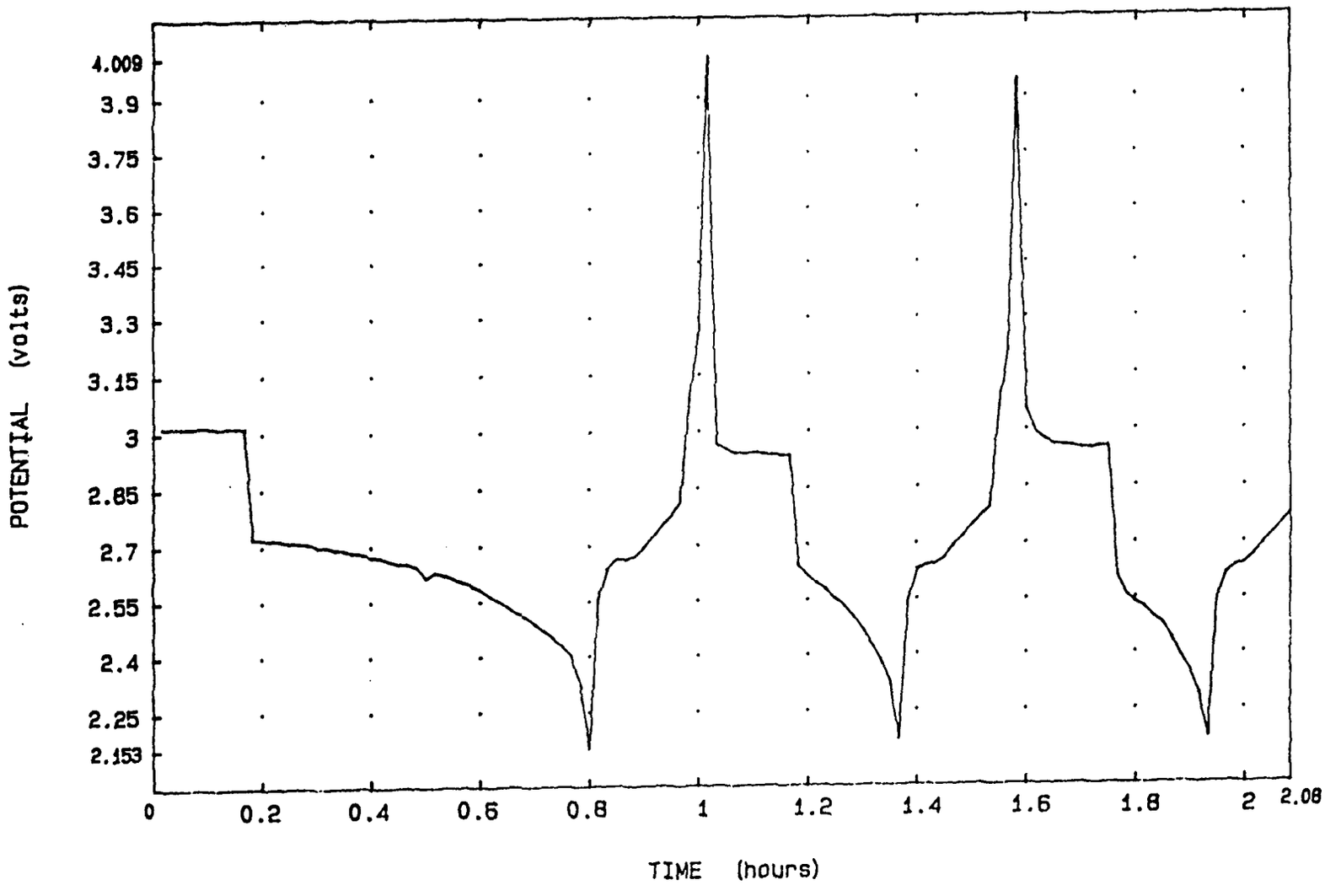

FIGURE 37. Cycle profile, cell #43-2-2: Li vs. C.
Separator: Hovosorb
Pos. screen/contact: Titanium
Electrolyte: 0.5M KBr; 0.5M LiBr

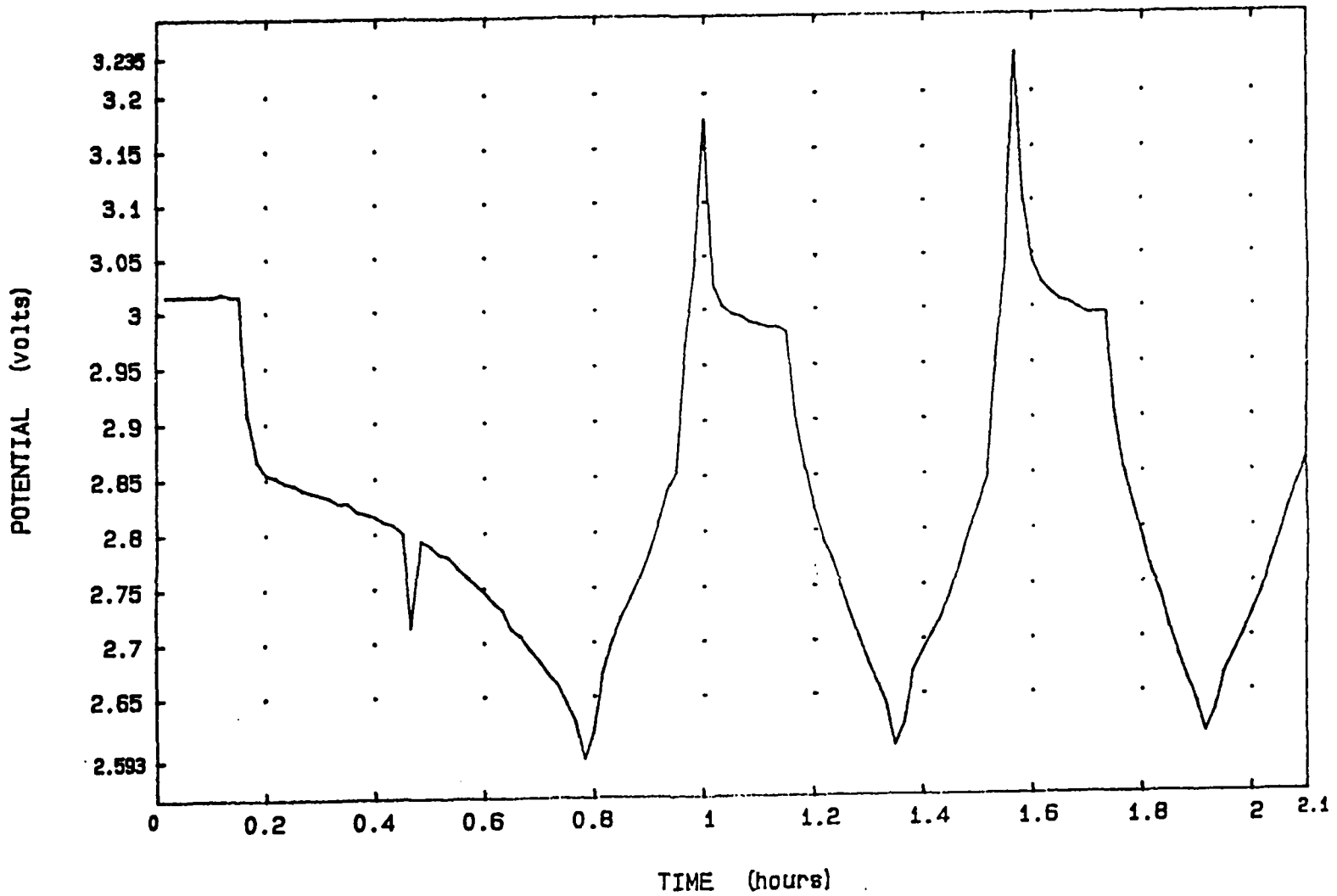

FIGURE 38. Cycle profile, cell #43-2-2: Ref. vs C.
Separator: Hovosorb
os. screen/contact: Titanium
Electrolyte: 0.5M KBr; 0.5M LiBr

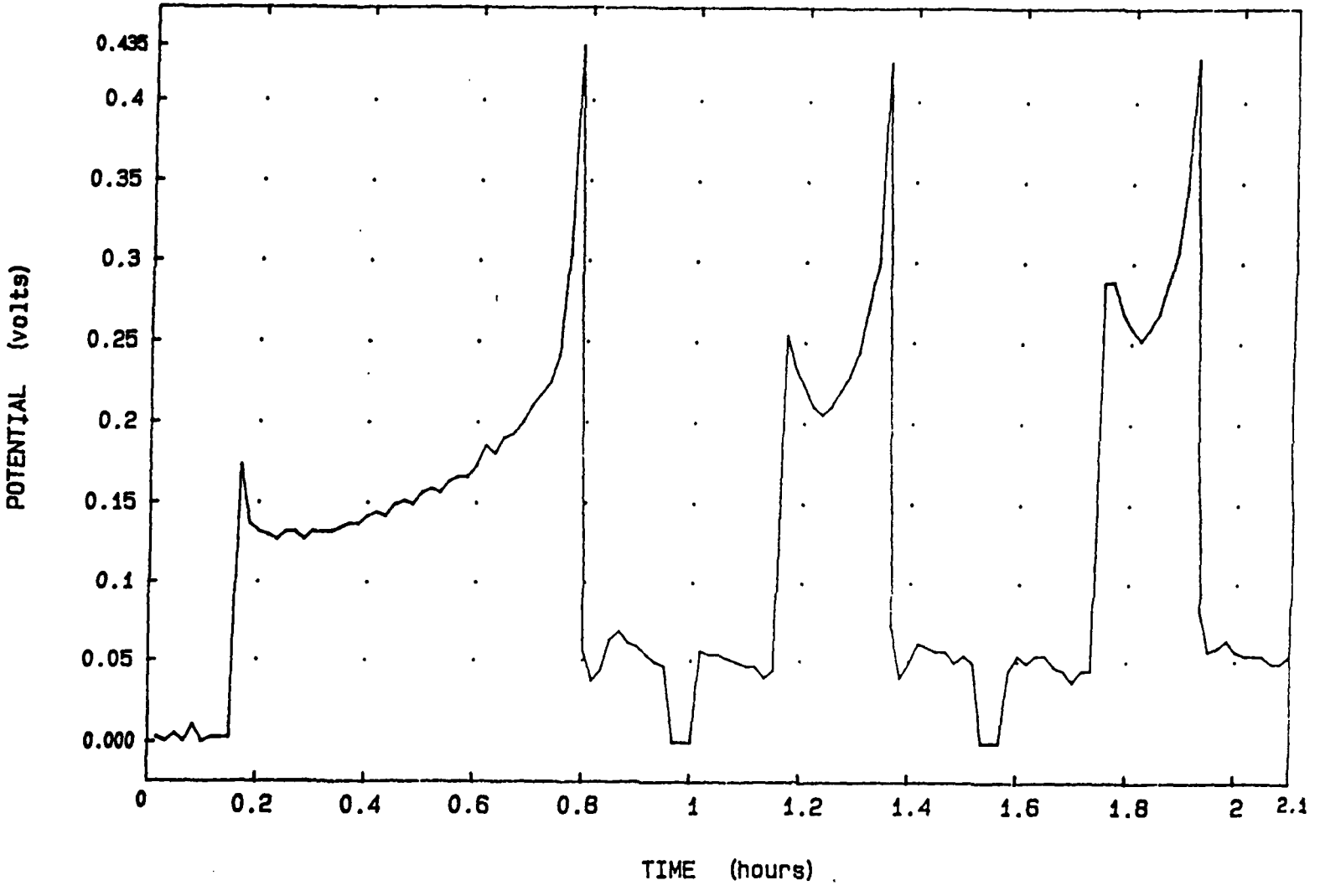

FIGURE 39. Cycle profile, cell #43-2-2: Ref. vs Li.
Separator: Hovosorb
Pos. screen/contact: Titanium
Electrolyte: 0.5M KBr; 0.5M LiBr

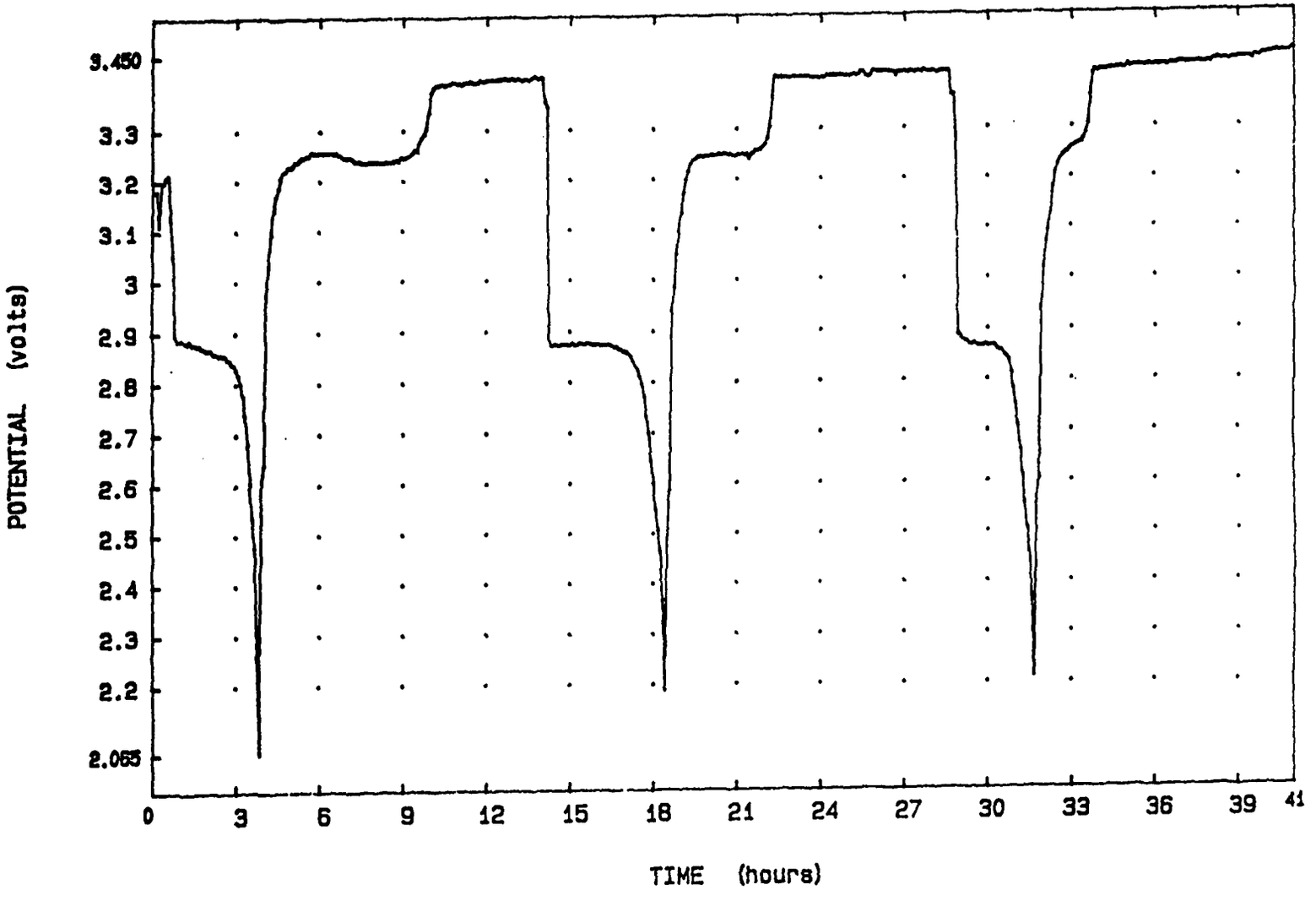

FIGURE 40. Cycle profile, cell #43-2-4: Li vs. C.
Separator: Hovosorb
Pos. screen/contact: Titanium
Electrolyte: 1M CsBr; 0.5M LiBr

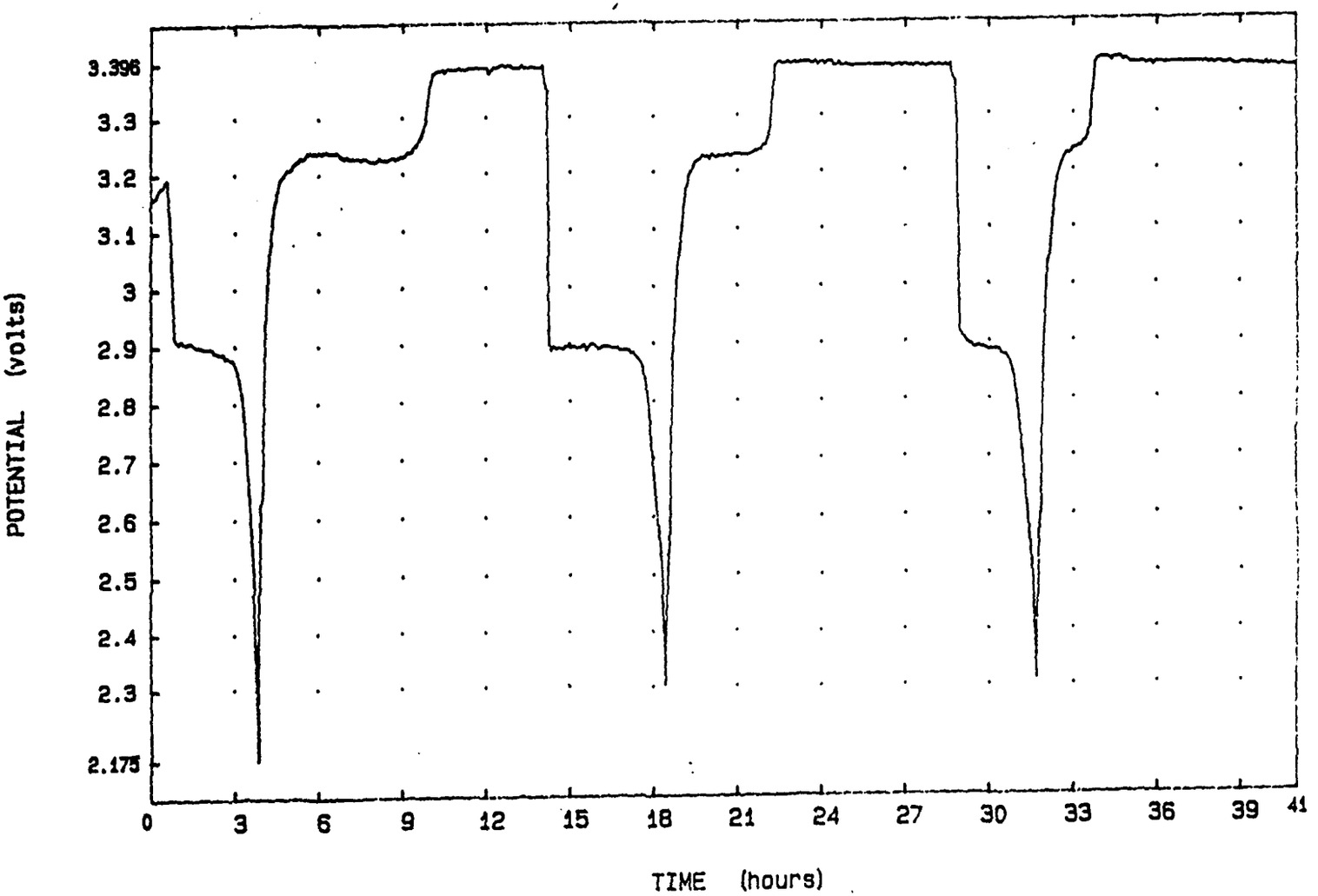

FIGURE 41. Cycle profile, cell #43-2-4: Ref. vs. C.
Separator: Hovosorb
Pos. screen/contact: Titanium
Electrolyte: 1M CsBr; 0.5M LiBr

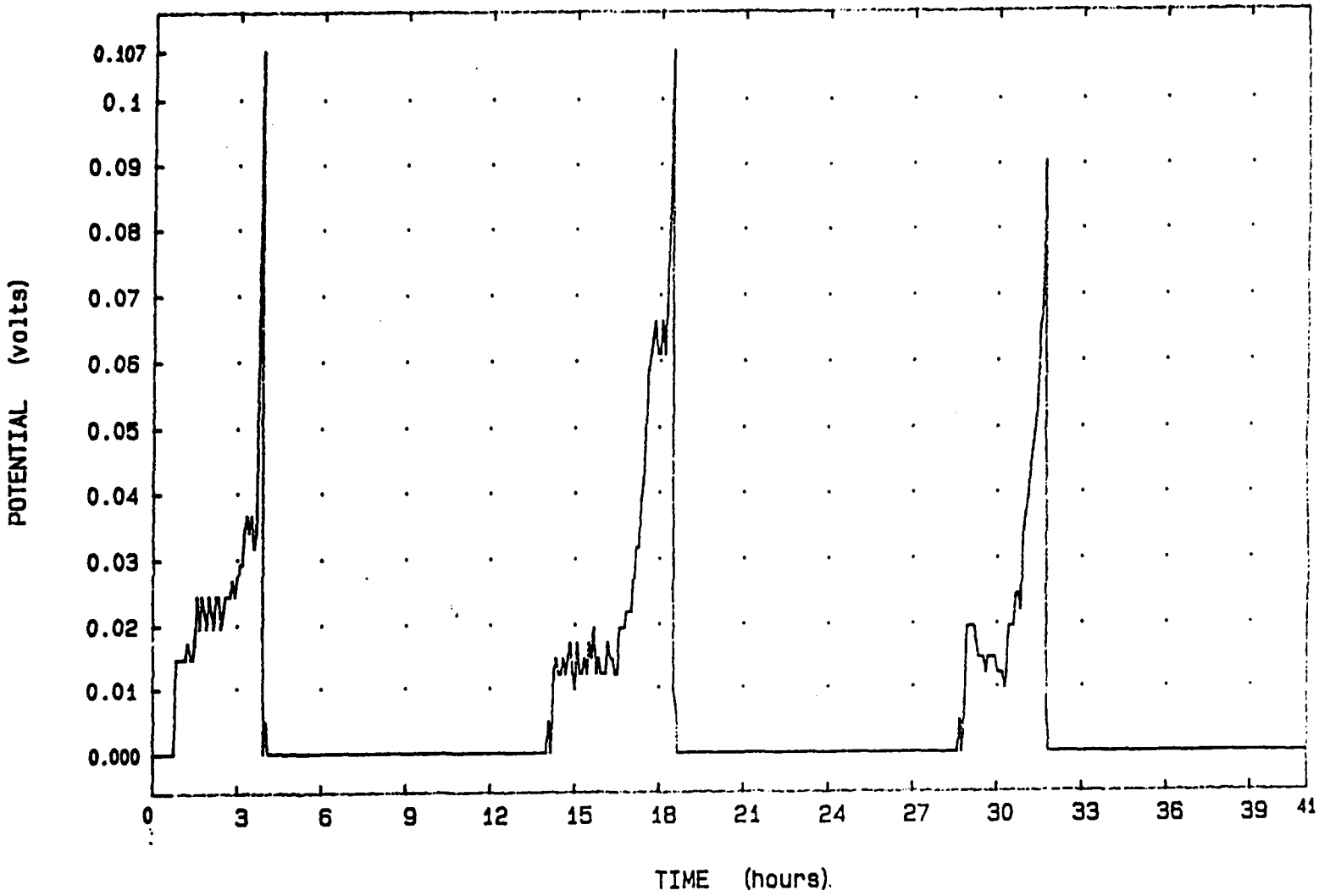

FIGURE 42. Cycle profile, cell #43-2-4: Ref. vs. Li.
Separator: Hovosorb
Pos. screen/contact: Titanium
Electrolyte: 1M CsBr; 0.5M LiBr

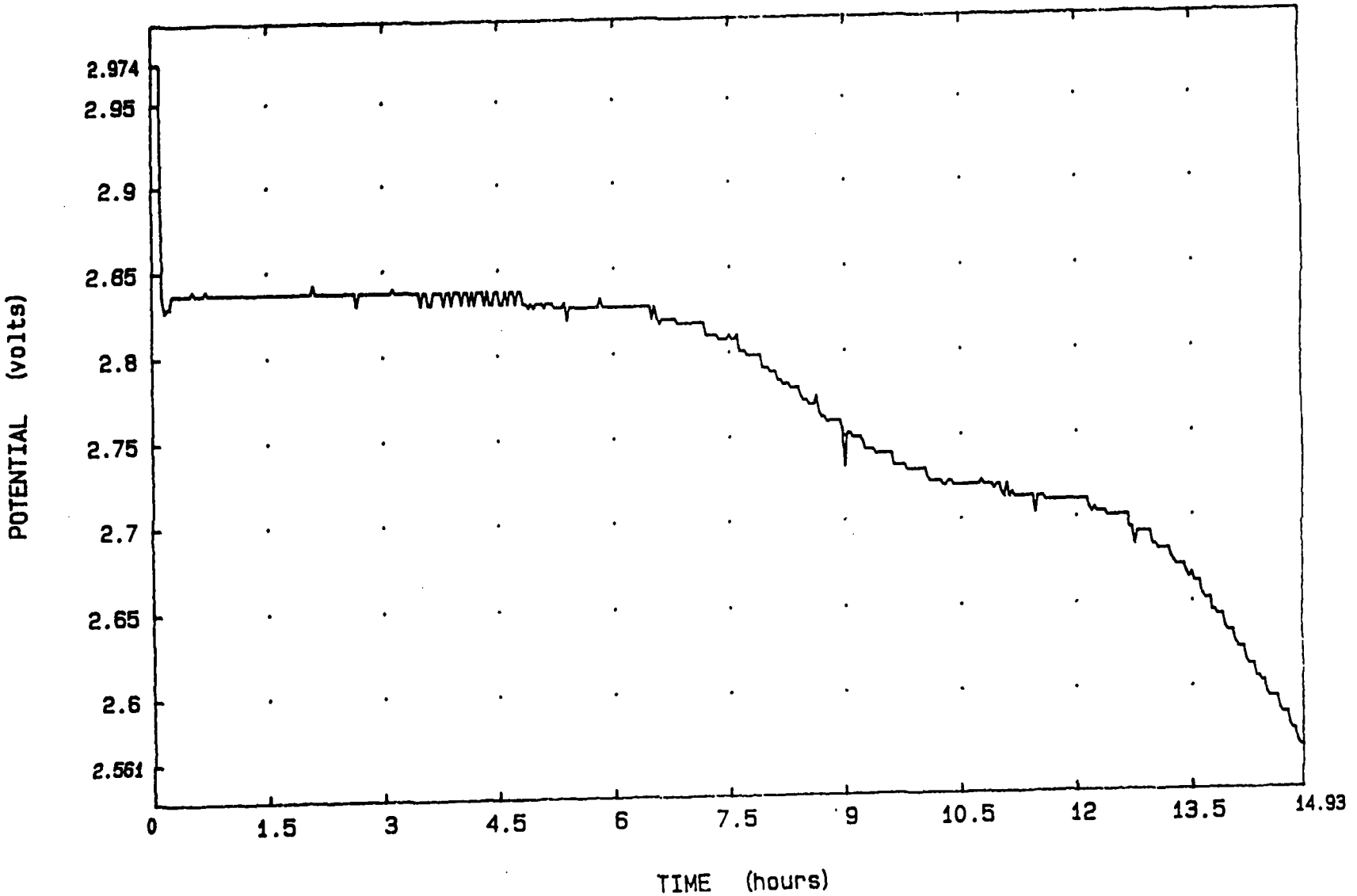

FIGURE 43. Discharge profile, cell #41-53-1. Cell potential (lithium vs. carbon)
Electrolyte: 1.25M CsBr/ 0.12M LiBr
Cathode: 75/25/5
Load: 100 ohms

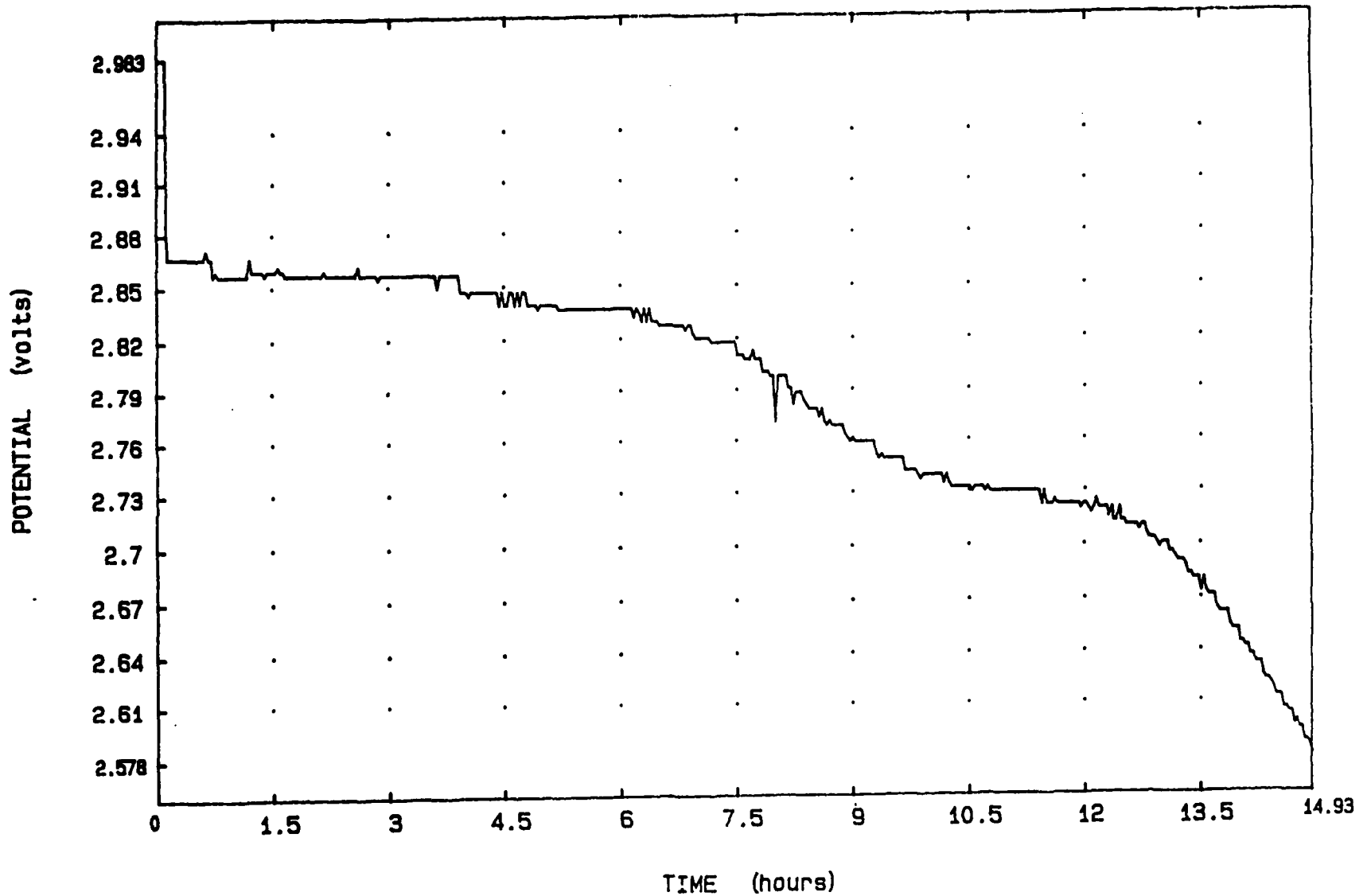

FIGURE 44. Discharge profile, cell #41-53-1. Cathode potential (reference vs. carbon)
Electrolyte: 1.25M CsBr/ 0.12M LiBr
Cathode: 75/25/5
Load: 100 ohms

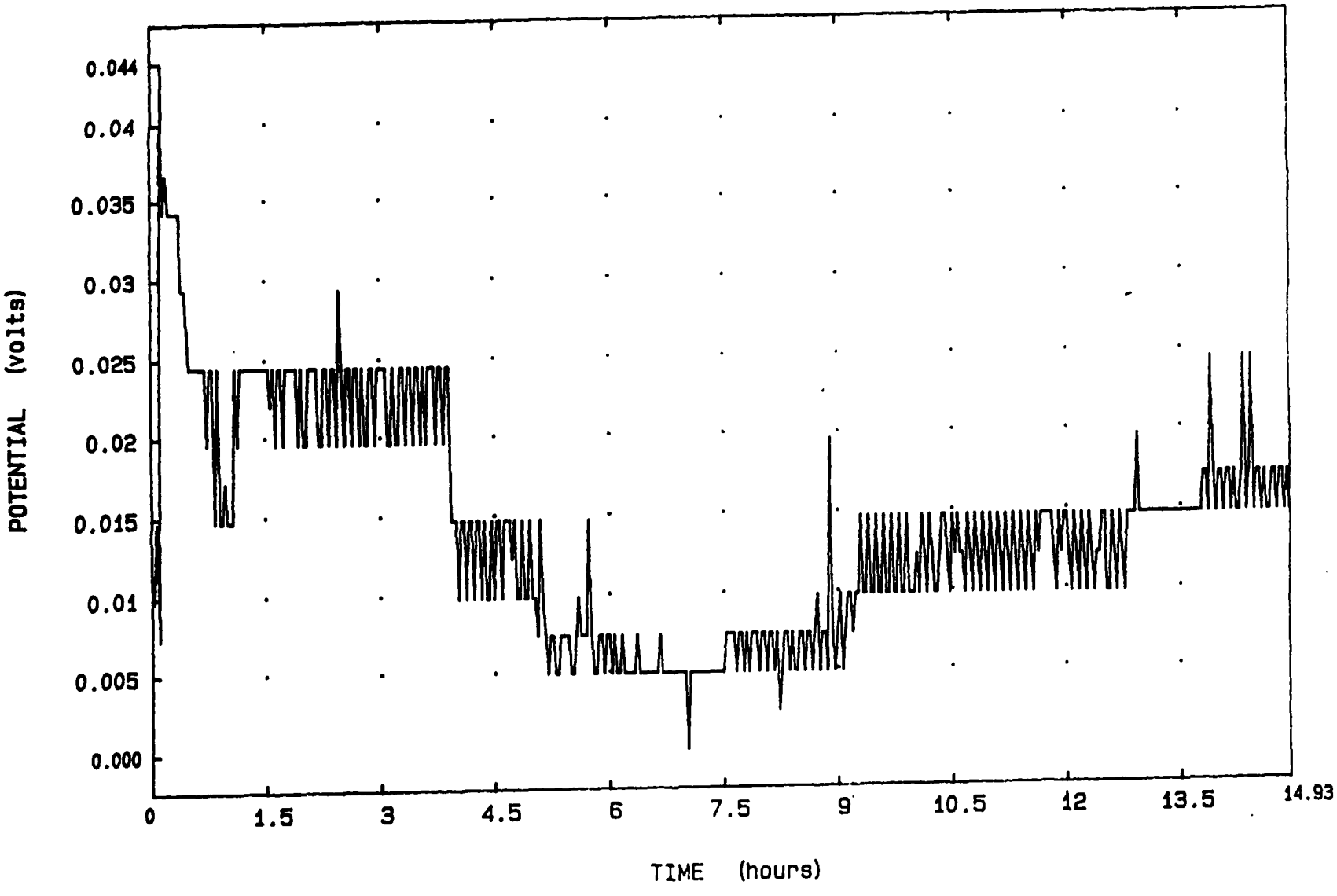

FIGURE 45. Discharge profile, cell #41-53-1. Anode potential (reference vs. lithium)
Electrolyte: 1.25M CsBr/ 0.12M LiBr
Cathode: 75/25/5
Load: 100 ohms

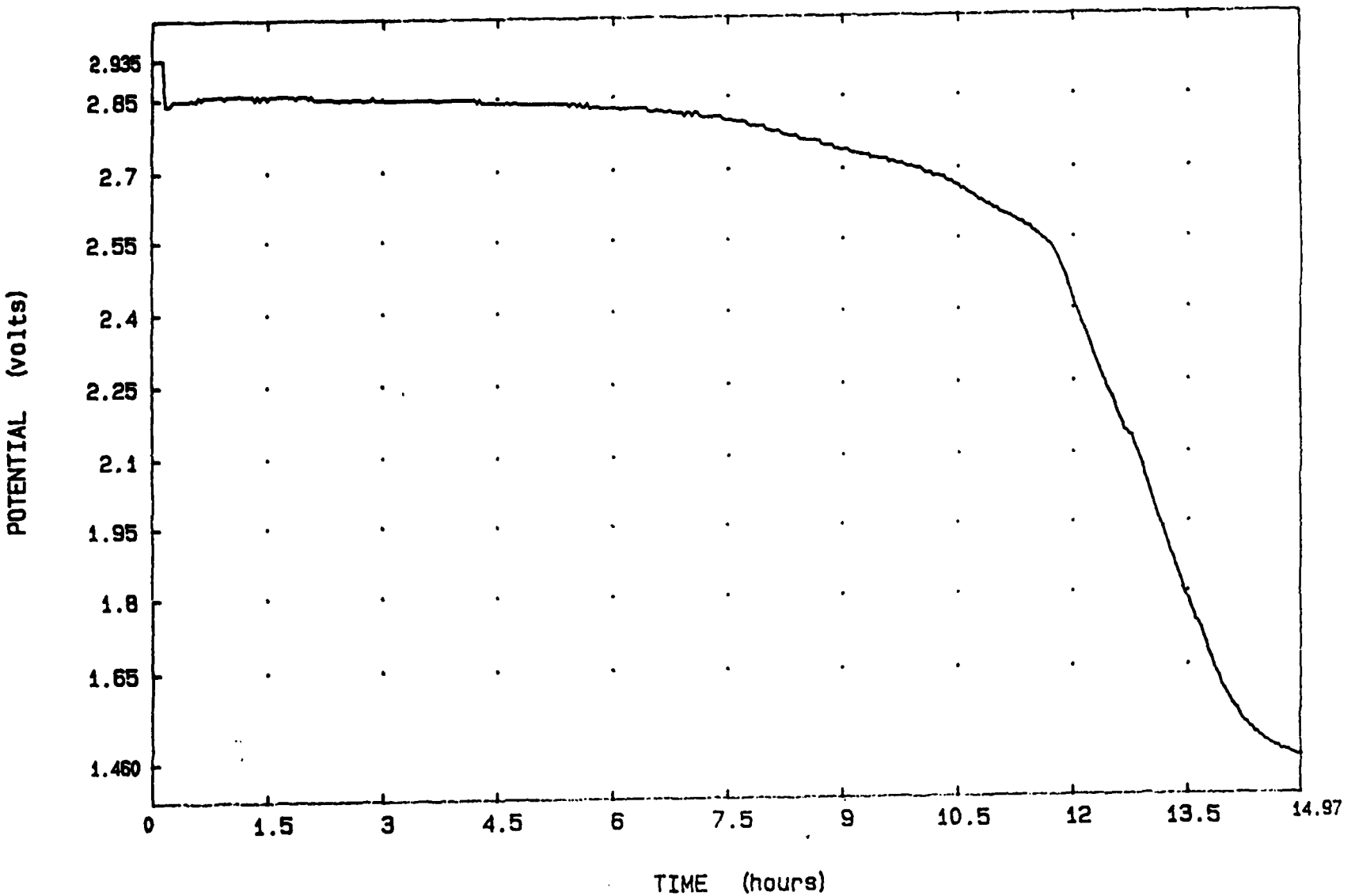

FIGURE 46. Discharge profile, cell #41-53-2. Cell potential (lithium vs. carbon)
Electrolyte: 1.25M CsBr/ 0.12M LiBr
Cathode: 75/25/5
Load: 100 ohms

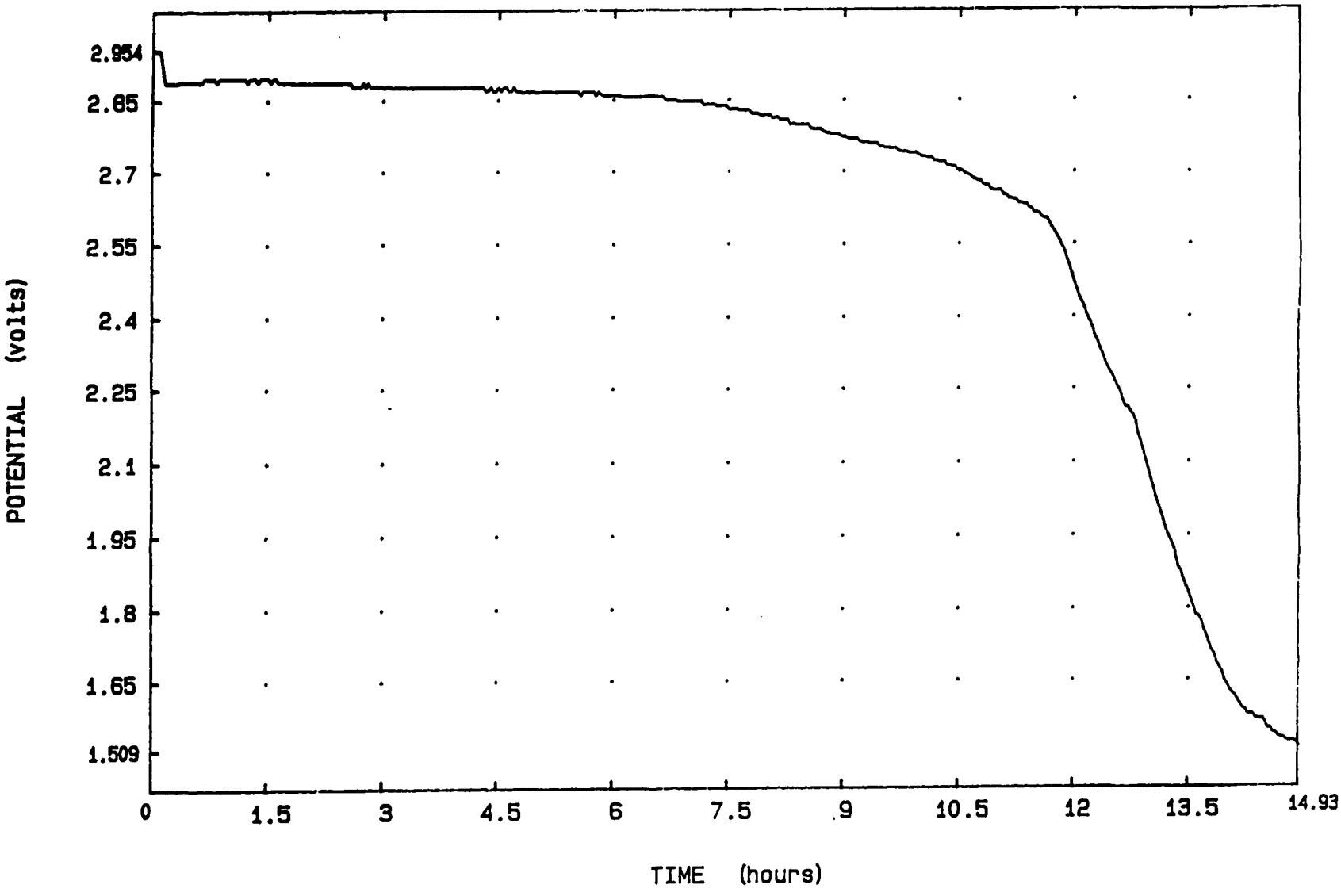

FIGURE 47. Discharge profile, cell #41-53-2. Cathode potential (reference vs. carbon)
Electrolyte: 1.25M CsBr/ 0.12M LiBr
Cathode: 75/25/5
Load: 100 ohms

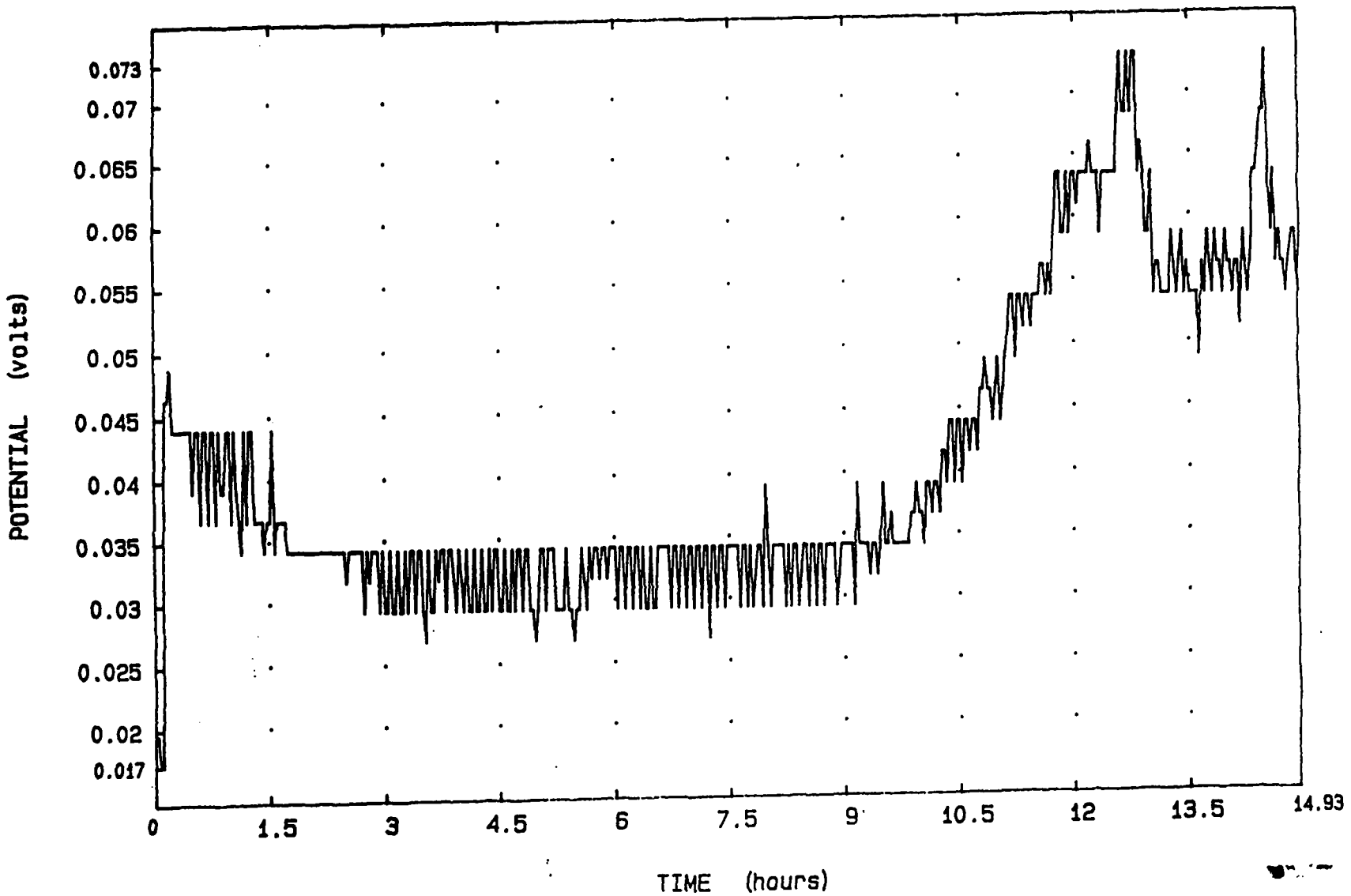

FIGURE 48. Discharge profile, cell #41-53-2. Anode potential (reference vs. lithium)
Electrolyte: 1.25M CsBr/ 0.12M LiBr
Cathode: 75/25/5
Load: 100 ohms

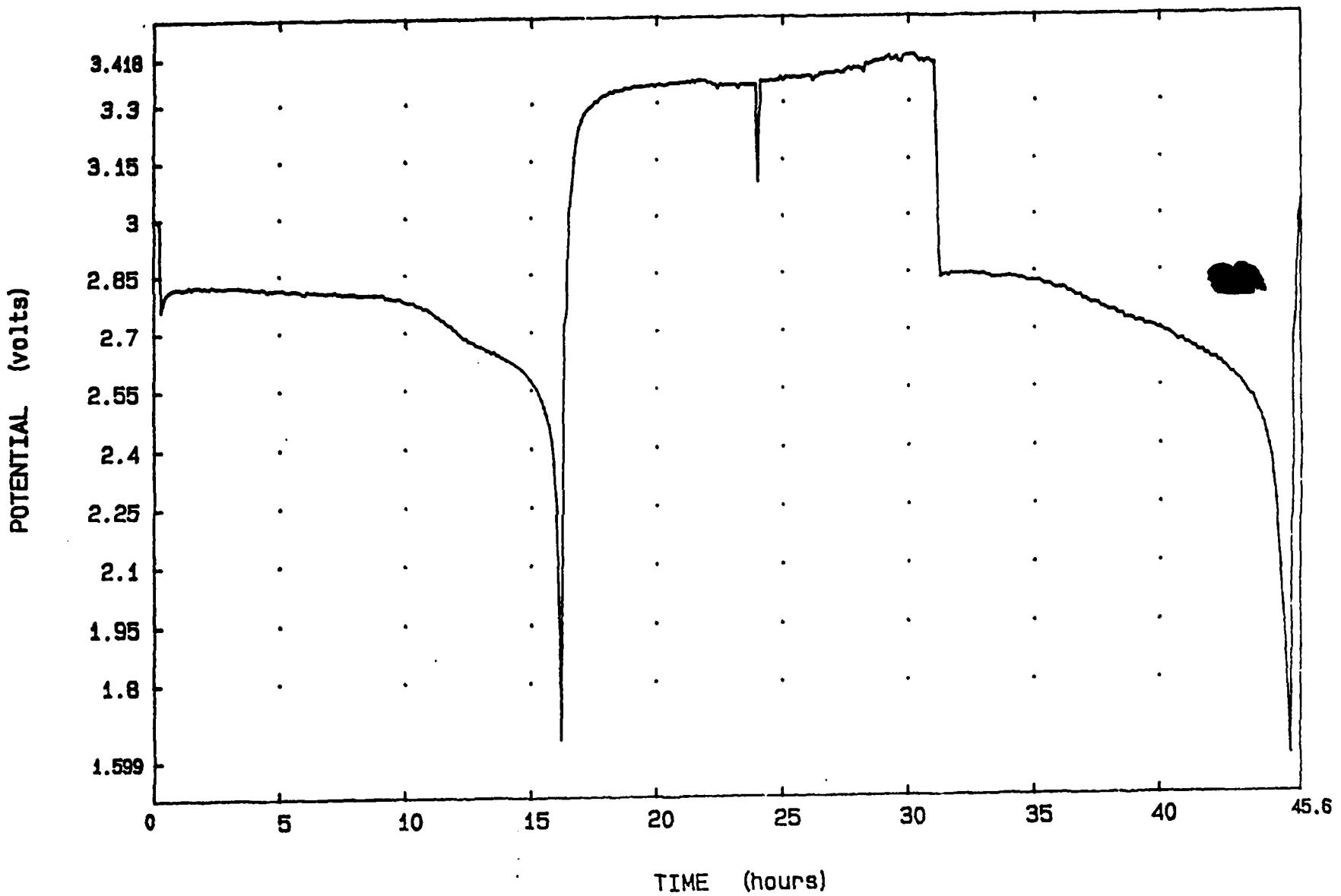

FIGURE 49. Cycle profile, cell #37-69-4, cycles 1,2
Separator: Hovosorb
Pos. screen/contact: Ti/ Ti
Electrolyte: 0.85M LiBr; 21.5% DME/ 6.5% PC

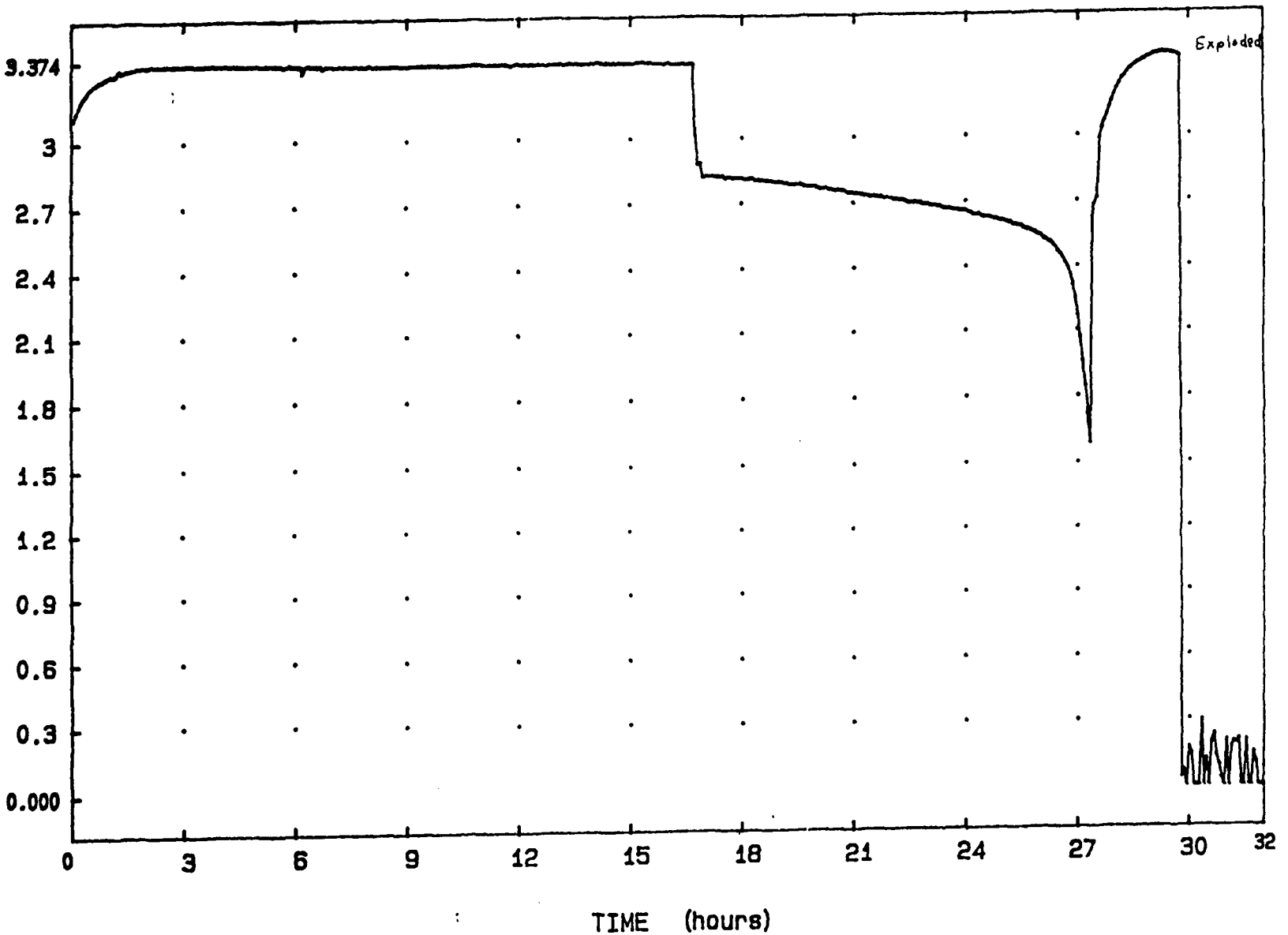

FIGURE 50. Cycle profile, cell #37-69-4, cycle 3
Separator: Hovosorb
Pos. screen/contact: Ti/ Ti
Electrolyte: 0.85M LiBr; 21.5% DME/ 6.5% PC

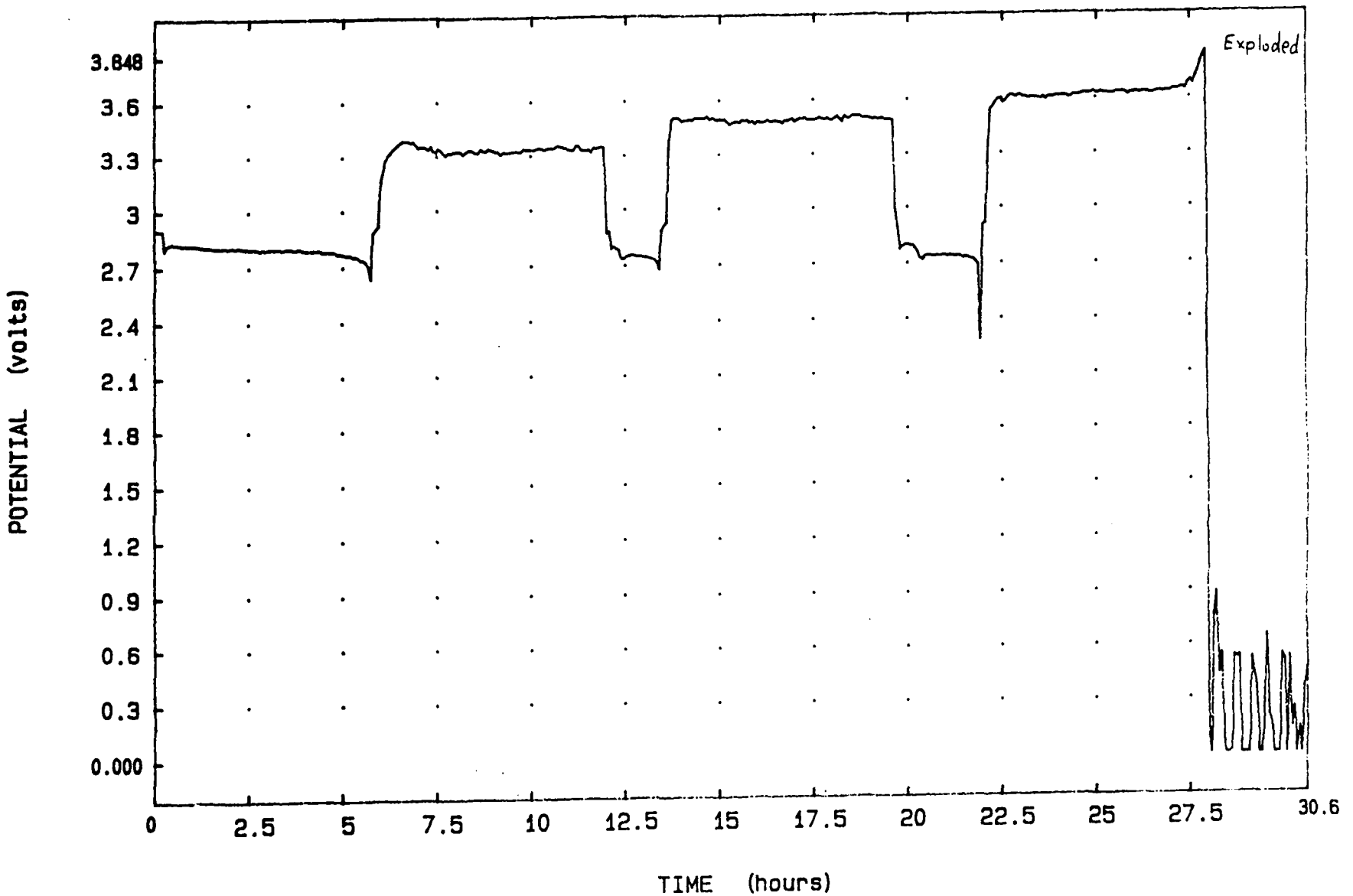

FIGURE 51. Cycle profile, cell #37-81-1
Separator: Hovosorb
Pos. screen/contact: Ti/ Ti
Electrolyte: 0.85M LiBr; 28% DME

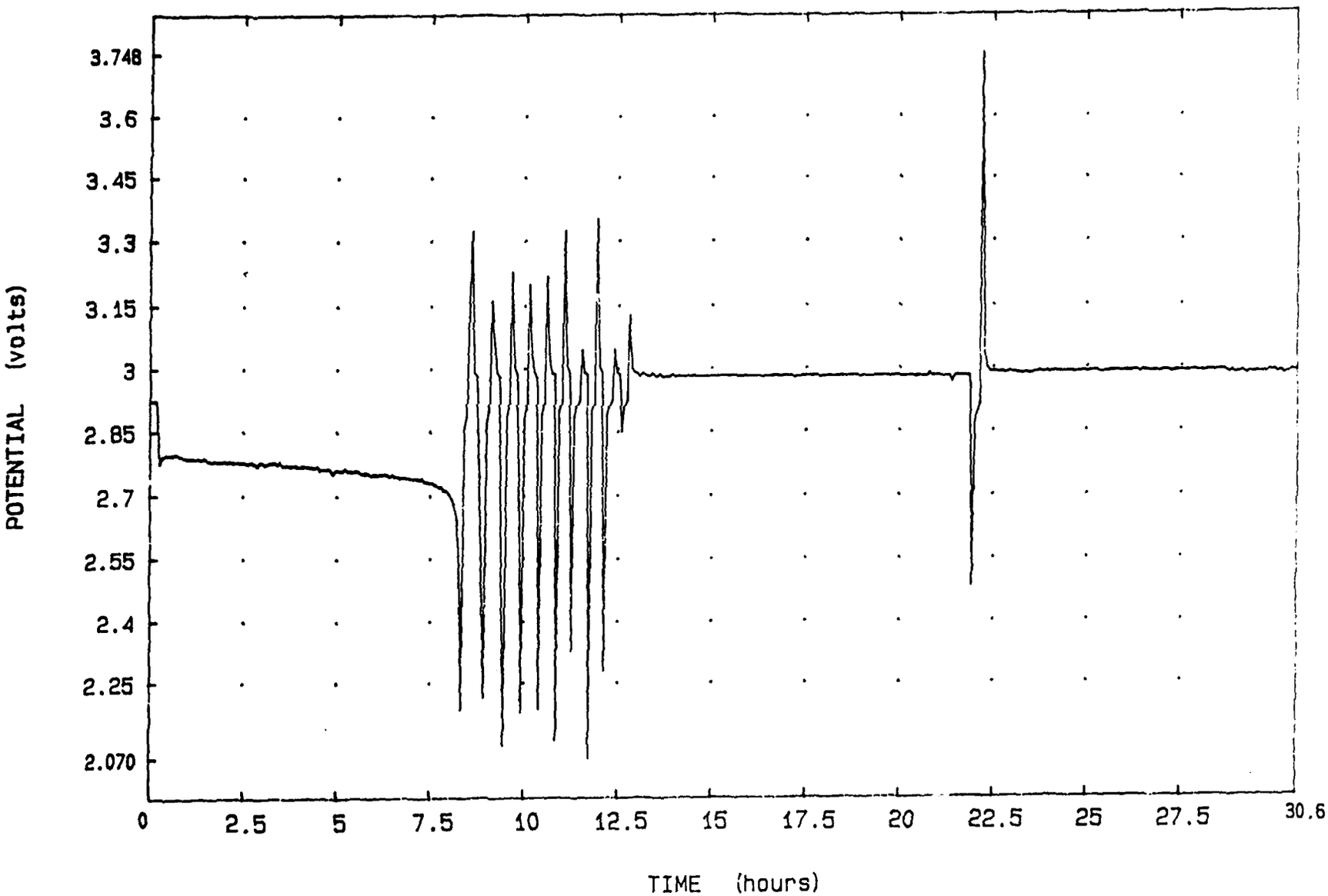

FIGURE 52. Cycle profile, cell #37-81-4
Separator: Tefzel
Pos. screen/contact: Ti/ Ti
Electrolyte: 0.85M LiBr; 28% DME

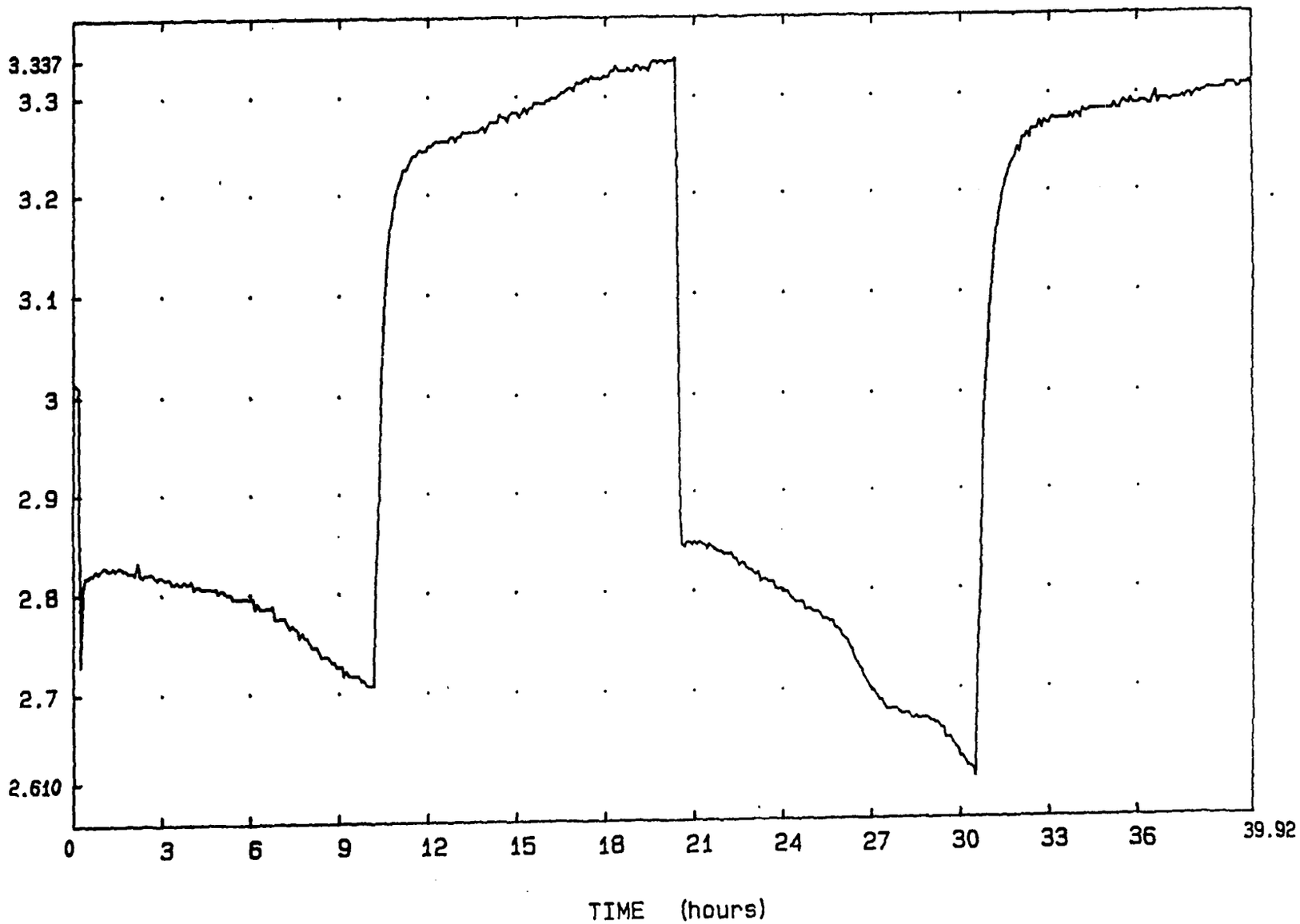

FIGURE 53. Cycle profile, cell #37-87-1, cycles 1,2
Separator: Hovosorb
Pos. screen/contact: Zr/ Zr
Electrolyte: 0.85M LiBr; 28% PC

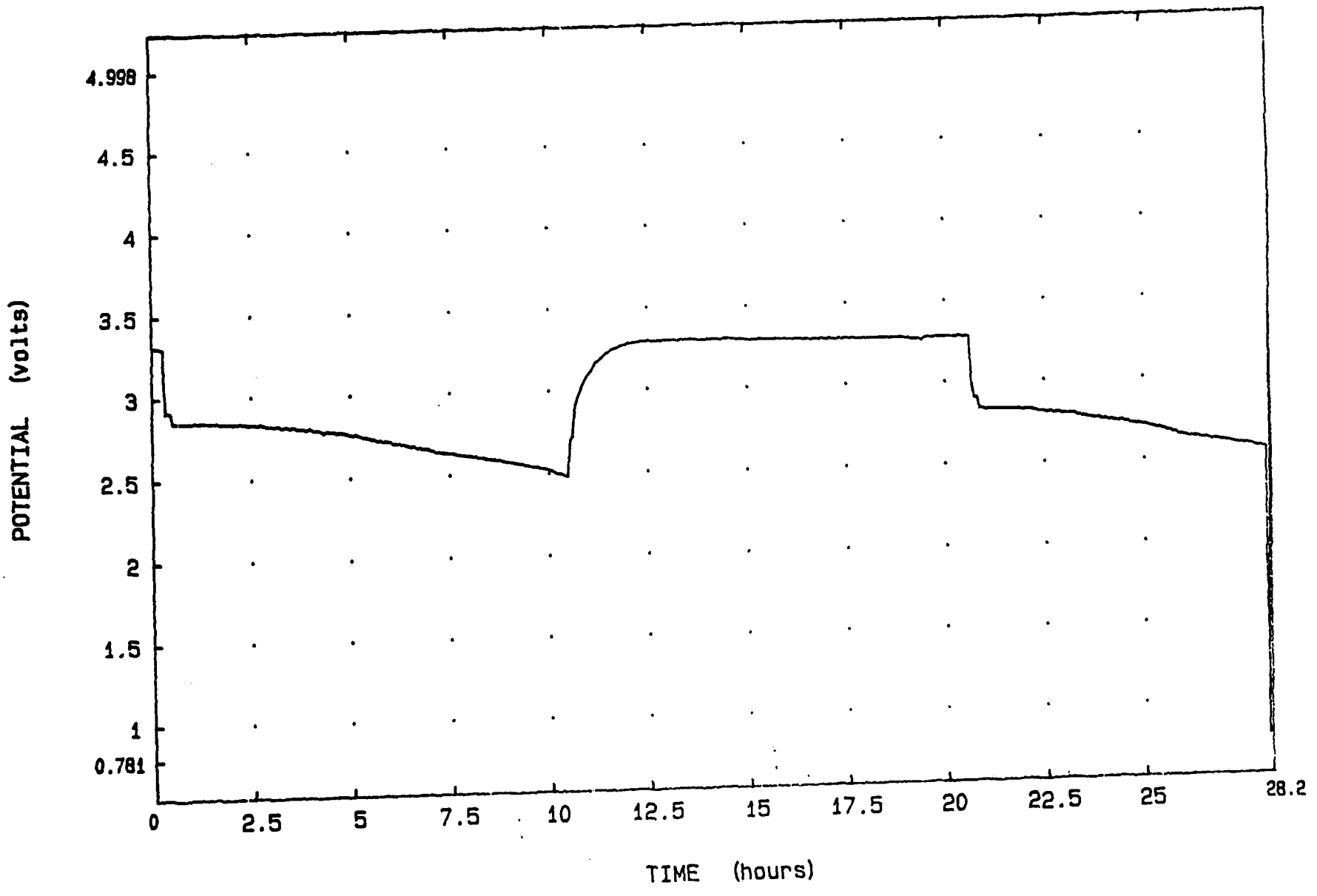

FIGURE 54. Cycle profile, cell #37-87-1, cycles 3,4
Separator: Hovosorb
Pos. screen/contact: Zr/ Zr
Electrolyte: 0.85M LiBr; 28% PC

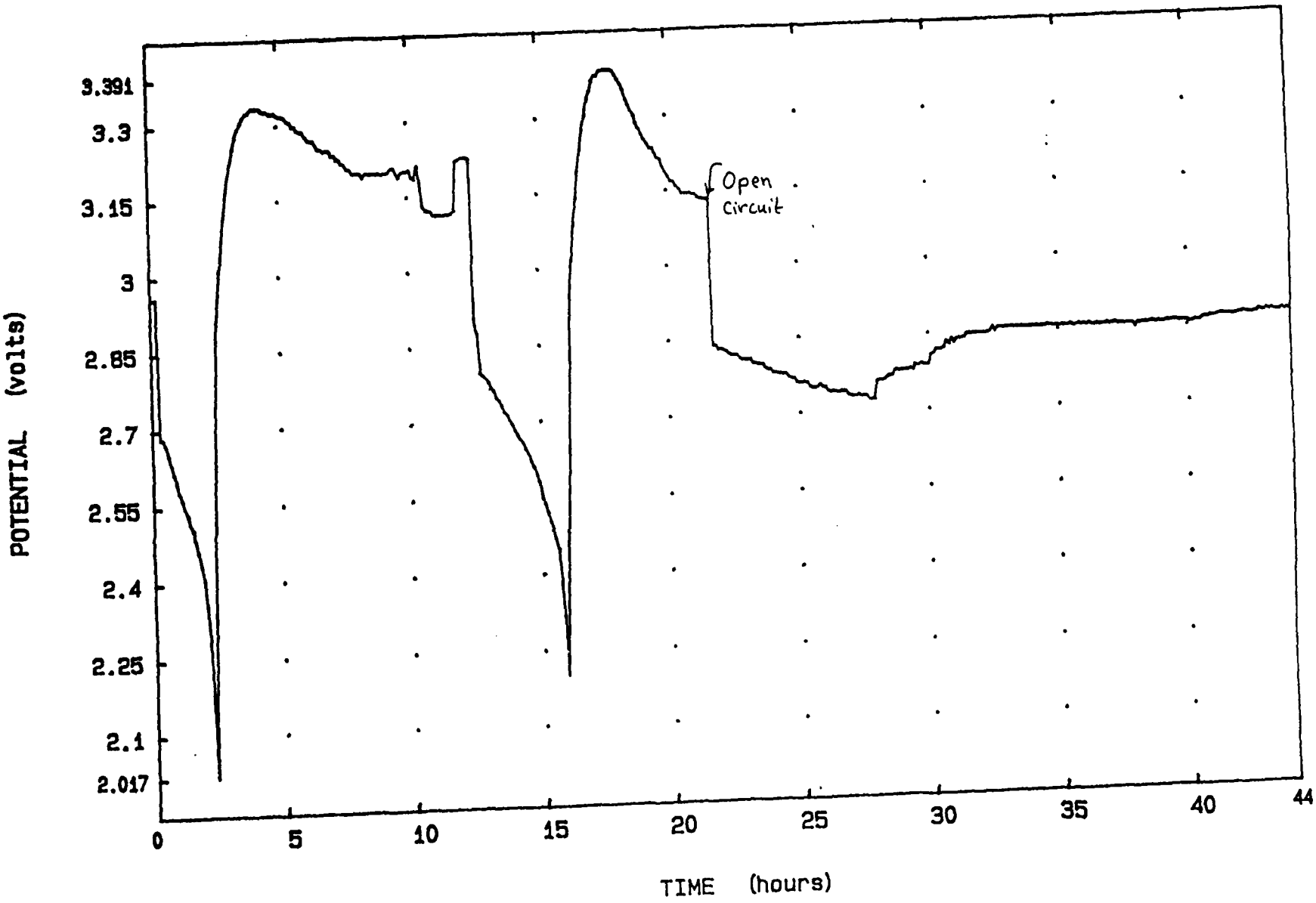

FIGURE 55. Cycle profile, cell #37-87-1, cycle 4, cont.;
cycle 5; open circuit
Separator: Hovosorb
Pos. screen/contact: Zr/ Zr
Electrolyte: 0.85M LiBr; 28% PC

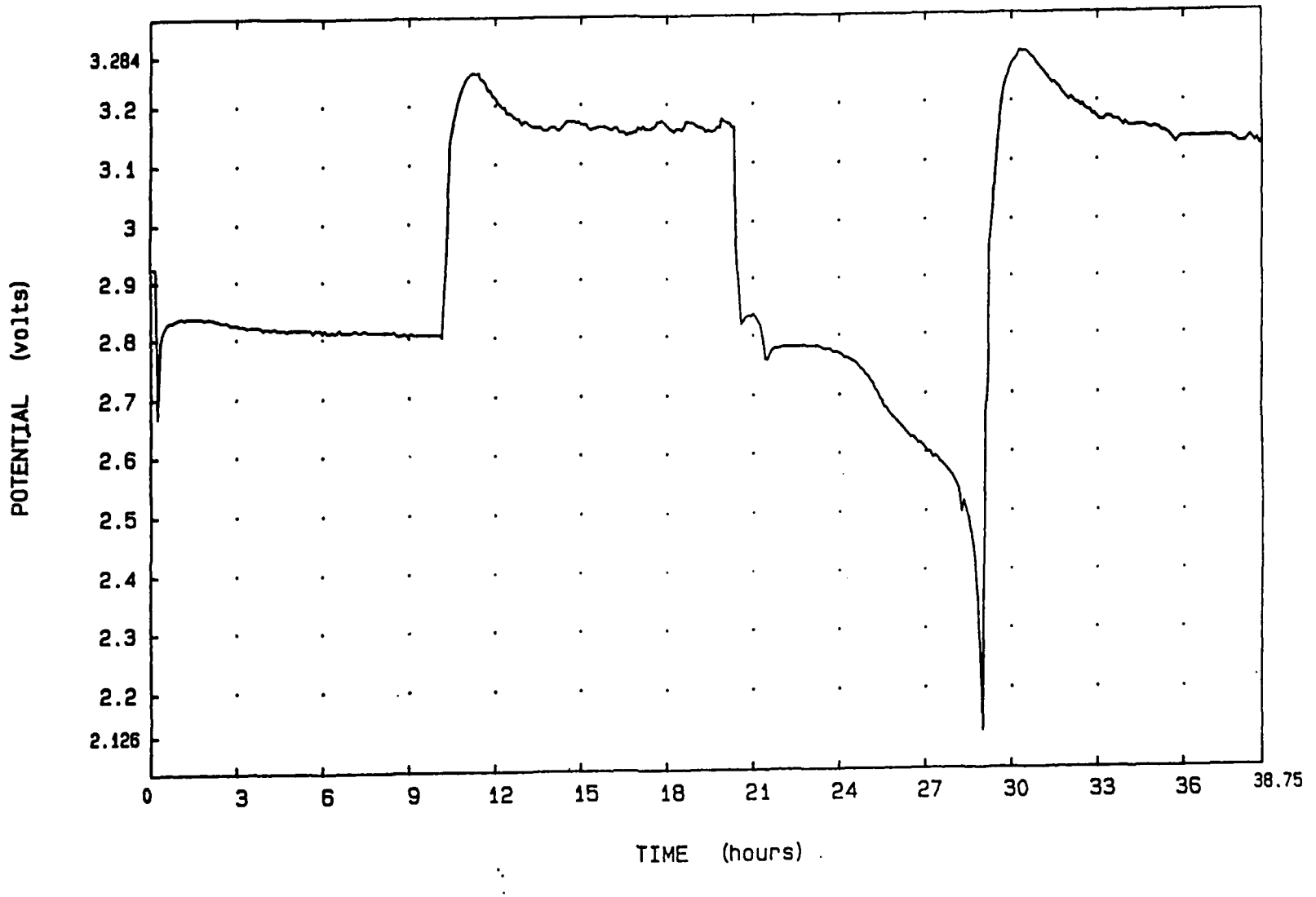

FIGURE 56. Cycle profile, cell #32-77-4
Separator: Hovosorb
Pos. screen/contact: Anodized Aluminum
Electrolyte: 0.85M LiBr; 14% DME; 14% PC

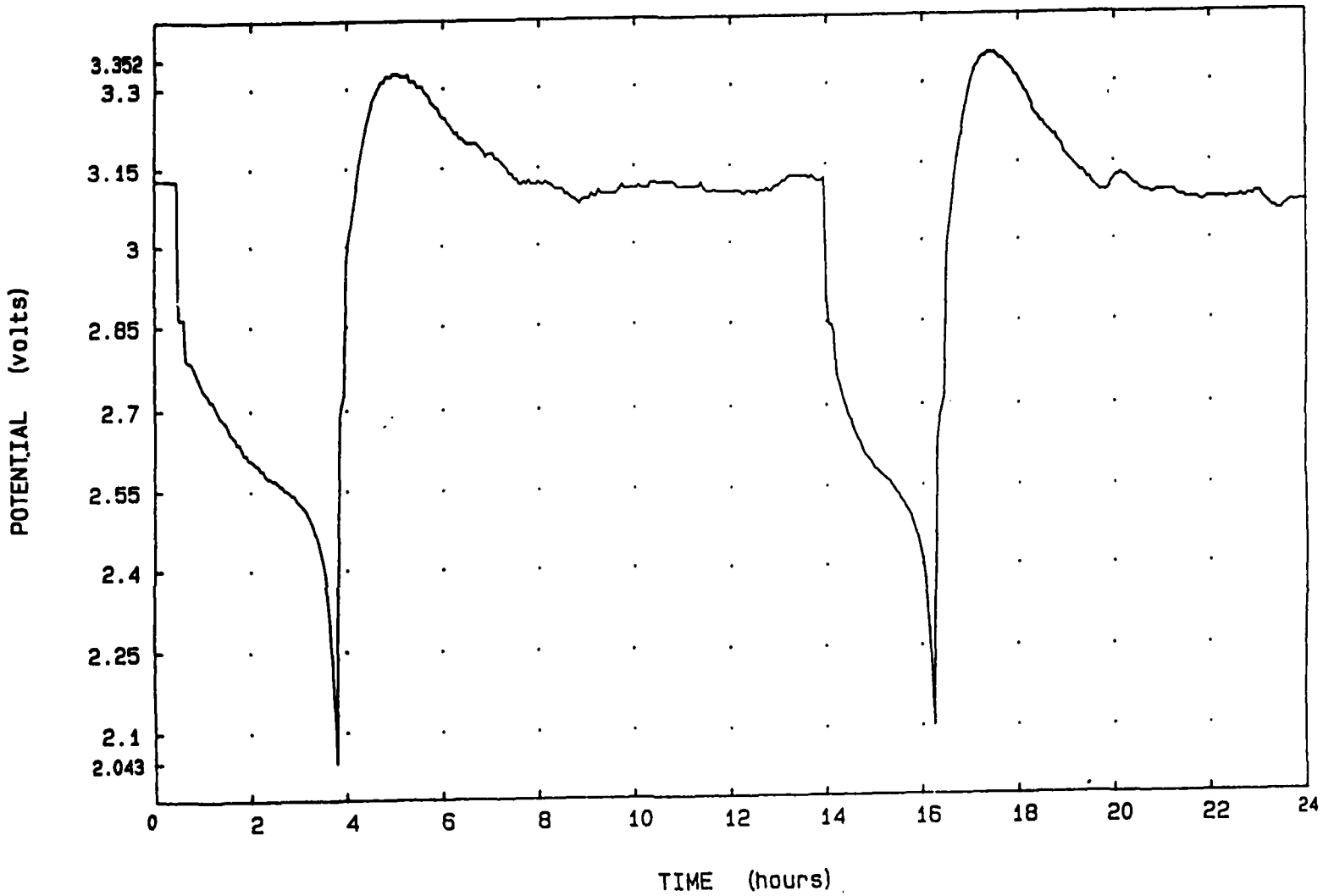

FIGURE 57. Cycle profile, cell #32-77-4: cycles #3 & 4.
Separator: Hovosorb
Pos. screen/contact: Anodized Aluminum
Electrolyte: 0.85M LiBr; 14% DME; 14% PC

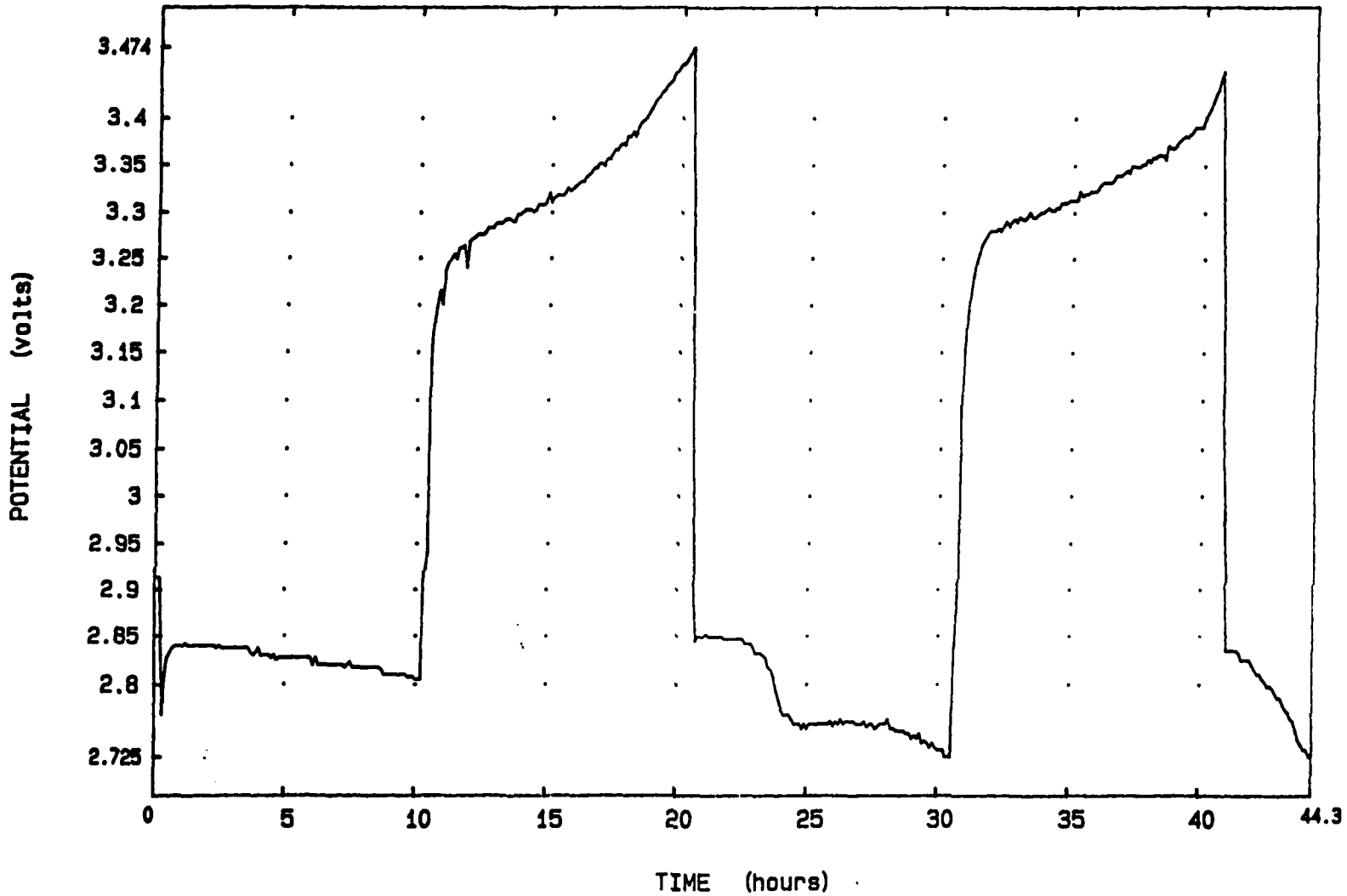

FIGURE 58. Cycle profile, cell #37-95-5
Separator: Fine Tefzel Mesh
Pos. screen/contact: Titanium
Electrolyte: 0.85M LiBr; 14% DME; 14% PC

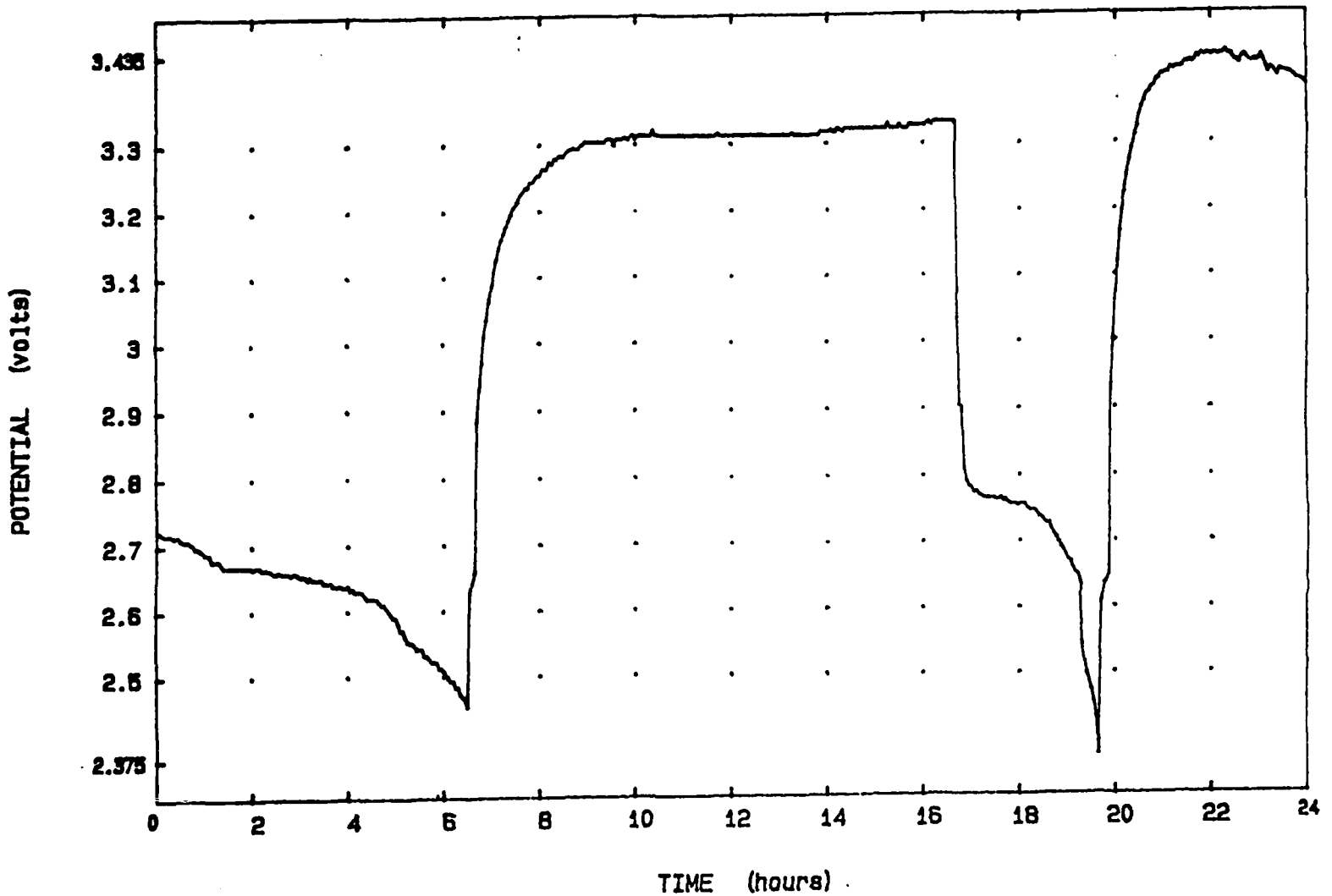

FIGURE 59. Cycle profile, cell #37-95-5: cycles #3 & 4.
Separator: Fine Tefzel Mesh
Pos. screen/contact: Titanium
Electrolyte: 0.85M LiBr; 14% DME; 14% PC

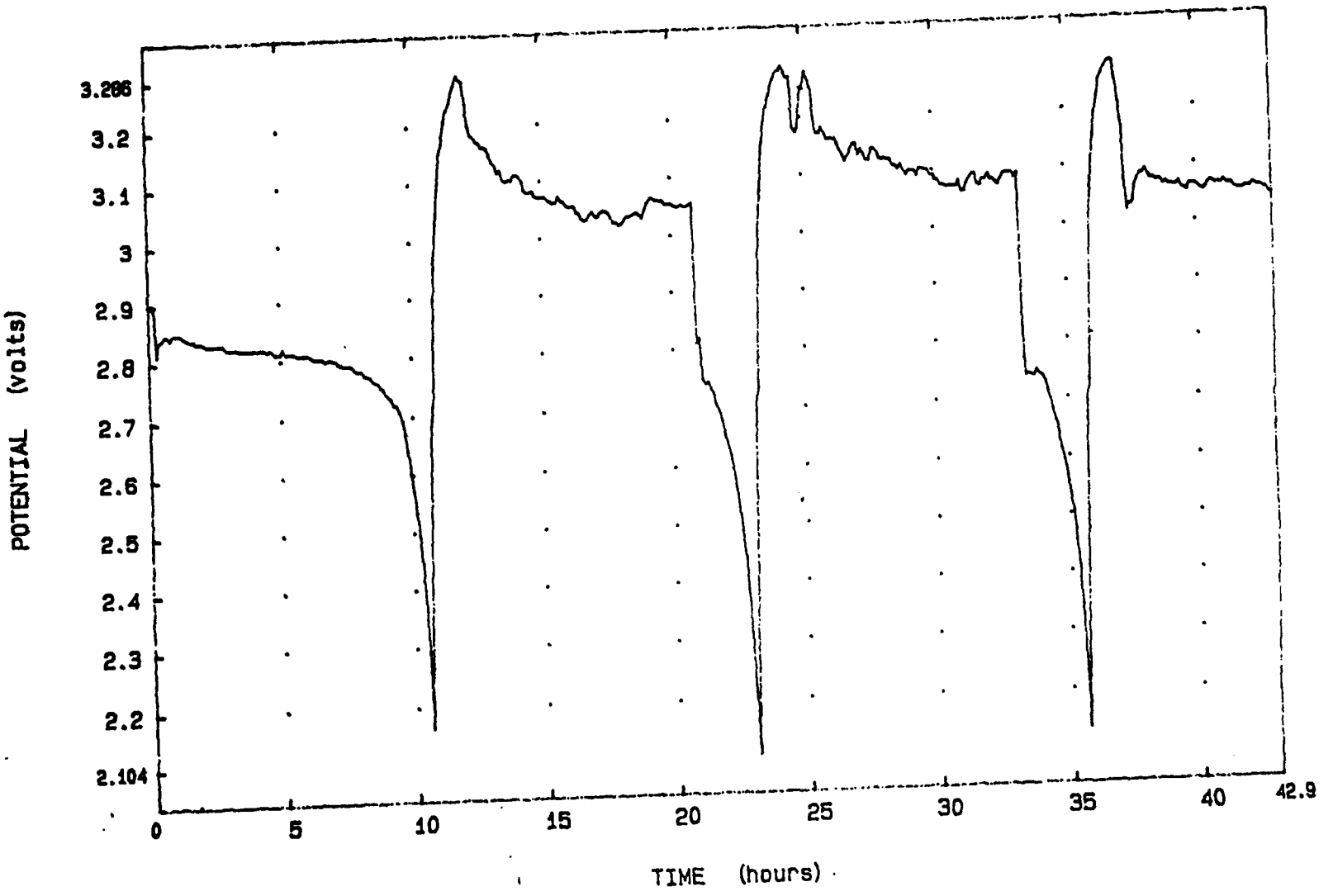

FIGURE 60. Cycle profile, cell #32-85-1
Separator: Hovosorb
Pos. screen/contact: Titanium
Electrolyte: 1M LiBr; 34% DME; 11% PC

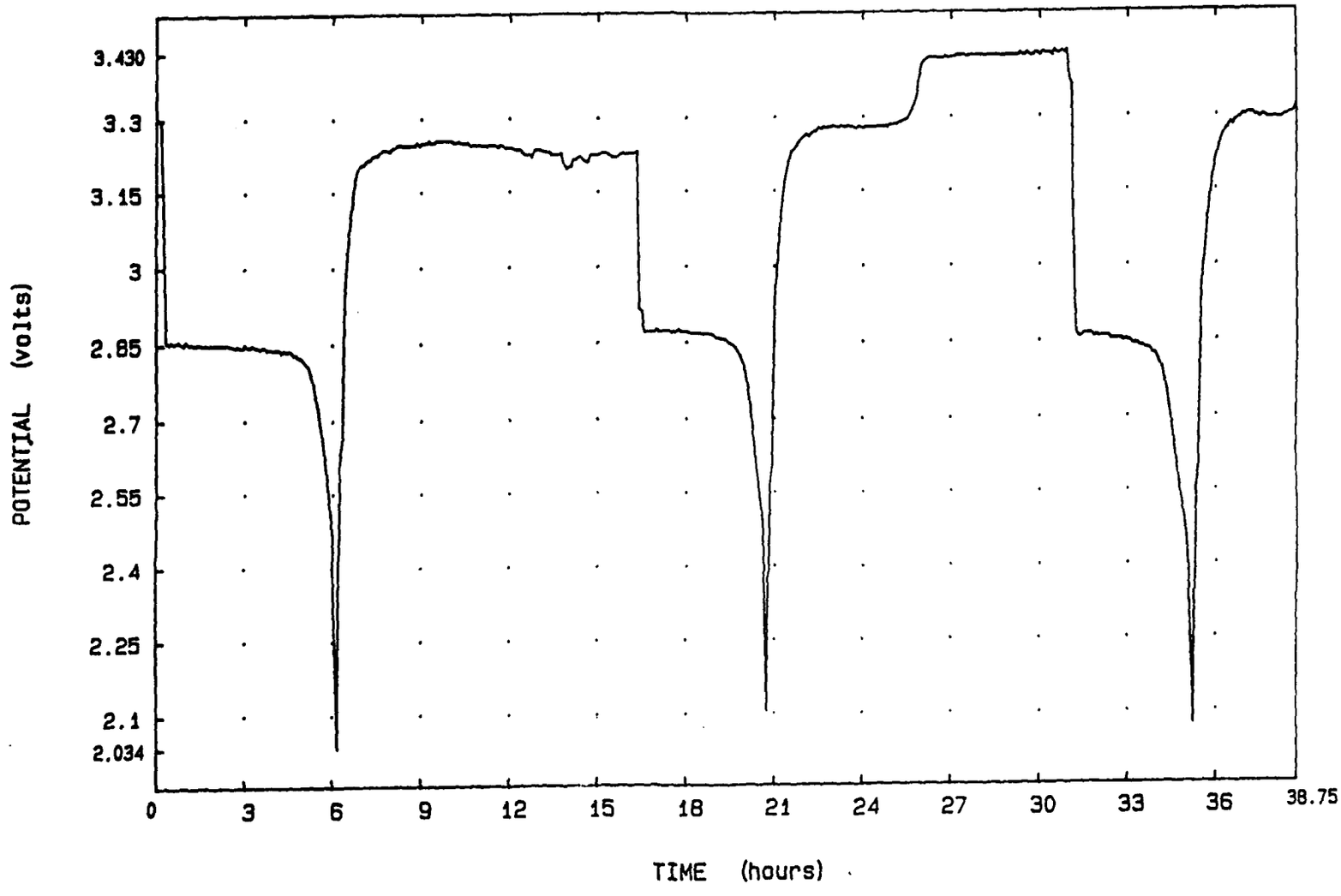

FIGURE 61. Cycle profile, cell #32-77-3
Separator: Hovosorb
Pos. screen/contact: Anodized Aluminum
Electrolyte: 1M CsBr; 0.5M LiBr

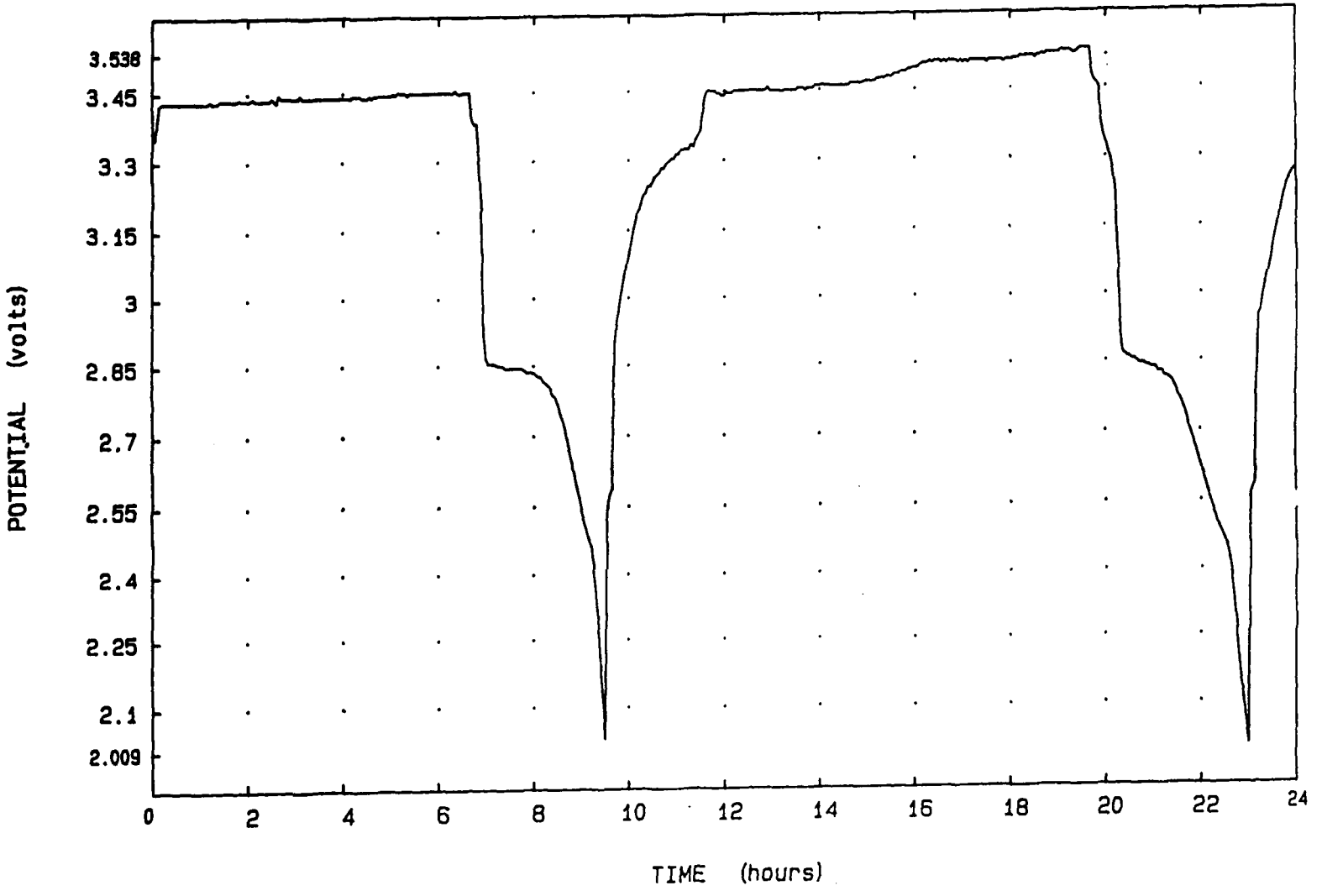

FIGURE 62. Cycle profile, cell #32-77-3: cycles 4 & 5.
Separator: Hovosorb
Pos. screen/contact: Anodized Aluminum
Electrolyte: 1M CsBr; 0.5M LiBr

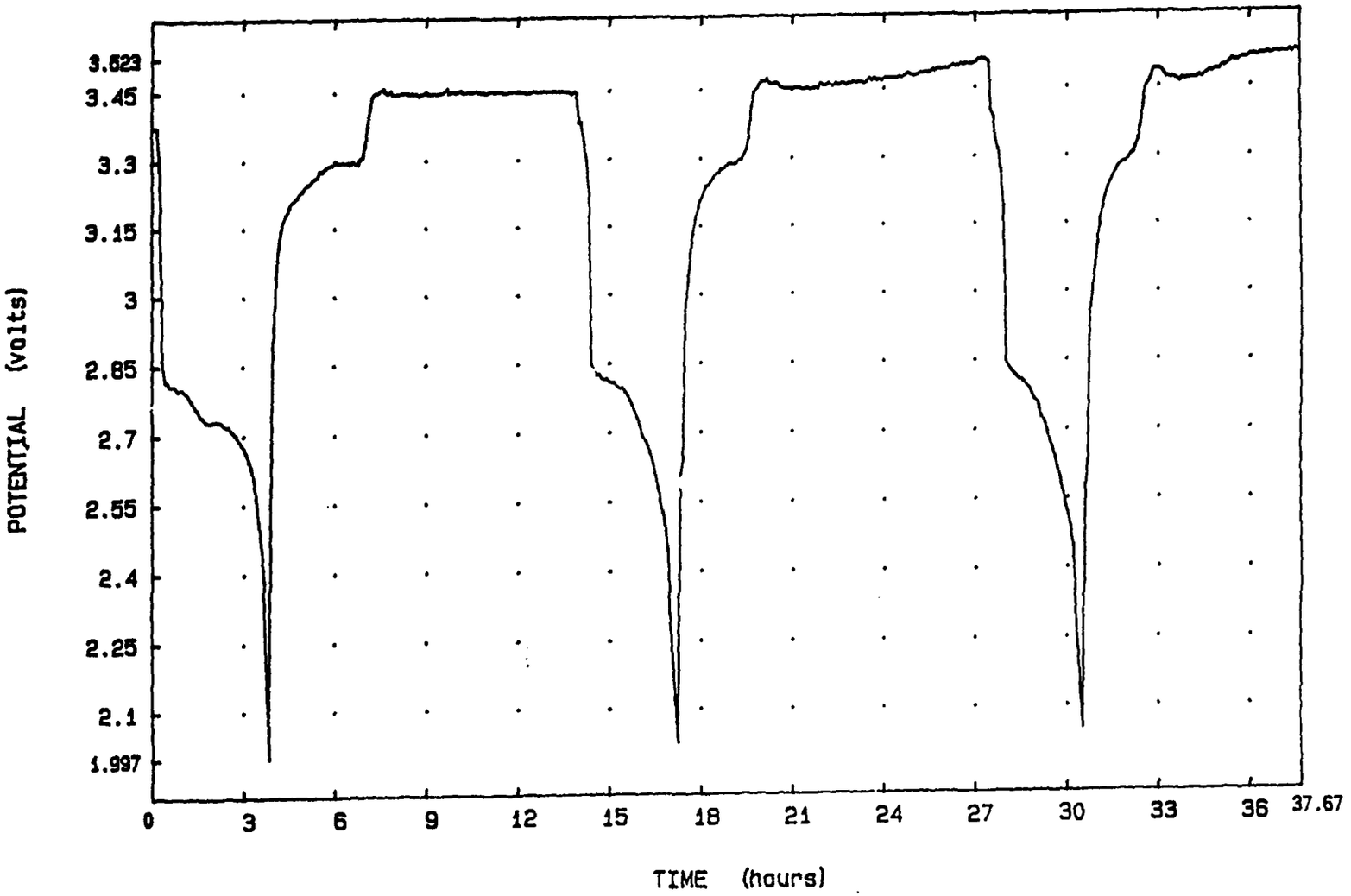

FIGURE 63. Cycle profile, cell #37-95-4
Separator: Coarse Tefzel Mesh
Pos. screen/contact: Titanium
Electrolyte: 1M CsBr; 0.5M LiBr

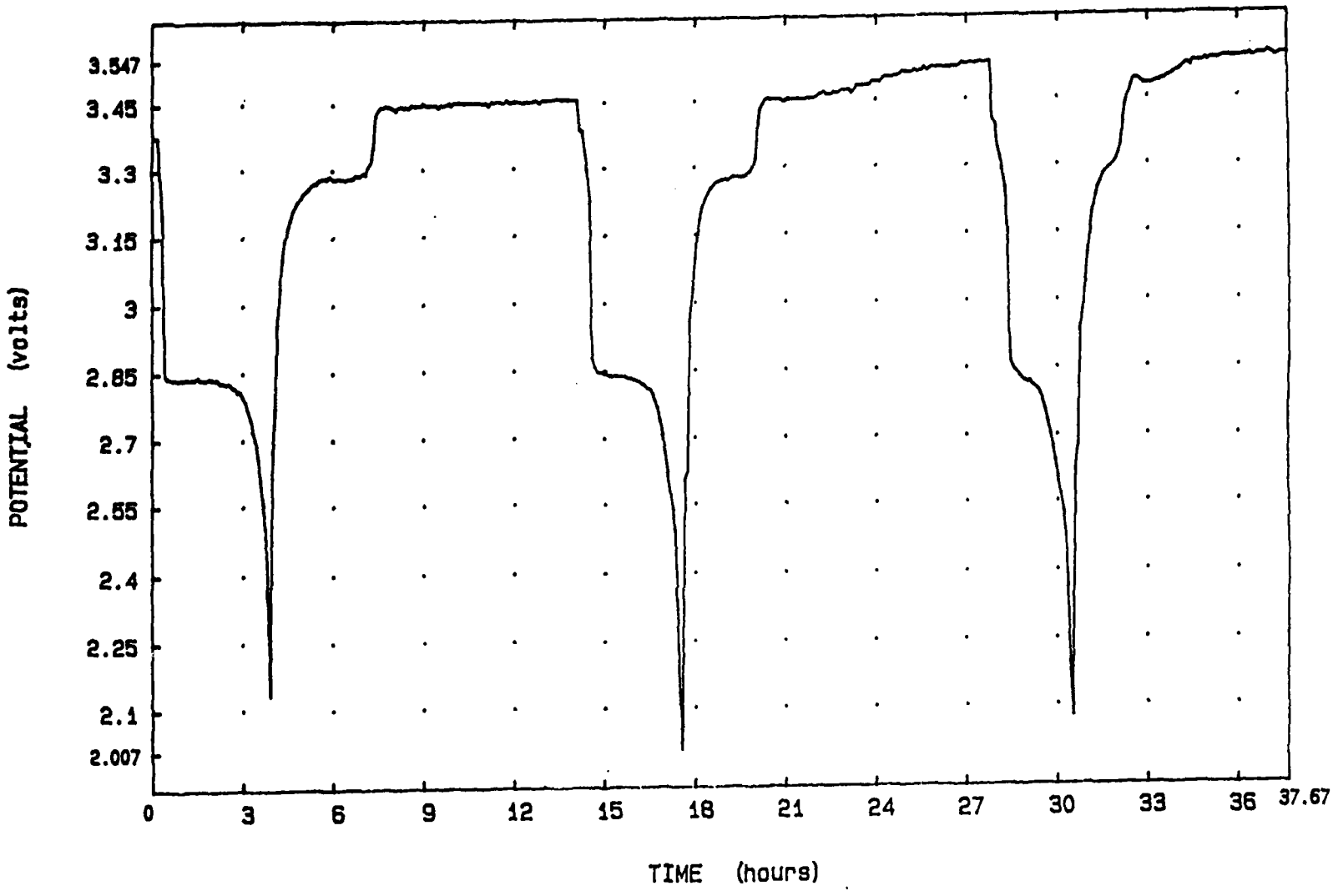

FIGURE 64. Cycle profile, cell #37-95-7
Separator: Fine Tefzel Mesh
Pos. screen/contact: Titanium
Electrolyte: 1M CsBr; 0.5M LiBr

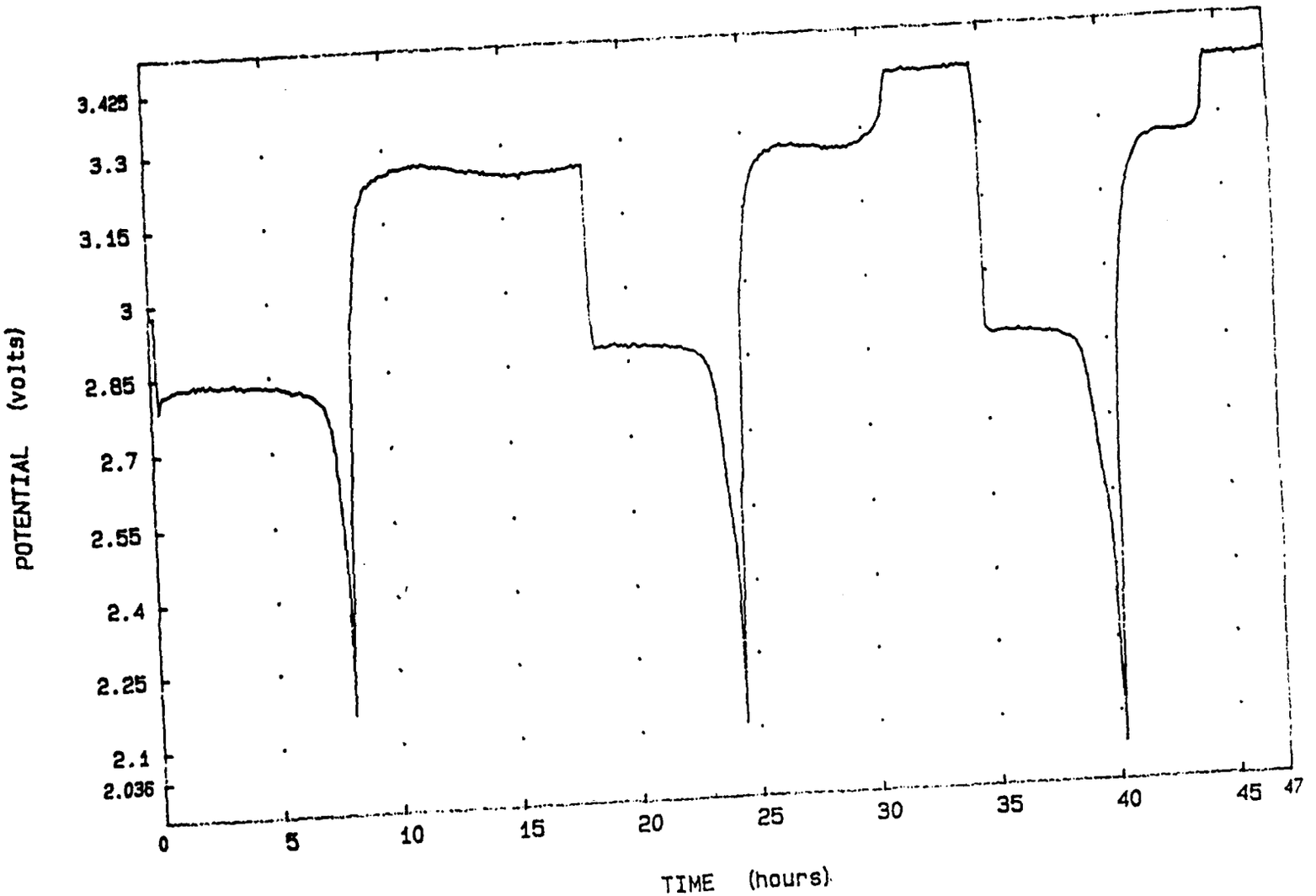

FIGURE 65. Cycle profile, cell #32-85-5
Separator: Hovosorb
Pos. screen/contact: Titanium
Electrolyte: 2M CsBr; 0.5M LiBr

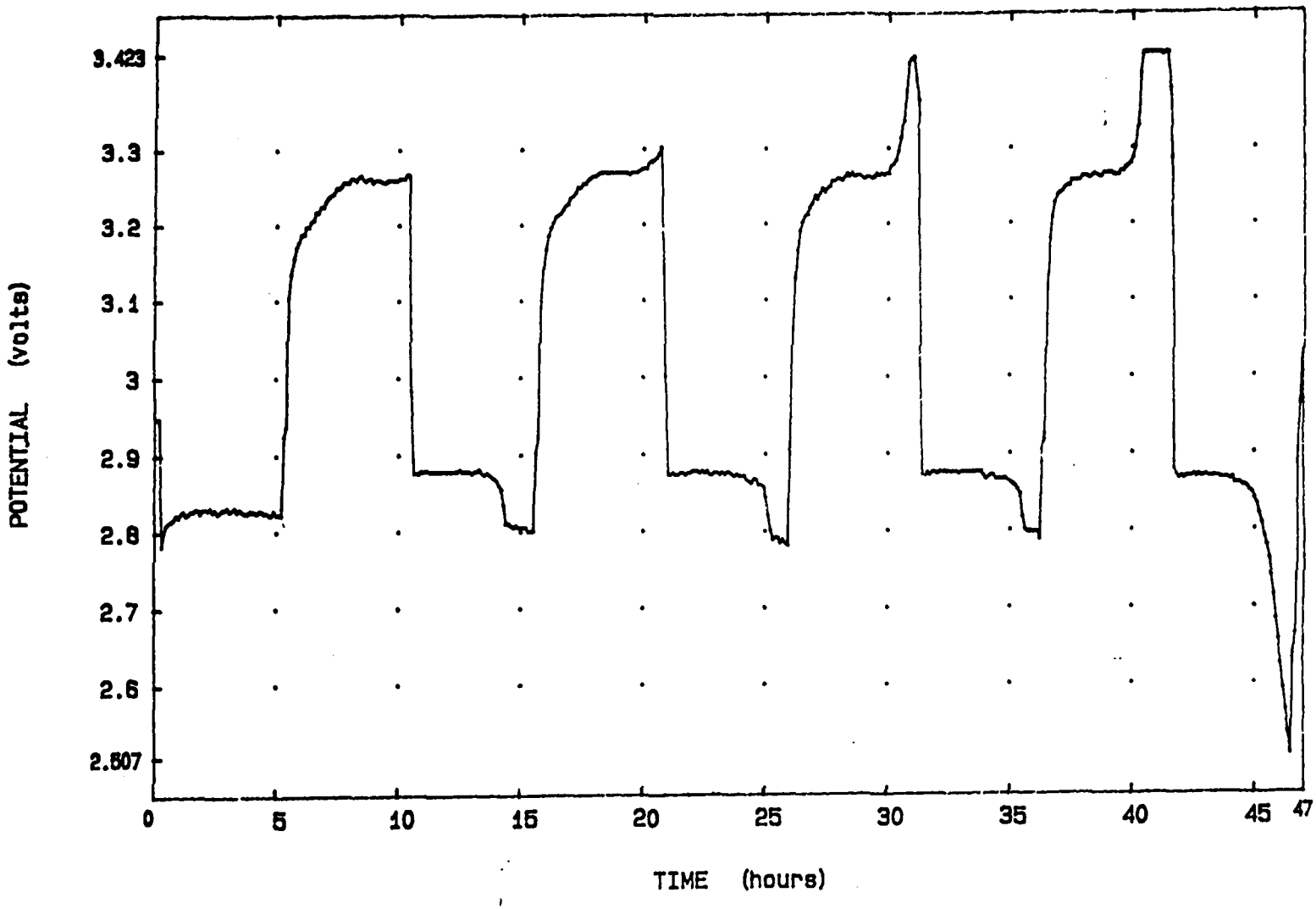

FIGURE 66. Cycle profile, cell #32-85-6
Separator: Hovosorb
Pos. screen/contact: Titanium
Electrolyte: 2M CsBr; 0.5M LiBr

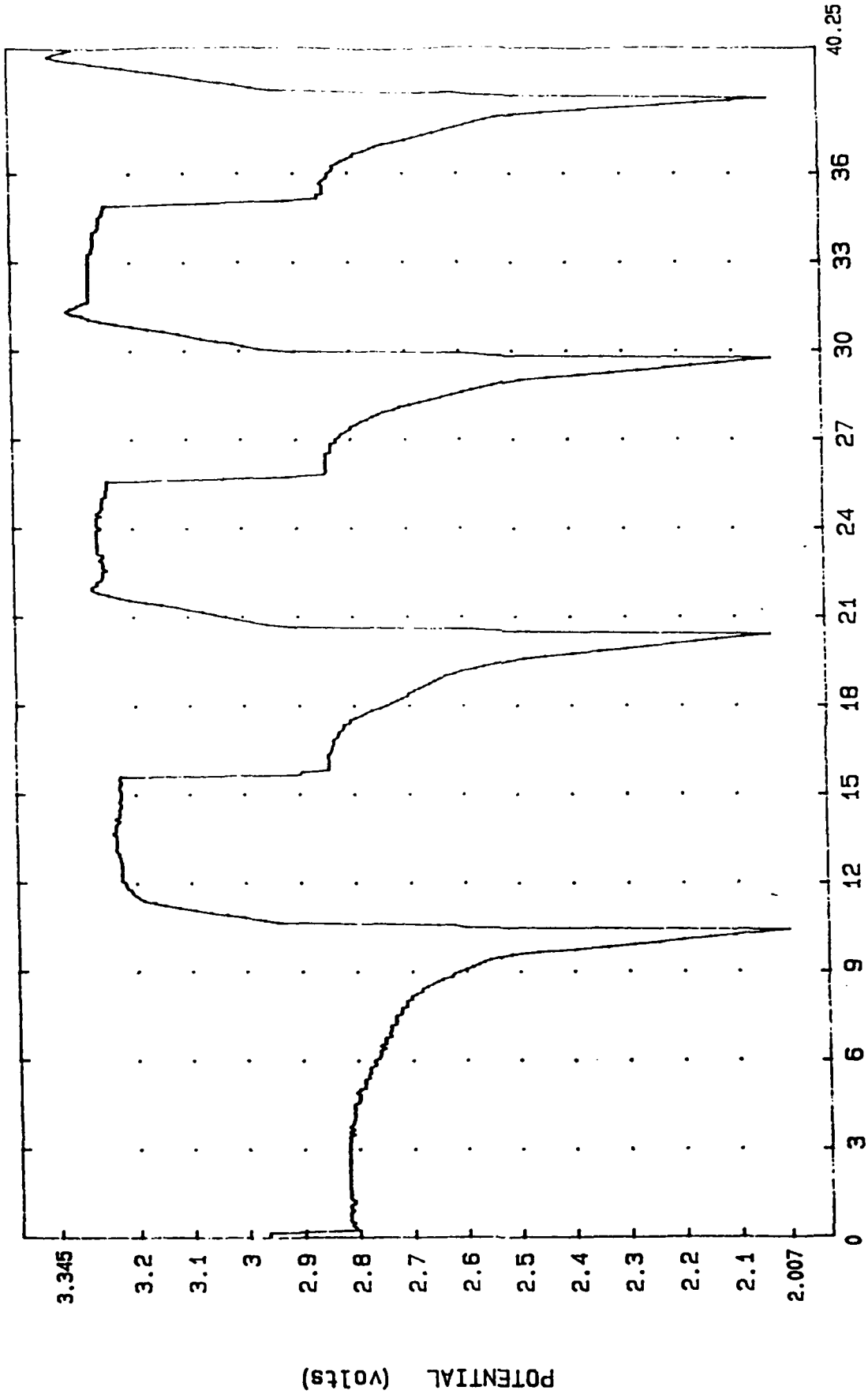

FIGURE 67. Beginning cycle profile, cell #41-26-1.
Electrolyte: 1.25M CsBr; 0.12M LiBr
Cathode: 75/25/10
Charge/ discharge current: 38.1 mA.

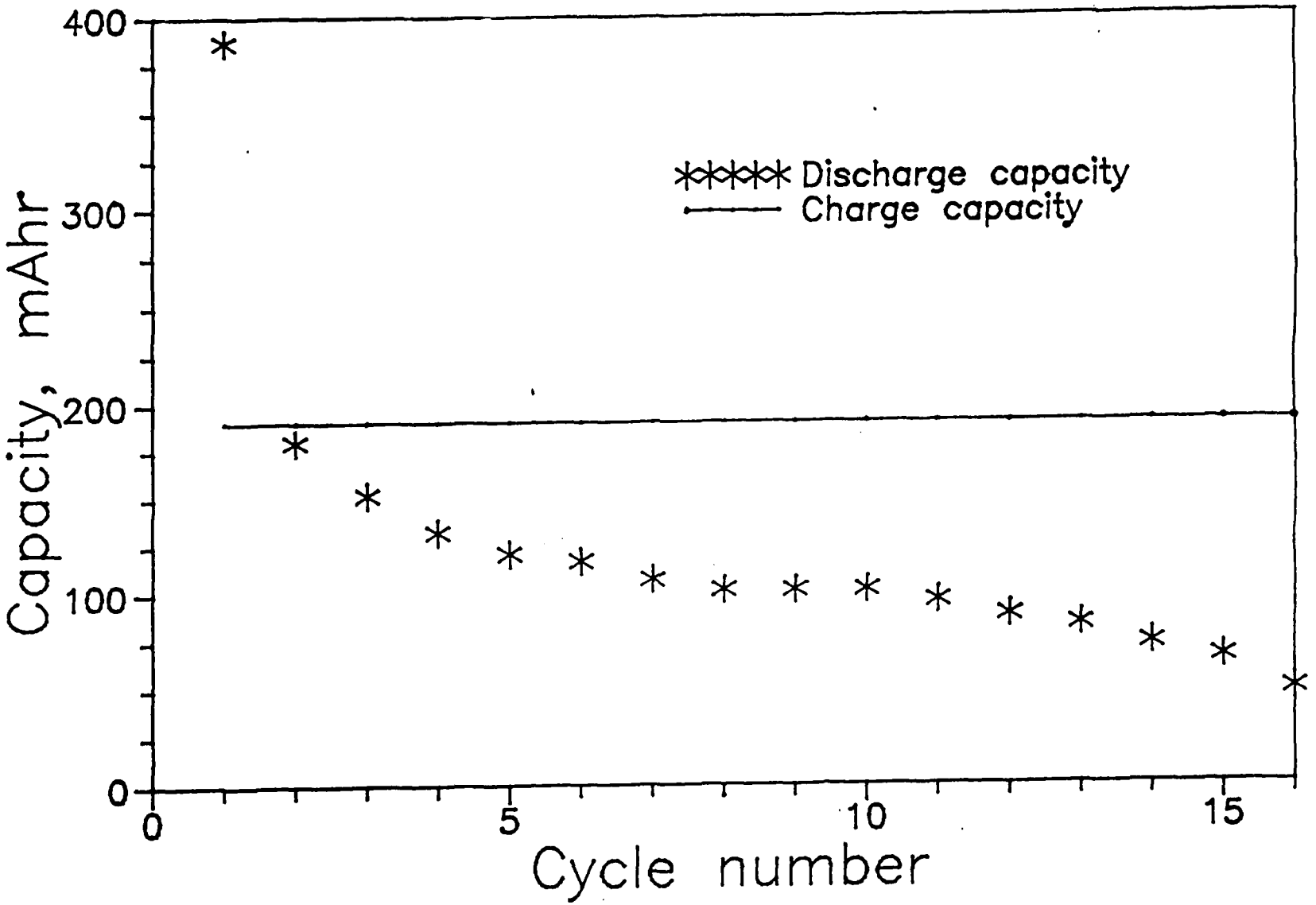

FIGURE 68. Capacity versus cycle number, cell #41-26-1
Time limited charge cycles: 38.1 mA x 5 hrs = 190.5 mAhr.

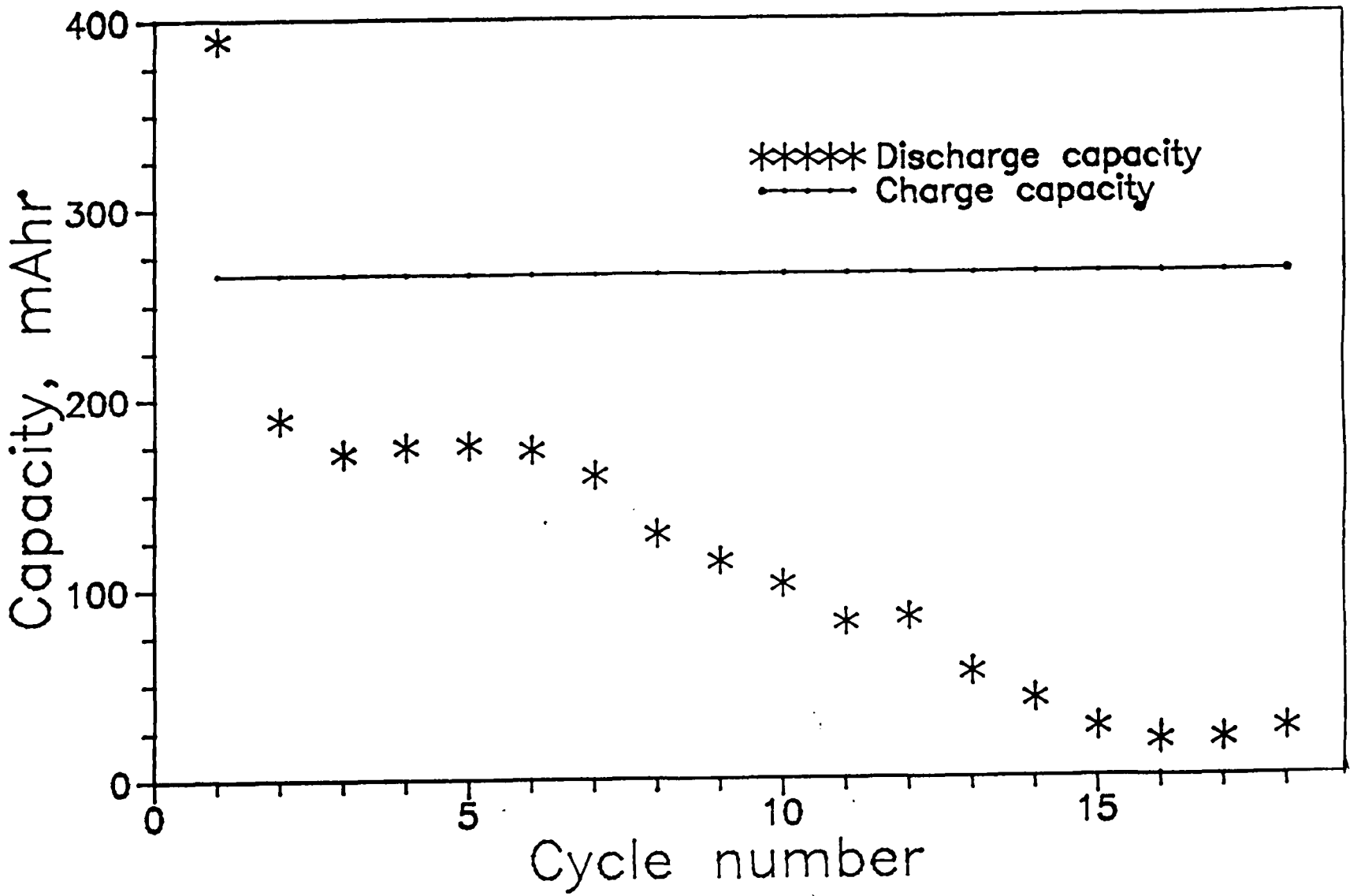

FIGURE 69. Capacity versus cycle number, cell #41-26-2
Time limited charge cycles: 53.1 mA x 5 hrs = 265.5 mAhr.

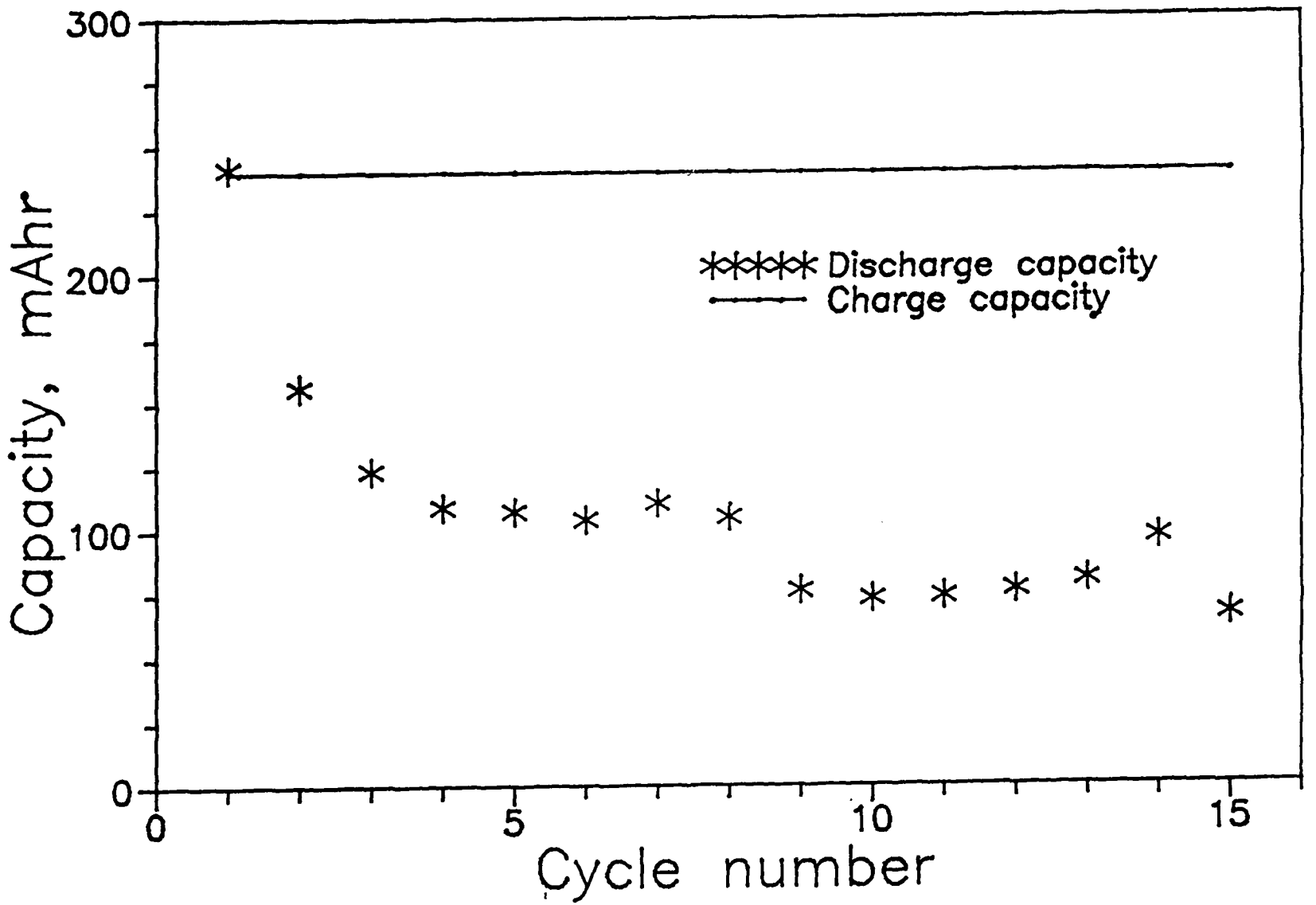

FIGURE 70. Capacity versus cycle number, cell #41-26-4
Time limited charge cycles: 48.0 mA x 5 hrs = 240.0 mAhr.

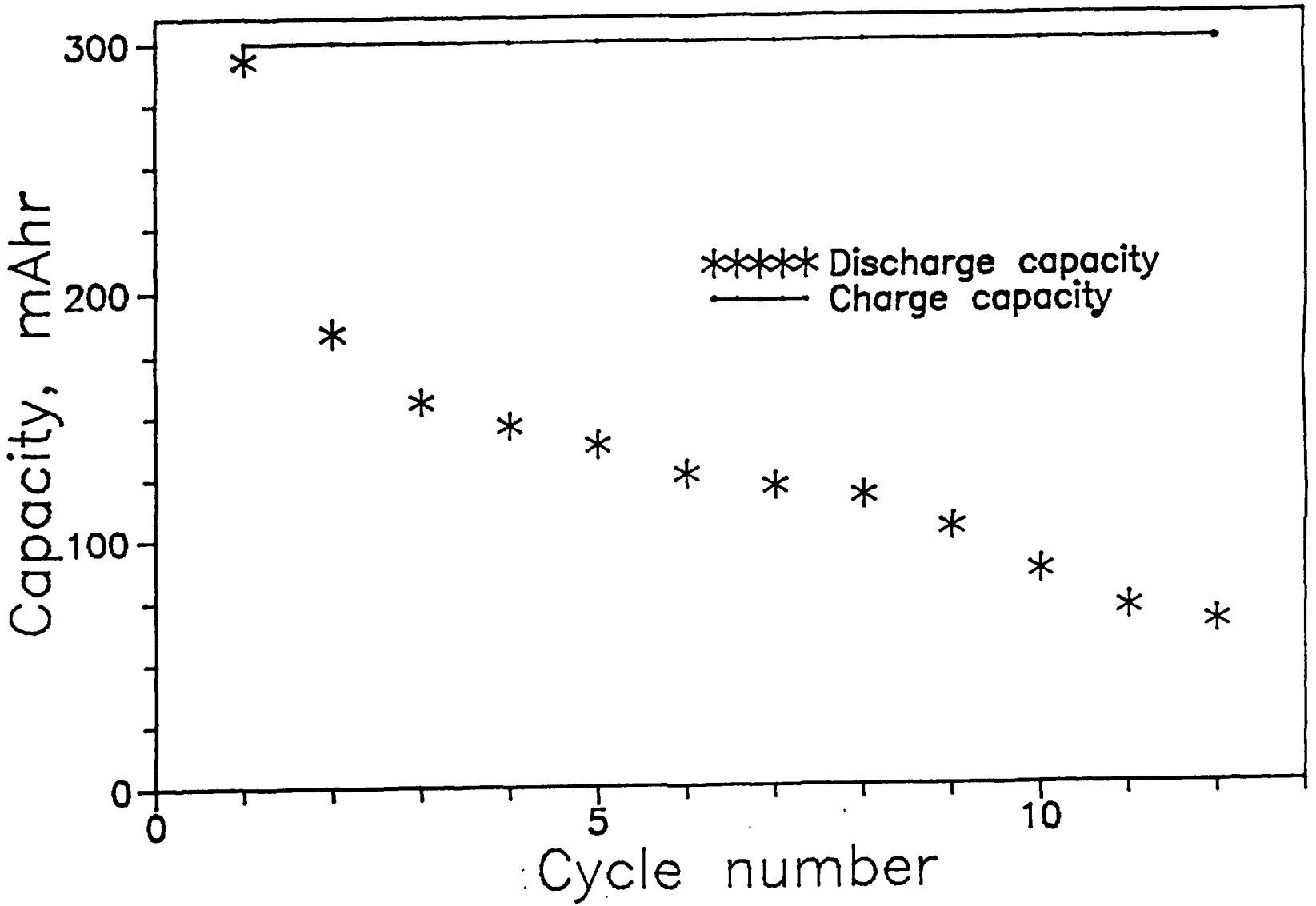

FIGURE 71. Capacity versus cycle number, cell #41-26-5
Time limited charge cycles: 60.0 mA x 5 hrs = 300.0 mAhr.

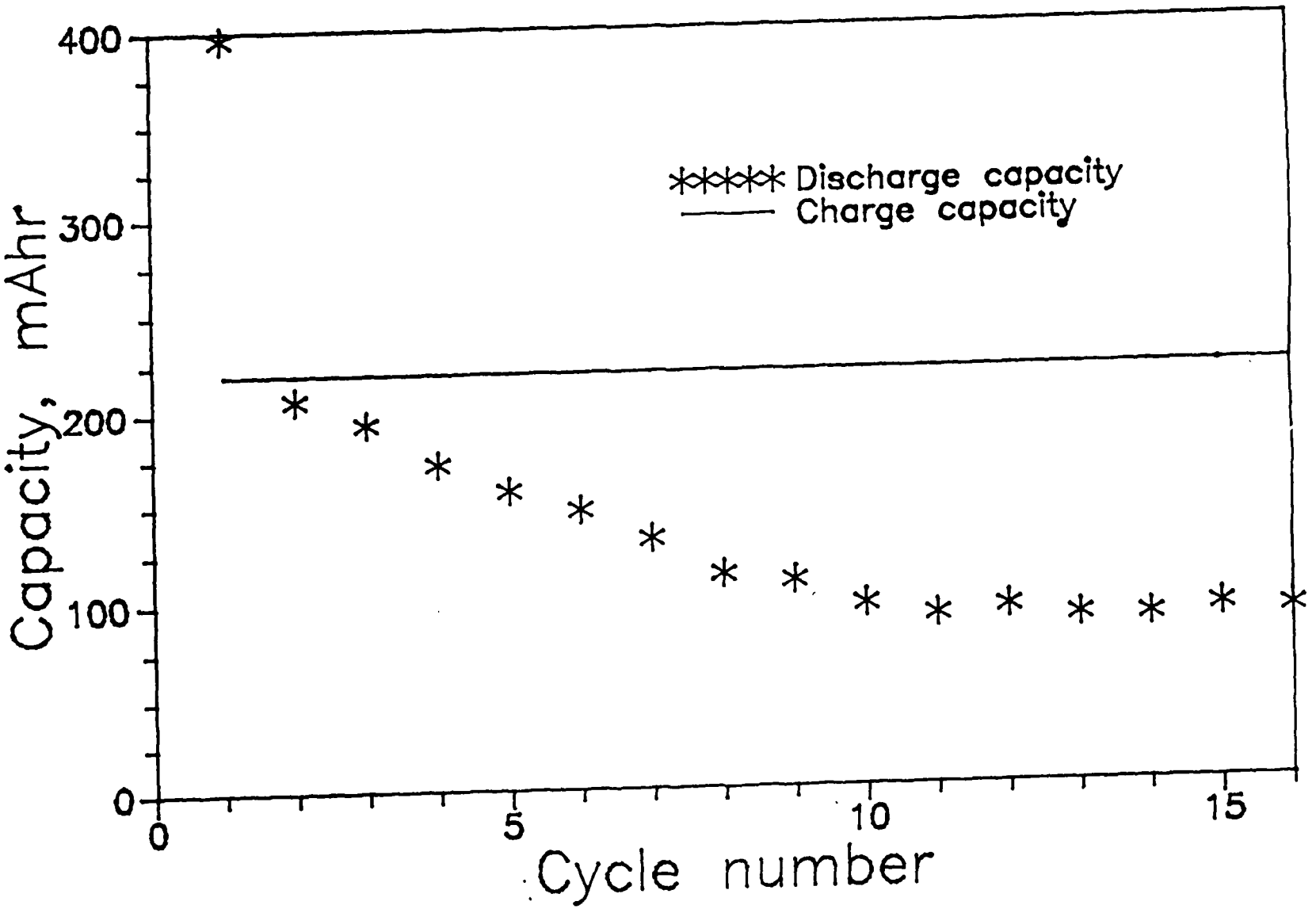

FIGURE 72. Capacity versus cycle number, cell #41-27-1
Time limited charge cycles: 43.9 mA x 5 hrs = 219.5 mAhr.

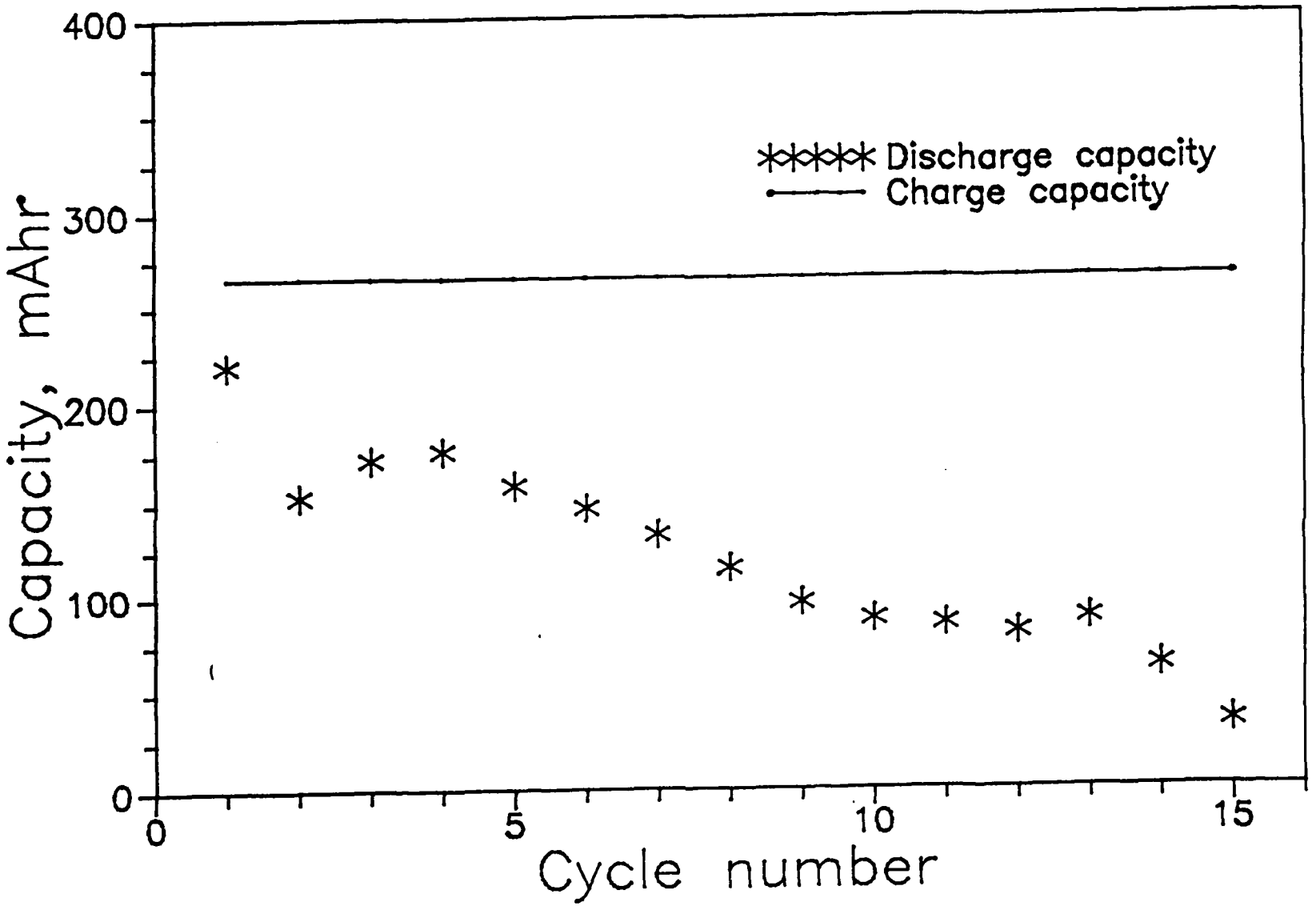

FIGURE 73. Capacity versus cycle number, cell #41-27-2
Time limited charge cycles: 53.1 mA x 5 hrs = 265.5 mAhr.

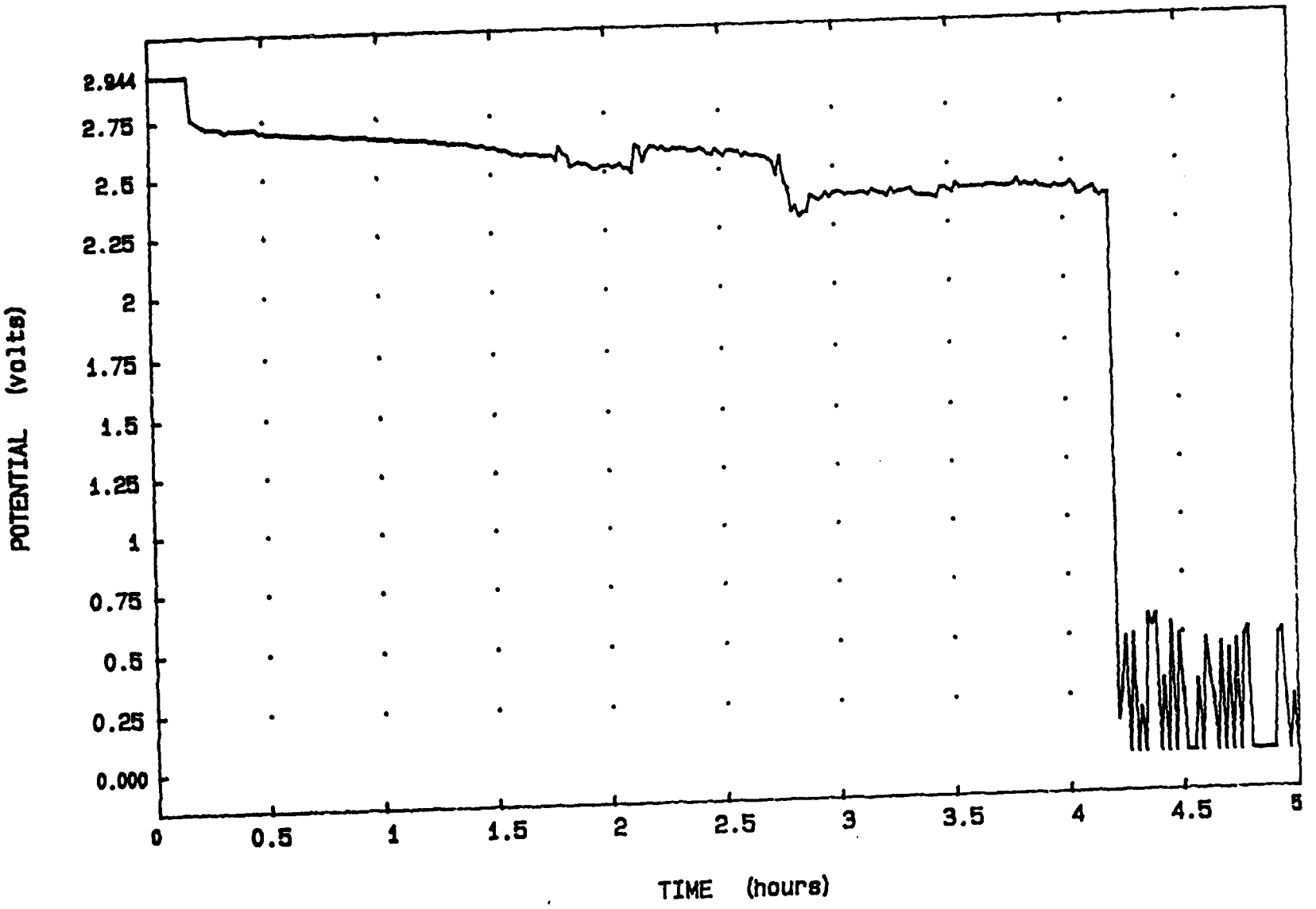

FIGURE 74. Beginning cycle profile, cell #41-31-3.
Electrolyte: 1.5M CsBr; 0.12M LiBr
Cathode: 75/25/5
Charge/ discharge current: 38.1 mA.
Cell exploded during discharge after 462 mAh.

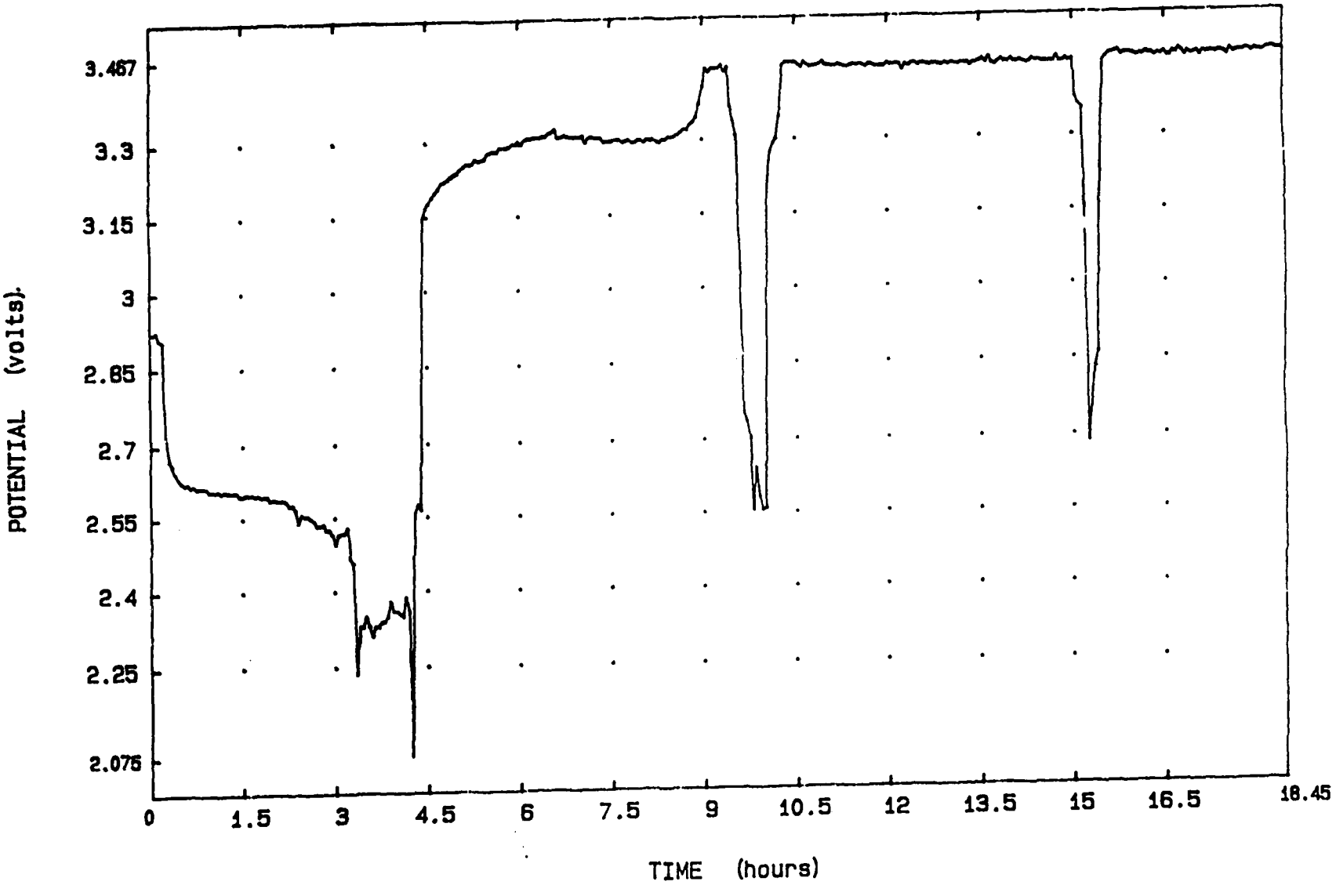

FIGURE 75. Beginning cycle profile, cell #41-31-4.
Electrolyte: 1.5M CsBr; 0.12M LiBr
Cathode: 75/25/5
Charge/ discharge current: 53.2 mA.
Time limited charge cycles: 115 mA x 5 hrs = 575 mAhr.

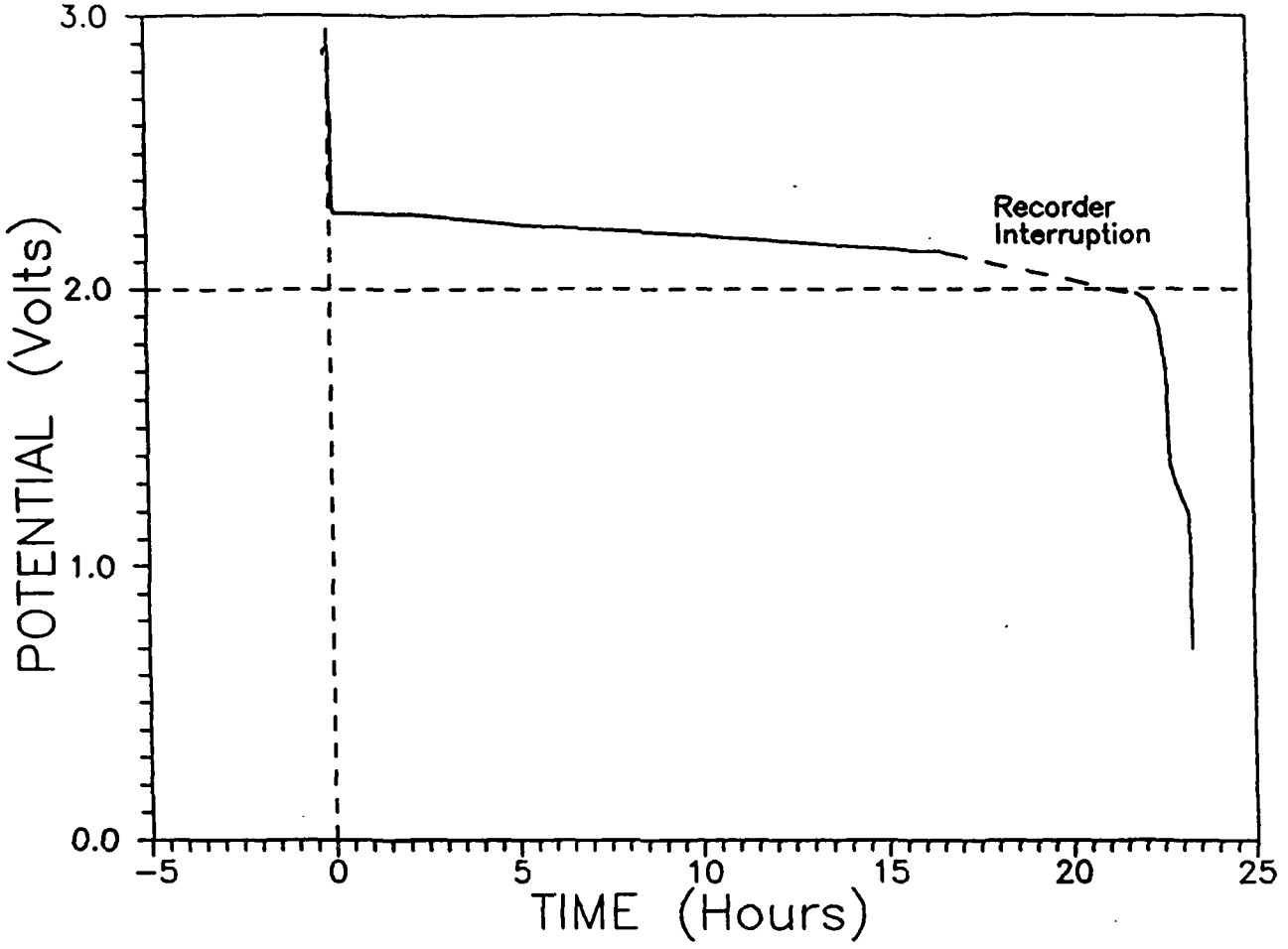

FIGURE 76. Cycle profile, cell #39-91-1
Separator: None
Pos. screen/contact: Tantalum
Electrolyte: 1.7M NEt_4Br; 43% DME; 13% PC

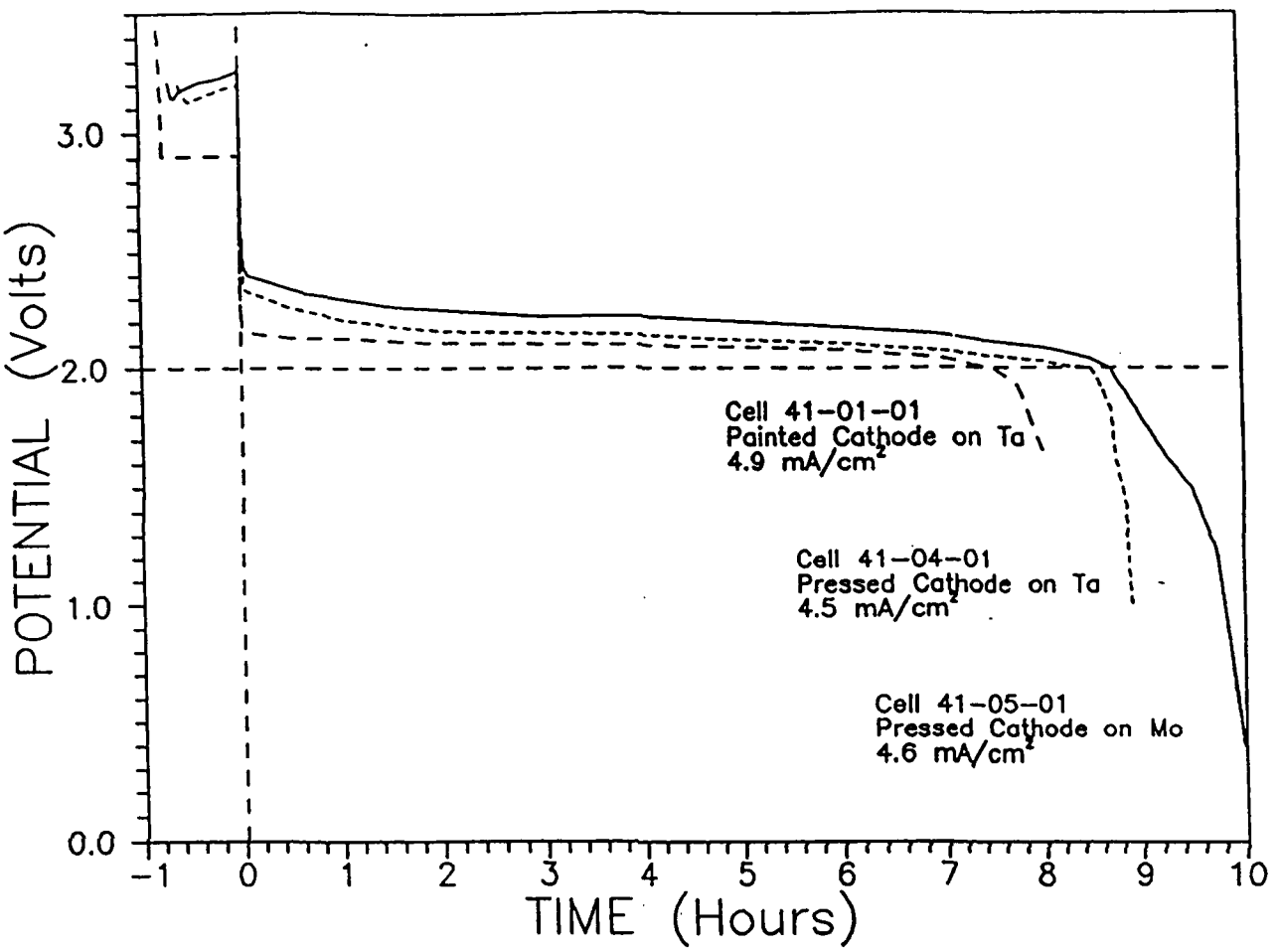

FIGURE 77. Cycle profile, cells #41-1-1; 41-4-1; 41-5-1.
Separator: Craneglass (None in #41-1-1)
Pos. screen/contact: Tantalum
Electrolyte: 1.7M NEt_4Br; 43% DME; 13% PC

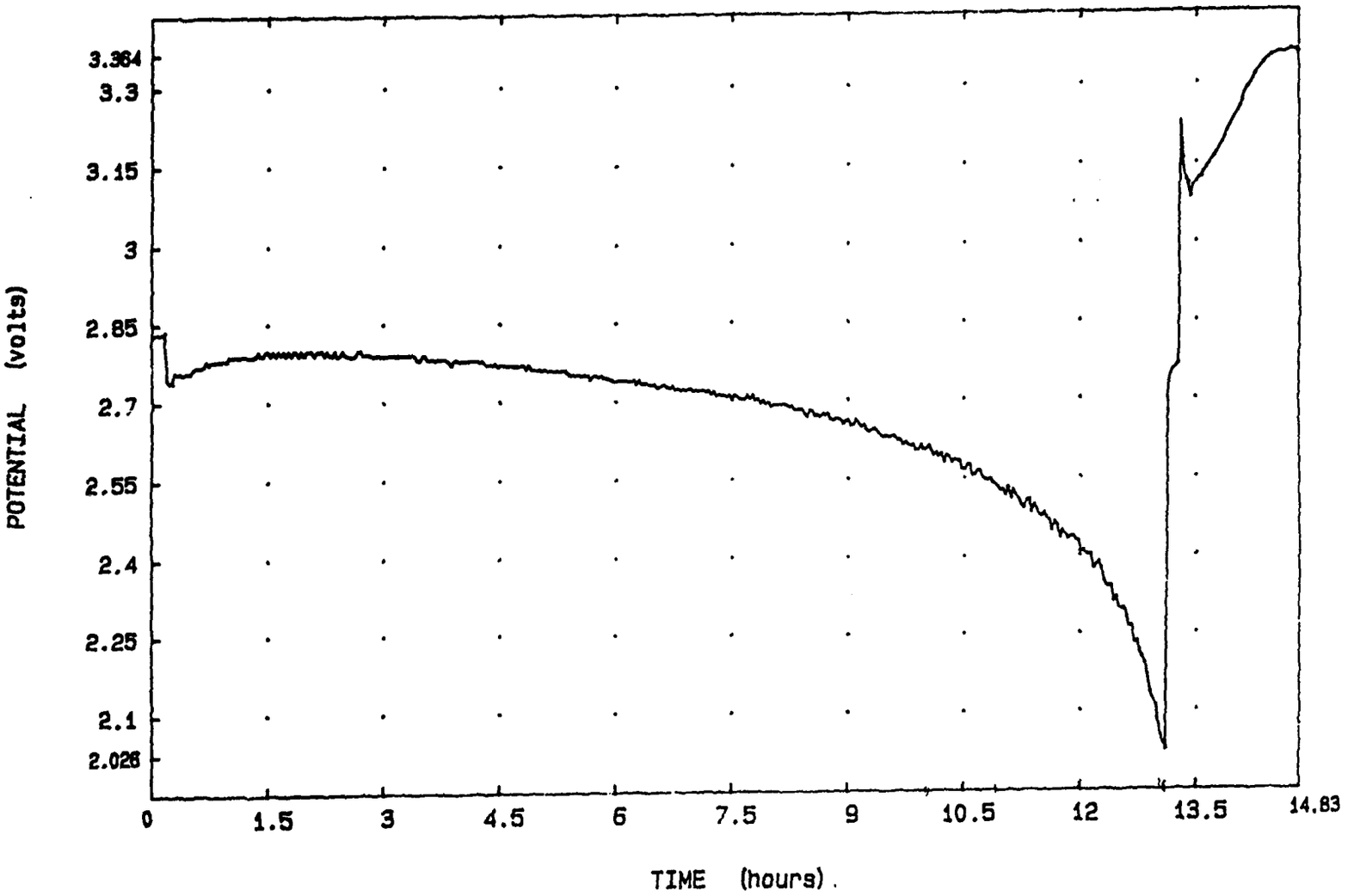

FIGURE 78. Cycle profile, cell #41-13-1: Li vs. C; cycle #2.
Separator: Craneglass
Pos. screen/contact: Molybdenum
Electrolyte: 1.7M LiBr; 43% DME: 13% PC

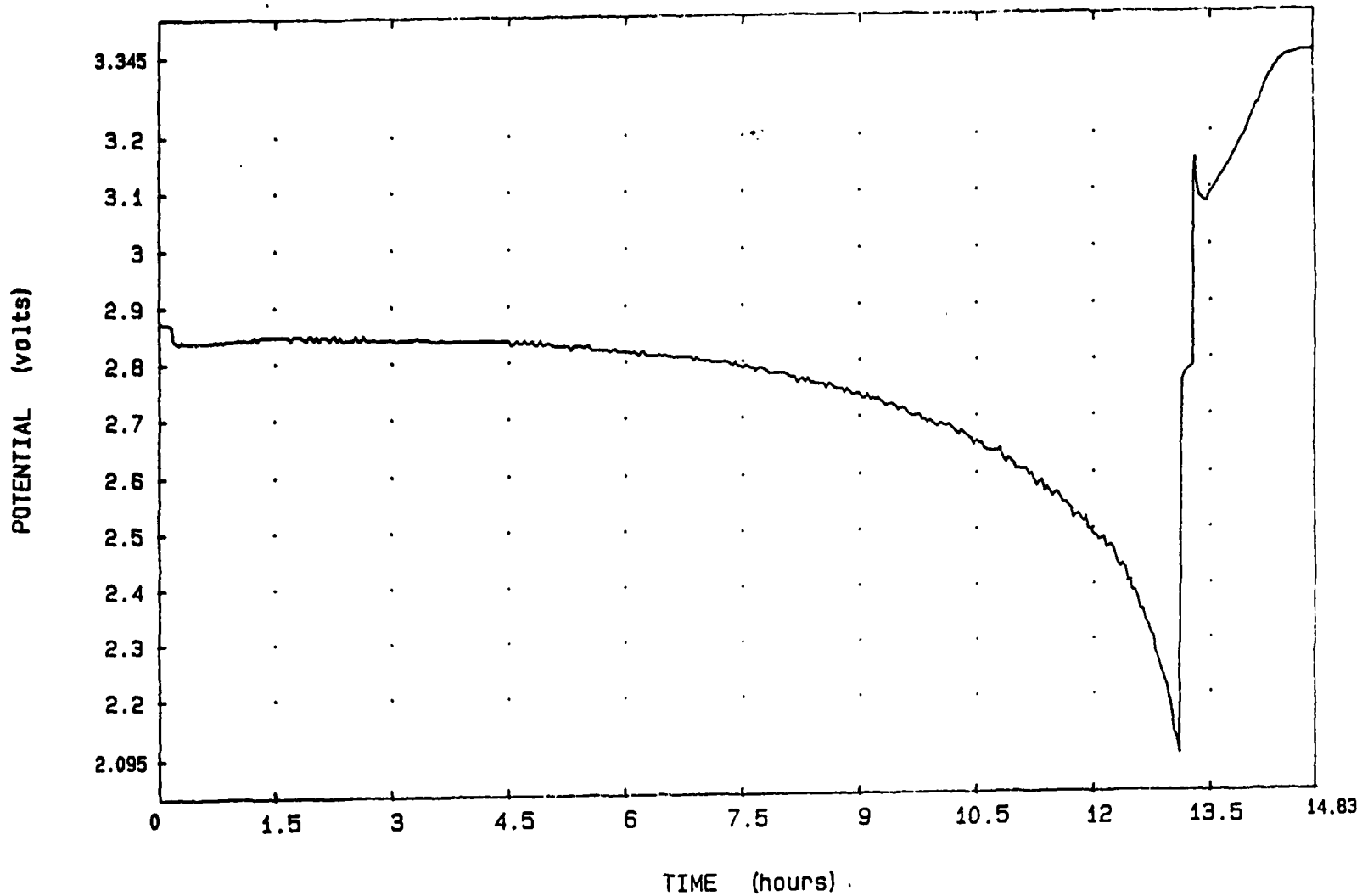

FIGURE 79. Cycle profile, cell #41-13-1: Ref. vs. C; cycle #2.
Separator: Craneglass
Pos. screen/contact: Molybdenum
Electrolyte: 1.7M LiBr; 43% DME: 13% PC

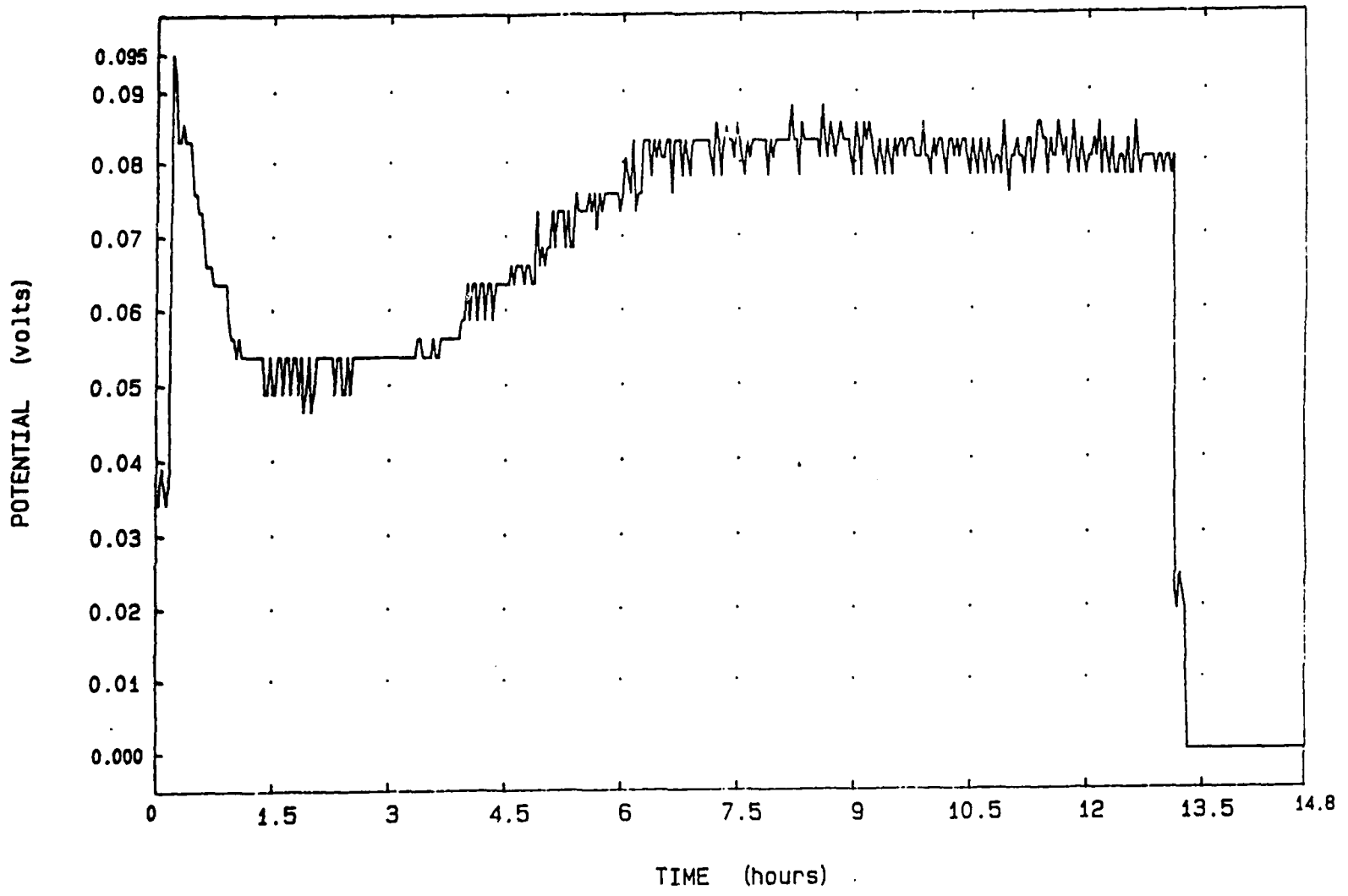

FIGURE 80. Cycle profile, cell #41-13-1: Ref vs. Li; cycle #2.
Separator: Craneglass
Pos. screen/contact: Molybdenum
Electrolyte: 1.7M LiBr; 43% DME: 13% PC

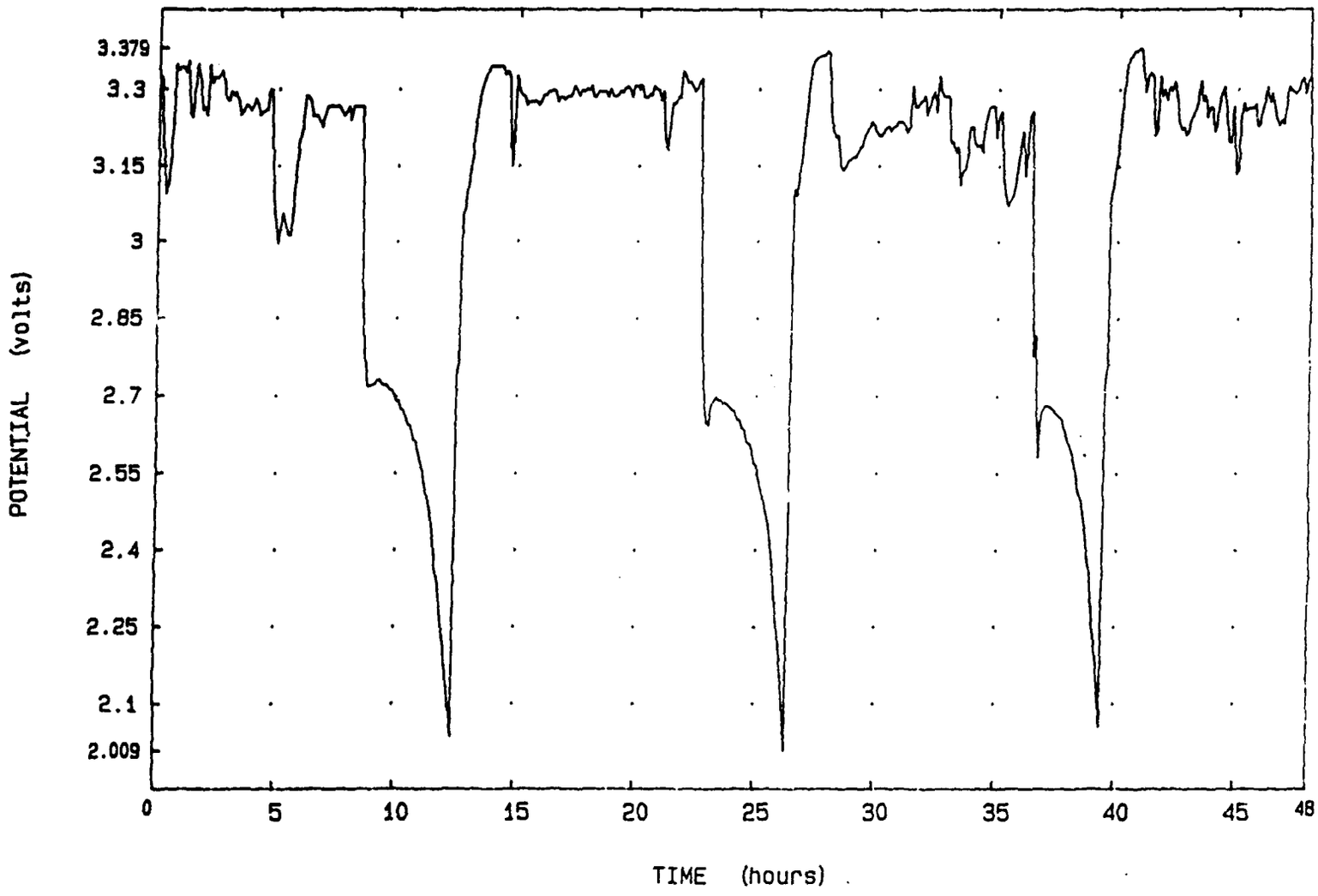

FIGURE 81. Cycle profile, cell #41-13-1: Li vs. C; cycles #3, 4, & 5
Separator: Craneglass
Pos. screen/contact: Molybdenum
Electrolyte: 1.7M LiBr; 43% DME: 13% PC

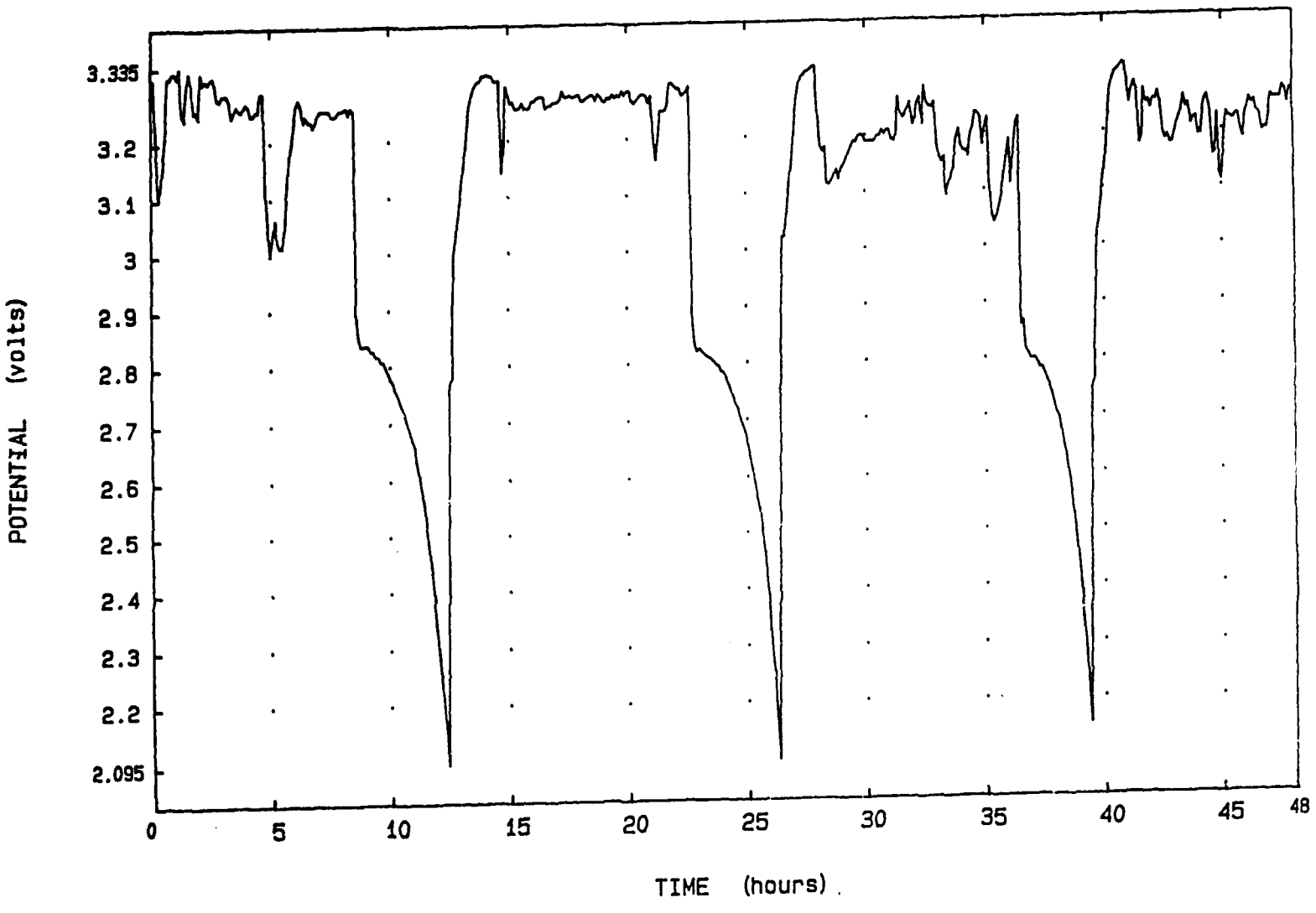

FIGURE 82. Cycle profile, cell #41-13-1: Ref vs. C; cycles #3, 4, & 5
Separator: Craneglass
Pos. screen/contact: Molybdenum
Electrolyte: 1.7M LiBr; 43% DME: 13% PC

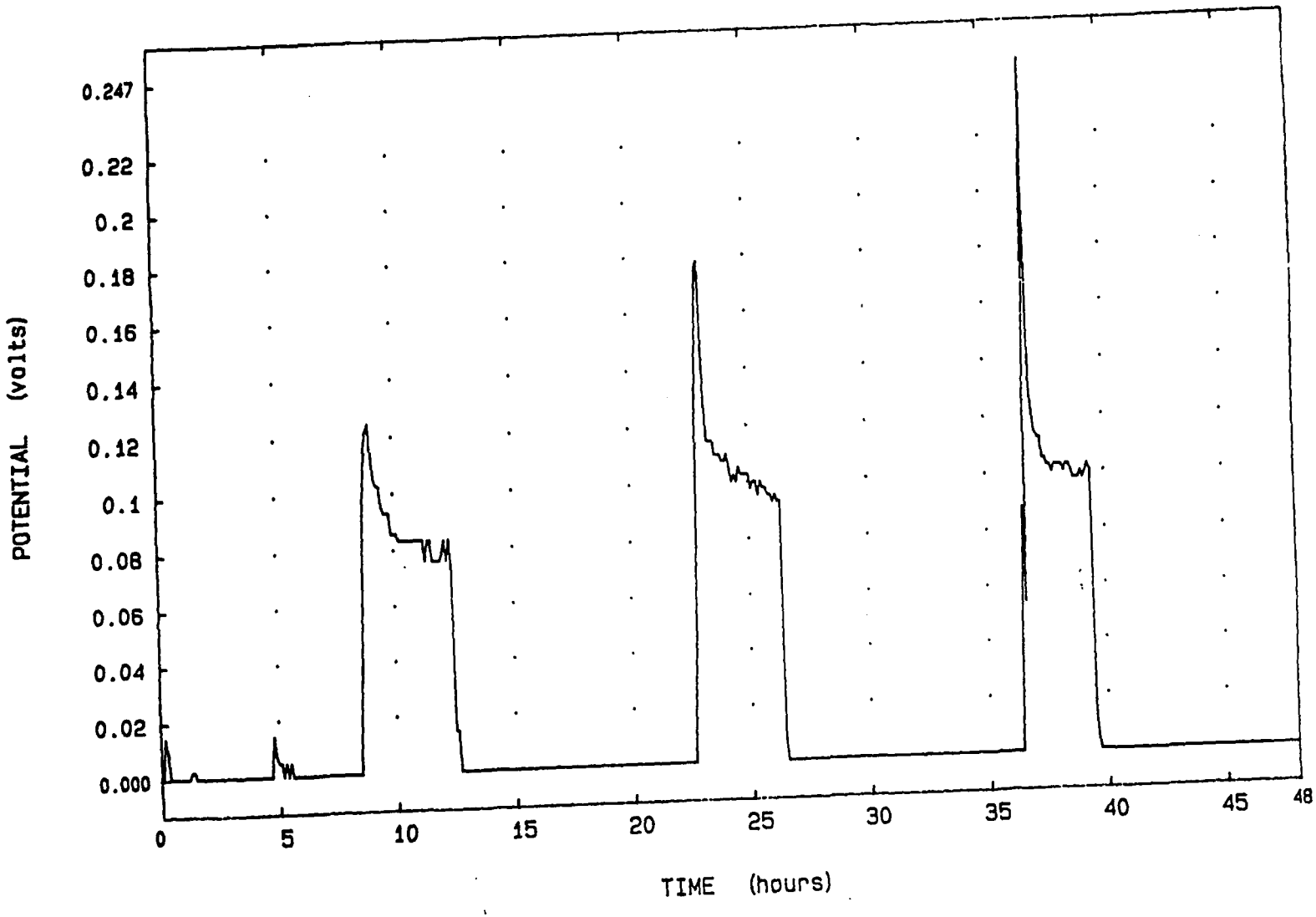

FIGURE 83. Cycle profile, cell #41-13-1: Ref. vs. Li; cycles #3, 4, & 5
Separator: Craneglass
Pos. screen/contact: Molybdenum
Electrolyte: 1.7M LiBr; 43% DME: 13% PC

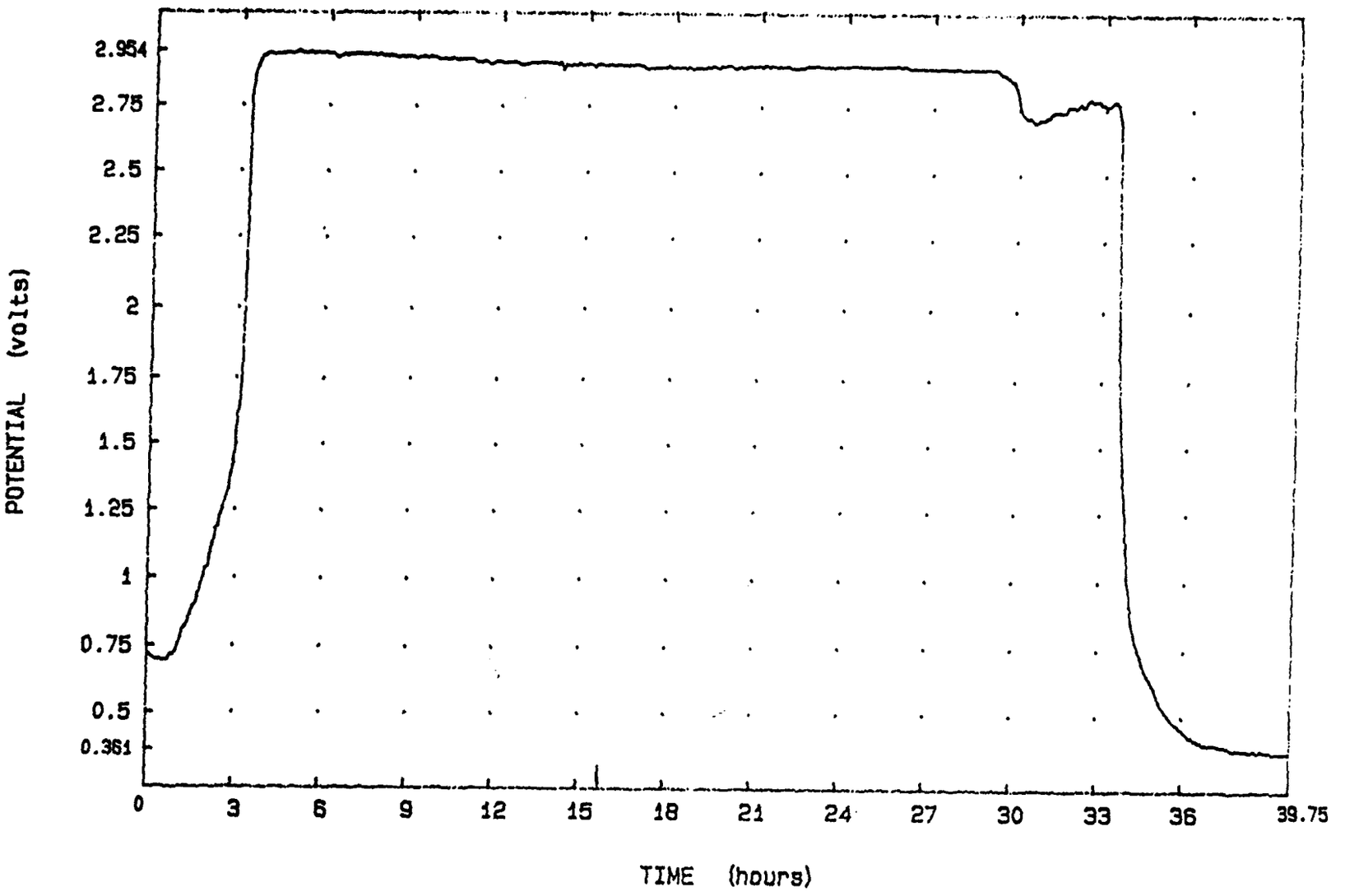

FIGURE 84. Open circuit potential versus time, cell #41-36-1.
Electrolyte: 0.75M $Cs(CF_3SO_3)$/ 0.12M LiBr.
Cathode: 75/25/5

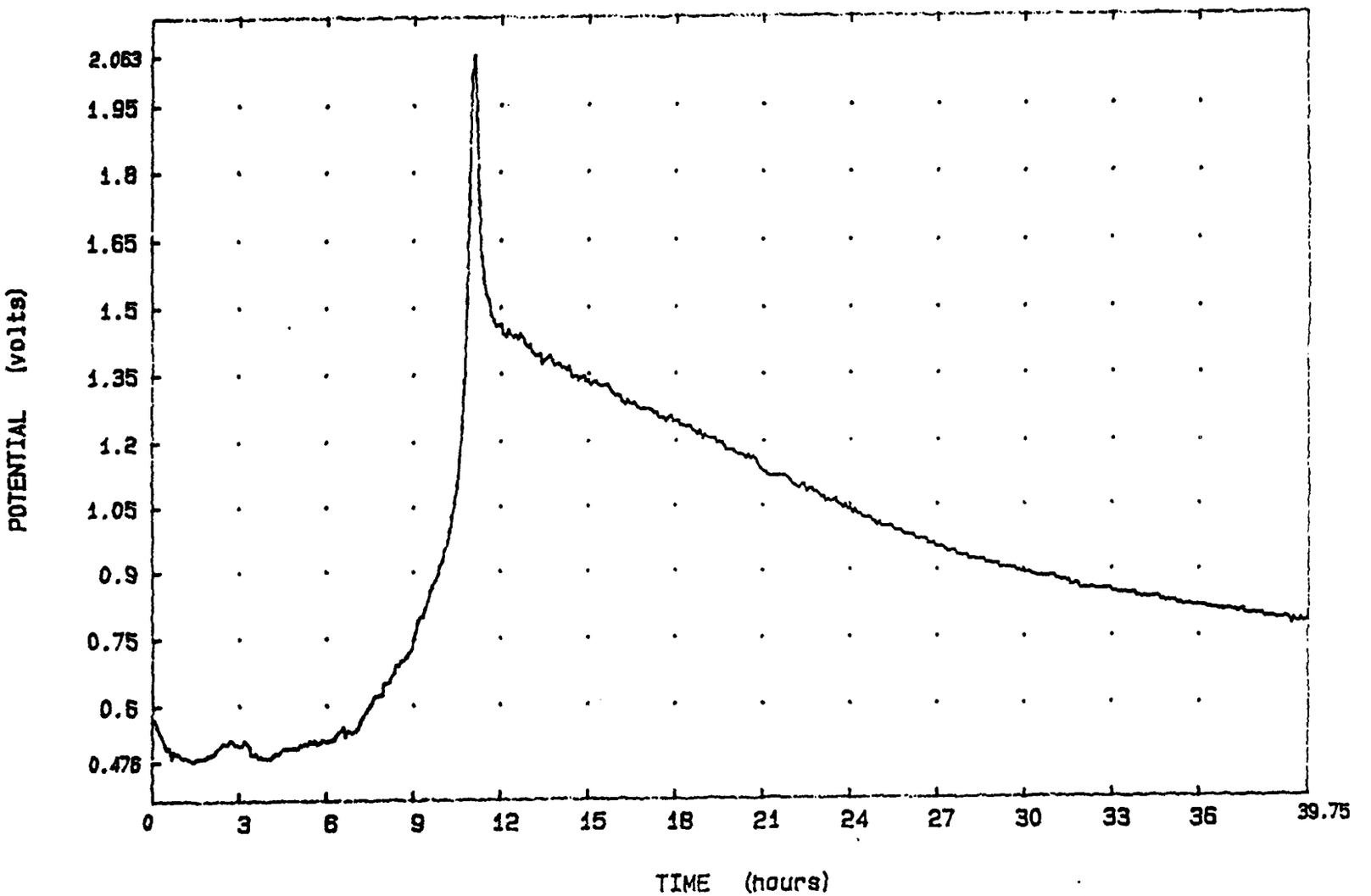

FIGURE 85. Open circuit potential versus time, cell #41-36-2.
Electrolyte: 0.75M $Cs(CF_3SO_3)$/ 0.12M LiBr.
Cathode: 75/25/5

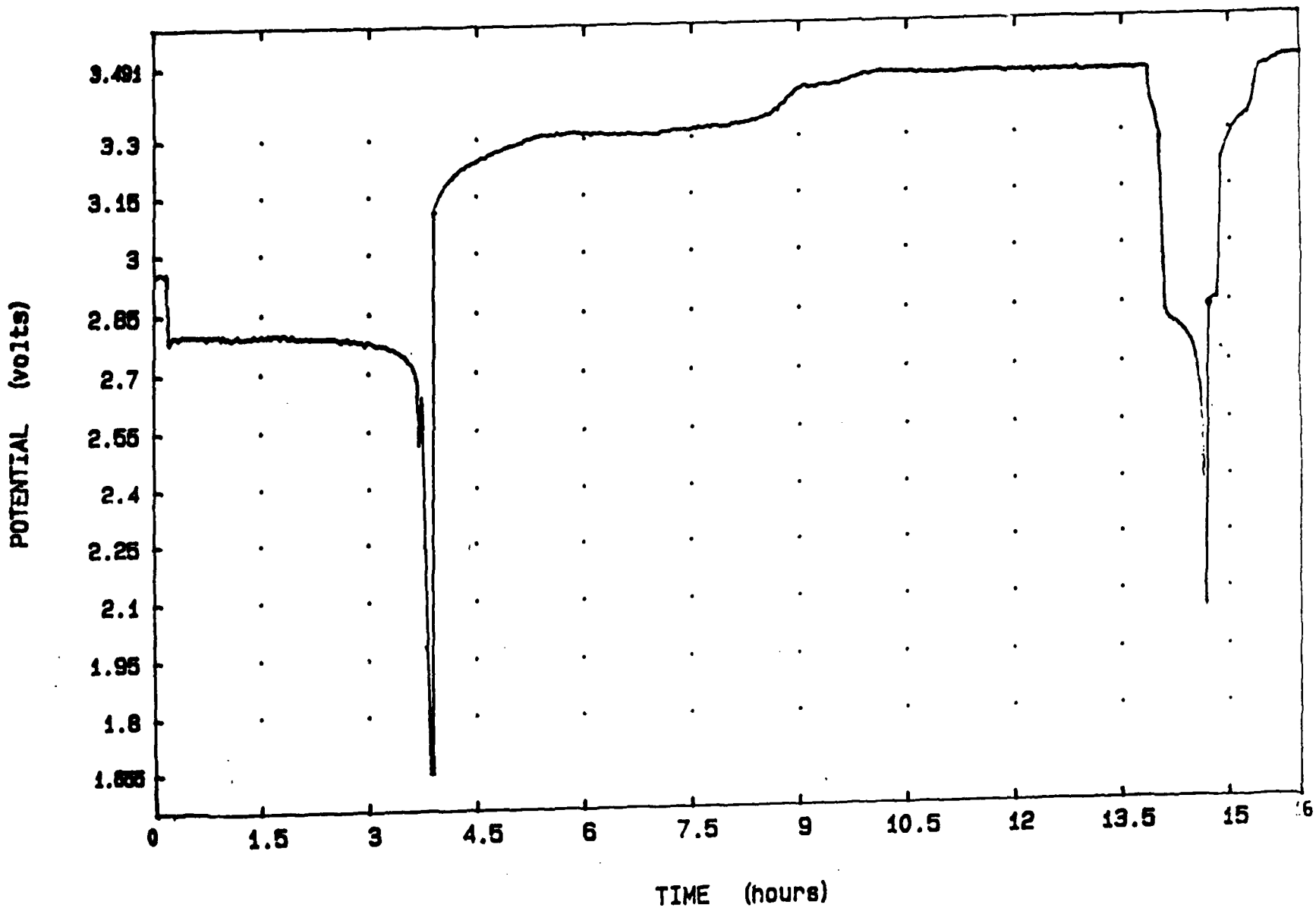

FIGURE 86. Cell 45-88-2. Discharge/ charge profile, potential versus time.
Electrolyte: 5M guanidine hydrobromide/ 0.7M LiBr
Positive: 23.7% Ketjenblack/ 71.2% acetylene black/ 5% Teflon binder; about 400 mg., on an anodized aluminum screen

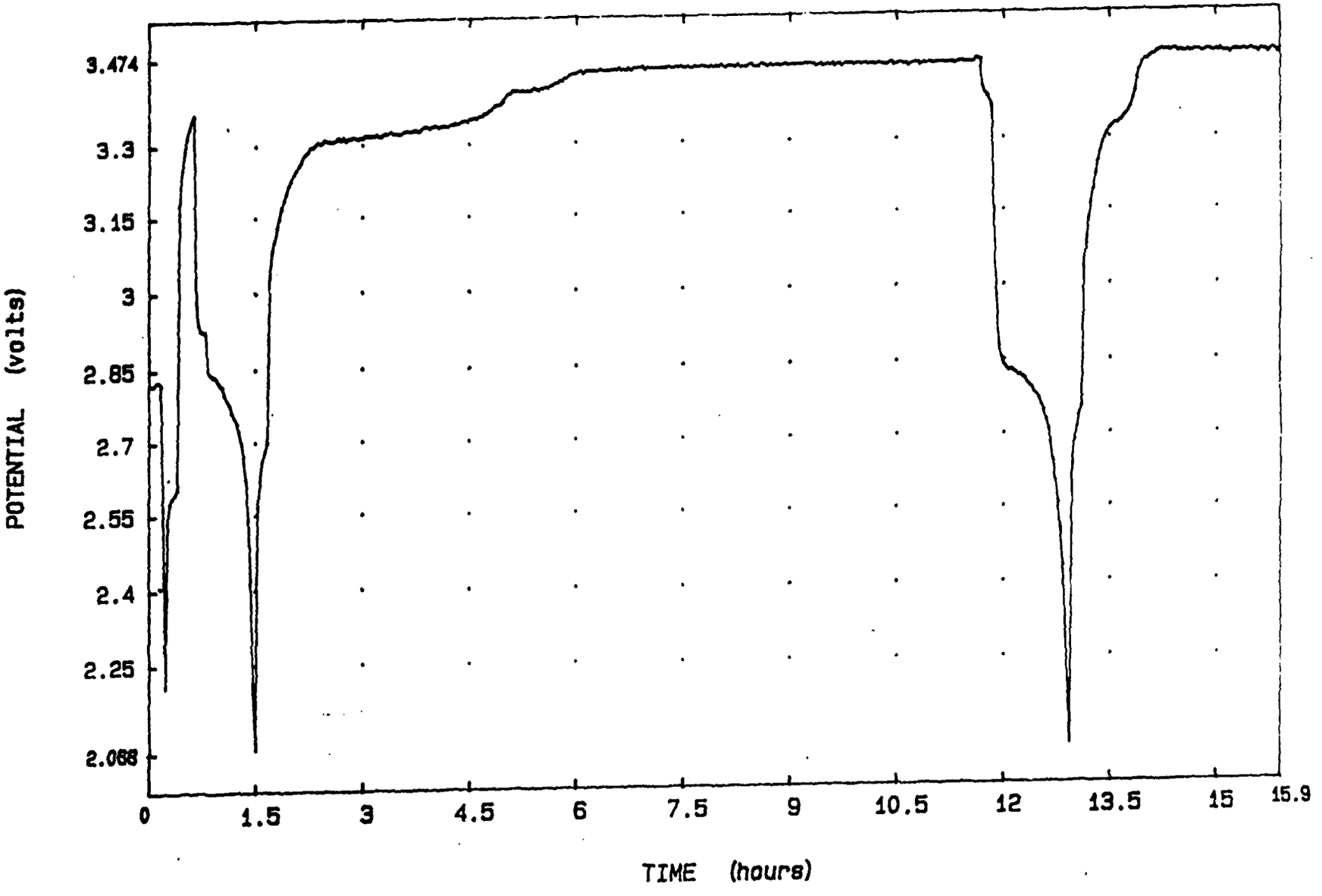

FIGURE 87. Cell 46-88-1. Discharge/ charge profile, potential versus time.
Electrolyte: 5M guanidine hydrobromide/ 0.7M LiBr
Positive: Painted; "Aquadag", 50/50 Aquadag/
Ketjenblack/ Aquadag; 116 cm^2; 350 mg, on anodized
aluminum foil.

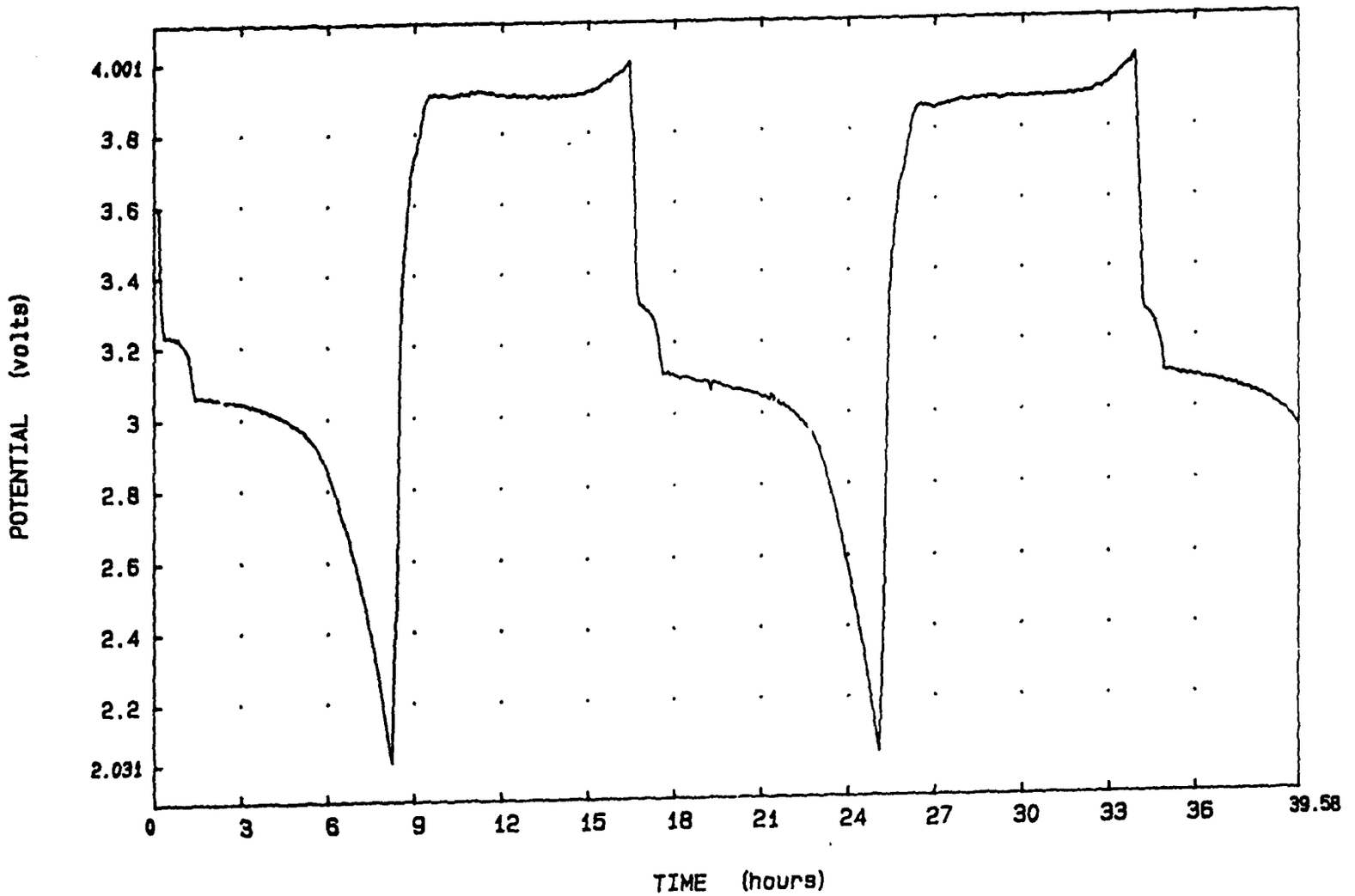

FIGURE 88. Discharge/charge profile, potential versus time, AA cell #50-15-3
Electrolyte: 2/1 (= dried $2LiCl \cdot CaCl_2 \cdot 4AlCl_3 \cdot 12SO_2$)
Positive electrode: 25Kj/75ab/10T
Charge/ discharge current: 1 mA/ cm^2 (50.8 mA).

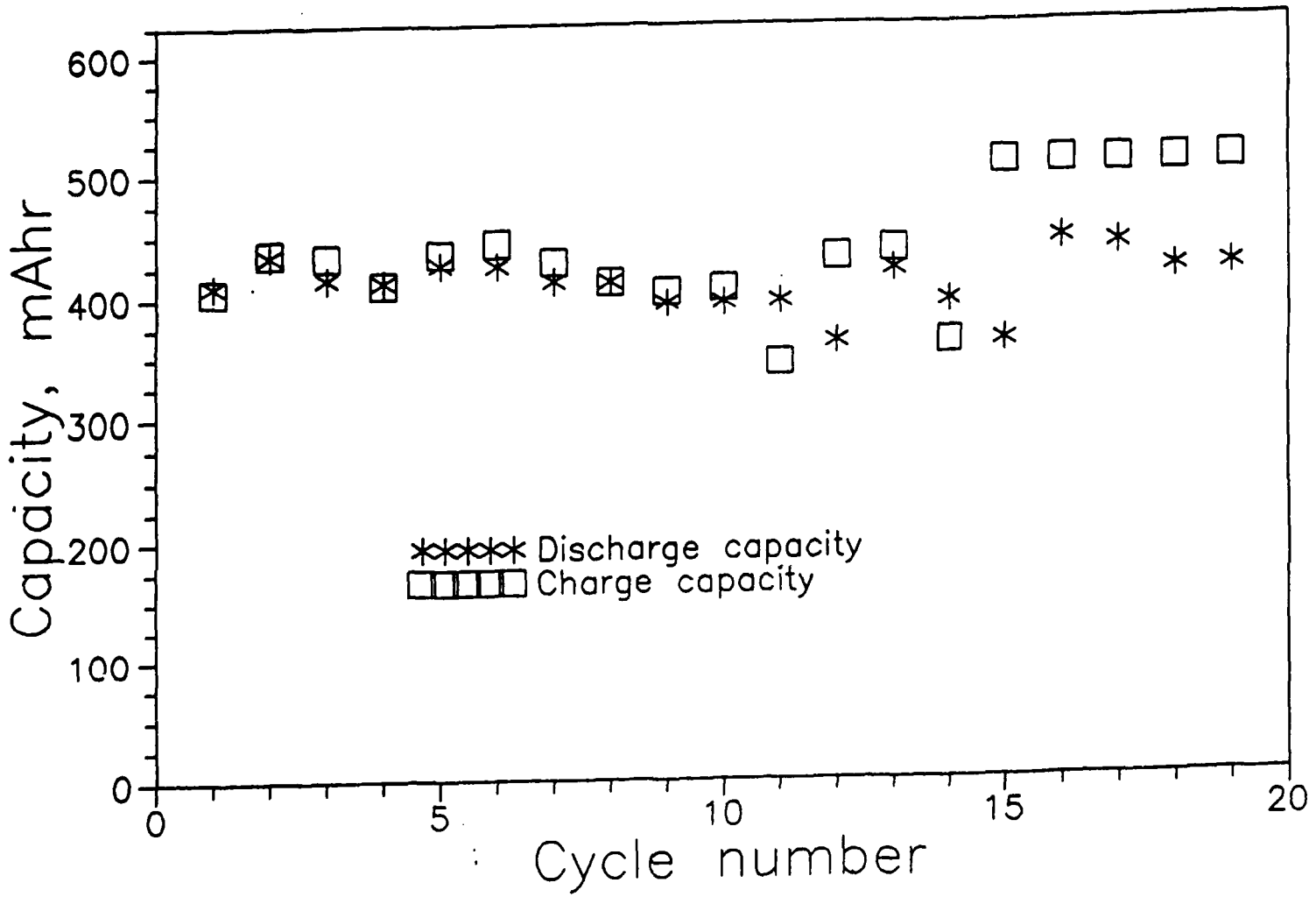

FIGURE 89. Capacity versus cycle number, AA cell #50-15-3
Electrolyte: 2/1 (≈ dried $2LiCl \cdot CaCl_2 \cdot 4AlCl_3 \cdot 12SO_2$)
Positive electrode: 25Kj/75ab/10T
Charge/ discharge current: 1 mA/ cm^2 (50.8 mA).
Charge cutoff potential limit: 4.0V; 4.1V at > cycle 14

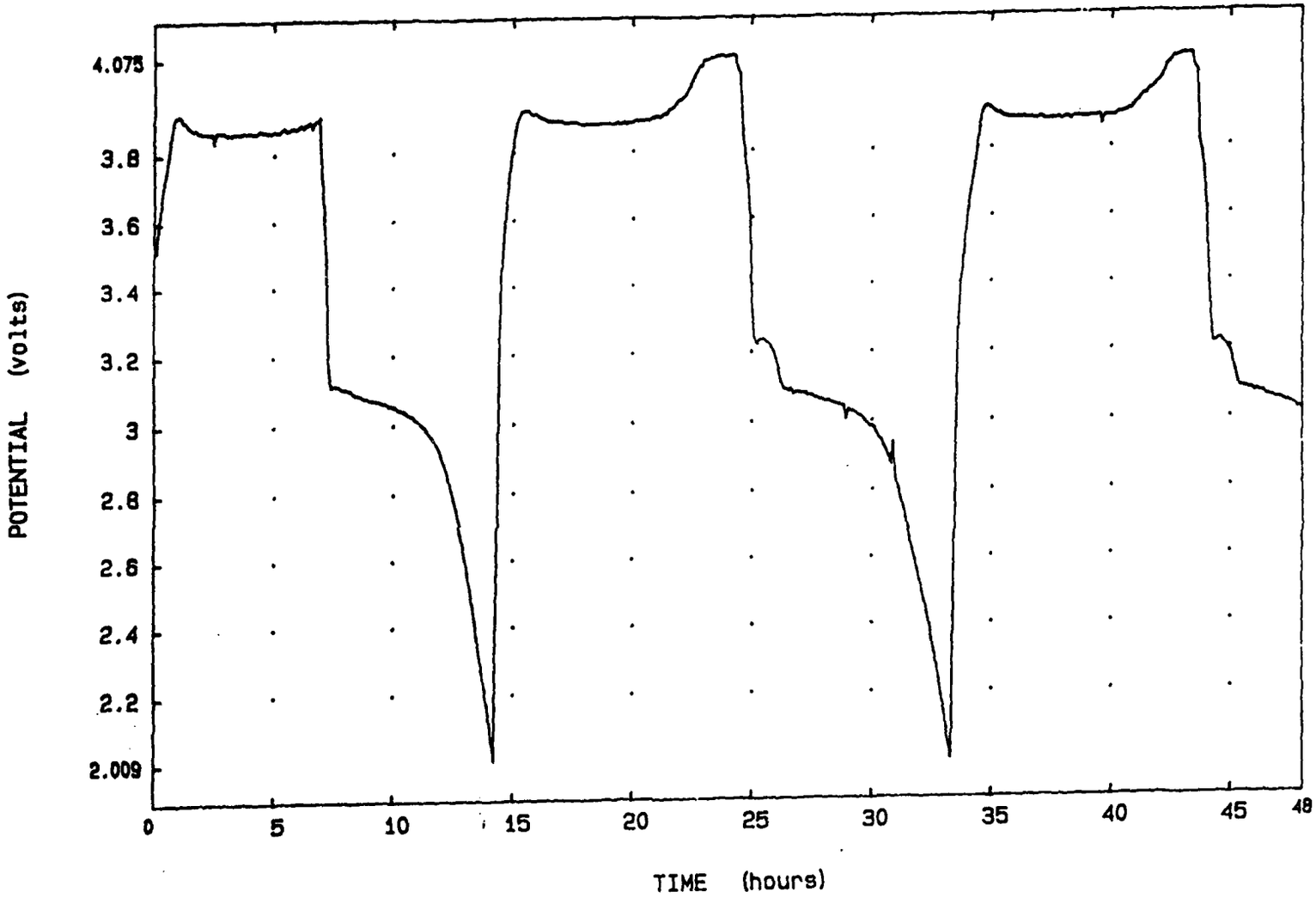

FIGURE 90. Discharge/charge profile, potential versus time, AA cell #50-15-3; cycles 15-16
Electrolyte: 2/1 (= dried $2LiCl \cdot CaCl_2 \cdot 4AlCl_3 \cdot 12SO_2$)
Positive electrode: 25Kj/75ab/10T
Charge/ discharge current: 1 mA/ cm^2 (50.8 mA).
Charge cutoff potential limit: 4.0V; 4.1V at ≥ cycle 14

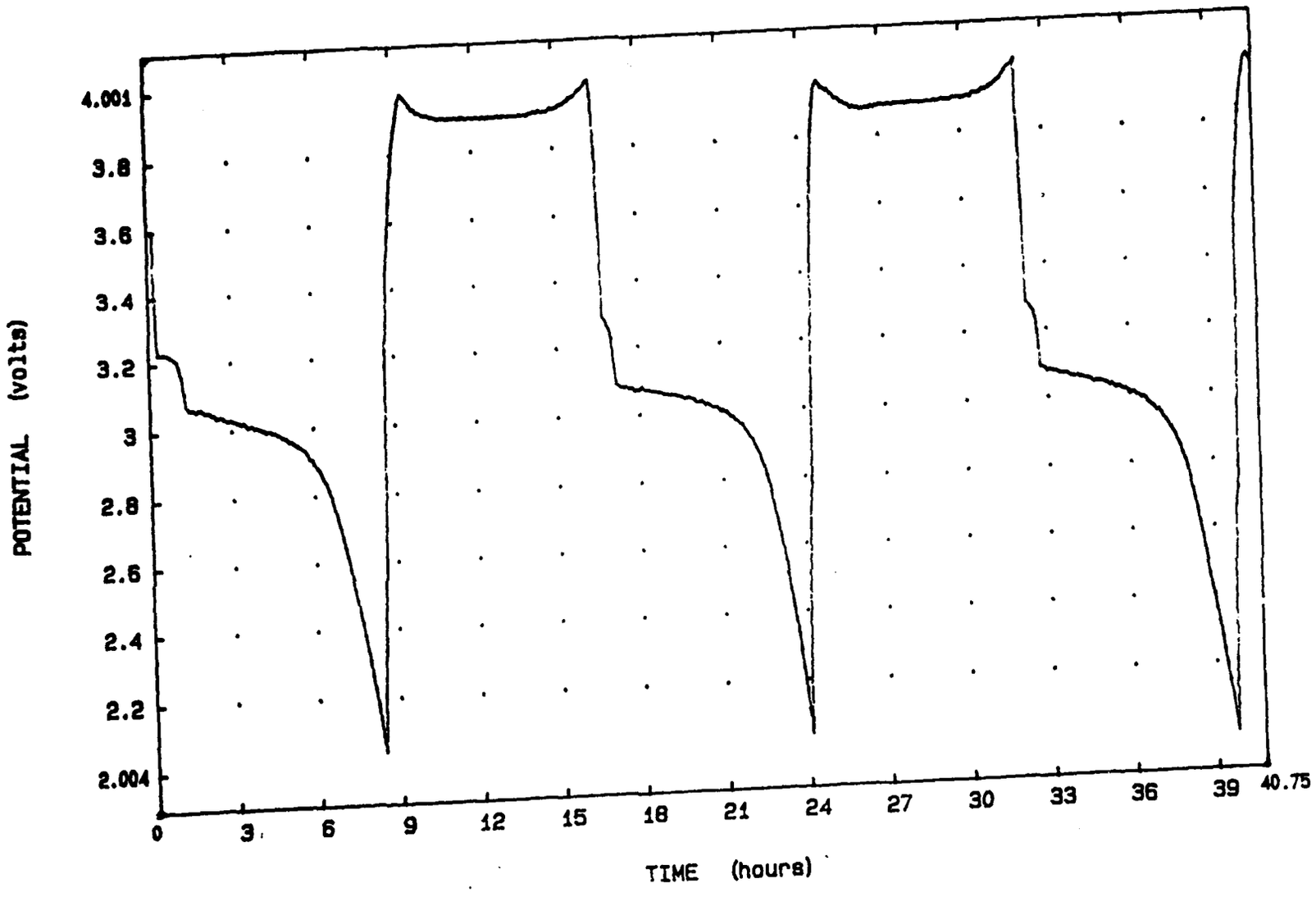

FIGURE 91. Discharge/charge profile, potential versus time, AA cell #45-79-3
Electrolyte: 3/1/1 (= dried $3LiCl \cdot CaCl_2 \cdot NaCl \cdot 6AlCl_3 \cdot 18SO_2$)
Positive electrode: 25Kj/75ab/10T
Charge/ discharge current: 1 mA/ cm^2 (50.8 mA).

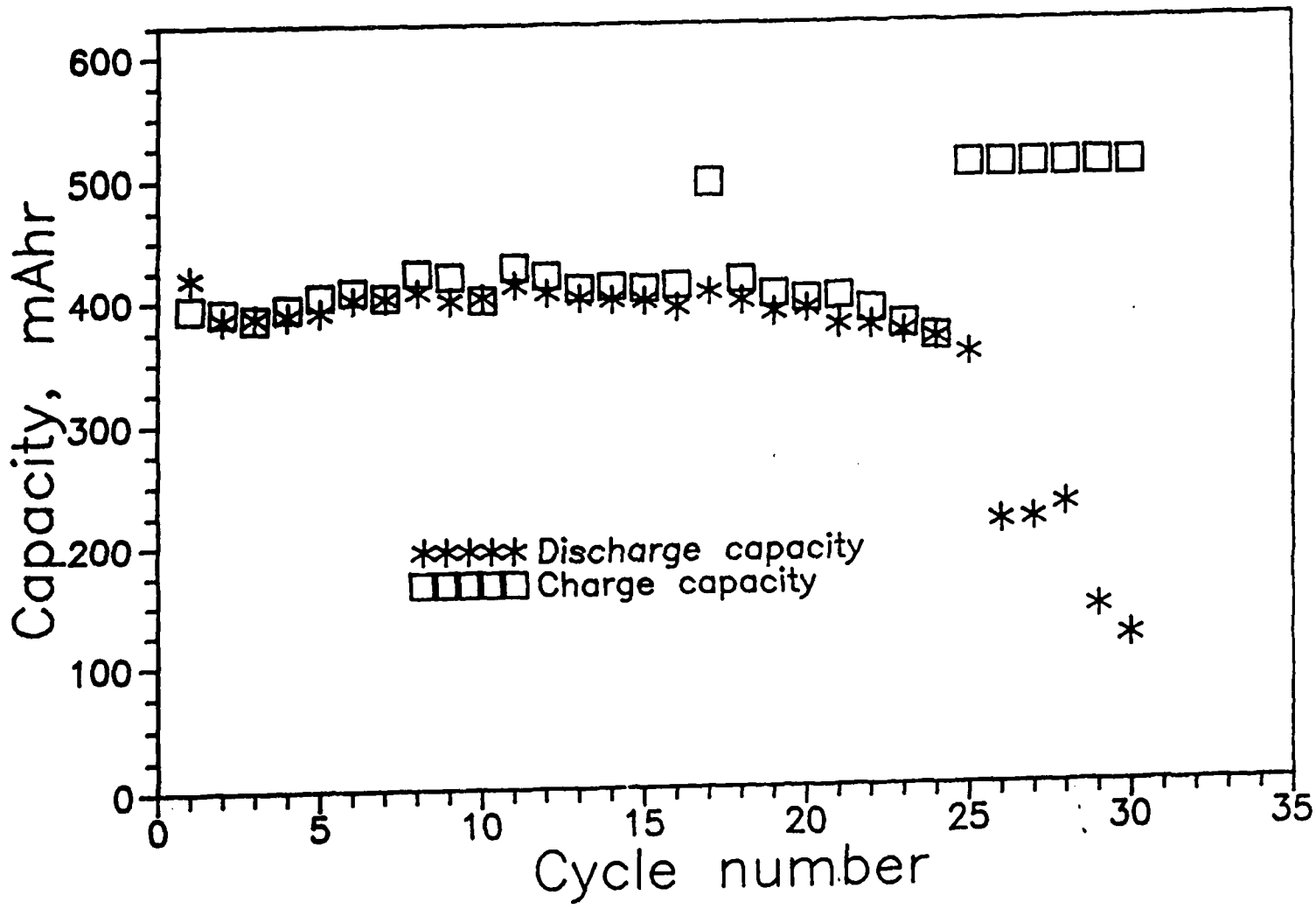

FIGURE 92. Capacity versus cycle number, AA cell #45-79-3
Electrolyte: 3/1/1 (= dried $3LiCl \cdot CaCl_2 \cdot NaCl \cdot 6AlCl_3 \cdot 18SO_2$)
Positive electrode: 25Kj/75ab/10T
Charge/ discharge current: 1 mA/ cm^2 (50.8 mA).
Charge cutoff potential limit: 4.0V only

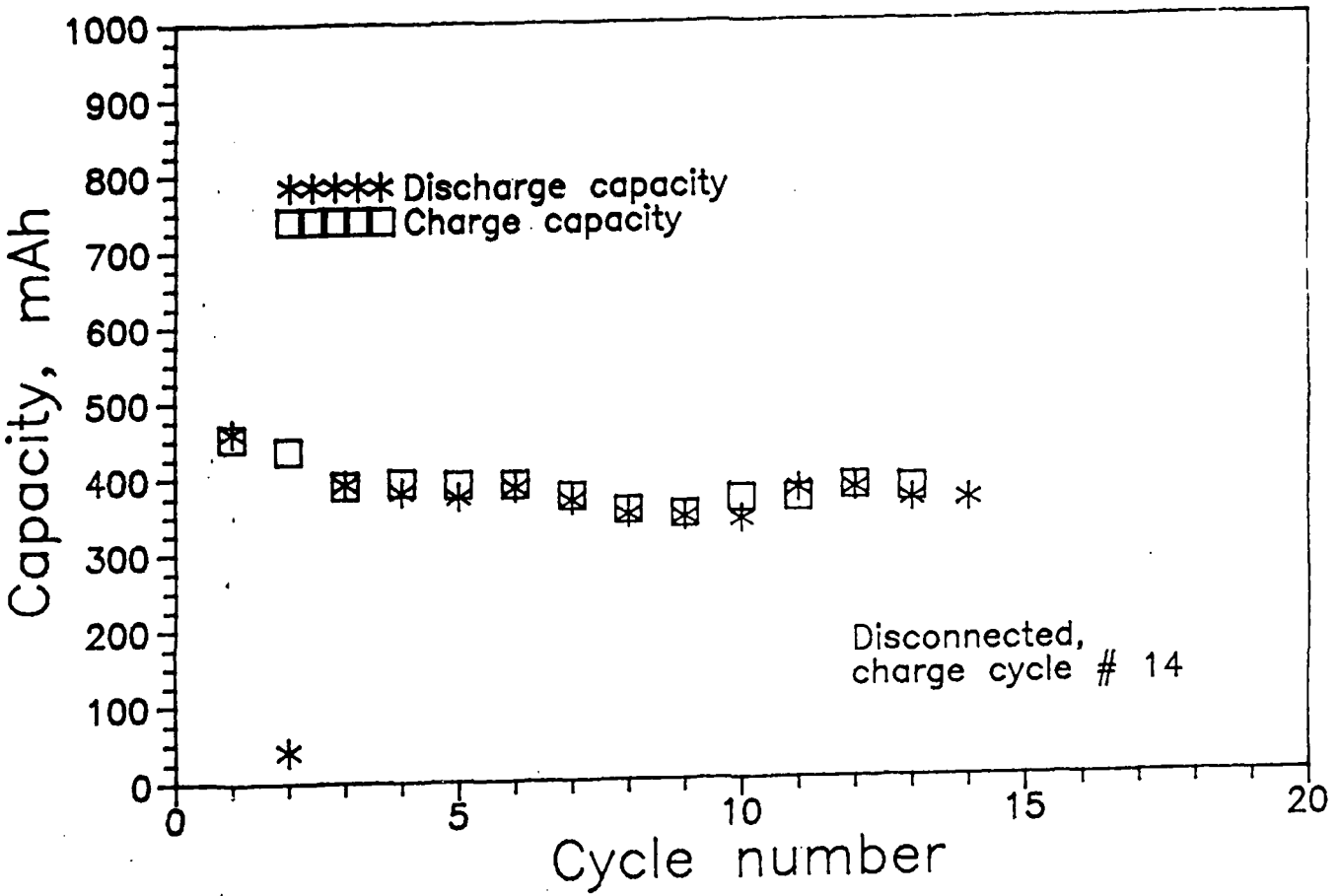

FIGURE 93. Discharge and Charge Capacities versus cycle number, AA cell #51-26-3.
Electrolyte: dried $LiCl \cdot CaCl_2 \cdot 4AlCl_3 \cdot 12SO_2$ (acid Electrolyte)
Positive electrode: 25Kj/75ab/10T (wet rolled)
Charge/ discharge current: 1 mA/ cm^2 (50.8 mA).

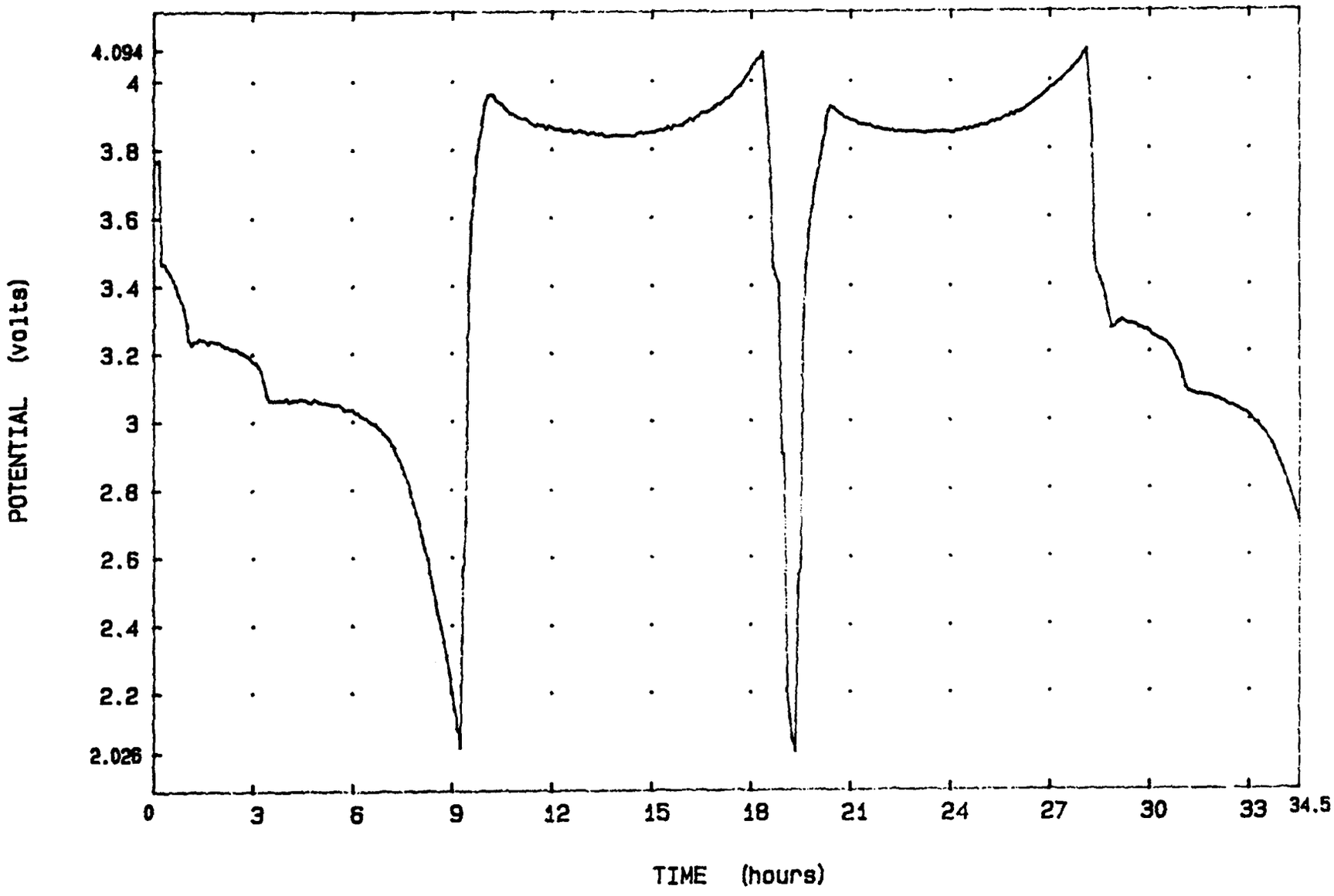

FIGURE 94. Discharge Profile, potential versus time
AA cell 51-26-3.
Electrolyte: dried $LiCl \cdot CaCl_2 \cdot 4AlCl_3 \cdot 12SO_2$ (acid electrolyte)
Positive electrode: 25Kj/75ab/10T (wet rolled)
Charge/ discharge current: 1 mA/ cm^2 (50.8 mA).

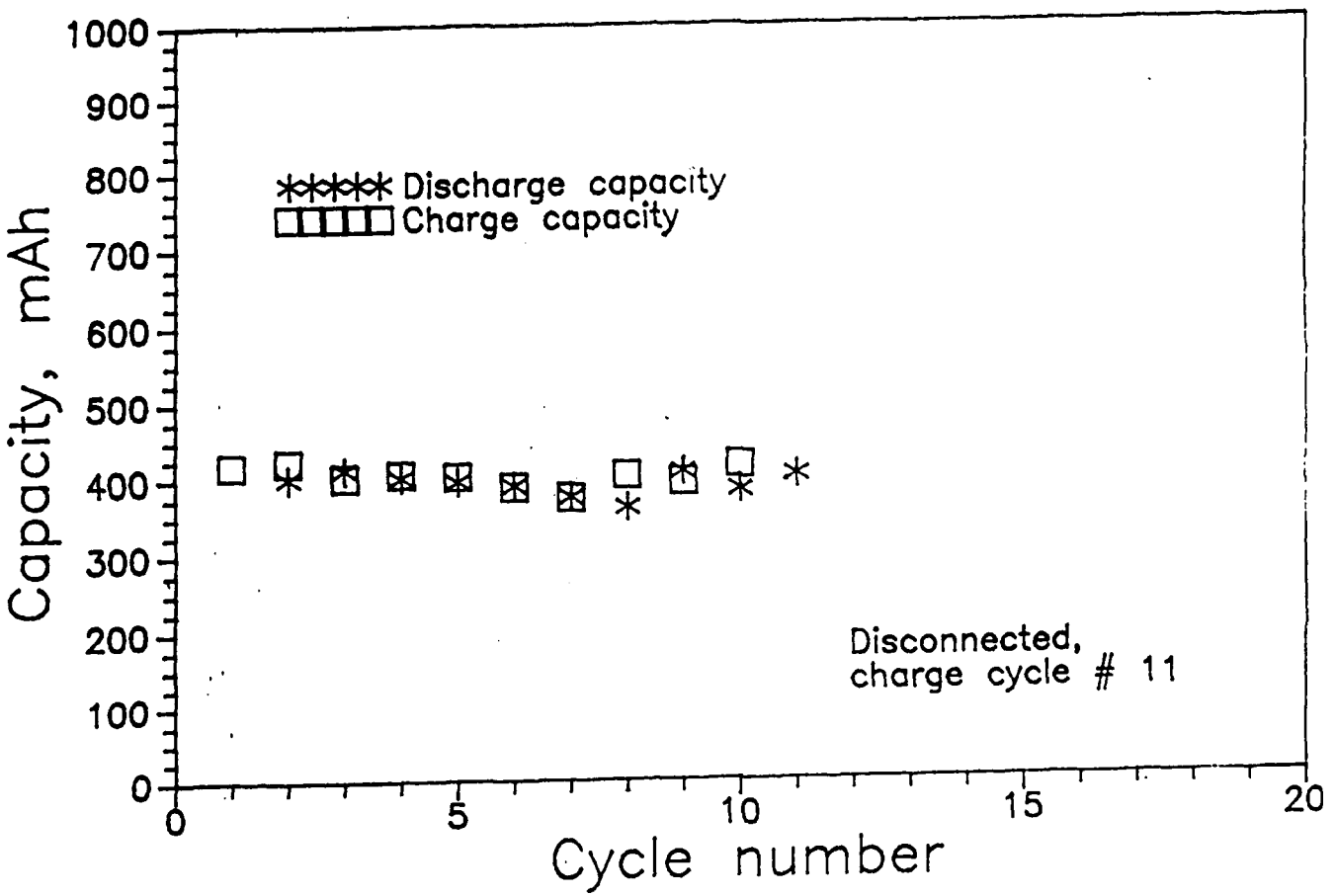

FIGURE 95. Discharge and Charge Capacities versus cycle number, AA cell #51-26-2.
Electrolyte: dried $2LiCl \cdot CaCl_2 \cdot 4AlCl_3 \cdot 12SO_2$
Positive electrode: 25Kj/75ab/10T (wet rolled)
Charge/ discharge current: 1 mA/ cm^2 (50.8 mA).

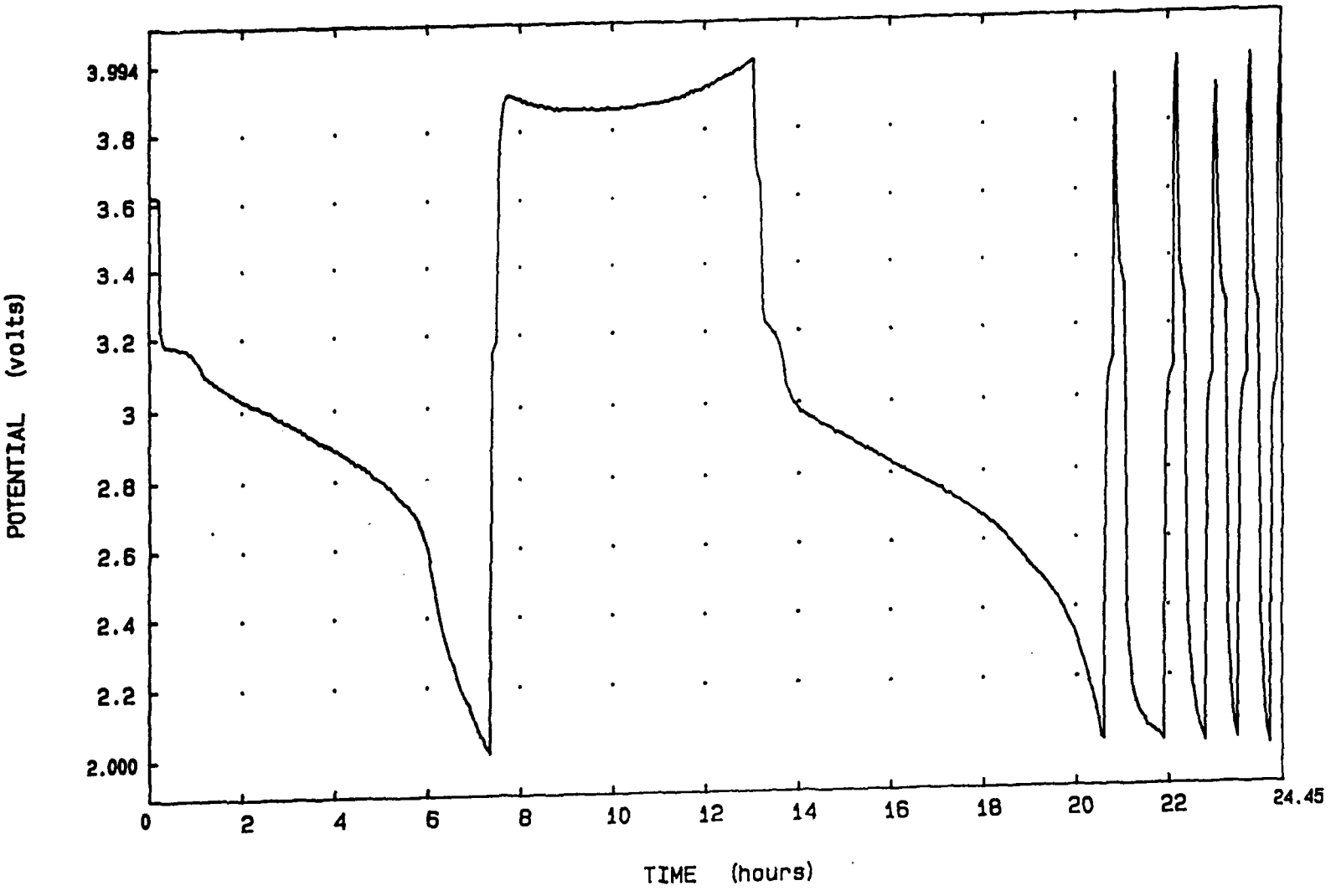

FIGURE 96. Discharge/charge profile, potential versus time, AA cell #45-94-1
Electrolyte: 2/1 (= dried $2LiCl \cdot CaCl_2 \cdot 4AlCl_3 \cdot 12SO_2$)
Positive electrode: 100Kj/5T
Charge/ discharge current: 1 mA/ cm^2 (50.8 mA).

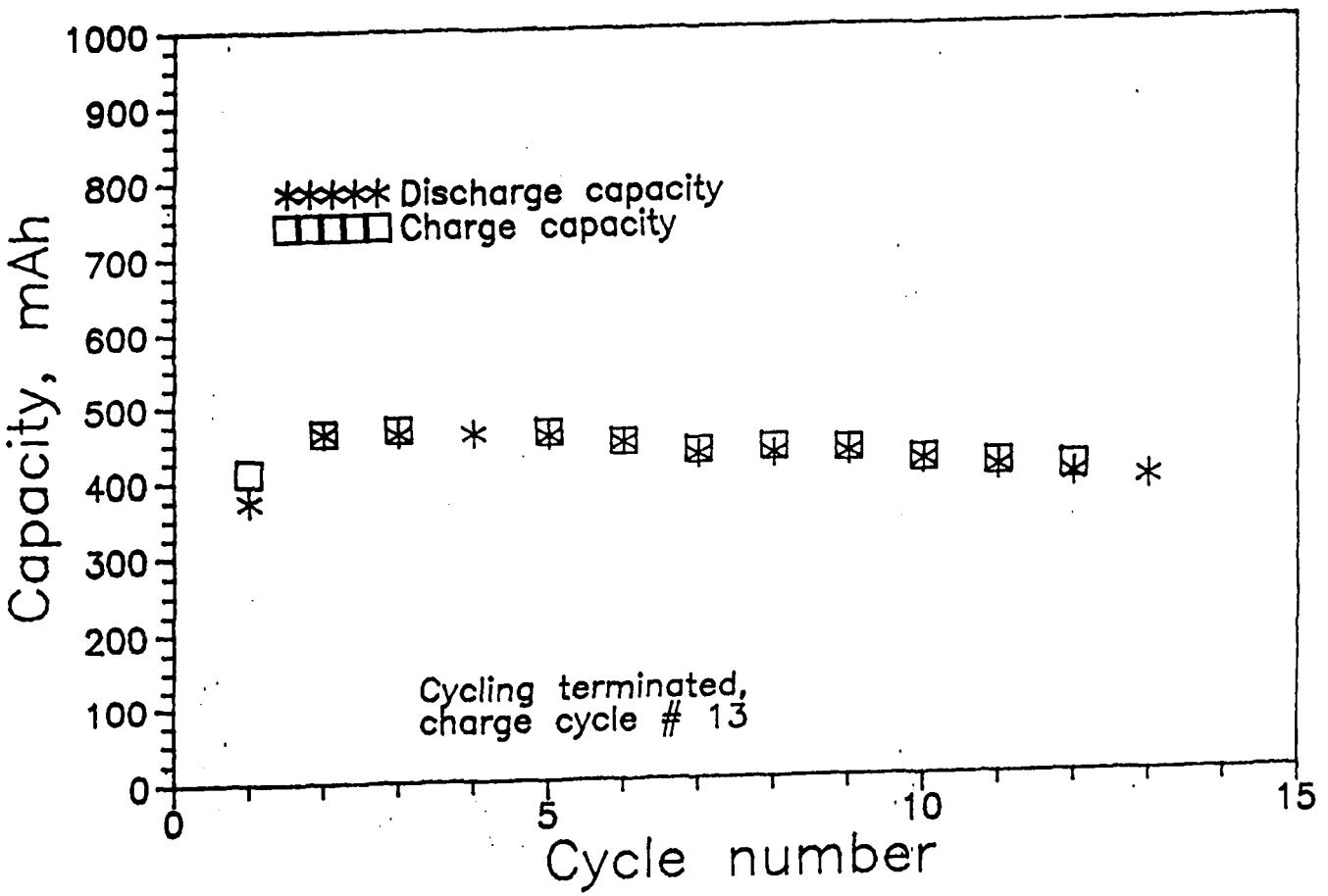

FIGURE 97. Discharge and Charge Capacities versus cycle number, AA cell #50-70-3.
Electrolyte: dried $2LiCl \cdot CaCl_2 \cdot 4AlCl_3 \cdot 12SO_2$
Positive electrode: 25Kj/75ab/10T
Charge/ discharge current: 1 mA/ cm^2 (50.8 mA).

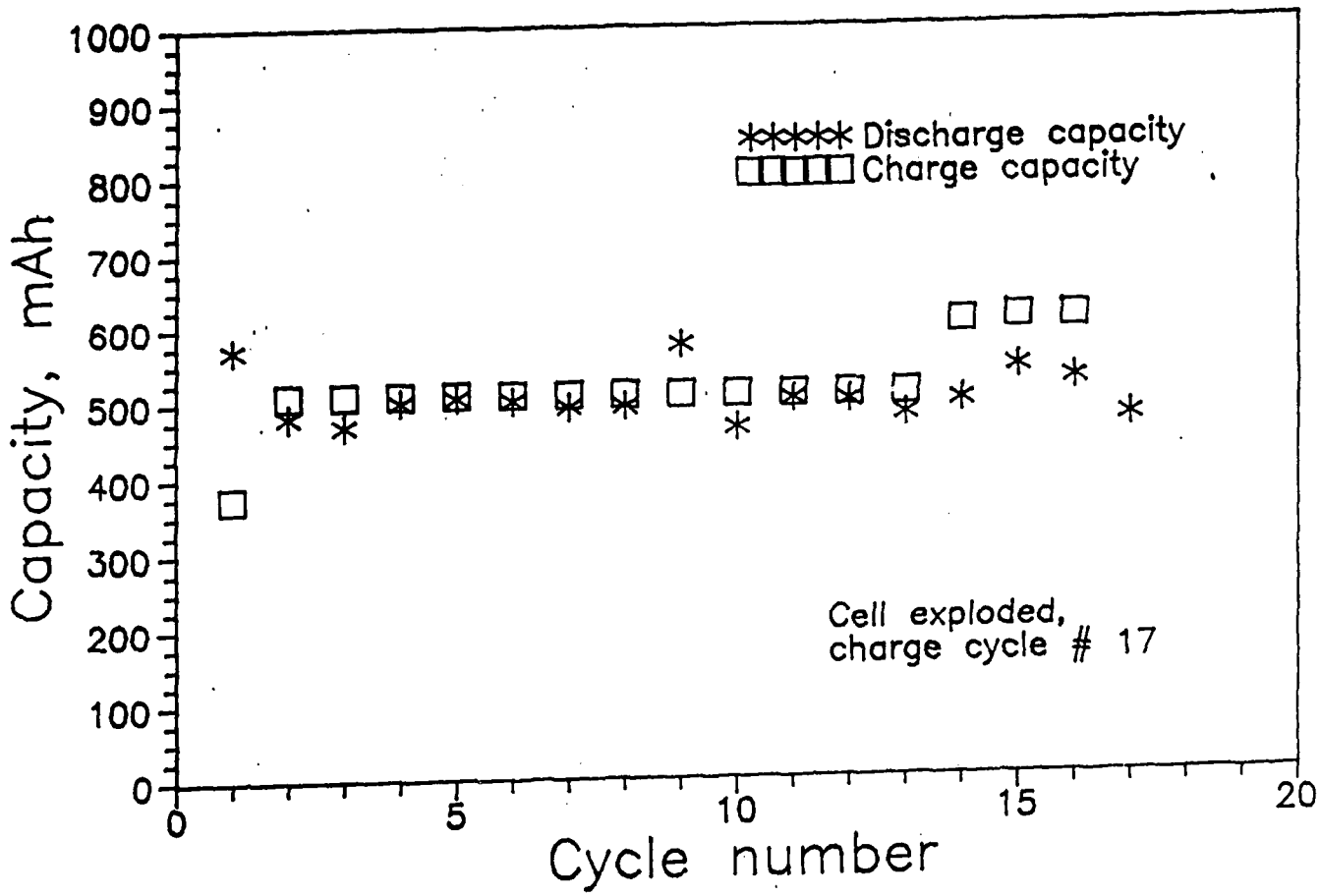

FIGURE 98. Discharge and Charge Capacities versus cycle number, AA cell #50-83-3.
Electrolyte: dried $2LiCl \cdot CaCl_2 \cdot 4AlCl_3 \cdot 12SO_2$
Positive electrode: 25D$_1$/25Kj/50ab/10T
Charge/ discharge current: 1 mA/ cm^2 (50.8 mA).

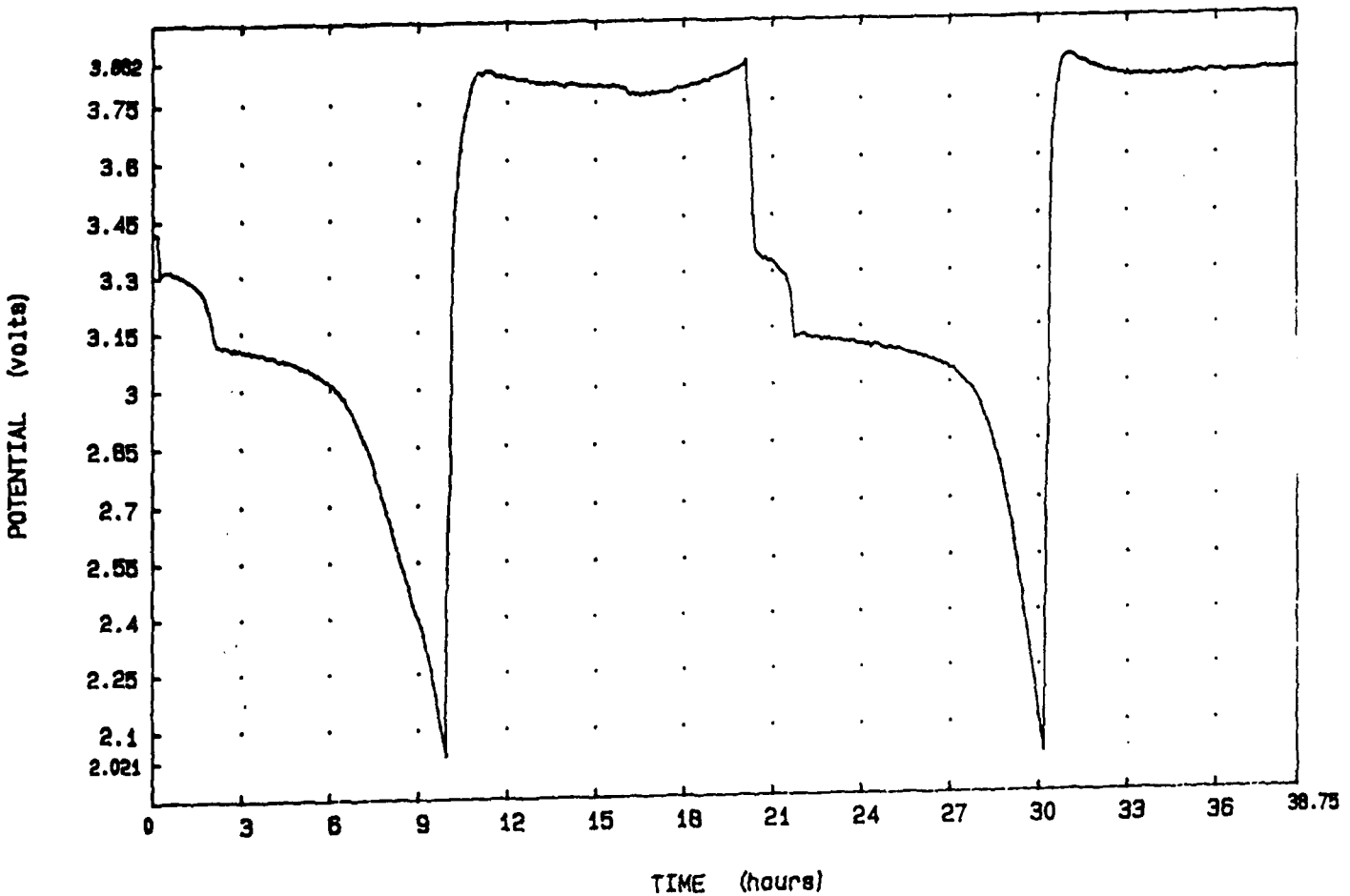

FIGURE 99. First two Discharge/ Charge Profiles, potential versus time, AA cell #56-2-1.
Electrolyte: dried $2LiCl \cdot CaCl_2 \cdot 4AlCl_3 \cdot 12SO_2$
Positive electrode: 25N/25Kj/50ab/10T
Charge/ discharge current: 1 mA/ cm^2 (50.8 mA).

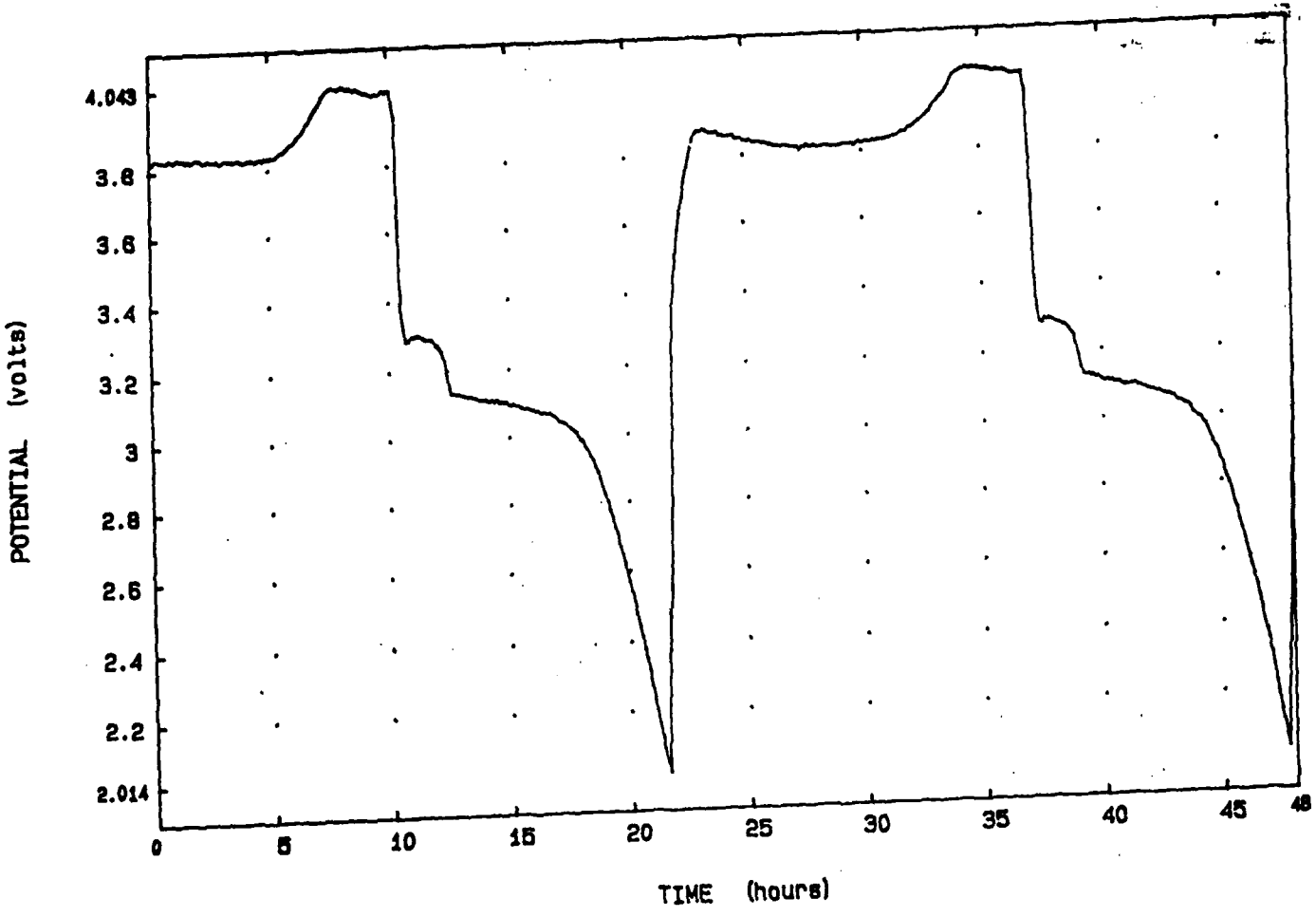

FIGURE 100. Discharge/ Charge Profiles #10 and 11 for AA cell #56-2-1, showing overcharge. Potential versus time.
Electrolyte: dried $2LiCl \cdot CaCl_2 \cdot 4AlCl_3 \cdot 12SO_2$
Positive electrode: 25N/25Kj/50ab/10T
Charge/ discharge current: 1 mA/ cm^2 (50.8 mA).

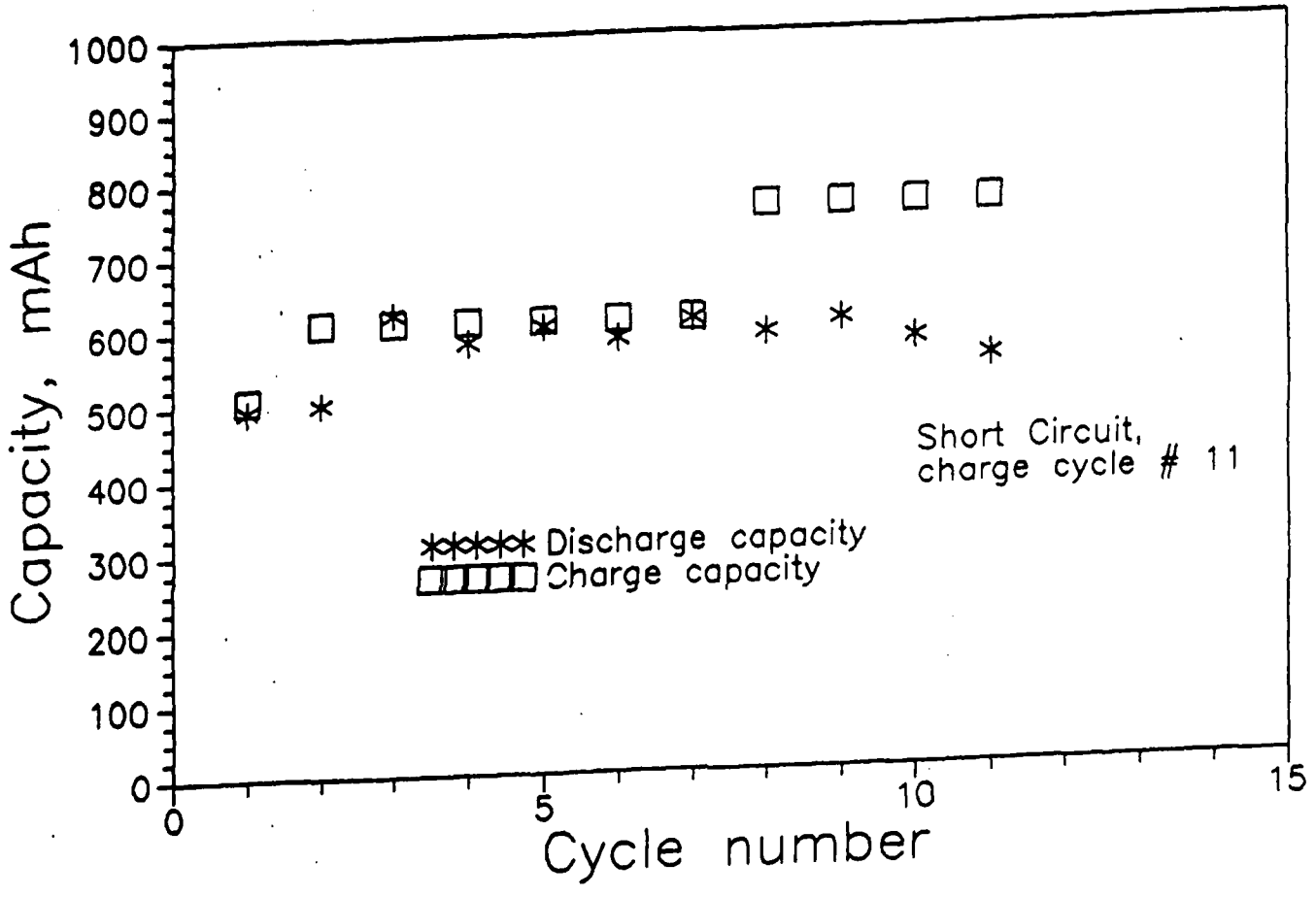

FIGURE 101. Discharge and Charge Capacities versus cycle number, AA cell #56-2-1.
Electrolyte: dried $2LiCl \cdot CaCl_2 \cdot 4AlCl_3 \cdot 12SO_2$
Positive electrode: 25N/25Kj/50ab/10T
Charge/ discharge current: 1 mA/ cm^2 (50.8 mA).

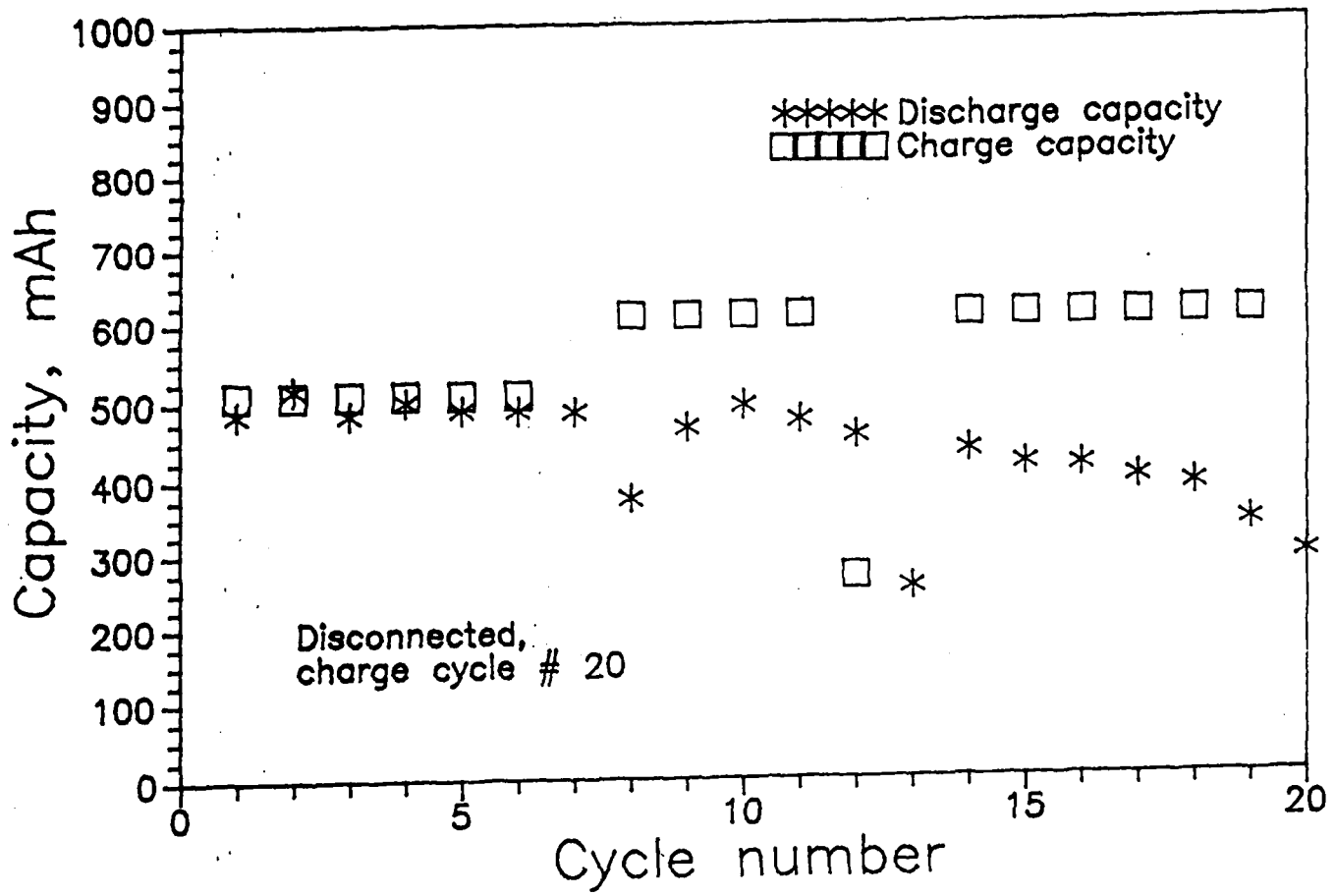

FIGURE 102. Discharge and Charge Capacities versus cycle number, AA cell #56-27-11.
Electrolyte: dried $2LiCl \cdot CaCl_2 \cdot 4AlCl_3 \cdot 12SO_2$
Positive electrode: $50D_1/25Kj/25ab/10T$
Charge/ discharge current: 1 mA/ cm^2 (50.8 mA).

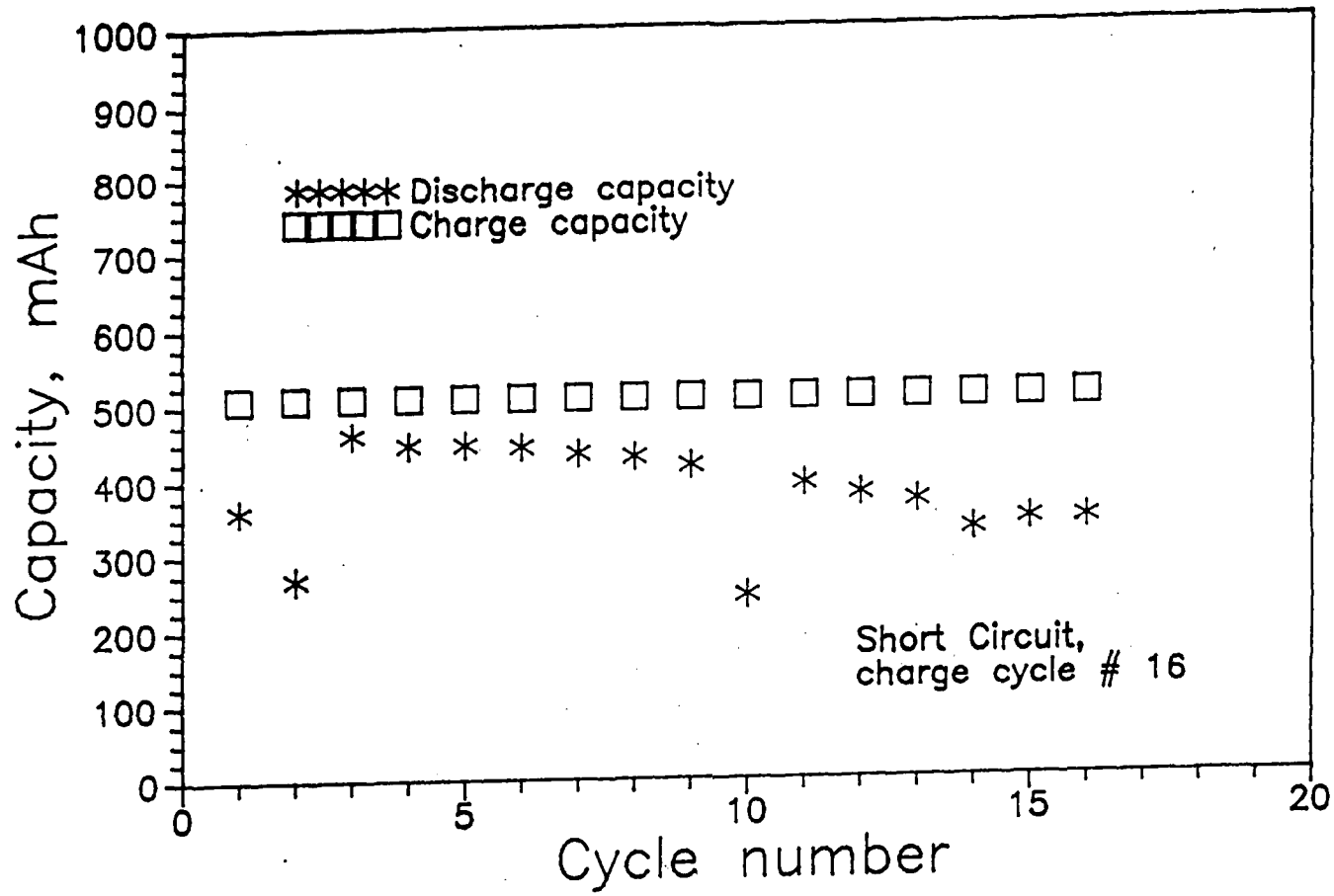

FIGURE 103. Discharge and Charge Capacities versus cycle number, AA cell #51-26-1.
Electrolyte: dried $2LiCl \cdot CaCl_2 \cdot 4AlCl_3 \cdot 12SO_2$
Positive electrode: 25Kj/75ab/10T (wr)
Charge/ discharge current: 1 mA/ cm^2 (50.8 mA).

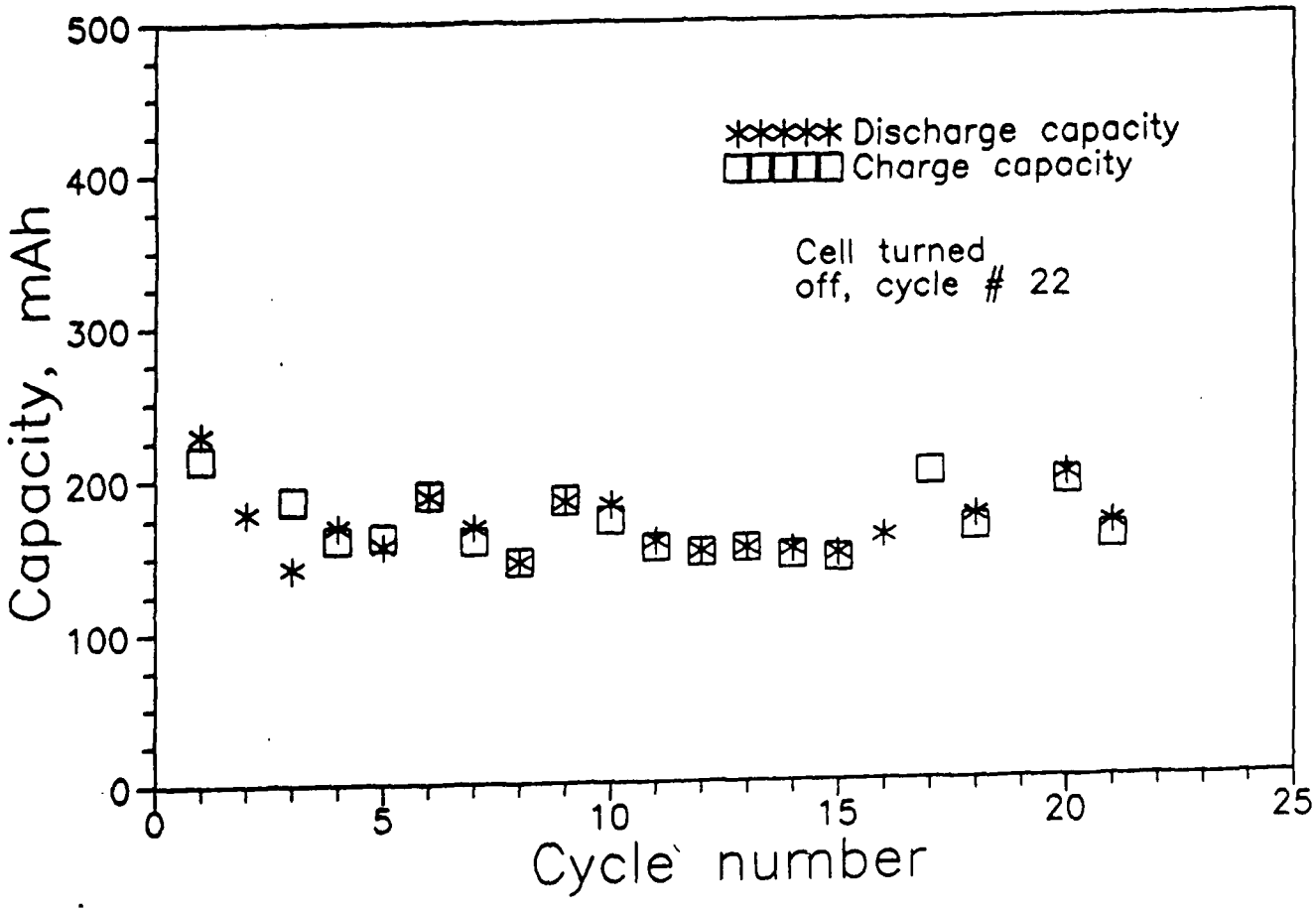

FIGURE 104. Discharge and Charge Capacities versus cycle number, AA cell #51-30-1.
Electrolyte: dried $2LiCl \cdot CaCl_2 \cdot 4AlCl_3 \cdot 12SO_2$
Positive electrode: 100ab/3T; annular bobbin
Charge/ discharge current: 1 mA/ cm^2 (50.8 mA).

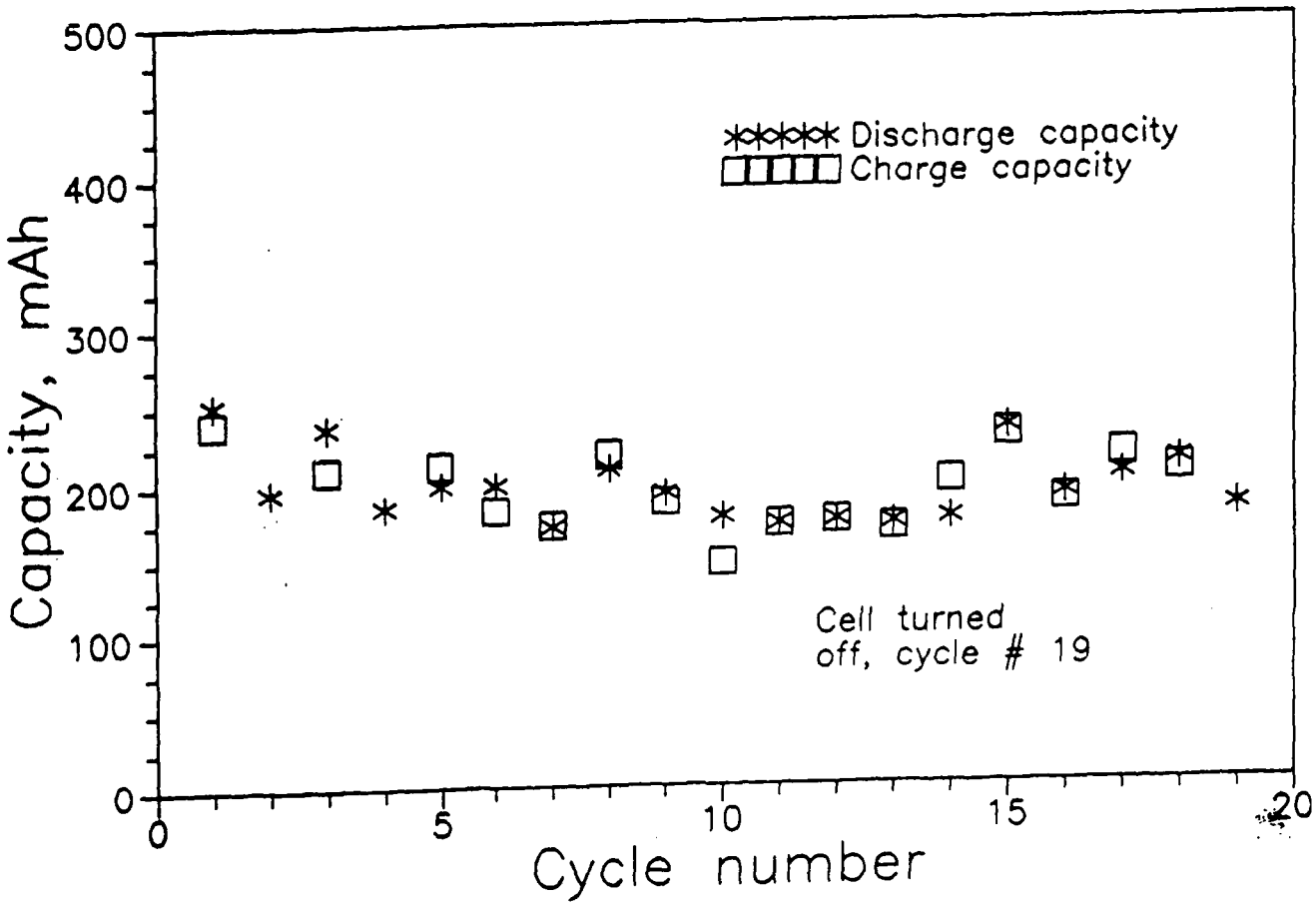

FIGURE 105. Discharge and Charge Capacities versus cycle number, AA cell #51-30-2.
Electrolyte: dried $2LiCl \cdot CaCl_2 \cdot 4AlCl_3 \cdot 12SO_2$
Positive electrode: 100ab/3T; annular bobbin
Charge/ discharge current: 1 mA/ cm^2 (50.8 mA).

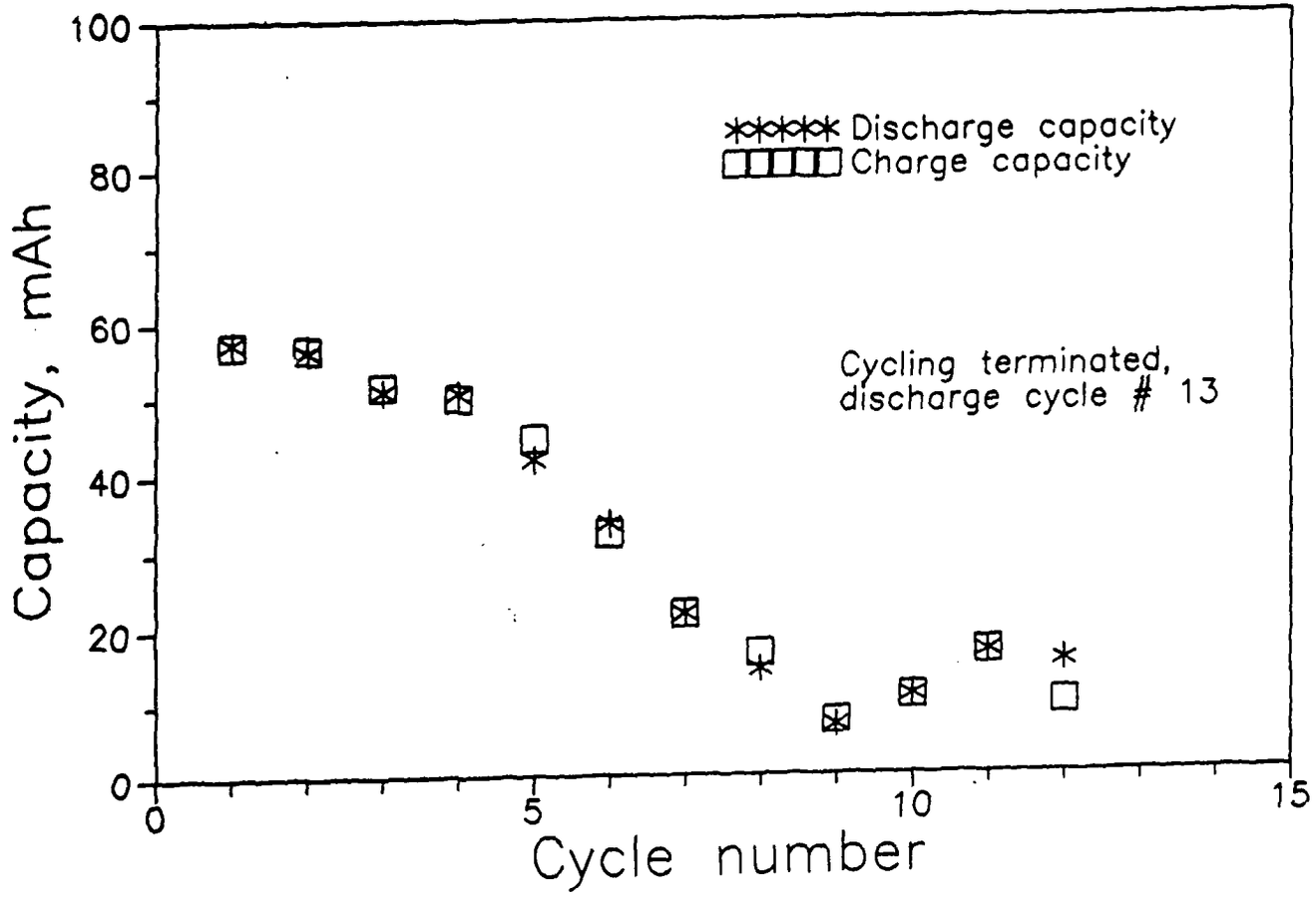

FIGURE 106. Discharge and Charge Capacities versus cycle number, AA cell #51-37-2.
Electrolyte: dried $2LiCl \cdot CaCl_2 \cdot 4AlCl_3 \cdot 12SO_2$
Positive electrode: 25Kj/75ab/10T (wr); flooded (7.26 cm^2)
Charge/ discharge current: 1 mA/ cm^2 (50.8 mA).

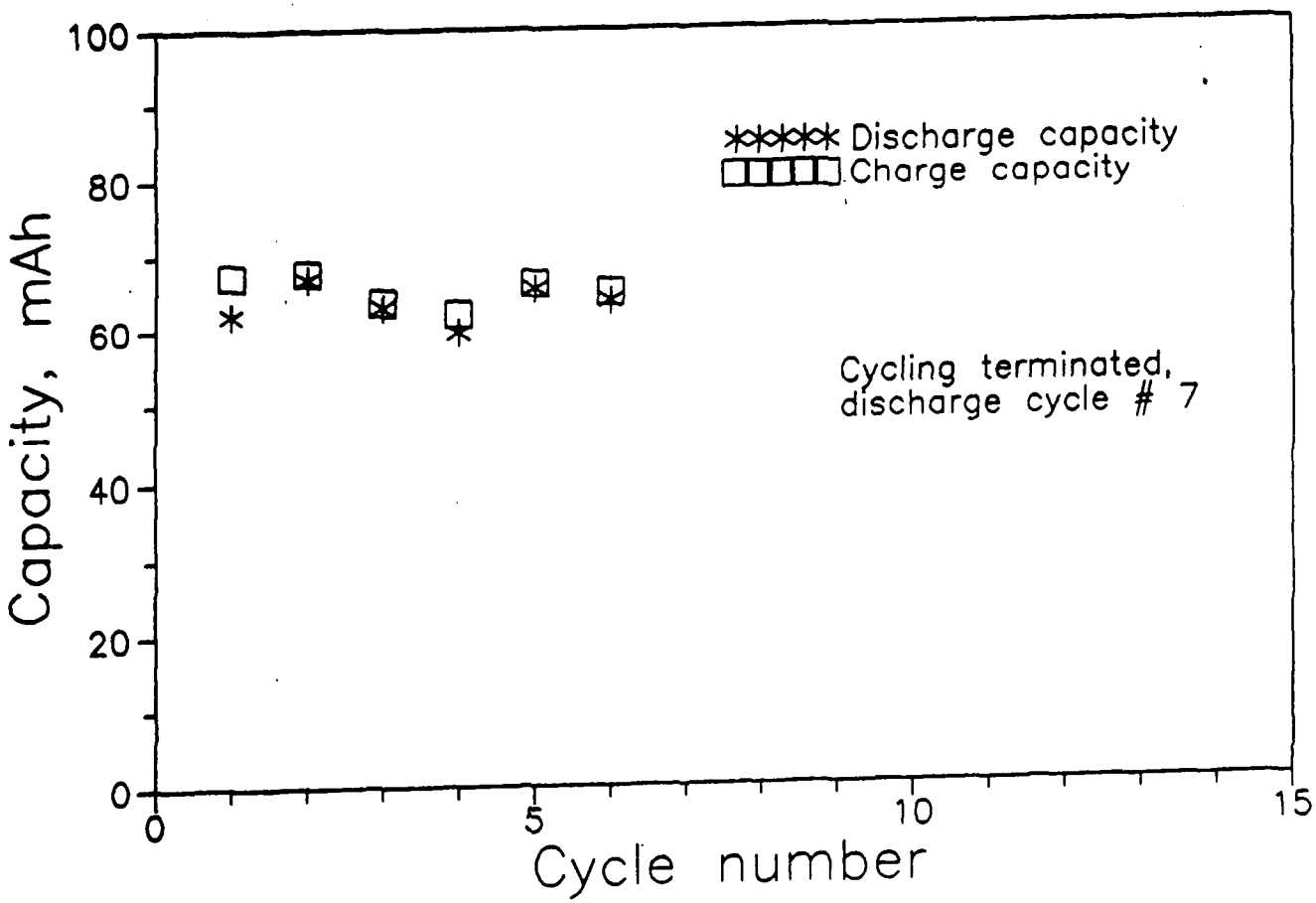

FIGURE 107. Discharge and Charge Capacities versus cycle number, AA cell #51-37-3.
Electrolyte: dried $2LiCl \cdot CaCl_2 \cdot 4AlCl_3 \cdot 12SO_2$
Positive electrode: 25Kj/75ab/10T (wr); flooded (7.26 cm^2)
Charge/ discharge current: 1 mA/ cm^2 (50.8 mA).

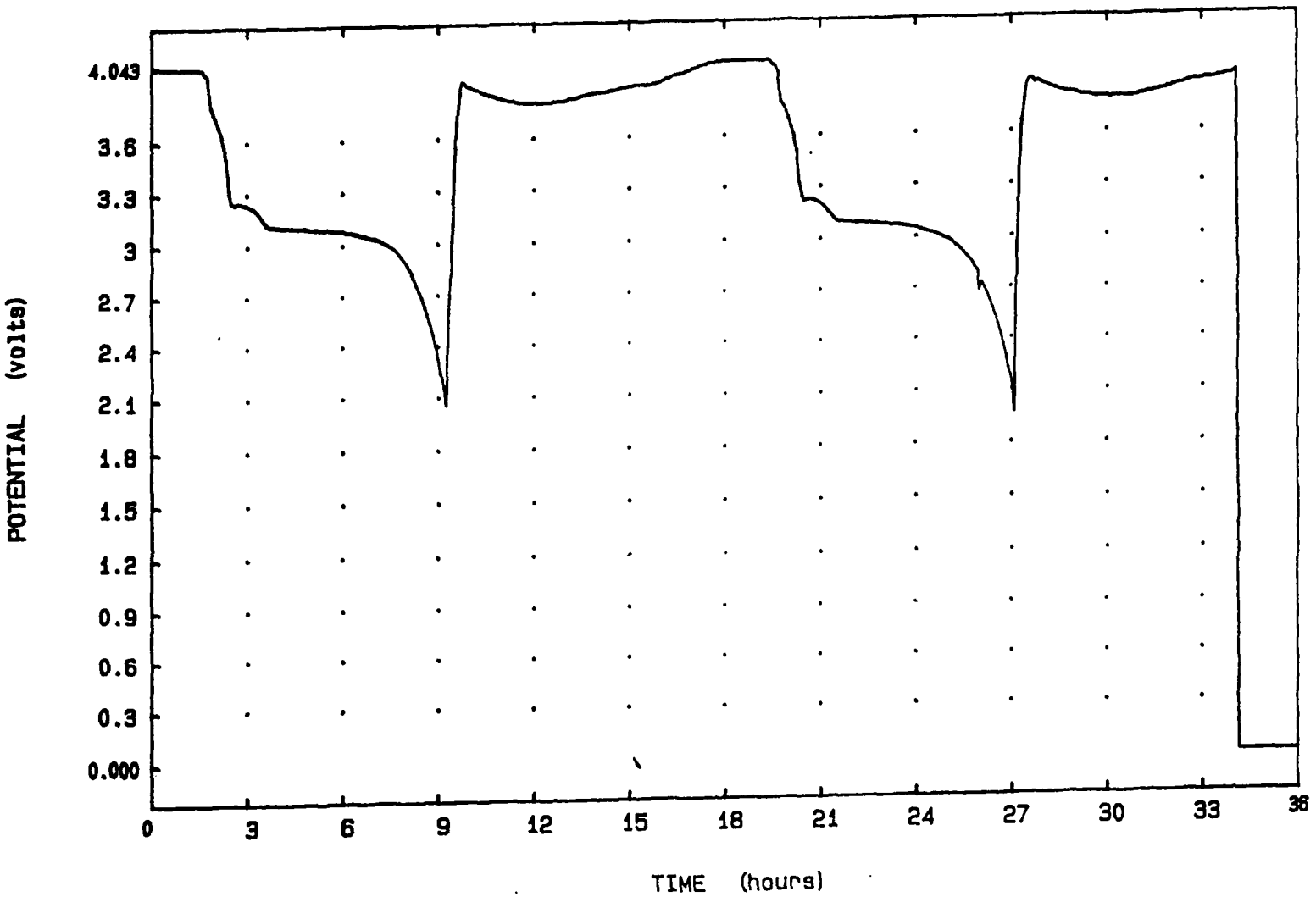

FIGURE 108. Discharge/charge profile, potential versus time, AA cell #50-41-4
Electrolyte: 2/1 (= dried $2LiCl \cdot CaCl_2 \cdot 4AlCl_3 \cdot 12SO_2$)
Positive electrode: 25Kj/75ab/10T/pore former
Charge/ discharge current: 1 mA/ cm^2 (50.8 mA).
Discharge/ charge cycles 16 and 17 (cell exploded during charge cycle #17).

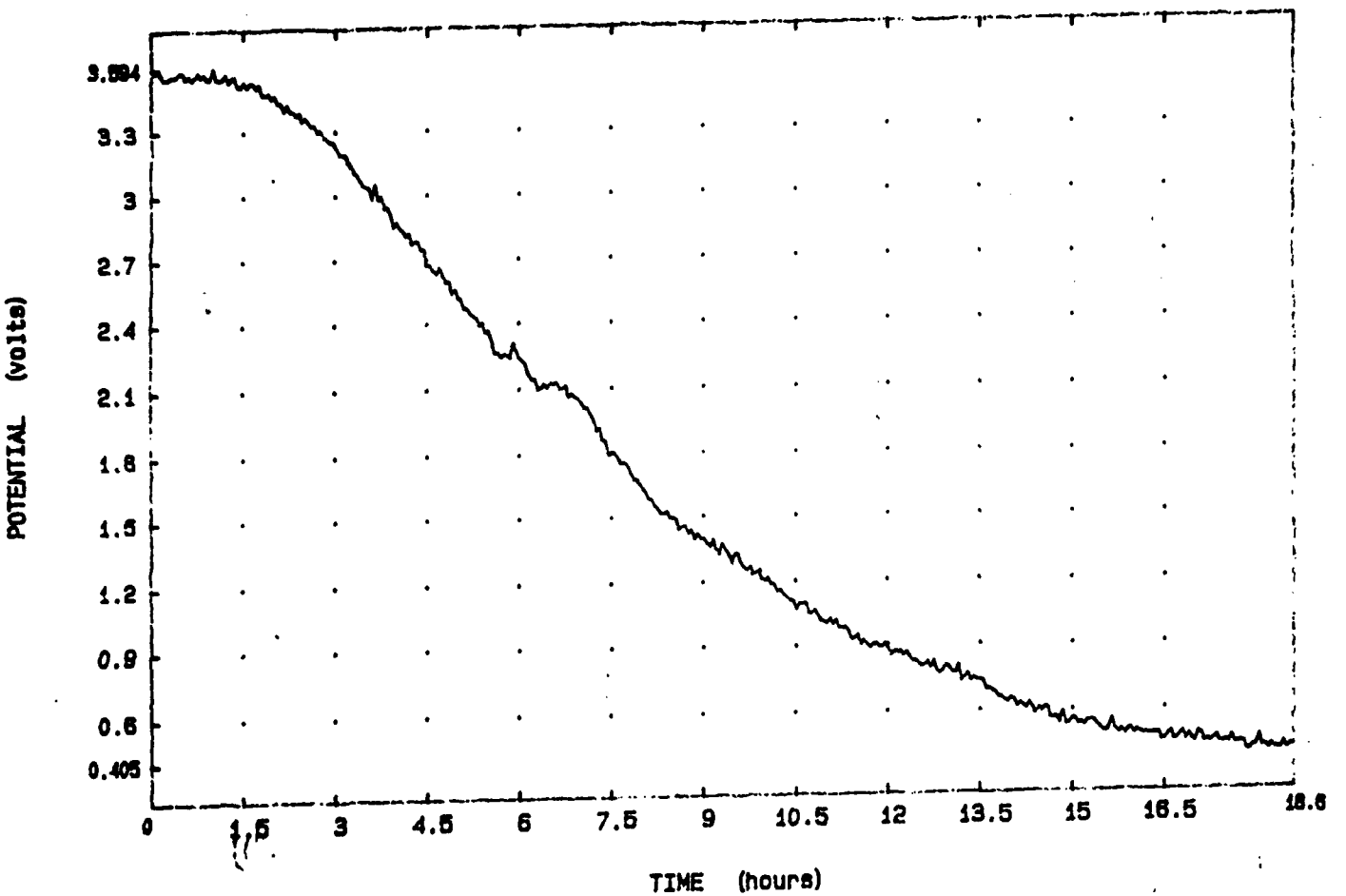

FIGURE 109. Discharge Profile, potential versus time, cathode versus anode, AA cell #55-3-1
Electrolyte: 15% Br_2/ 2M LiBr·$AlCl_3$/ CH_2ClCCl_O
Positive electrode: 25Kj/75ab/10T
Discharge constant load: 100 ohms.

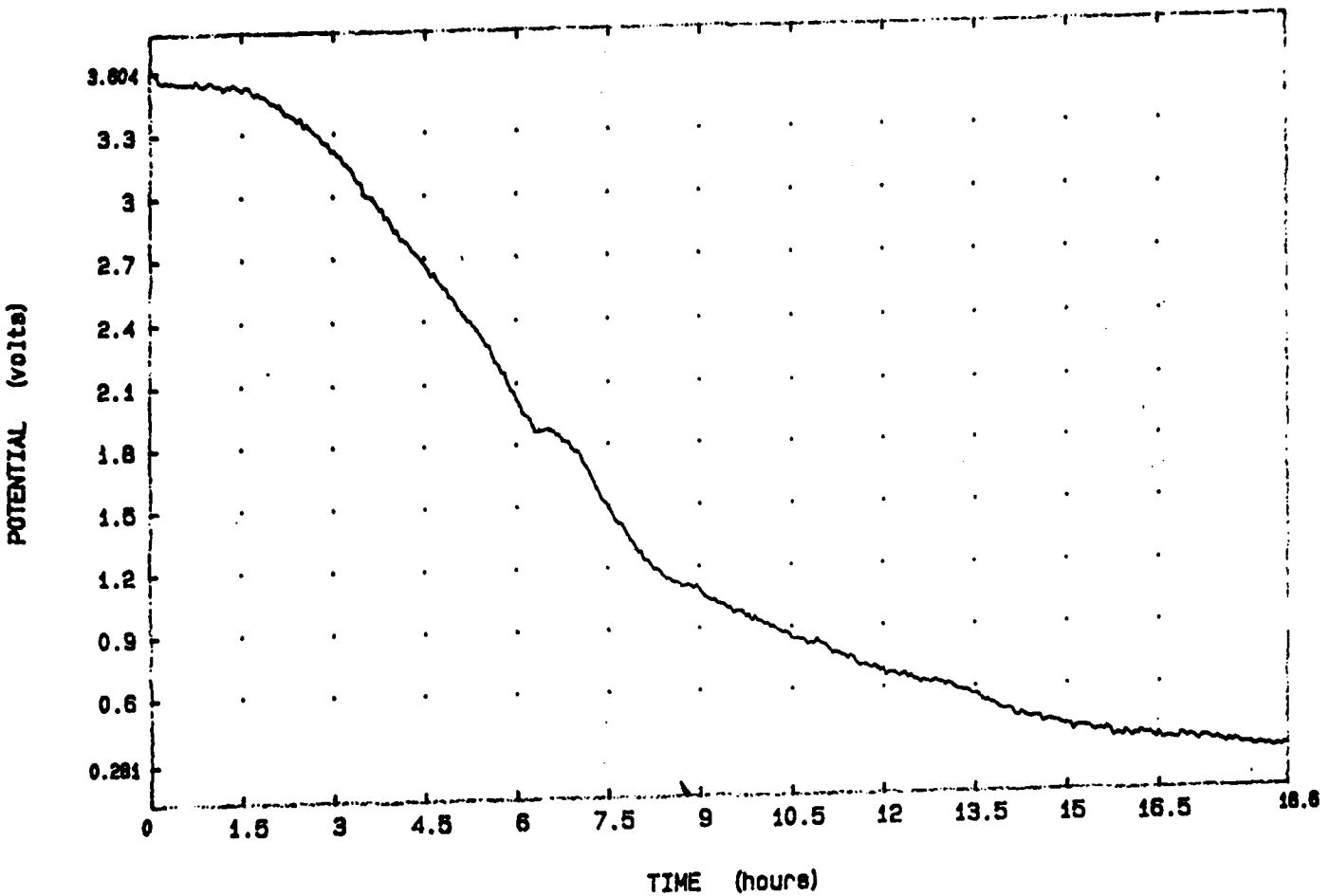

FIGURE 110. Discharge Profile, potential versus time, cathode versus reference, AA cell #55-3-1
Electrolyte: 15% Br_2/ 2M LiBr·$AlCl_3$/ CH_2ClCCl_3
Positive electrode: 25Kj/75ab/10T
Discharge constant load: 100 ohms.

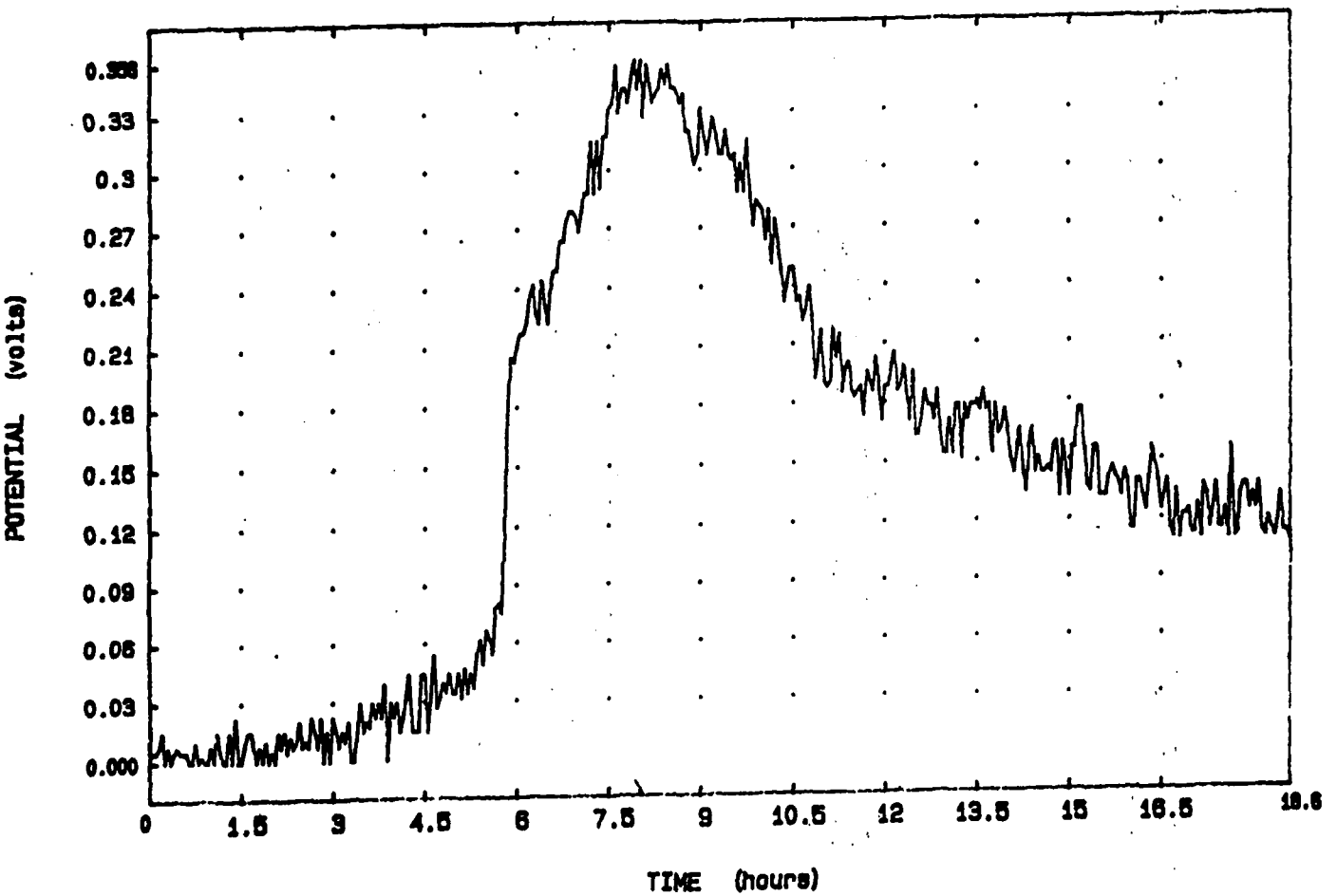

FIGURE 111. Discharge Profile, potential versus time, anode versus reference, AA cell #55-3-1
Electrolyte: 15% Br_2/ 2M $LiBr \cdot AlCl_3$/ $CH_2ClCClO$
Positive electrode: 25Kj/75ab/10T
Discharge constant load: 100 ohms.

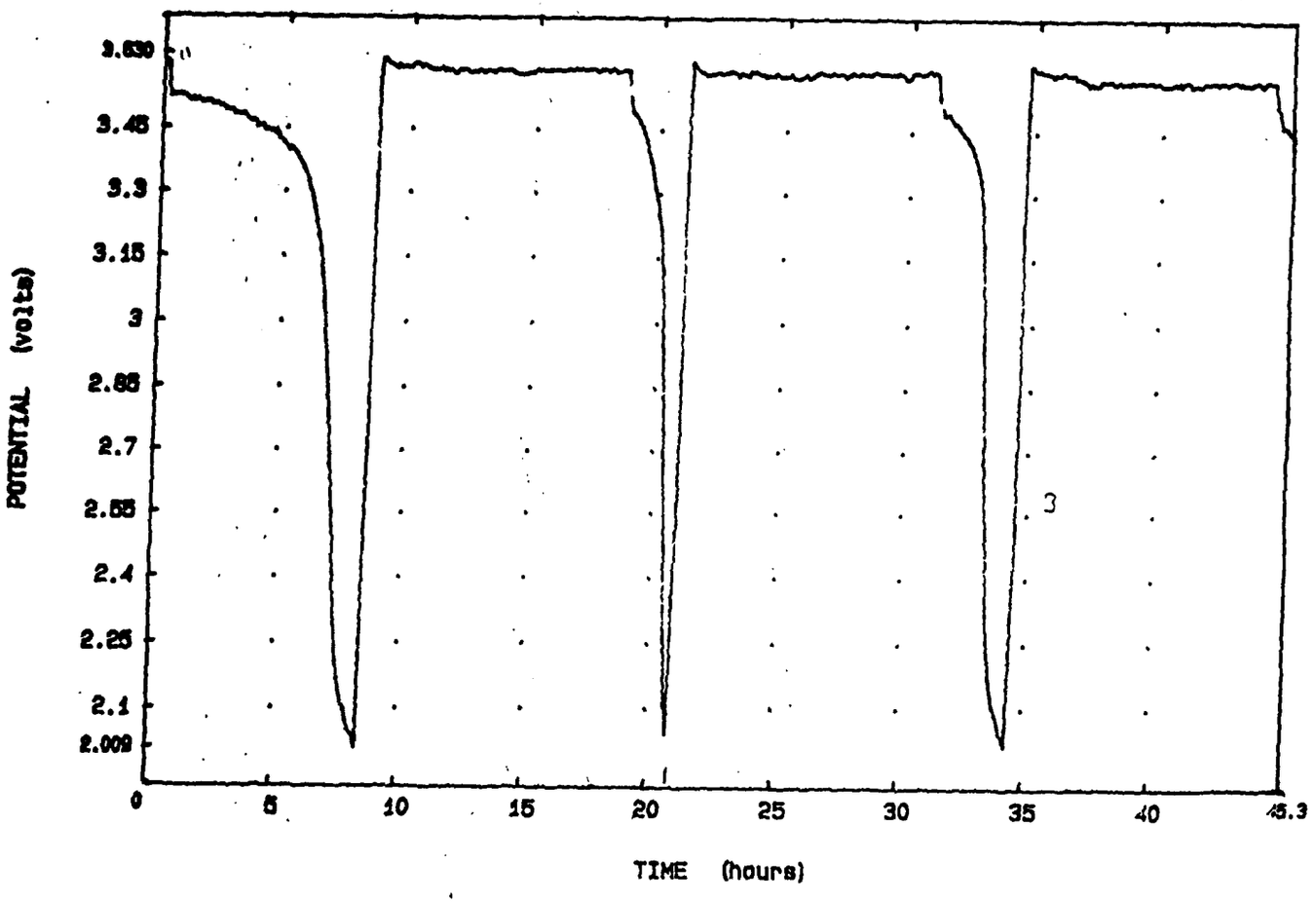

FIGURE 112. Discharge/ Charge Profiles, potential versus time, AA cell #55-15-5
Electrolyte: 20% Br_2/ 2M $LiBr \cdot AlCl_3$/ $CH_2ClCClO$
Positive electrode: Alupower
(layered, with graphite fibers and Teflon)
Charge/ discharge current: 1 mA/ cm^2 (50.8 mA).

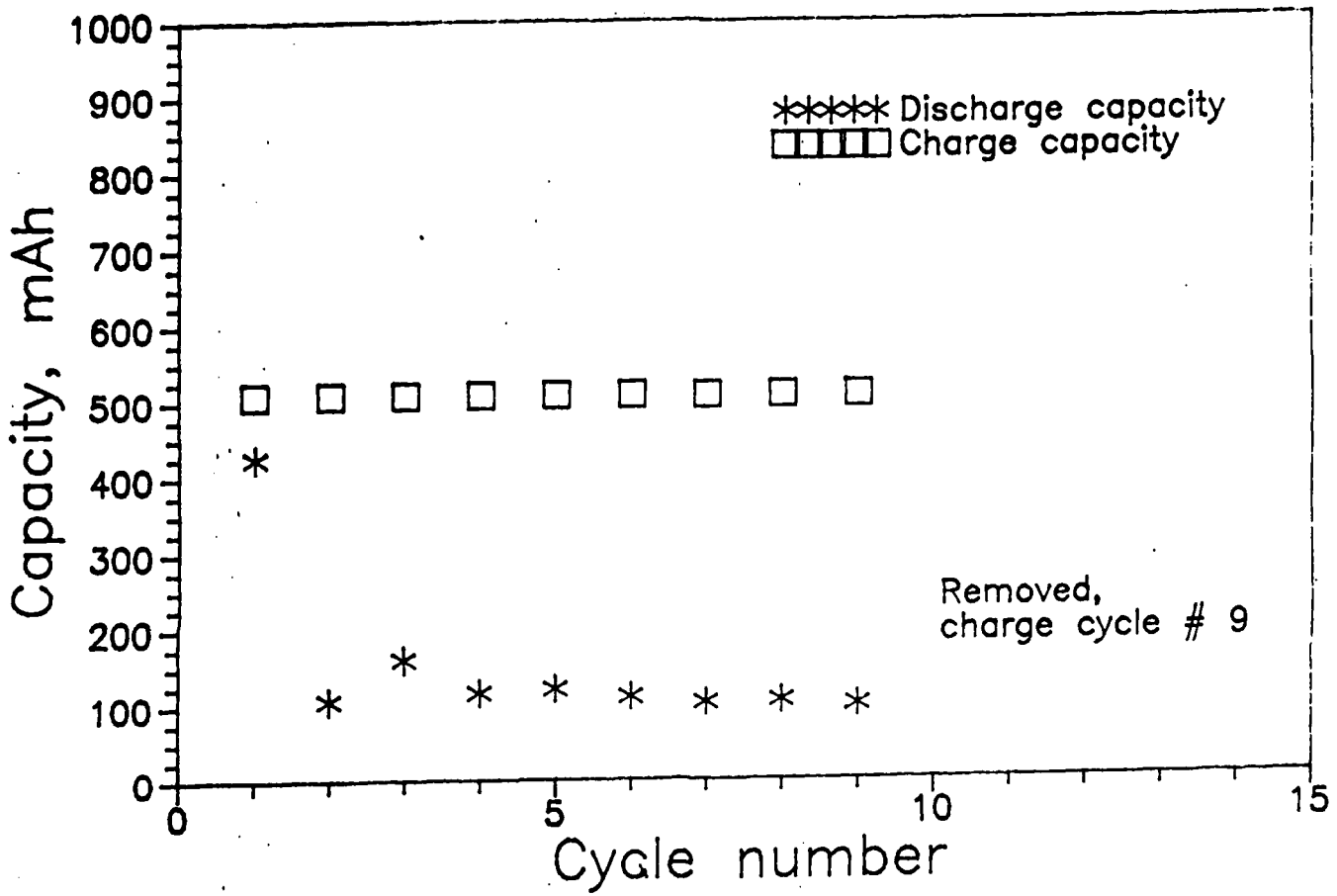

FIGURE 113. Discharge and Charge Capacities versus cycle number, AA cell #55-15-5
Electrolyte: 20% Br_2/ 2M LiBr·$AlCl_3$/ CH_2ClCCl_O
Positive electrode: Alupower
(layered, with graphite fibers and Teflon)
Charge/ discharge current: 1 mA/ cm^2 (50.8 mA).

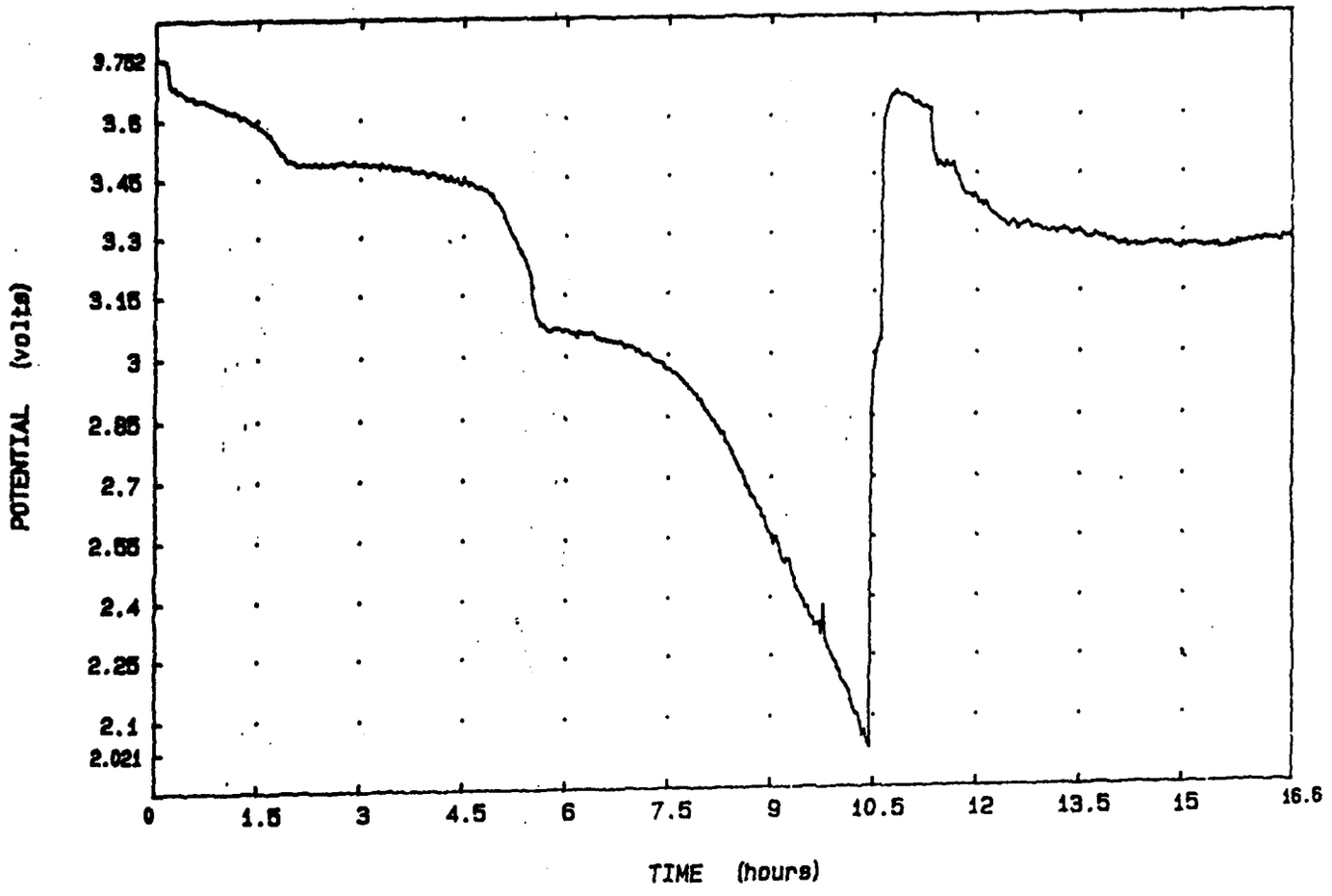

FIGURE 114. Discharge/ Charge Profiles, potential versus time, AA cell #55-69-4
Electrolyte: dried $2LiCl \cdot CaCl_2 \cdot 4AlCl_3 \cdot 12SO_2$/ 20% Br_2
Positive electrode: 100Kj/10T; with "Panex", either side
Charge/ discharge current: 1 mA/ cm^2 (50.8 mA).

ELECTRONICS TECHNOLOGY AND DEVICES LABORATORY
MANDATORY DISTRIBUTION LIST
CONTRACT OR IN-HOUSE TECHNICAL REPORTS

Defense Technical Information Center*
ATTN: DTIC-FDAC
Cameron Station (Bldg 5)
Alexandria, VA 22304-6145

(*Note to Contractor: Two copies for DTIC will be sent from STINFO Office, Fort Monmouth, NJ.)

Director
US Army Material Systems Analysis Actv
ATTN: DRXSY-MP
001 Aberdeen Proving Ground, MD 21005

Commander, AMC
ATTN: AMCDE-SC
5001 Eisenhower Ave.
001 Alexandria, VA 22333-0001

Commander, LABCOM
ATTN: AMSLC-CG, CD, CS (In turn)
2800 Powder Mill Road
001 Adelphi, Md 20783-1145

Commander, LABCOM
ATTN: AMSLC-CT
2800 Powder Mill Road
001 Adelphi, MD 20783-1145

Commander
US Army Laboratory Command
Fort Monmouth, NJ 07703-5000
1 - SLCET-DD
2 - SLCET-DT (M. Howard)
1 - SLCET-DB
35 - Originating Office

Commander, CECOM
R&D Technical Library
Fort Monmouth, NJ 07703-5000
1 - ASQNC-ELC-IS-L-R (Tech Library)
3 - ASQNC-ELC-IS-L-R (STINFO)

Advisory Group on Electron Devices
201 Varick Street, 9th Floor
002 New York, NY 10014-4877

Director
Naval Research Laboratory
ATTN: CODE 2627
001 Washington, DC 20375-5000

Cdr, PM JTFUSION
ATTN: JTF
1500 Planning Research Drive
001 McLean, VA 22102

Rome Air Development Center
ATTN: Documents Library (TILD)
001 Griffiss AFB, NY 13441

Deputy for Science & Technology
Office, Asst Sec Army (R&D)
001 Washington, DC 20310

HQDA (DAMA-ARZ-D/Dr. F.D. Verderame)
001 Washington, DC 20310

Dir, Electronic Warfare/Reconnaissance
Surveillance and Target Acquisition Ctr
ATTN: AMSEL-EW-D
001 Fort Monmouth, NJ 07703-5000

Dir, Reconnaissance Surveillance and
Target Acquisition Systems Directorate
ATTN: AMSEL-EW-DR
001 Fort Monmouth, NJ 07703-5000

Cdr, Marine Corps Liaison Office
ATTN: AMSEL-LN-MC
001 Fort Monmouth, NJ 07703-5000

Dir, US Army Signals Warfare Ctr
ATTN: AMSEL-SW-OS
Vint Hill Farms Station
001 Warrenton, VA 22186-5100

Dir, Night Vision & Electro-Optics Ctr
CECOM
ATTN: AMSEL-NV-D
001 Fort Belvoir, VA 22060-5677

Cdr, Atmospheric Sciences Lab
LABCOM
ATTN: SLCAS-SY-S
001 White Sands Missile Range, NM 88002

Cdr, Harry Diamond Laboratories
ATTN: SLCHD-CO, TD (In turn)
2800 Powder Mill Road
001 Adelphi, MD 20783-1145

Altus Corporation
1610 Crane Court
San Jose, CA 95112
ATTN: Technical Library

Duracell Inc.
Duracell Research Center
37 A Street
Needham, MA 02194
ATTN: Dr. A.N. Dey

Eagle-Picher Industries, Inc.
C & Porter Streets
PO Box 47
Joplin, MO 64801
ATTN: Technical Library

Stonehart Associates, Inc.
17 Cottage Road
P.O. Box 1220
Madison, Connecticut 06443
ATTN; Paul Stonehart

EIC Laboratories, Inc.
111 Downey Street
Norwood, MA 02062
ATTN: Technical Library

Electrochimica Corporation
20 Kelly Court
Menlow Park, CA 94025
ATTN: Dr. Morris Eisenberg

Whittaker-Yardney
Lithium Battery Operations
520 Winter Street
Waltham, MA 02254
ATTN: Dr. Robert MacDonald

Honeywell, Inc.
Power Sources Center
104 Rock Road
Harsham, PA 19044
ATTN: Technical Library

Honeywell, Inc.
Sensors and Signal Processing Lab.
10701 Lyndale Avenue South
Bloomington, Minnesota 55420
ATTN: H.V. Venkatasetty

Jet Propulsion Laboratory
4800 Oak Grove Drive
Pasadena, CA 91109
ATTN: Technical Library

Power Conversion, Inc.
280 Midland Avenue
Saddle Brook, NJ 07662
ATTN: Dr. Thomas Reddy

SAFT America, Inc.
Advanced Battery Systems
107 Beaver Court
Cockeysville, MD 21030
ATTN: Technical Library

Union Carbide Corporation
Section A-2
Battery Products Division
Old Ridgebury Rd.
Danbury, CT 06817
ATTN: Mr. Berger

AT&T Bell Laboratories
600 Mountain Avenue, 7A-317
Murray Hill, NJ 07974
ATTN: Karrie Hanson

Jet Propulsion Laboratory
Mail Stop 277-212
Pasadena, CA 91109
ATTN: Mr. Halpert

Tracor Battery Technology Ctr
1601 Research Blvd
Rockville, MD 20850
ATTN: Dr. Nehemiah Margalit

Gates Energy Products
P.O. Box 114
Gainesville, FL 32602
Attn: Library/T. Brown

Alupower, Inc.
6 Claremont Road
Bernardsville, NJ 07924
ATTN: Dr. Robert P. Hamlen

Catalyst Research
3706 Crondall Lane
Owings Mills, MD 21117
ATTN: Dr. Steven P. Wicelinski

Center for Electrochemical Systems
and Hydrogen Research
238 Wisenbaker ERC
Texas A&M University
College Station, TX 77843
ATTN: A. John Appleby

SRI International
333 Ravenswood Avenue
Menlo Park, CA 94025
ATTN: Digby D. MacDonald

Oxley Research, Inc.
71 Edgehill Road
New Haven, CT 06511
ATTN: Dr. James E. Oxley

Combustion Engineering
1000 Prospect Hill Road
Dept 9351-0501
Windsor, CT 06095-0500
ATTN: David N. Palmer

Lithium Energy Assoc., Inc.
246 Sycamore Street
Watertown, MA 02172
ATTN: Dr. Fred Dampier, Ph.D.

Dr. George Blomgren
Dr. J. C. Bailey
Battery Products Division
Union Carbide Corporation
Westlake, OH 44145

Dr. Sam Levy
Dr. Frank Delnick
Sandia National Laboratories
PO Box 5800
Acbuquerque, NM 87185

Dr. Graham Cheek
Chemistry Department
US Naval Academy
Annapolis, MD 21402

Dr. Boyd Carter
Jet Propulsion Lab
Pasadena, CA 91109

Dr. Nicola Marincic
Battery Engineering Inc.
Hyde Park, MA 02136

Dr. D. M. MacArthur
G. M. Research Laboratory
Tech. Center
Warren, MI 48090-9055

Dr. M. Gopikanth
Chemtech. Corporation
PO Box 280
Brookline, MA 02146

Dr. Kim Kinoshita
Lawrence Berkeley Lab
University of California
1 Cyclotron Road
Berkeley, CA 94720

Dr. Darrel Unterreker
Promeon Inc.
6700 Shingle Creek Pkwy
Brooklyn Center, MN 55430

Dr. Tom Watson
1711 Hunter Green Rd.
Upperco, MD 21155

Dr. K. C. Tsai
Pinnacle Research Inst.
10432 N. Tantau Ave.
Cupertino, CA 95014

Dr. Clive Scorey
Pfizer Corporation
21 Toelles Rd.
PO Box 5807
Wallingford, CT 06492